An examination of essential and non-essential metals in cacao (*Theobroma cacao* L.) using concentrations and stable isotope compositions

---

By Elnaz Barati

A thesis submitted as part of the requirements for a Doctor of Philosophy

Earth Science and Engineering

Imperial College London

June 2023

Declaration of Originality and Copyright

I solemnly declare that the research outlined in this Ph.D. thesis is my own work and all other resources have been appropriately referenced.

The copyright of this thesis rests with the author. Unless otherwise indicated, its contents are licensed under a Creative Commons Attribution-Non Commercial-No Derivatives 4.0 International Licence (CC BY-NC-ND).

Under this licence, you may copy and redistribute the material in any medium or format on the condition that; you credit the author, do not use it for commercial purposes and do not distribute modified versions of the work.

When reusing or sharing this work, ensure you make the licence terms clear to others by naming the licence and linking to the licence text.

Please seek permission from the copyright holder for uses of this work that are not included in this licence or permitted under UK Copyright Law.

Acknowledgements

First and foremost, I would like to thank my supervisors, Professor Mark Rehkämper and Dr. Rebekah E. T. Moore, for helping me get through my Ph.D. research. I am grateful for their dedication and support in my supervision and for always being ready to provide guidance when I needed it. I appreciate Mark's prompt, detailed and constructive feedback on my Ph.D. research. I also appreciate Rebekah's constructive feedback on my research, and her assistance in helping me learn the research methodology, namely in training me on ion exchange chromatography and MC-ICP-MS measurements. I would also like to thank Dr. Katharina Kreissig for her technical assistance and advice whilst working in the MAGIC laboratories, and most importantly for her lending an empathetic ear when I needed it. And of course, I would like to thank Mr. Barry J. Coles for the numerous times he provided technical assistance and helped me navigate using the MC-ICP-MS instrument.

Thank you also to all the lovely people at the London Metallomics Facility at King's College London, Dr. Alex Griffith, Ms. Renata Magueta, and Dr. Alex Morrell, for their patience, guidance and technical assistance whilst I completed my ICP-Q-MS measurements. I would also like to thank all the gracious collaborators that allowed for me to successfully complete my Ph.D. thesis, Professor Jim Dunwell and Dr. Ihsan Ullah at the University of Reading, Mr. James Weeks at King's College London, Dr. Laurence Maurice, Dr. Eva Schreck and Ms. Laudine Marchive at Géosciences Environnement Toulouse (GET), Observatoire Midi Pyrénées, Université de Toulouse.

Thank you to my dear family, Roya, Mohammadreza, Sanaz, Elham, Sahar, Pasha and Mohammad, for supporting me all along the way. And, of course, thank you to my friend Cate for listening to my countless tangents on my Ph.D. research.

Finally, I would like to thank all those working hard at the Department of Earth Science and Engineering that allowed me to successfully complete my Ph.D. thesis.

Abstract

High Cd concentrations observed in cacao beans (*Theobroma cacao* L.) grown in South and Central America pose global health concerns. This Ph.D. thesis aims to understand whether elements, primarily Zn and Cd, use similar mechanisms for their uptake, storage and translocation in hydroponic- and soil-cacao systems. If similar mechanisms are used for Cd and other elements, there are mitigation opportunities to reduce Cd uptake and subsequent transport to cacao beans. Firstly, using anion exchange chromatography and MC-ICP-MS, Zn isotope and concentration analyses were conducted on 19 cacao genotypes grown in hydroponic solutions under Cd stress. The results demonstrated all 19 genotypes preferentially removed isotopically light Zn from hydroponic solutions, which was also observed for Cd; and the roots were enriched in isotopically heavy Zn isotopes compared to aerial organs. This isotope partition trend between roots and aerial organs is opposite to what was observed for previously published Cd isotope data from the same plants. Secondly, using ICP-Q-MS, element concentration measurements were conducted on cacao, soil leachate and bulk soil samples from Ecuador. The results showed cacao trees had similar uptake patterns for Zn and Cd and for Mn and Cu from bioavailable pools, represented by soil leachates, indicating possible shared physiological mechanisms for uptake. Additionally, based on the concentration analyses and elemental distributions for cacao fruit, leaves, woody biomass and roots, the elements fell into three primary groups: Zn, Cd, Mg, Al, and Fe; Cu, Mn, As and Mo; and Co and Ni. Lastly, a critical review on Zn and Cd isotope fractionation in plant systems demonstrated that most plant species: preferentially take up isotopically light Zn and Cd from nutrient mediums; and isotopically heavy Zn and light Cd are sequestered in the root, whereas isotopically light Zn and heavy Cd are preferentially translocated from the root to aerial organs.

Publications and Conference Presentations

Published

Barati, E., Moore, R.E.T., Ullah, I., Kreissig, K., Coles, B., Dunwell, M. J., &. Rehkämper, M. (2023). An investigation of zinc isotope fractionation in cacao (*Theobroma cacao* L.) and comparison of zinc and cadmium isotope compositions in hydroponic plant systems under high cadmium stress. *Scientific Reports,* 13, 4682.

Conference Presentations

Barati, E., Moore, E. T. R., Ullah, I., Kreissig, K., Coles, B., Dunwell, M. J., &. Rehkämper, M. (2022). Investigating cadmium and zinc interactions in cacao using stable isotope analyses, Oral Talk, *20th Biennial National Atomic Spectroscopy Symposium*, Manchester, UK, June 28-29, 2022.

Barati, E., Moore, E. T. R., Ullah, I., Kreissig, K., Coles, B., Dunwell, M. J., &. Rehkämper, M. (2022). Investigating cadmium and zinc interactions in cacao using stable isotope analyses, Oral Talk, *Earth Science and Engineering Student Conference*, London, UK, September 30, 2022.

Table of Contents

Section		Title	Page
		List of Figures	**11**
		List of Tables	**14**
1.0		**Chapter 1: Introduction**	**16**
	1.1	Research motivation	17
	1.2	Overview of Ph.D. research objectives	20
	1.3	References	21
2.0		**Chapter 2: Background and overview of the research methodology**	**24**
	2.1	Chapter overview	25
	2.2	Single collector quadrupole ICP-MS instrument	25
	2.2.1	Sample preparation for ICP-Q-MS measurements	25
	2.2.2	Overview of ICP-Q-MS instrument mechanics	26
	2.3	MC-ICP-MS instrument	29
	2.3.1	MC-ICP-MS for isotope ratio measurements	29
	2.3.2	Sample preparation and ion exchange chromatography	30
	2.3.3	Spectral interferences in MC-ICP-MS instruments	31
	2.3.4	Overview of MC-ICP-MS instrument mechanics	32
	2.4	Non-spectral interferences in ICP-MS instruments	34
	2.5	Data reduction	35
	2.5.1	Overview of instrumental drift and calibration solutions in ICP-Q-MS	35
	2.5.2	Overview of mass bias correction using the double-spike method	37
	2.6	Fundamentals behind isotope fractionation	42
	2.7	References	45
3.0		**Chapter 3: Background on cadmium and zinc in vascular plant-soil systems**	**48**
	3.1	Chapter Overview	49
	3.2	Background on Zn and Cd in minerals, soils and soil solutions	49
	3.2.1	Zinc and Cd formation in primary and secondary (soil) minerals	49
	3.2.2	Zinc and Cd concentrations in soils and aqueous (soil) solutions	51
	3.3	Zn and Cd soil and aqueous chemistry	53
	3.3.1	Characteristics defining Zn and Cd solubility in soils	53
	3.3.2	Understanding Zn and Cd adsorption in soils	55
	3.4	Background on Cd and Zn uptake and transport in plants	57
	3.4.1	Uptake of Zn and Cd in plants	57
	3.4.2	Translocation of Zn and Cd in plants	59
	3.5	Overview of the biochemical, molecular, and physiological mechanisms for regulating Zn and	60

	Cd in plants	
3.5.1	Excluder strategy	61
3.5.1.1	Reducing soil metal bioavailability	61
3.5.1.2	Controlling of metal influx	62
3.5.2	Tolerance strategy	63
3.5.2.1	Promoting metal efflux	63
3.5.2.2	Sequestering and immobilising metals	64
3.6	Application of stable isotope analyses to vascular plant systems	65
3.7	Elements in cacao plants	66
3.7.1	Cd concentrations in cacao	67
3.7.2	Cd uptake and transport in cacao	67
3.7.3	Other element uptake and transport in cacao	68
3.8	References	70
4.0	**Chapter 4: An investigation of zinc isotope fractionation in cacao (*Theobroma cacao* L.) and a comparison of zinc and cadmium isotope compositions in hydroponic plant systems under high cadmium stress**	**77**
4.1	Declaration of research contributions	78
4.2	Introduction	78
4.3	Methods	82
4.3.1	Samples	82
4.3.1.1	Cultivation of cacao plant	82
4.3.1.2	Plastic leaching experiment	84
4.3.2	Sample preparation	85
4.3.2.1	Digestion	85
4.3.2.2	Zinc separation chemistry	86
4.3.3	Zinc concentration and stable isotope measurements	87
4.3.4	Calculations and data analysis	88
4.4	Results	89
4.4.1	Quality control	89
4.4.1.1	Blank contributions and reference materials	89
4.4.1.2	Zinc data for biological and analytical replicates of cacao plant samples	90
4.4.2	Zinc data for the 19 cacao genotypes	91
4.4.3	Zinc data for plants treated with 0, 5, and 20 $\mu mol\ L^{-1}\ CdCl_2$	93
4.5	Discussion	99
4.5.1	Stable isotope fractionation during Zn uptake	99
4.5.2	Stable isotope fractionation during Zn translocation	101
4.5.3	Comparison of Zn and Cd stable isotope fractionation in cacao plants	103
4.6	Conclusion	107
4.7	References	109
5.0	**Chapter 5: Uptake and translocation of essential and non-essential elements in cacao (*Theobroma cacao* L.): an Ecuador field study**	**118**
5.1	Declaration of research contributions	119

5.2	Introduction	119
5.3	Samples	122
5.3.1	Cacao farms	122
5.3.2	Sample collection and initial preparation	122
5.4	Analytical methods	123
5.4.1	Laboratories and reagents	123
5.4.2	Analyses at the LMF	124
5.4.2.1	Digestion of cacao samples	124
5.4.2.2	Preparation of soil leachates	125
5.4.2.3	Elemental concentration measurements by ICP-Q-MS	125
5.4.3	Analyses at the GET and PAPC Laboratories	127
5.4.3.1	Determination of physico-chemical properties of soils	127
5.4.3.2	Determination of elemental concentrations of soils	128
5.4.4	Analyses at the MAGIC Laboratories	129
5.5	Data analysis and calculations	130
5.5.1	Elemental (mass) distribution calculation	130
5.5.2	Bioaccumulation and translocation factors	130
5.6	Results	131
5.6.1	Quality control	131
5.6.1.1	Cacao samples	132
5.6.1.2	Bulk soil samples	133
5.6.1.3	Soil leachate samples	133
5.6.2	Cacao samples	134
5.6.2.1	Elemental concentrations of cacao organs	134
5.6.2.2	Elemental distributions in the cacao trees	137
5.6.3	Soils	139
5.6.3.1	Physico-chemical properties of bulk soils	139
5.6.3.2	Element concentrations of bulk soils	139
5.6.3.3	Element concentrations of the soil leachates	139
5.7	Discussion	142
5.7.1	Element uptake and bioaccumulation by cacao trees	142
5.7.1.1	Bioaccumulation factors between total plants and bulk soils	142
5.7.1.2	Bioaccumulation values between total plants and bioavailable pools	146
5.7.2	Element translocation in cacao trees	149
5.7.2.1	Element enrichments in the roots	150
5.7.2.2	Element enrichments in the woody biomass	150
5.7.2.3	Element enrichments in the leaves and fruit	154
5.7.2.4	Hitchhiker elements and their rides: Cd-Zn and Co-Ni	155
5.8	Conclusions	160
5.9	References	164

6.0	**Chapter 6: A critical review of zinc and cadmium stable isotope fractionation in vascular plant systems**	**174**
6.1	Introduction	175
6.2	Zinc and Cd isotope ratio notation	177
6.3	Quality control in Zn and Cd stable isotope studies of vascular plant species	181

	6.4	Brief overview of kinetic and equilibrium isotope effects and high- and low-affinity transport systems in vascular plant species	182
	6.5	Isotopic fractionation of Zn and Cd during uptake by vascular plants	184
	6.5.1	Summary of apparent isotope fractionation for uptake of Zn in vascular plant species	184
	6.5.2	Summary of apparent isotope fractionation for uptake of Cd in vascular plant species	188
	6.5.3	Comparison of apparent isotope fractionation for uptake of Zn and Cd in vascular plant species	191
	6.5.4	Understanding uptake mechanism(s) for Zn and Cd using stable isotope analyses	194
	6.5.5	Key takeaways on the uptake of Zn and Cd stable isotopes in vascular plants	206
	6.6	Isotopic fractionation of Zn and Cd translocation in vascular plants	207
	6.6.1	Summary of apparent isotope fractionation for the translocation of Zn in vascular plant species	207
	6.6.2	Summary of apparent isotope fractionation for the translocation of Cd in vascular plant species	210
	6.6.3	Comparison of apparent isotope fractionation for uptake of Zn and Cd in vascular plant species	210
	6.6.4	Understanding translocation mechanism(s) for Zn and Cd using stable isotope analyses	212
	6.6.5	Key takeaways on the translocation of Zn and Cd stable isotopes in vascular plants	222
	6.7	Influence of plant height on Zn and Cd isotope fractionation during translocation	223
	6.8	Genotype-specific influences on Zn and Cd isotope fractionation during uptake and translocation	224
	6.9	Conclusion and recommendations	225
	6.9.1	Key recommendations	225
	6.10	References	230
7.0		**Chapter 7: Conclusion and future research opportunities**	**242**
	7.1	Summary of key findings	243
	7.2	Future research opportunities	245
8.0		**Appendices**	**248**
		Appendix I	**249**
		Appendix II	**264**
		Appendix III	**297**

List of Tables

Table 2.1. Common isobaric and polyatomic interferences for Zn.

Table 3.1 Trace elements coprecipitated with secondary (soil) minerals and soil humus, adapted from Sposito [1].

Table 3.2. Soil pH and total Cd and Zn concentrations (mg kg^{-1}) for topsoils for Ecuadorian cacao farms.

Table 3.3. Summary of Cd concentrations (mg kg^{-1}) for different cacao plant tissues.

Table 3.4. Summary of element concentrations (mg kg^{-1}) for different cacao plant tissues.

Table 4.1. Zinc mass fractions (*f*), concentrations (mg kg^{-1}) and stable isotope compositions ($\delta^{66}Zn$) of leaves, stems and roots for 19 cacao genotypes grown with 20 µmol L^{-1} $CdCl_2$.

Table 4.2. Zinc masses (µg), concentrations (mg kg^{-1}) and stable isotope compositions ($\delta^{66}Zn$) for total plants and Zn stable isotope differences ($\Delta^{66}Zn$) and fractionation factors ($\varepsilon^{66}Zn$).

Table A4.1. Cacao clone names, accession numbers and donor organizations for the cacao germplasms used in this study.

Table A4.2. Composition of the half-strength Hoagland solutions with additional $CdCl_2$.

Table A4.3. Zinc concentrations ([Zn]; mg kg^{-1}) and stable isotope compositions ($\delta^{66}Zn$) for quality control materials.

Table A4.4. Summary of mass fractions (*f*), Zn concentrations ([Zn]; mg kg^{-1}) and Zn stable isotope compositions (δ^{66} Zn) for leaves, stems and roots determined for biological and analytical replicates.

Table A4.5. Dry weights (g) of the different plant organs treated with 20 µmol L^{-1} $CdCl_2$.

Table A4.6. Summary of Zn concentration data (mg kg^{-1}) for cacao leaves from this study and the literature.

Table A4.7. Summary of mean dry weights (g), mass fractions (*f*), Zn concentrations ([Zn]; mg kg^{-1}) and Zn stable isotope compositions (δ^{66} Zn) of leaves, stems and roots and total plant dry weights (g) for seedlings of the NA 702 genotype treated with 0, 5, and 20 µmol L^{-1} $CdCl_2$.

Table A4.8. Summary of $\Delta^{66}Zn$ for uptake, and Zn stable isotope compositions (δ^{66} Zn) for root, shoot and leaf published for different plant species.

Table A5.1. Location of the farms as well as the number, genotype and age of each of the cacao trees grown on the farms.

Table A5.2. Limits of detection (LOD) and quantification (LOQ) for cacao samples, and certified and measured element concentrations (mean ± SD; μg g^{-1}) for reference materials analysed by ICP-Q-MS together with cacao samples at the LMF.

Table A5.3. Certified and measured Cd concentrations (mean ± SD; μg g^{-1}) for reference materials analysed alongside cacao plant organ samples at the MAGIC Laboratories by MC-ICP-MS using the isotope dilution method.

Table A5.4. Limits of detection (LOD) and quantification (LOQ) for bulk soils, and certified and measured element concentrations (mean ± SD; μg g^{-1}) for a reference material analysed primarily by ICP-Q-MS at GET laboratories, except for Cd concentrations which were analysed at the MAGIC Laboratories by MC-ICP-MS using the isotope dilution method.

Table A5.5. Limits of detection (LOD) and quantification (LOQ) for soil leachates, and certified and measured element concentrations (mean ± SD; μg g^{-1}) for a reference material analysed by ICP-Q-MS at the LMF alongside soil leachate samples.

Table A5.6. Element concentrations (μg g^{-1}) determined for analytical replicates of cacao plant organs from Farms 3, 4 and 6.

Table A5.7. Element concentrations (μg g^{-1}) determined for analytical replicates of bulk soil (0-20 cm) samples from the six farms.

Table A5.8. Element concentrations (μg g^{-1}) determined for analytical replicates of soil leachates extracted using Mehlich-3, EDTA-AA and AA.

Table A5.9. Median, min and max element concentrations (μg g^{-1}) in the cacao plant organs from the six farms.

Table A5.10. Element concentrations (in μg g^{-1}) in the organs of the cacao trees.

Table A5.11. Mean and median elemental (mass) distributions (%) for the cacao tree reservoirs roots, woody biomass, leaves and fruit.

Table A5.12. Physico-chemical properties and element concentrations of bulk topsoils from the six farms.

Table A5.13. Element concentrations (μg g^{-1}) of leachates extracted from the bulk topsoil samples of the six farms using Mehlich-3, EDTA-AA and AA.

Table A5.14. Fractions of elements extracted (%) from bulk topsoil of the six farms using Mehlich-3, EDTA-AA, and AA.

Table A5.15. Bioaccumulation factors (BF) determined for elements between the cacao trees of Farms 3 to 6 and bulk topsoils as well as the Mehlich-3, EDTA-AA, and AA soil leachates.

Table A5.16. Mean and median elemental (mass) distributions (%) for the cacao tree reservoirs woody biomass, leaves and fruit.
Table A5.17. Translocation factors (TF) determined for elements between the roots and different aboveground organs of cacao tree from the six farms.
Table 6.1. Summary of glossary terms important to understanding isotope fractionation in vascular plant systems.
Table 6.2. Summary of soil pH, δ^{114}Cd (‰) and δ^{66}Zn (‰) values for bulk soil, soil extract and/or solution and summary of Δ^{114}Cd (‰) and Δ^{66}Zn (‰) values.
Table A6.1. Summary of measured Zn concentration ± SD (mg kg^{-1}) and δ^{66}Zn (‰) values of certified reference materials used in published studies.
Table A6.2. Summary of measured Cd concentration ± SD (mg kg^{-1}) and δ^{114}Cd (‰) values of certified reference materials used in published studies.
Table A6.3. Summary of Δ^{66}Zn (‰) values associated with uptake and translocation and δ^{66} Zn (‰) values for roots, shoots and leaves for different vascular plant species.
Table A6.4. Summary of Δ^{114}Cd (‰) values associated with uptake and translocation and δ^{114}Cd (‰) values for roots, shoots and leaves for different vascular plant species.

List of Figures

Figure 2.1. An example demonstrating (a) on-mass mode and (b) mass shift mode to remove $^{40}Ar^{40}Ar^{+}$ interference on $^{80}Se^{+}$, modified from Sugiyama & Shikamori [6].

Figure 2.2. Schematic drawing of the Nu Plasma HR MC-ICP-MS instrument taken from Rehkämper et al. [5].

Figure 2.3. An example of a calibration curve produced by the external calibration solutions, which is used to determine the Zn concentrations in a sample set.

Figure 2.4. Schematic drawing of the application of the DS method modified from Yang [9].

Figure 2.5. Schematic plot of the error in α for ^{64}Zn-^{67}Zn DS from Arnold et al. [10].

Figure 4.1. Zinc stable isotope compositions ($\delta^{66}Zn$) of leaves, stems and roots versus mass fractions (*f*) of Zn in leaves, stems and roots for the 19 cacao genotypes treated with 20 µmol L^{-1} $CdCl_2$.

Figure 4.2. Mean Zn stable isotope compositions ($\delta^{66}Zn$) versus mass fractions (*f*) of Zn in leaves, stems and roots relative to the total plant Zn inventory for NA702 plants treated with 0 µmol L^{-1} (yellow, *n*=3), 5 µmol L^{-1} (green, *n*= 2), and 20 µmol L^{-1} (blue, *n*=1) $CdCl_2$.

Figure 4.3. Zinc stable isotope difference ($\Delta^{66}Zn_{mob\text{-}total\ plant}$) between mobilised Zn in cacao leaves (mob) and total plant Zn inventory versus mass fraction (*f*) of Zn present in cacao leaves for the 19 cacao genotypes treated with 20 µmol L^{-1} $CdCl_2$.

Figure A4.1. Zinc stable isotope compositions ($\delta^{66}Zn$) versus Zn concentrations ([Zn]; mg kg^{-1}) for leaves, stems, roots, and whole plants of the 19 cacao genotypes treated with 20 µmol L^{-1} $CdCl_2$.

Figure A4.2. Leaf Zn concentrations ([Zn]; mg kg^{-1}) versus total plant Zn concentrations (mg kg^{-1}) for the 19 cacao genotypes.

Figure A4.3. (a) Dry weights (g) and (b) mass fraction (%) for organs of NA 702 plants cultured with 0, 5 and 20 µmol L^{-1} $CdCl_2$ and mean results for the other 18 cacao genotypes cultured with 20 µmol L^{-1} $CdCl_2$.

Figure A4.4. Mean Zn stable isotope compositions ($\delta^{66}Zn$) for leaves, stems and roots versus mean Zn concentrations ([Zn]; mg kg^{-1}) of the NA702 seedlings treated with 0 µmol L^{-1} (yellow), 5 µmol L^{-1} (green) and 20 µmol L^{-1} (blue) $CdCl_2$.

Figure A4.5. Cadmium stable isotope compositions ($\delta^{114}Cd$) versus Zn stable isotope composition ($\delta^{66}Zn$) for roots and leaves of the 19 cacao genotypes treated with 20 µmol L^{-1} $CdCl_2$.

Figure 5.1. Element concentrations (µg g^{-1}) of cacao plant organs from the six farms.

Figure 5.2. Median elemental (mass) distributions (%) determined for (a) total trees with root, woody biomass, leaf and fruit reservoirs and (b) aboveground tree parts with woody biomass, leaf and fruit reservoirs.
Figure 5.3. Element concentrations (μg g^{-1}) for bulk soil samples and the Mehlich-3, AA and EDTA-AA soil leachates from the six farms.
Figure 5.4. Median BF values for elements between six total cacao trees from Farms 3 to 6 and (a) bulk topsoils, and the (b) Mehlich-3, (c) EDTA-AA and (d) AA soil leachates.
Figure 5.5. The range of BF values A) between (i) cacao beans and bulk (top)soils from previously published literature compared to this study's BF values for (ii) ripe cacao beans and (iii) total cacao trees versus bulk soils; and range of BF values B) between (i) cacao leaves and bulk (top)soils from previously published literature compared to this study's BF values between (ii) mature leaves and (iii) total cacao trees and bulk soils.
Figure 5.6. Median TF values for elements between plant organs and roots.
Figure A5.1. Sampling locations situated near the three Ecuadorian villages of Mompiche, Esmeraldas, Atacames, Esmeraldas, and Puerto Inca, Guayas [83].
Figure A5.2. Median elemental (mass) distributions (%) determined for (a) total trees with root, woody biomass, leaf and fruit reservoirs and (b) aboveground tree parts with woody biomass, leaf and fruit reservoirs.
Figure 6.1. Zn and Cd uptake. Summary of apparent isotope fractionation values between total plant and medium (a) $\Delta^{66}Zn_{\text{total plant-medium}}$ and (b) $\Delta^{114}Cd_{\text{total plant-medium}}$ for different vascular plant species, whereby the medium represents hydroponic solution, soil solution or extract, and/or bulk soil.
Figure 6.2. Summary of $\Delta^{66}Zn_{\text{total plant-medium}}$ (‰) and $\Delta^{114}Cd_{\text{total plant-medium}}$ (‰) values for cacao and wheat, whereby medium represents the nutrient medium such as a hydroponic solution or soil extract.
Figure 6.3. Summary of apparent isotope fractionations ($\Delta^{114}Cd$ and $\Delta^{66}Zn$) between total plant and medium and between aerial plant parts, and processes responsible for Zn and Cd isotope fractionation during uptake and translocation.
Figure 6.4. Zn and Cd translocation. Summary of apparent isotope fractionation values between shoot and root or total plant (a) $\Delta^{66}Zn_{\text{shoot- root/total plant}}$ and (b) $\Delta^{114}Cd_{\text{shoot- root/total plant}}$ for different vascular plant species.
Figure 6.5. Plot shows the $\Delta^{66}Zn$ (‰) and $\Delta^{114}Cd$ (‰) during translocation for wheat and cacao.

Chapter 1
Introduction

1.1. Research motivation

Over the last few decades, the growing presence of Cd, a trace toxic heavy metal, in cocoa-based products has become a global health and safety concern [1]. With a biological half-life of between 10 and 30 years in humans, the long-term exposure and progressive accumulation of Cd in the human body through air, water, soil, and food can lead to adverse health complications [1,2]. These health complications include permanent damage to the urinary and skeletal systems and different types of cancers [2]. As a result of these adverse health impacts, the European Union (EU) recently established a new strict upper limit of between 0.1 to 0.8 mg kg^{-1} for Cd present in final cacao-based products sold to consumers, effective January 1, 2019 [3].

With these newly established upper limits, cacao producers are now confronted with the difficult challenge of reducing high Cd concentration levels in their products to meet these limits. This is particularly relevant to cacao producers in South and Central America, as studies have documented higher concentration levels of Cd in cocoa powder and cocoa-based products using cacao beans from South and Central American countries, when compared to similar products originating from African countries [4,5]. For example, a study by Argüello et al. [6] found that, based on a nationwide survey of 159 cacao farms in Ecuador, 254 of 560 cacao bean samples (or 45%) exceeded concentrations of 0.6 mg kg^{-1} for Cd (the threshold limit for the study). Other studies of cacao beans from Ecuador and Honduras also documented Cd concentrations in a large portion of cacao bean samples that far exceeded the EU upper limits [7,8,9]. The prevalence of high Cd concentration in cacao beans from South and Central America, and specifically Ecuador, has negative ramifications for the livelihoods of thousands of small-scale cacao farmers and their

families. This reflects that Ecuador exports a large portion of its cacao beans and cocoa-based products to the EU [10, 11]. Specifically, in 2014, Ecuador's cacao bean exports reached over 236,000 MT, the equivalent of $775 million (USD), with 42% of exports going to the US, followed by 27% to the EU and 11% to Mexico [11]. Losing some, or all, of its exports to the EU will have adverse consequences for cacao farmers in Ecuador, and to other South and Central American countries that rely heavily on the export of cacao beans and cocoa-based products.

To mitigate the high Cd concentration levels in cacao beans and subsequent cocoa-based products, further research is required to understand the underlying origins of and/or mechanisms for the observed Cd enrichments. There are presently still notable uncertainties about whether the high Cd concentrations of cacao beans are mainly of natural origin, and associated with soil properties, or whether they are a consequence of anthropogenic processes related to land management and agricultural practices. For land management and agricultural practices, specifically, it is unclear to what extent cultivation, fertilization and soil conditioning affect Cd concentration levels in soils and cacao cultivars [7,9,12,13]. It is also unclear to what extent tree age and cultivar type, including the distinct physiological mechanisms that are characteristic of different cultivars, impact the uptake and enrichment of Cd [13,14,15,16]. There is also limited understanding to what extent other elements, including essential micronutrients (e.g., Zn, Cu, Fe, Mn) and other toxic, non-essential metals (e.g., As, Pb), influence the uptake mechanisms of Cd in cacao cultivars. In particular, research has yet to provide basic understanding about whether (and which) other essential and non-essential elements use similar uptake and translocation mechanisms as Cd in cacao, and whether different uptake and translocation mechanisms work synergistically or antagonistically to either increase or decrease the uptake and translocation of Cd

in cacao cultivars [17, 18, 19]. Antagonism occurs when the addition of one element decreases the level of another element, while synergism occurs when the addition of one element increases the level of another element in a plant [20].

State-of-art methodologies, namely ion exchange chromatography and MC-ICP-MS methodologies, can help to understand how the availability of essential micronutrient elements, such as Zn, influence the uptake and translocation of Cd to aerial plants organs in cacao cultivars. Notably, previous work on wheat soil-plant systems have shown that such coupled concentration and stable isotope data collected through MC-ICP-MS methodologies can provide vastly improved constraints on: (i) whether high concentrations of Cd available for plant uptake in soils are of natural or anthropogenic origins; (ii) the mechanisms employed by plants to regulate uptake of Cd and translocation of the metal from the roots to the edible parts [21,22]; and (iii) the extent to which other metals such as Zn impact the uptake of Cd and translocation from the roots to aerial parts of a plant [23]. Similarly, the use of single collector ICP-MS allows for multi-element concentration measurements of cacao plant parts, which help to further understand the relationship between and transport of Cd and other essential and non-essential elements (e.g., Zn, Ni, Cu, Fe, Mn) across different plant parts [7,9,19].

This Ph.D. research helps ongoing efforts to understand and develop agricultural practices that yield cacao beans with safe Cd levels for human consumption, whilst supporting the livelihoods of farmers in South and Central American countries.

1.2. Overview of Ph.D. research objectives

This Ph.D. thesis aims to support the development of mitigation strategies to reduce the high Cd concentrations of cacao beans by addressing various uncertainties and gaps in the existing relevant research. In particular, the research will focus on examining whether there are significant relationships between the uptake and translocation mechanisms of Cd and other essential and non-essential elements, namely chemically similar Zn, in cacao plants. If similar mechanisms exist for Cd and Zn, notably for uptake, there is an opportunity to use Zn to mitigate or reduce the uptake of Cd by cacao plants. The Ph.D. research objectives will be achieved by: (1) introducing briefly the research methodology; (2) briefly introducing Cd and Zn in vascular plant-soil systems; (3) analysing and comparing Cd and Zn concentrations and stable isotope compositions of 19 diverse, juvenile cacao genotypes that were hydroponically grown under high Cd stress at the University of Reading (UK); (4) analysing Cd and other essential and non-essential element concentrations in bulk soil, soil leachate and cacao plant samples from diverse localities in Ecuador; (5) further understanding Cd and Zn isotope fractionation in vascular plant species through a comprehensive critical review; and (6) summarizing the thesis' findings and outlining opportunities for future research.

1.3. References

1. Maddela, N. R. *et al.* Cocoa-laden cadmium threatens human health and cacao economy: A critical view. *Science of The Total Environment* **720**, 137645 (2020).
2. Rahimzadeh, R. M., Rafati Rahimzadeh, M., Kazemi, S., & Moghadamnia, A. A., Review Article Cadmium toxicity and treatment: An update. *Caspian Journal of Internal Medicine* **8**, 135 (2017).
3. The European Commission. Commission Regulation (EU) No 488/ 2014 of 12 May 2014 Amending Regulation (EC) No. 1881/2006 as regards maximum levels of cadmium in foodstuffs. *Official Journal of European Union* **138**, 75–79 (2014).
4. Abt, E., Sam, F. J., Gray, P. & Robin, P. L. Cadmium and lead in cocoa powder and chocolate products in the US Market, *Food Additives & Contaminants: Part B* **11(2),** 92-102 (2018).
5. Mounicou, S., Szpunar, J., Andrey, D., Blake, C., & Lobinski, R. Concentrations and bioavailability of cadmium and lead in cocoa powder and related products. *Food Additives & Contaminants* **20**, 343–352 (2003).
6. Argüello, D. *et al*. Soil properties and agronomic factors affecting cadmium concentrations in cacao beans: A nationwide survey in Ecuador. *Science of the Total Environment* **649**, 120-127 (2019).
7. Chavez, E. *et al*. Concentration of cadmium in cacao beans and its relationship with soil cadmium in southern Ecuador. *The Science of the Total Environment* **533**, 205-214 (2015).

8. Barraza, F. *et al*. Cadmium bioaccumulation and gastric bioaccessibility in cacao: A field study in areas impacted by oil activities in Ecuador. *Environmental Pollution* **229**, 950-963 (2017).
9. Gramlich, A. *et al*. Soil cadmium uptake by cocoa in Honduras. *The Science of the Total Environment* **612**, 370-378 (2018).
10. Díaz-Montenegro, J., Varela, E., & J. M. Gil. Livelihood strategies of cacao producers in Ecuador: Effects of national policies to support cacao farmers and specialty cacao landraces, *Journal of rural studies* **63**, 141–156 (2018).
11. Vega, H., & Beillard, J.M. Ecuador Cocoa Update and Outlook (Foreign Agricultural Service Global Agricultural Network, Trans.) GAIN Report. *Quito: United States Department of Agriculture*, 2015. Retrieved from: https://apps.fas.usda.gov/newgainapi/api/report/downloadreportbyfilename?filename=Ecuador%20Cocoa%20Update%20and%20Outlook_Quito_Ecuador_2-18-2015.pdf [accessed 10/11/2022].
12. Barraza, F. *et al*. Distribution, contents and health risk assessment of metal(loid)s in small-scale farms in the Ecuadorian Amazon: An insight into impacts of oil activities. *The Science of the Total Environment* **622-623**, 106-120 (2018).
13. Scaccabarozzi, D. *et al.* Soil, Site, and Management Factors Affecting Cadmium Concentrations in Cacao- Growing Soils. *Agronomy* **10**, 806, (2020).
14. Barraza, F. *et al.* Cadmium isotope fractionation in the soil – cacao systems of Ecuador: A pilot field study. *RSC Advances* **58(9)**, 34011-34022, (2019).
15. Engbersen, N. *et al.* Cadmium accumulation and allocation in different cacao cultivars. *Science of the Total Environment* **678**, 660–670, (2019).

16. Moore, R. *et al.* Cadmium isotope fractionation reveals genetic variation in Cd uptake and translocation by *Theobroma cacao* and role of natural resistance-associated macrophage protein 5 and heavy metal ATPase-family transporters. *Horticulture Research* **7**, 71 (2020).
17. dos Santos, M. L. S. *et al*. Mitigation of cadmium toxicity by zinc in juvenile cacao: Physiological, biochemical, molecular and micromorphological responses. *Environmental and Experimental Botany* **179**, 104201 (2020).
18. Arévalo-Gardini, E., Arévalo-Hernández, C. O., Baligar, V. C., & He, Z. L. Heavy metal accumulation in leaves and beans of cacao (Theobroma cacao L.) in major cacao growing regions in Peru. *The Science of the Total Environment* **605-606**, 792–800 (2017).
19. Barraza, F. *et al.* Beyond cadmium accumulation: Distribution of other trace elements in soils and cacao beans in Ecuador. *Environmental research* **192**, 110241 (2021).
20. Green, C., Chaney, R. & Bouwkamp, J. Increased zinc supply does not inhibit cadmium accumulation by rice (Oryza sativa L.). *Journal of Plant Nutrition* **40(6)**, 869-877 (2016).
21. Wiggenhauser, M. *et al.* Cadmium Isotope Fractionation in Soil- Wheat Systems. *Environmental Science & Technology* **50(17)**, 9223–9231 (2016).
22. Imseng, M. *et al.* Fate of Cd in agricultural soils: A stable isotope approach to anthropogenic impact, soil formation and soil-plant cycling. *Environmental Science & Technology* **52**, 7b05439 (2018).
23. Wiggenhauser, M. *et al.* Zinc isotope fractionation during grain filling of wheat and a comparison of zinc and cadmium isotope ratios in identical soil-plant systems. *The New Phytologist* **219(1),** 195– 205 (2018).

Chapter 2

Background and overview of the research methodology

2.1. Chapter overview

This chapter will briefly introduce all the research methods used in this Ph.D. thesis, which include discussing sample preparation, single and multiple collector ICP-MS instruments, spectral and non-spectral interferences, data reduction and the fundamentals behind isotope fractionation. Furthermore, in this chapter, Zn will be mostly used as the example analyte.

2.2. Single collector quadrupole ICP-MS instrument

The single collector quadrupole ICP-MS (ICP-Q-MS) is a type of mass spectrometer that can be used to measure multiple elemental concentrations in environmental, clinical, and geological samples [1,2]. In this Ph.D. research, ICP-Q-MS is used to conduct accurate multi-element concentration measurements of plant samples.

2.2.1. Sample preparation for ICP-Q-MS measurements

The ICP-Q-MS is useful for direct determination of concentrations for multiple interference-prone elements in a given sample without using any chemical separation procedures, such as ion exchange chromatography used for multiple collector ICP-MS (MC-ICP-MS) sample measurements. Whilst ICP-Q-MS does not require chemical separation procedures, it does still require sample preparation. In particular, all samples must be digested to produce liquid sample solutions that can be introduced to the instrument's desolvating sample introduction system for measurements [1, 2]. Sample digestion is accomplished through microwave digestion techniques

and protocols, which employ the use of a microwave digestion system and different analytical reagents (e.g., HNO_3, HF, H_2O_2) [3].

2.2.2. Overview of ICP-Q-MS instrument mechanics

The ICP-Q-MS instruments use a conventional argon (Ar) plasma source that reaches between 5000–7400 K and is connected to a desolvating sample introduction system fitted with a spray chamber nebuliser. The power supply is also provided through a radiofrequency (RF) generator. Once a liquid sample solution is introduced to the ICP-Q-MS, it is desolvated, vaporized and ionised by the Ar plasma source [1,2,4]. Subsequently, the ionised sample passes through three cones (sampler, skimmer and hyperskimmer cones), each with a small orifice to allow the transfer of a tiny fraction of the positively charged ions, while removing excess electrons. The ion stream then enters the 'reaction or collision cell' whereby spectral interferences, namely elemental isobaric and polyatomic interference species can be removed [1,2,4].

In all ICP-MS instruments, including in both ICP-Q-MS and MC-ICP-MS instruments, there are two main types of spectral interferences that can occur during measurements, namely elemental isobaric and polyatomic ion interferences (see Table 2.1, as an example). Elemental isobaric interferences occurs when in the sample solution being analysed there are nuclides of the same mass as the analyte element of interest [1,5]. In contrast, polyatomic ions, such as argides, oxides and nitride ions, form in ICP-MS instruments when two or more isotopes from the same or different element react with one another in the Ar plasma. These polyatomic ions can interfere with measurements of the analyte of interest when they share the same nominal mass [1,5]. For

instance, $^{40}Ar^{+}$ reacts with oxide to produce $^{40}Ar^{16}O^{+}$ which interferes with the major Fe isotope of $^{56}Fe^{+}$ [1]. In addition, acids, buffers, salts, solvents and other reagents that generate oxide, hydroxide, chloride- and sulphur-containing polyatomic ion species present in the sample matrix can produce interferences during all ICP-MS measurements [1]. As such, ICP-Q-MS is susceptible to isobaric and polyatomic interferences, and a 'reaction and collision cell' can be used to reduce these interferences.

Table 2.1. Common isobaric and polyatomic interferences for Zn.

Isotope	Isobaric Interferences	Polyatomic Interferences
^{64}Zn	^{64}Ni, $^{32}S_2^{+}$	$^{32}S^{16}O_2^{+}$, $^{48}Ti^{16}O^{+}$, $^{36}Ar^{14}N_2^{+}$
^{66}Zn	$^{132}Ba^{2+}$	$^{50}Ti^{16}O^{+}$, $^{34}S^{16}O_2^{+}$, $^{33}S_2^{+}$
^{67}Zn	$^{134}Ba^{2+}$	$^{35}Cl^{16}O_2^{+}$, $^{33}S^{34}S^{+}$, $^{34}S^{16}O_2{}^{1}H^{+}$
^{68}Zn	$^{136}Ba^{2+}$	$^{40}Ar^{14}N_2^{+}$, $^{35}Cl^{16}O^{17}O^{+}$, $^{40}Ar^{12}C^{16}O^{+}$
^{70}Zn	^{70}Ge	$^{35}Cl^{35}Cl^{+}$, $^{40}Ar^{14}N^{16}O^{+}$, $^{34}S^{18}O_2^{+}$

The 'reaction and collision cell' of an ICP-Q-MS instrument consists of two different instrumental configuration settings for the analysis of an analyte(s) in a sample: the dynamic reaction cell (DRC) or reaction mode and the kinetic energy discrimination (KED) or collision mode. The DRC or reaction mode uses reaction chemistry to eliminate isobaric interferences. DRC uses reactive gases such as H_2, O_2 or NH_3 to remove isobaric interferences by either (Figure 2.1): (1) converting the interfering species into a new species or reaction product ion that no longer interferes with the identification of the analyte ion at its 'natural' isotopic mass (called on-mass mode); or (2) converting the analyte ion of interest into a reaction product ion that can be easily identified free from the inferring species at another mass-to-charge ratio than that of the original analyte ion of interest (called on mass-shift mode). In contrast to DRC mode, the KED or collision mode uses non-reactive gases such as He to promote fragmentation of polyatomic ions. Polyatomic ions are larger than analyte ions of the same mass, and therefore they have larger cross-sections.

Collisions with a non-reactive gas causes polyatomic ions to lose more kinetic energy as they pass through the pressurized reaction and collision cell. These polyatomic ions can subsequently be prevented through energy filtering from entering the quadruple (Q) mass analyser. Energy filtering ensures that lower kinetic energy ions formed in the reaction or collision cell are unable to overcome the potential energy barrier, and thus prevented from passing into Q mass analyser and towards the ion detector [1,2,4].

After departing the 'reaction and collision cell', the ions enter the Q mass analyser. In the Q mass analyser, mass-selection occurs whereby positively charged ions within a specific mass-to-charge window (between 0-240 atomic mass units) can be selected, and those ions falling outside this selected mass-to-charge window are omitted or rejected. Finally, after departing the Q mass analyser cell, the analyte ions reach the ion detectors interference-free and subsequently provide accurate element concentration measurements [1,2,4].

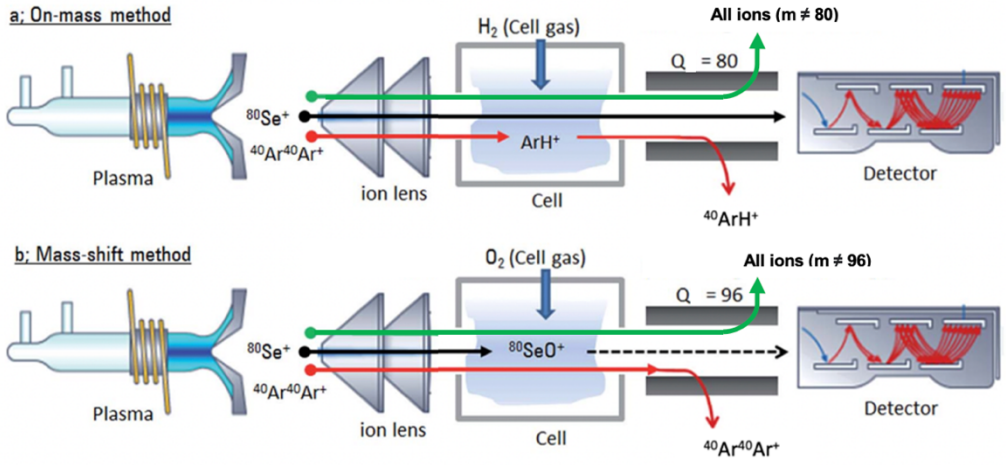


Figure 2.1. An example demonstrating (a) on-mass mode and (b) mass shift mode to remove $^{40}Ar^{40}Ar^{+}$ interference on $^{80}Se^{+}$, modified from Sugiyama & Shikamori [6]. In the figure, 'cell' denotes the reaction and collision cell, Q denotes the mass analyser set to a specific mass-to-charge, and 'm' denotes mass-to-charge.

2.3. MC-ICP-MS instrument

Through advancements in mass spectrometry, namely in MC-ICP-MS, small natural variations in isotope compositions have been readily discovered for an increasing number of elements (e.g., Mg, Si, Ca, Cr, Fe, Ni, Cu, Zn, Se, Mo, Ru, Ag, Cd) in environmental, clinical, and geological samples [7,8,9,10,11]. The MC-ICP-MS instrument allows for the simultaneous collection and analyses of multiple isotopes, which was previously not possible through other mass spectrometry instruments such as the single collector ICP-MS instrument. In this Ph.D. research, MC-ICP-MS is used for all isotope ratio measurements as opposed to thermos-ionization mass spectrometer (TIMS) and ICP-Q-MS instruments for reasons outlined in the proceeding section.

2.3.1. MC-ICP-MS for isotope ratio measurements

Modern mass spectrometers use a combination of multiple-Faraday detectors and a magnetic mass analyser for isotope ratio analyses. However, the ion source for different mass spectrometers varies. For example, TIMS uses thermal ionisation via a heated coil or filament (e.g., W, Re) to ionise metal salts, whereas the ICP-Q-MS and MC-ICP-MS use Ar plasma to ionise solution sprays or solid aerosols [8,12]. Through the Ar plasma used in MC-ICP-MS (and ICP-Q-MS) instruments, at high temperatures (~6000-8000 K), elements with ionisation potentials of up to 10 eV are readily ionised to 75% or more. For instance, Zn and Cd have ionisation potentials of between 8 eV to10 eV with between 30% to 90% degree in ionisation using the Ar plasma [5]. As such, through an Ar plasma source, MC-ICP-MS can readily ionise nearly all elements in the periodic table with high precision [5,9]. The TIMS instrument, however, cannot ionise most

elements with high ionisation potentials (e.g., more than 7 eV) at high precision, as high temperatures achieved through the Ar plasma of MC-ICP-MS are not possible for thermal ionisation used in TIMS [5]. Thus, MC-ICP-MS is a superior mode for element ionisation of samples with high ionisation potentials as compared to TIMS.

In contrast to MC-ICP-MS instruments, ICP-Q-MS instruments have comparatively poor isotope ratio measurements for analytical data [5,8], with precisions of isotope ratio measurements usually being greater than > 5‰ for many elements [5]. The poor isotope ratio precision in ICP-Q-MS instruments is attributed to poor peak shape, namely a triangular shape, observed with quadrupole-based units even at low mass resolution (~300 M/ΔM) [5,8]. On the other hand, MC-ICP-MS instruments display flat-topped peaks at low mass resolution (~400 M/ΔM) and high mass resolution (>5000 M/ΔM) with high precision for isotope ratio measurements [5,9,17]. For instance, using MC-ICP-MS at low mass resolution (~400 M/ΔM), the precision of isotope ratio measurements for Zn have been documented between 0.02‰ and 0.10‰ in environmental and biological samples [10,11]. Moreover, MC-ICP-MS provides high precision of isotope ratios even at low mass resolution not obtained through ICP-Q-MS instruments. To this end, given the limitations in element ionisation of TIMS and poor precision of isotope ratio measurements for ICP-Q-MS, the MC-ICP-MS instrument is used for all isotope ratio measurements in this Ph.D. research.

2.3.2. Sample preparation and ion exchange chromatography

Prior to MC-ICP-MS instrumental analysis, all samples need to undergo sample preparation. As with ICP-Q-MS sample preparation, all samples must be dissolved and digested to produce liquid sample solutions with no bonded molecules, in order to measure individual elements. However, for isotope composition analysis, samples also need to undergo additional chemical separation to isolate specific elements (e.g. Zn) from the rest of the matrix before measurements via MC-ICP-MS. The most common method is ion exchange chromatography or 'column chemistry' [10,11,12,13,14,15,16]. Through ion exchange chromatography, all or most elements that could cause isobaric interferences can be kept out of the fraction containing the analyte of interest either by using specific mineral acids to (i) eliminate from the sample matrix through elution or (ii) keeping them on the resin while the analyte of interest is eluted [10,11,12,13,14,15,16]. It is important to note that column chemistry can cause isotope discrimination, whereby different isotopes are more easily separated from the resin than others. In this case, when there is incomplete separation, the collected analyte will not have the same isotope composition as it started with and will bias results [13]. After separation, the extracted analyte fractions can then be used directly for isotope measurements or to take preconcentrate measurements. The preconcentrate measurements examine the expected and observed analyte ion beam intensities during isotope measurements by the MC-ICP-MS, and whether there are discrepancies in measurements due to possible spectral interferences introduced during quantitative chemical separation [11].

2.3.3. Spectral interferences in MC-ICP-MS instruments

Given that high precision of isotope ratios can be achieved at low mass resolution, almost all MC-ICP-MS instruments operate at low mass resolution with minimal loss in transmission due to wide source and collector slits [5]. At low mass resolution, however, ions of the same mass-to-charge ratio (e.g., ^{64}Zn and $^{32}S^{16}O_2^+$) are not readily separated and induce analytical artefacts and polyatomic interferences, which are not possible to monitor and correct for during isotope measurements. As such, great care needs to be taken during sample preparation and chemical separation to reduce sources of contamination (e.g., analytical reagents, solvents) that can result in polyatomic interferences [1,5,9,18]. In contrast, unlike polyatomic interferences, isobaric interferences can be monitored and corrected for during isotope measurements by the MC-ICP-MS instrument. For example, ^{64}Ni can interfere with the reading of ^{64}Zn on the MC-ICP-MS, and therefore the interference can be monitored and subsequently corrected for mathematically using the measurements from ^{60}Ni and/or ^{62}Ni flat-topped peaks. However, the isobaric interference correction can only be accomplished, if most of the isobaric interferences have been successfully removed during chemical separation through ion exchange chromatography [10, 15, 16].

2.3.4. Overview of MC-ICP-MS instrument mechanics

During this Ph.D. research, all isotope ratio measurements were conducted with a Nu Plasma HR MC-ICP-MS instrument at the MAGIC laboratories in the Department of Earth Science and Engineering at Imperial College London. All Nu Plasma HR MC-ICP-MS instruments are double-focusing mass spectrometers that are fitted with up to 12 Faraday detectors, with a RF for its power supply (Figure 2.2) [9]. In this research, the Nu Plasma HR MC-ICP-MS instrument used an Aridus II (CETAC Technologies) desolvating nebuliser system, which was fitted with a

glass or PFA nebuliser. The desolvating nebuliser system introduces the sample to the MC-ICP-MS instrument, whereby the sample is mixed with Ar gas to produce an aerosol that is then passed through the plasma heat source that has temperatures of more than 6000 K to ionise the sample [5,11,13]. The ionised sample then travels along the ion beam through a sampler cone and subsequently a skimmer cone that permits <1% of the sample ions to pass through an electrostatic field, whereby excess electrons are then removed. The positively charged ions emerge from the electrostatic field guided by an electrostatic analyser (ESA). The ESA provides the focusing energy required to help separate isotopes by mass in the magnetic field of the MC-ICP-MS, by adjusting for kinetic energies, without affecting the large spread of ion energies in the ion beam and the flat-topped peaks produced. Subsequently, the positively charged ions that reach the magnetic field are then separated according to their mass-to-charge ratio prior to reaching the Faraday detectors for signal detection. An additional feature on the Nu Plasma HR MC-ICP-MS instrument is the variable dispersion zoom lens system, which is situated just after the magnetic (field) sector. The zoom lens system allows for the positively charged ions in the multiple ion beams that reflect different masses to be guided to the appropriate Faraday detectors with fixed positions for isotope measurements [5].

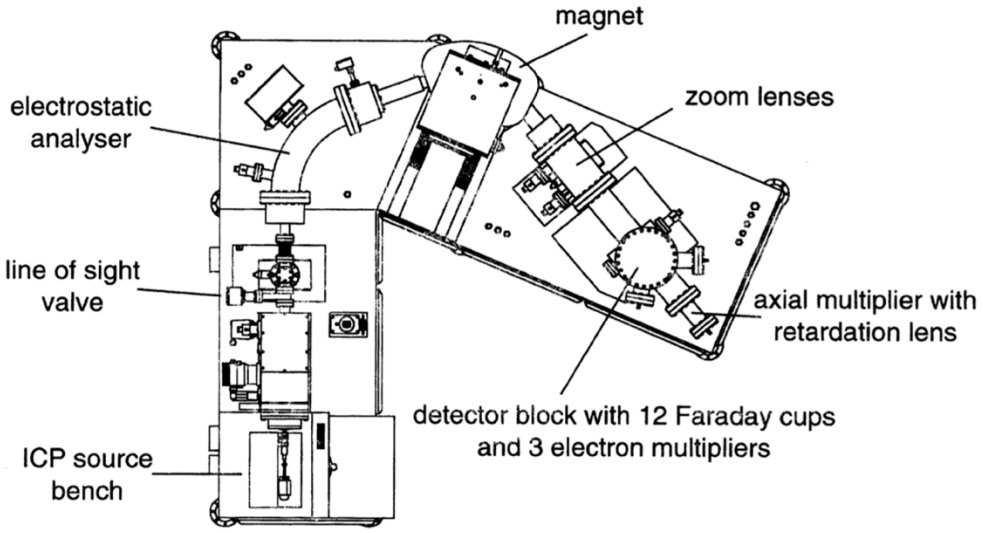


Figure 2.2. Schematic drawing of the Nu Plasma HR MC-ICP-MS instrument taken from Rehkämper et al. [5].

2.4. Non-spectral interferences in ICP-MS instruments

There are three main types of non-spectral interferences that can affect sample measurements for all ICP-MS instruments, namely matrix effects, memory effects, and physical effects. Matrix effects refer to the suppression or enhancement of an analyte ion in the presence of the sample matrix, when compared with the signal of the same analyte ion in the absence of the sample matrix [1,5]. For instance, organic residues or compounds, such as from column resins used during ion exchange chromatography, or metallic elements present in the sample matrix may react or collide with the analyte ion of interest during ionisation or passage through sampler and skimmer cones. In turn, this may enhance or diminish signal intensity of the analyte ion of interest [1,18]. As such, care must be taken during sample preparation and chemical separation to mitigate against sample-induced matrix effects in the ICP-MS instrument.

Memory effects refer to the persistence of a signal intensity for an analyte ion after completing the analysis of a given sample with adequate rinse time [1,5]. Certain elements such as Cd, Hg and Au are known to induce memory effects, and can propagate errors during measurements between different sample analyses. To minimize memory effects, there should be prolonged washout time between samples with 1 to 5% HNO_3 to remove memory from previous samples. As a disadvantage, longer washout times mean longer analysis times and lower throughputs [1].

Physical effects result from samples containing high levels of matrix elements and compounds such as salts or oxides that clog the nebuliser or are nebulised, deposited, and clogged onto the sampler and skimmer cones. As a result of the clogging of the nebuliser and sampling orifices, there are physical interference effects whereby there is a downward drift in the signal intensity of the analyte ion. To combat physical interference effects the spray-chamber, nebuliser, elbow joint, peristaltic pump tubing, sampler and skimmer cones need to be regularly cleaned with mineral acids such as 5% HNO_3. The sampler and skimmer cones need to be further cleaned and polished using an abrasive metal polish and rinsed with ultrapure water [1].

2.5. Data reduction

2.5.1. Overview of instrumental drift and calibration solutions in ICP-Q-MS

Instrumental drift in ICP-Q-MS instruments is primarily due to fluctuations in the electronics and in the Ar plasma. This drift can result from differences in the chemical composition

of a given sample, salt and oxide build-up and partial clogging at sampler or skimmer cone that impact the precision and accuracy in ICP-Q-MS measurements [1]. A common way to monitor and correct for instrumental drift is through the addition of multiple external calibration standard solutions, which are used to generate an external calibration curve for each element of interest and are measured before and after sample analyses (Figure 2.3). The external calibration standard solutions require the samples to be matrix-matched to them. Additionally, the unknown concentration of a particular analyte is subsequently determined by comparing signal intensities (counts per second, cps) of the analyte in the sample to the established calibration curve (Figure 2.3) [1,2].

Usually, an internal standard is also used in conjunction with external calibration standard solutions. An internal standard is a solution with a known, predetermined elemental concentration(s) that is added to each sample and external calibration standard solution. The internal standard can then be used to correct for any deviations in analyte(s) measurements between the external calibration standard solution and the sample [1,2]. This is accomplished through adding, in equal concentration, the same quantity of the internal standard to each sample and calibration standard solution. Choosing an appropriate internal standard for sample analyses requires that: (1) elements present in the internal standard solution must not be present in the sample; (2) elements in the internal standard solution must have similar physical and chemical properties as the analyte of interest; (3) the internal standard solution must consist of interference-free elements; and (4) the internal standard solution must not be a source of spectral interference with the analyte of interest [1]. For example, in this PhD research, ^{71}Ga was used as the internal standard for ^{66}Zn as it meets all the aforementioned conditions for a suitable internal standard.

Most importantly, in plant (biological) samples Ga is not present in quantifiable concentrations, and therefore not a source of spectral interference with Zn.

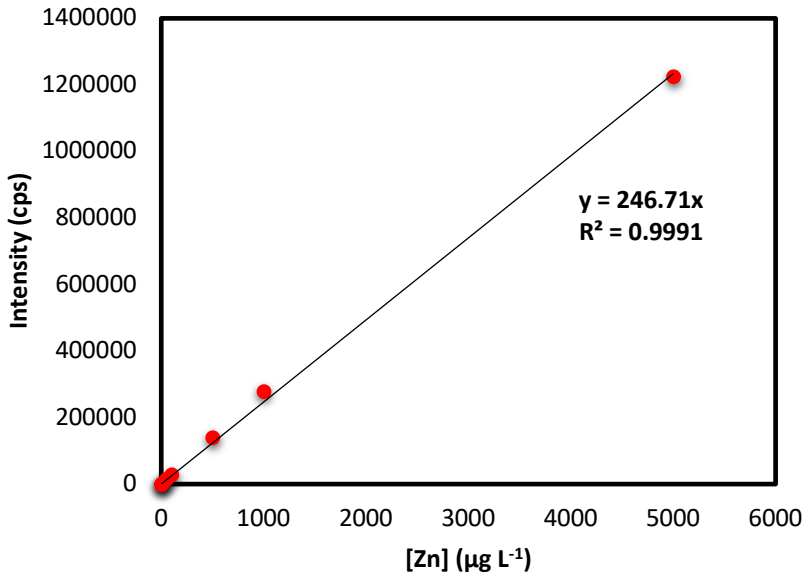


Figure 2.3. An example of a calibration curve produced by the external calibration solutions, which is used to determine the Zn concentrations in a sample set.

2.5.2. Overview of mass bias correction using the double-spike method

Although MC-ICP-MS provides high precision isotope ratio measurements, they suffer from large instrumental mass bias, whereby during the process of plasma ionisation there is a preferential extraction and transmission of heavier ions [5,9,12]. The mass bias results in the raw isotope ratio measurements deviating from their 'true' values by a certain percentage (%) per atomic mass unit [8]. For example, raw isotope ratios measurements for Li by plasma source ICP-MS instruments can deviate from their 'true values' by up to 25% per atomic mass unit [9]. The exact causes for the mass bias phenomena seen in MC-ICP-MS, and other Ar plasma source mass

spectrometry instruments is not fully understood. It is suggested, however, that mass bias is due to supersonic expansion of ions through the sampler cone, namely the expansion of the neutral plasma into the vacuum between the sampler and skimmer cones [5,9]. Between the sample and skimmer cones, ions gain kinetic energy by supersonic expansion, whereby lighter ions gain less kinetic energy than heavier ions, and therefore are more inclined to be deflected away from the beam axis when collisions occur with Ar neutrals [1,13]. This phenomenon preferentially favours the transmission of heavy isotopes of an analyte into the MC-ICP-MS instrument. As a result, this phenomenon generates different transmission efficiencies for the ions of different mass-to-charge ratios to produce a non-uniform response across the mass range [1,5,9,12]. Several techniques have been developed to correct for this mass bias, including sample-standard bracketing, elemental doping and double-spike (DS) methods. In this Ph.D. research, a combination of sample-standard bracketing and DS methods are employed to help address mass bias [5,9,12,15].

The sample-standard bracketing method requires that the MC-ICP-MS instrument to be in stable operating condition and that the sample matrix matches that of the standard solution. Once these requirements are met, the sample-standard bracketing method assumes that the mass bias for the sample can be corrected for using the mass bias for the standard solution, which is measured before and after the sample analysis by the MC-ICP-MS [8,9,12,15]. For this method, it can only be effectively applied when the sample and standard solutions are near identical, which assumes the sample and standard solution have matching concentrations and assumes almost perfect chemical separation of the analyte from the sample matrix. Due to possible isotope discrimination that may occur during ion exchange chromatography, the sample-standard bracketing also requires a sample recovery and yield of 100% during chemical purification. The sample-standard

bracketing method can be used in conjunction with either elemental doping or DS methods [8,9]. In this Ph.D. research, the sample-standard bracketing method primarily helps to monitor instrumental drift, whereby there is a drop or change in the signal intensity for the analyte of interest.

The elemental doping method, otherwise known as 'external normalisation', for mass bias correction is done by using the isotopic ratios of a different element that is simultaneously measured with the element under consideration by the MC-ICP-MS instrument. The chosen element for doping is assumed to behave similarly as the element under consideration with respect to mass bias, and therefore the element used for doping has a similar mass number as the element under consideration. Due to possible isotope discrimination that may occur during ion exchange chromatography, the elemental doping method requires sample recovery and yield of 100% during chemical purification. An example of elemental doping is the use of Cu doping for mass bias correction for Zn in stable isotope analyses [14].

The DS method for mass bias correction can be employed if the element under consideration has four or more stable isotopes. A DS contains two artificially enriched isotopes that have a known, predetermined ratio. This is then mixed with a sample with a natural (N), but unknown isotope composition, producing a mixture (M) [9,12,13]. Subsequently, the 'true' isotope ratio of the sample (N), can all be mathematically derived through solving a series of linear algebra equations after measurements are taken using an iterative technique to account for the instrumental mass fractionation (β) (Figure 2.4) [4,12]. The DS method can be a more robust alternative to elemental doping, as it not only corrects for mass bias, but if the DS is added to the sample before

chemical purification, it produces precise isotope compositions for the samples, even if the analyte yield after ion exchange chromatography was not 100%. This is because the analyte in the DS and the sample will undergo the same isotope fractionation during chemical separation and this can be corrected for as the initial isotope composition of the DS is known [5,12]. There are, however, disadvantages to the DS method such as the high cost associated with obtaining high purity enriched DS, the effort required to accurately calibrate the compositions of DS, and the DS requires the element under consideration to have at least four isotopes [9,12,19].

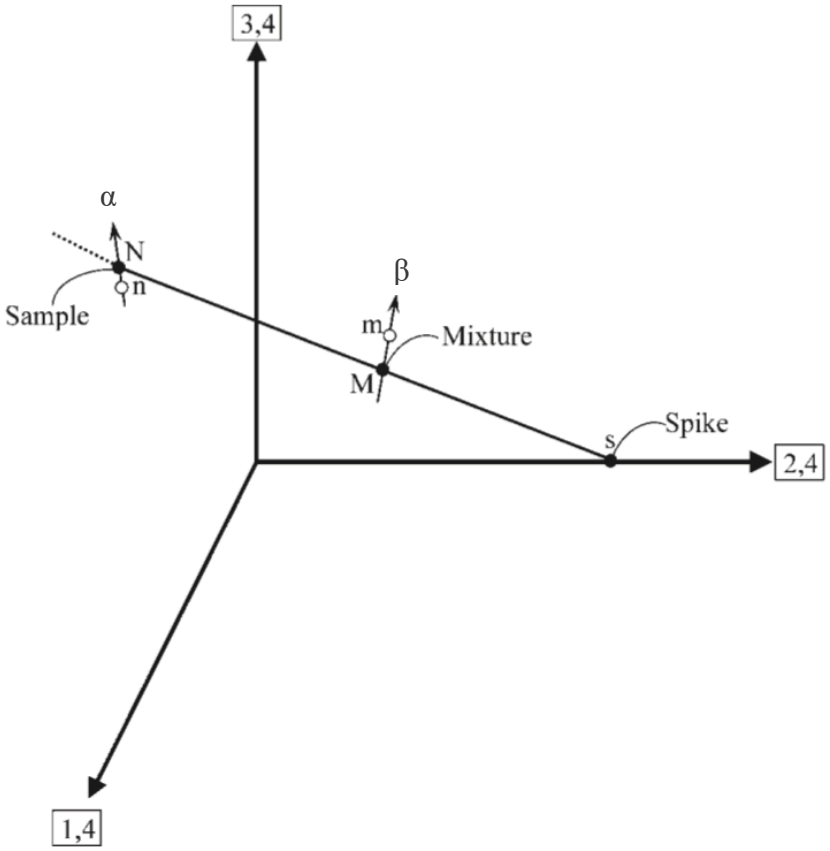


Figure 2.4. Schematic drawing of the application of the DS method modified from Yang [9]. The double spike is referred to as spike (s). N denotes the sample under consideration. 'M' denotes the mixture of the spike (s) with sample (N). The mixture 'M' undergoes instrumental mass fractionation with a mass fractionation factor (β), so that a different composition of 'm' is measured by the MC-ICP-MS. The

composition ‘n’ denotes a mass fractionation from ‘N’ with a mass fractionation factor of α. For stable isotope analyses, the ‘n’ is the composition of the standard solution measured by MC-ICP-MS and α the mass fractionation that occurs in nature. The DS method mathematically solves for α, β, N and M through inputs of isotope ratios for n, m, and s [9,19].

The precision of the DS method may suffer as all isotope ratio measurements propagate errors into the final measurements. The error propagation, however, can be minimised through proper calibration and optimisation of DS [9,10]. A reduction in error propagation in the mass fractionation can be achieved through optimising the proportion of enriched isotopes in the DS and the proportion of DS in the DS-sample mixture to reduce the error in mass fractionation factor α (Figure 2.5) [9,10,19]. For example, Zn isotope compositions in samples can be accurately determined over a large range of DS-sample ratios [10, 16]. Arnold et al. [10] and Amet & Fitoussi [16] demonstrated that the DS method produces accurate isotope compositions when the DS contributes a proportion of between 0.40 to 0.70 of the total Zn present in the DS-sample mixtures, with the optimum proportion being at approximately 0.55 (Figure 2.5). At higher and lower proportions of DS present in the DS-sample mixtures, the precision and accuracy of the data deteriorates (Figure 2.5) [10,16,19]. Further, for DS-sample mixtures, this optimum proportion of 0.55 translates to a molar ratio (S/N) for the spike-derived Zn (from the DS spike solution) to natural (total) Zn of approximately 1 [10,11,16].

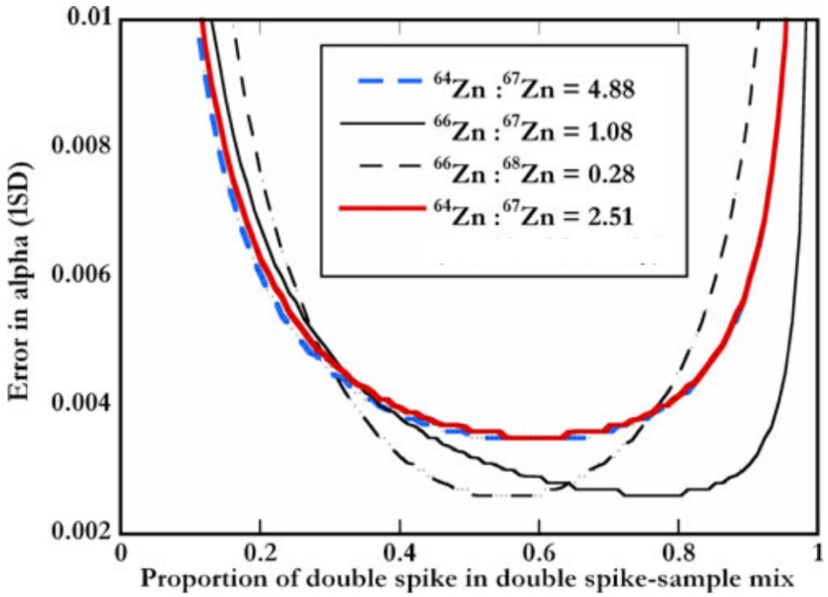


Figure 2.5. Schematic plot of the error in α for ^{64}Zn-^{67}Zn DS from Arnold et al. [10]. The horizontal axis denotes the proportion of DS in DS-sample mixture. The vertical axis denotes the error propagation in natural fractionation factor, α (1SD). Arnold et al. [10] determined four favourable Zn DS compositions using MATLAB error minimization code from Rudge et al. [19]. The different curves denote the uncertainty in the α as a function of the proportion of DS in the DS-sample mixture [10]. For the lowest error propagation in α, the optimum proportion of DS in the DS-sample mixture is at approximately 0.55. However, there is an acceptable range of 0.40 to 0.70 for producing low error propagation in α [10,16,19].

2.6. Fundamentals behind isotope fractionation

Isotopes of a given element display the same number of electrons, and thus largely exhibit similar chemical behaviours [7]. However, small differences in physical and chemical behaviours can still occur between isotopes of a given element because of differences in mass, namely the differences in the number of neutrons in the nucleus of an element [7,8]. Due to these small differences in mass, isotopes of the same element may participate in physical processes and

(bio)chemical reactions with different efficiencies. Mass-dependent isotope fractionation results from these different efficiencies, whereby there are slight differences in the equilibrium for isotopic molecules (i.e., thermodynamic or equilibrium isotope effect) or in the rate by which the isotopes participate in a chemical reaction (i.e., kinetic isotope effect) [7,8]. Through mass-dependent isotope fractionation effects, insights can be gained about the physical processes and chemical reactions that occurred and the conditions in which they occurred in [7]. It is assumed in this Ph.D. thesis, that all isotope fractionation occurring in plant systems are fundamentally mass-dependent.

Mass-dependent isotope fractionation in chemical reactions, namely equilibrium (or thermodynamic) isotope fractionation, is a quantum-mechanical phenomena that depends on vibrational energies and chemical bonds in molecules (i.e., intramolecular bonds) [7,8]. That is to say, the isotope fractionation is largely governed by the difference in vibrational energy levels of both the reactant(s) and product(s) in a chemical reaction, which is a function of an isotope's mass. At equilibrium, the reactant(s) or product(s) with the strongest chemical bond will be enriched in the heavier isotope [8].

A reaction is considered kinetic in nature, if equilibrium cannot be achieved, due to several reasons, including: (1) the reaction is unidirectional such as in enzymatic reactions; (2) the reaction is proceeding at a low temperature; or (3) when reaction products are formed, they are removed. Kinetic isotope fractionation is largely governed by the difference in vibrational energy levels of the reactant(s) and the activation energy complex. In general, light isotopes in molecules react more readily compared to their heavy isotope counterparts and will thus be present at a higher

relative abundance in the chemical reaction's product(s) than in the reactant(s). This, in turn, results in kinetic isotope fractionation [7,8]. In this Ph.D. thesis, equilibrium or kinetic isotope fractionation will be further discussed throughout different chapters in the context of plant systems, notably in Chapter 6.

2.7. References

1. Balaram, V. Strategies to overcome interferences in elemental and isotopic geochemical analysis by quadrupole inductively coupled plasma mass spectrometry: A critical evaluation of the recent developments. *Rapid Communications in Mass Spectrometry* **35**, e9065 (2021).
2. Pröfrock, D. & Prange, A. Inductively Coupled Plasma–Mass Spectrometry (ICP-MS) for Quantitative Analysis in Environmental and Life Sciences: A Review of Challenges, Solutions, and Trends. *Applied Spectroscopy* **66**, 843-868 (2012).
3. Hassan, N.., Rasmussen, P.., Dabek-Zlotorzynska, E., Celo, V. & Chen, H. (2007) Analysis of Environmental Samples Using Microwave-Assisted Acid Digestion and Inductively Coupled Plasma Mass Spectrometry: Maximizing Total Element Recoveries. *Water, Air, and Soil Pollution* **178(1-4)**, 323–334.
4. Balcaen, L., Bolea-Fernandez, E., Resano, M. & Vanhaecke, F. Inductively coupled plasma – Tandem mass spectrometry (ICP-MS/MS): A powerful and universal tool for the interference-free determination of (ultra)trace elements – A tutorial review. *Analytica chimica acta* **894**, 7-19 (2015).
5. Rehkämper, M., Schönbächler, M., & Stirling, C.H. Multiple collector ICP-MS: Introduction to instrumentation, measurement techniques and analytical capabilities. *Geostandards Newsletter* **25**, 23–40 (2001).
6. Sugiyama, N. & Shikamori, Y. Removal of spectral interferences on noble metal elements using MS/MS reaction cell mode of a triple quadrupole ICP-MS. *Journal of Analytical Atomic Spectrometry* **30(12)**, 2481–2487 (2015).

7. Vanhaecke, F., & Kyser, K. The isotopic composition of the elements. In F. Vanhaecke & P. Degryse (Eds.), Isotopic analysis: fundamentals and applications using ICP-MS, *Weinheim, Germany: Wiley-VCH* 1–29 (2012).
8. Vanhaecke, F., Balcaen, L. & Malinovsky, D. Use of single-collector and multi-collector ICP-mass spectrometry for isotopic analysis. *Journal of Analytical Atomic Spectrometry* **24**, 863 (2009).
9. Yang, L. Accurate and precise determination of isotopic ratios by MC-ICP-MS: A review. *Mass Spectrometry Reviews* **28**, 990-1011 (2009).
10. Arnold, T. *et al*. Measurement of zinc stable isotope ratios in biogeochemical matrices by double-spike MC-ICPMS and determination of the isotope ratio pool available for plants from soil. *Analytical and Bioanalytical Chemistry* **398**, 3115-3125 (2010).
11. Moore, R. E. T., Larner, F., Coles, B. J. & Rehkämper, M. High Precision Zinc Stable Isotope Measurement of Certified Biological Reference Materials Using the Double Spike Technique and Multiple Collector-ICP-MS. *Analytical and Bioanalytical Chemistry* **409**, 2941-2950 (2017).
12. Li, W. *et al*. Environmental applications of metal stable isotopes: Silver, mercury and zinc. *Environmental Pollution* **252**, 1344-1356 (2019).
13. Murphy, K., Rehkämper, M., Kreissig, K., Coles, B. & van de Flierdt, T. Improvements in Cd stable isotope analysis achieved through use of liquid–liquid extraction to remove organic residues from Cd separates obtained by extraction chromatography. *Journal of Analytical Atomic Spectrometry* **31**, 319-327 (2016).

14. Maréchal, C.N., Télouk, P. & Albarède, F. (1999) Precise analysis of copper and zinc isotopic compositions by plasma-source mass spectrometry. *Chemical Geology* **156(1)**, 251–273.

15. Makishima, A. & Nakamura, E. Low-blank chemistry for Zn stable isotope ratio determination using extraction chromatographic resin and double spike-multiple collector-ICP-MS. *Journal of Analytical Atomic Spectrometry* **28**, 127-133 (2012).

16. Amet, Q. & Fitoussi, C. Chemical procedure for Zn purification and double spike method for high precision measurement of Zn isotopes by MC-ICP-MS. *International Journal of Mass Spectrometry* **457**, 116413 (2020).

17. Albarède, F. et al. Precise and accurate isotopic measurements using multiple-collector ICPMS. *Geochim Cosmochim Acta,* **68**, 2725–2744 (2004).

18. Wei, R. *et al*. An analytical method for precise determination of the cadmium isotopic composition in plant samples using multiple collector inductively coupled plasma mass spectrometry. *Analytical Methods* **7**, 2479-2487 (2015).

19. Rudge, J. F., Reynolds, B. C. & Bourdon, B. The double spike toolbox. *Chemical Geology* **265**, 420-431 (2009).

Chapter 3

Background on cadmium and zinc in vascular plant-soil systems

3.1. Chapter Overview

This Chapter aims to provide a brief overview of Zn and Cd in vascular plant-soil systems. In particular, this Chapter will focus on five key areas relevant to this Ph.D. thesis: (1) background on Zn and Cd in minerals, soils, and soil solutions; (2) basic Zn and Cd soil and aqueous chemistry; (3) background on Zn and Cd uptake and transport in vascular plants; (4) brief overview of Cd and Zn isotope studies in soils and vascular plants; and (5) brief overview of Cd, Zn and other relevant elements in cacao plants.

3.2. Background on Zn and Cd in minerals, soils and soil solutions

This section will focus on providing a general background introduction of Zn and Cd distribution in primary and secondary (soil) minerals and their concentrations in soil and aqueous (soil) solutions.

3.2.1. Zinc and Cd formation in primary and secondary (soil) minerals

The chemical process that underlies the occurrence of trace elements, notably Cd and Zn, in primary and secondary minerals and in soil humus is coprecipitation. Coprecipitation is the result of the simultaneous precipitation of a particular element with another element by physico-chemical mechanism(s) at a specific rate(s). One broad type of coprecipitation is adsorption which is discussed throughout this section and subsequent sections of this Chapter [1].

Cadmium and Zn are both naturally present in the earth's crust and coprecipitate as part of primary minerals formed in the parent material. Zinc is largely present in Zn-rich ores, such as Zn

sulfide (sphalerite or wurtzite) and Zn carbonates (smithsonite) or Zn silicates (hemimorphite) [1, 2]. In contrast, there are only a few naturally occurring Cd-specific minerals in the environment such as Cd sulfides (greenockite) and Cd carbonates (otavite) [3, 4]. In nature, Cd is more often a substitute for other divalent cations such as Ca, Fe, Zn, Pb, and Co in different minerals, due primarily to having a similar ionic radius as these elements. In particular, Cd often substitutes Zn in sphalerite or smithsonite [1, 3, 4]. As such, given its substitution abilities, Cd more commonly occurs in Zn minerals (i.e. Zn blende ore), with a typical Cd:Zn mass ratios of 1:200 [3]. Cadmium is also readily present in other ores such as phosphate ores [4].

Trace elements coprecipitated with secondary (soil) minerals are formed through physico-chemical mechanisms (e.g., weathering, leaching) that breakdown the parent material(s) [1]. For example, Cd and Zn (alongside numerous other elements) coprecipitate with Fe and Al oxides (Table 3.1) [1, 2, 3]. In addition, organic matter such as humic substances, which are dark, microbially transformed organic materials present at different horizons of the soil, coprecipitate with an assortment of elements such as Zn and Cd (Table 3.1). The two most common humic substances are humic acid ($C_{185}H_{191}O_{90}N_{10}S$) and fulvic acid ($C_{186}H_{245}O_{142}N_9S_2$) [1].

Table 3.1 Trace elements coprecipitated with secondary (soil) minerals and soil humus, adapted from Sposito [1].

Solid	Coprecipitated trace elements
Fe and Al oxides	B,P,Ti,V,Cr,Mn,Co,Ni,Cu,Zn,Mo,As,Se,Cd,Pb
Mn oxides	P, Fe, Co, Ni, Cu, Zn, Mo, As, Se, Cd, Pb
Ca carbonates	P,V,Mn,Fe,Co,Cd,Pb
Illites	B,V,Ni,Co,Cr,Cu,Zn,Mo,As,Se,Pb
Smectites	B,Ti,V,Cr,Mn,Fe,Co,Ni,Cu,Zn,Pb
Humus	B,Al,V,Cr,Mn,Fe,Ni,Cu,Zn,Se,Cd,Pb

3.2.2. Zinc and Cd concentrations in soils and aqueous (soil) solutions

The presence of Zn and Cd in soils is highly dependent on the composition of the parent material, and the physico-chemical mechanism(s) (e.g., weathering, leaching) that break down the parent material(s) [1, 2, 3]. Further, additional Zn and/or Cd can be added to soils above the natural background levels through contributions from human activities (e.g., mining, agriculture). The average global Zn and Cd concentrations in uncontaminated soils are between 50 to 55 mg kg^{-1} and 0.2 to 0.36 mg kg^{-1}, respectively, though soil concentrations vary widely between continents, countries, and soil types [2, 3, 4].

In Chapter 5 of this Ph.D. thesis, soils are sampled from Ecuador, and in particular Ecuadorian cacao farms. The average total Zn and Cd concentrations in bulk topsoils (0-20 cm) that have been previously reported for Ecuadorian cacao farms are between 24 to 404 mg kg^{-1} and 0.02 to 10 mg kg^{-1}, respectively (Table 3.2) [5,6,7,8]. The soils from the cacao farms are predominately circumneutral or acidic, depending on sampling location within Ecuador (Table 3.2; pH = 4 to 8) [5,6,7,8]. Based on reported values, the total Cd and Zn concentrations in Ecuador largely exceed the global averages for both elements.

Table 3.2. Soil pH and total Cd and Zn concentrations (mg kg^{-1}) for topsoils for Ecuadorian cacao farms.

Soil depth (cm)	Soil pH	Cd concentration (mg kg^{-1})	Zn concentration (mg kg^{-1})	Reference
0-20	4.3-6.0	0.052-0.47	53.8-106.1	Barraza et al. [5]
0-20	4.2-8.0	0.19-1.02	-	Barraza et al. [6]
5-15	5.5- 7.9	0.52-2.39	-	Chavez et al. [7]
5- 15	4.1–7.9	0.02–10.4	24.5-404.0	Argüello et al. [8]

In pH neutral soil solutions. global average Zn and Cd concentration ranges are estimated to be between 0.005 to 5 mg L^{-1} and 0.1 to 5 μg L^{-1}, respectively [3,4]. There are no studies that have empirically quantified both Cd and Zn concentrations in soil solutions, namely porewater, from Ecuadorian cacao farm soils. A few studies have attempted to examine the bioavailable portion, or the readily accessed (and acidified portion) of the soil by plants (i.e. rhizosphere), through soil leachate extraction [7,9]. Though not a direct comparison, the estimated global average Cd concentration in soil solutions (0.1 to 5 μg L^{-1}) are substantially less than concentrations reported for bioavailable pools from Ecuadorian cacao farms. For instance, previous studies reported for bioavailable pools from Ecuadorian cacao farms, represented by soil leachates extracted from bulk soils (5-15cm) using Mehlich-3 values of between 10 to 1000 μg L^{-1} [7]. This observed higher Cd concentrations are plausible for bioavailable pools on Ecuadorian cacao farms, as the total Cd soil concentrations on the Ecuadorian cacao farms (0.02 to 10 mg kg^{-1}) are orders of magnitude higher than the global average, total Cd concentration in soils (0.2 to 0.36 mg kg^{-1}). Previous studies have noted that soils in South American countries such as Ecuador are naturally rich in Cd, as compared to many other geographical areas on Earth [4,8,9]. In addition, anthropogenic sources could contribute to observed higher Cd concentrations in soils (and bioavailable pools) on Ecuadorian cacao farms such as from the use of contaminated irrigation water by mining activities and phosphate fertilisers [9]. Thus, the observed higher Cd concentrations in soils and bioavailable pools from Ecuadorian cacao farms, are likely due to either geogenic or anthropogenic sources or a combination of both. Previous studies have not previously investigated Zn concentrations in the bioavailable pool on Ecuadorian cacao farms. As a result, a comparison between Zn and Cd on Ecuadorian cacao farms cannot be made due to limited past research.

3.3. Zn and Cd soil and aqueous chemistry

In this section, there will be a brief overview of the Zn and Cd soil and aqueous chemistry responsible for the observed Zn and Cd distributions in the secondary (soil) minerals and concentrations in soil and aqueous (soil) solutions. In particular, this section will discuss why Zn and Cd are *largely* 'chemical analogues' of one another [10].

3.3.1. Characteristics defining Zn and Cd solubility in soils

Two important characteristics help define metal elements and their biogeochemical behaviours in soils and aqueous (soil) solutions: (1) ionic potential and (2) polarizability [1,10]. Together, alongside pH, these two characteristics of metal ions help to understand the behaviour of these ions in terms of their solubility and complexation formation [1].

The first important characteristic is ionic potential (IP), which refers to the valence of a metal cation divided by its ionic radius in nanometers (nm). The ionic potential indicates how strongly, or weakly a given ion will be electrostatically attracted to another ion of the opposite charge, and to what extent it will repel other ions of the same charge. Ionic potential helps to estimate a metal ion's tendency towards forming an ionic bond. Notably, metal cations with IP < 30 nm^{-1} are usually found in circumneutral aqueous solutions (pH ~6.5 and ~7.5) as solvated chemical species or free cations rarely ionically bound to other species [1, 2, 3]. Both Zn and Cd have +II oxidation states in soil and soil solutions, with low IP values of 27 nm and 21 nm, respectively [1, 2, 3]. In circumneutral or acidic soils (pH<7.5), the *principal* or primary metal

species for Zn(II) and Cd(II) in aqueous (soil) solutions are Zn^{2+} and $Cd^{2+}$and $CdCl^{+}$, respectively. In alkaline soils (pH>7.5), *principal* metal species for Zn(II) and Cd(II) in aqueous (soil) solutions are usually Zn^{2+}, $ZnHCO_3^{+}$ and/or Zn-organic complexes, and Cd^{2+}, $CdCl^{+}$ and $CdHCO_3^{+}$, respectively [1, 11]. Typically, in alkaline soils, Zn^{2+} and Cd^{2+} ions bind with small organic ligands (i.e. citrates) and inorganic ligands (i.e. bicarbonates) in the soil solutions [2,3,4,11].

The second important characteristic defining metal elements is their polarizability or "Class A" vs "Class B" behaviours. A metal cation is classified as Class A if it has (1) low polarizability and (2) can readily form stronger complexes with O-containing donor ligands (e.g., carboxylate, phosphate or water molecules) than with N- or S-containing donor ligands (e.g., amines or thiols). Polarizability is a measure of how easily electrons in an ion can be pulled away from its nucleus. In contrast, a metal cation is classified as Class B if it has (1) high polarizability and (2) can form stronger bonds with N- or S-containing donor ligands than with O-containing donor ligands. A metal cation is considered *borderline,* if it is neither Class A nor Class B [1, 10]. Cadmium is considered to be a Class B metal, whereas Zn is considered to be *borderline*, and is capable of behaving as Class A or Class B, depending on its valence and local bonding environment (i.e. its stereochemistry) [1,3,10]. It is important to note that Class A metals tend to form stronger hydrophilic (water-loving) complexes with ligands in aqueous (soil) solutions through ionic or electrostatic bonding, whilst Class B metals usually form strong *lipophilic* (fat-loving) complexes with ligands in aqueous (soil) solutions through covalent bonding [1]. Moreover, Class B metal cations such as Cd are usually less soluble and more resistant to dissociation in aqueous (soil) solutions than Class A metal cations. As a *borderline* metal cation, Zn is capable of being either

soluble or insoluble depending on its bonding environment. As such, Zn can behave similarly or identically to Cd contingent on its local bonding environment.

Together, both characteristics demonstrate that Zn can behave like Cd, depending on its bonding environment. Furthermore, in instances these elements solvate into aqueous (soil) solution, notably in circumneutral or acidic soils, they are present largely as free cations [1, 2, 3].

3.3.2. Understanding Zn and Cd adsorption in soils

Coprecipitation through adsorption or ligand exchange (or 'inner sphere' complexes) can contribute to the reduction of trace elements present in aqueous (soil) solutions. Clay minerals, soil organic matter and oxyhydroxides of Fe, Al and Mn are the three primary Cd and Zn adsorbents in soils. Through adsorbing Cd^{2+} and Zn^{2+} ions onto the surface of these minerals and soil organic matter, there is a reduction of free cations in aqueous (soil) solutions [1, 2, 3].

During adsorption, protons (H^+) are the main competing cations for Zn^{2+} and Cd^{2+} sorption sites on soil organic matter or oxyhydroxides because Zn^{2+} and Cd^{2+} binds to the surface of O atoms of hydroxyl groups of organic matter or oxyhydroxides through ligand exchange [2, 3, 4]. A general, simplified sorption equation can be used for both Zn and Cd [2, 3]:

$$S\text{-}OH + Zn^{2+} \leftrightarrow S\text{-}OZn^{+} + H^{+} \qquad \text{(Equation 3.1)}$$

$$S\text{-}OH + Cd^{2+} \leftrightarrow S\text{-}OCd^{+} + H^{+} \qquad \text{(Equation 3.2)}$$

with S-OH a surface hydroxyl group of soil organic matter or oxyhydroxides. These equations predict that increasing the H^+ ion concentration, decreases sorption sites drastically for free cations, such as Zn^{2+} and Cd^{2+} ions. A reduction of adsorption to the sorption sites in soils for Zn and Cd results in increased Zn^{2+} and Cd^{2+} ions in aqueous (soil) solutions. Alternatively, decreasing H^+ ion concentrations, increases the sorption sites drastically for free cations, Zn^{2+} and Cd^{2+} ions. As such, the increased adsorption of Zn and Cd to various components in soils results in a reduction of Zn^{2+} and Cd^{2+} ions in aqueous (soil) solutions. Furthermore, these adsorption reactions, shown through equations 3.1 and 3.2, are usually (weakly) selective, reversible and pH dependent [2,3]. In particular, as previously discussed with changing H^+ concentrations, Cd and Zn adsorption increases with increasing soil pH, and desorption increases with decreasing soil pH [1, 2, 3, 10]. Additionally, between soil pH of 3 to 8, some degree of adsorption occurs for Cd^{2+} and Zn^{2+} ions in soils, either with soil organic matter, clay minerals and/or oxyhydroxides [4]. For example, speciation modelling has shown that at a lower soil pH (<6.5), the majority of Cd^{2+} and Zn^{2+} ions (~40% to ~70%) of the total adsorbed Zn and Cd present in soils were preferentially bound to organic matter. In contrast, at a higher pH (>6.5) oxyhydroxides, notably Fe-oxides, become the primary and most important adsorptive constituent, with ~80% to ~100% of total adsorbed Cd and Zn being bound to Fe-oxides in soils [3, 12]. Depending on soil type and type of organic matter, soil pH influences strongly both the level of metal adsorption occurring and the type of constituent that both Cd and Zn are preferentially adsorbing to in soils. Thus, these two elements, largely share similar adsorption preferences, chemical behaviours and distributions in soils.

3.4. Background on Cd and Zn uptake and transport in plants

This section will focus on understanding how the presence of both Zn and Cd in a nutrient medium (e.g., soils and hydroponics) influences the uptake and translocation of these elements in vascular plant species, in particular edible fruit trees and food crops. Previous investigations have suggested that Cd competes with essential micronutrients such as Fe, Mn, Cu and Zn for the same membrane transport protein(s) [13,14], and that the application of these essential micronutrients to nutrient mediums may help decrease the uptake and translocation of Cd across plant organs, in particular the roots, stems and leaves [13,14,15,16,17]. Current studies have been examining how the application of Zn can be used to effectively reduce the uptake and translocation of Cd in plant species [13,14,16,17,18,19,20,21]. However, previous studies demonstrate that the ability of Zn to either inhibit or promote the uptake, translocation and accumulation of Cd in plants is a multifaceted and interconnected phenomenon that is dependent on (i) the doses and concentrations of Cd and Zn [13,14,16,17,18,19,20,21], (ii) the timing and duration of exposure [21,22], and (iii) the plant species and genotype [19, 23, 24]. At present, however, the focus of the current body of research has largely been on understanding how differing concentrations of Zn impact the uptake and translocation of Cd in plants, which is further explored and discussed in the sections below.

3.4.1. Uptake of Zn and Cd in plants

Depending on its concentration, Zn can act antagonistically or synergistically to increase or decrease the uptake of Cd in plants [18]. Antagonism occurs when the addition of one element decreases the level of another element, and synergism occurs when the addition of one element increases the level of another element [15]. Several studies found that when higher concentrations

of Zn are applied to nutrient mediums (e.g., hydroponic solutions and soils) of Cd stressed plants, there is an antagonistic effect in which Zn reduces the uptake of Cd in plants [13, 14, 17, 19, 20, 21]. Sharma & Agrawal [13], for instance, determined in their study examining the uptake and accumulation of Cd and Zn in carrots that a higher concentration of Zn (300 μg mL^{-1}) combined with Cd (100 μg mL^{-1}) resulted in a lower uptake (3.98 μg $g^{-1}d^{-1}$) of Cd in carrots compared to lower concentration of Zn (100 μg mL^{-1}) combined with Cd (10 μg mL^{-1}) in carrots (4.30 μg $g^{-1}d^{-1}$). Green et al. [15] determined in their study that unless extremely high and toxic concentrations of Zn (31μM Zn) were added to Cd stressed rice, there were no significant reductions in Cd uptake. However, Nan et al. [25] found, in their study examining Cd and Zn uptake and translocation in soil-wheat and -corn systems under actual field conditions, that higher concentrations of Zn (227 and 235 mg kg^{-1} DW) worked synergistically with Cd (10.11 and 10.36 mg kg^{-1} DW) to increase the uptake of Cd in both wheat and corn. Studies also found that in Cd stressed plants, adding low concentrations of Zn to the nutrient medium, further increases the uptake of Cd in these plants [13,19]. Moreover, there are mixed and conflicting findings on how the application of Zn to nutrient mediums cause either an increase or decrease in the uptake of Cd in plants.

There are still significant gaps in understanding how different concentrations of both Zn and Cd influence the uptake of these metals in vascular plant species, notably edible fruit trees and food crops. At the same time, the mixed and conflicting findings could reflect different experimental conditions and differences in physiological mechanisms across plant species and genotypes that are resulting in the observed differences in the uptake of these metals.

3.4.2. Translocation of Zn and Cd in plants

Most studies have found that independent of the concentration of Zn added to nutrient mediums of Cd stressed plants, namely edible fruit trees and food crops such as carrots, cacao, rice and wheat, the root tissues *usually* store the highest concentrations of Cd followed by stem tissues then leaf tissues [13,14,15,16,18,19,20, 21, 22]. It is suggested as Cd enters plant root cells, as part of an internal tolerance strategy to cope with trace toxic heavy metals, the plant's root system either precipitates and/or adsorbs Cd to the cell wall (i.e. apoplast), or within the symplast of a root cell (i.e. the cytoplasm), or it further sequesters and immobilises Cd in the organelles (i.e. vacuole) of a root cell. Thus, preventing Cd from leaving the root cells and being translocated to aerial plant organs (i.e. stem and leaves) [17, 19, 20, 26, 27].

Aside from the internal tolerance strategies employed by plant species to prevent Cd from leaving its root tissues, the specific underlying mechanisms for how plant species prevent Cd translocation to stem and leaf tissues in the presence of Zn are not well understood [17, 22]. It is believed that since Zn plays a crucial role in multiple enzyme reactions to maintain stem and leaf tissue growth, and Cd as a non-essential element does not play a crucial role, Zn is preferentially transferred to aerial plant organs. That is to say, once Cd is in the plant root cells and is mobile, a series of complex membrane transport proteins preferentially select and load Zn over Cd onto the xylem (which carries nutrients and water upwards from the roots to the stems and leaves), and thus preventing the mobile Cd from reaching the stem and leaf tissues [17,27,28]. With that said, certain studies have found results to suggest that when higher concentrations of Zn are added to nutrient mediums, although the overall amount of Cd taken up by the whole plant decreases, the fraction of Cd increases in the stem and leaf tissues [16, 21, 29]. For example, in their study on

adding Zn to regulate the uptake of Cd in four rice genotypes, Cai et al. [21] found that although the total Cd taken up decreased with higher Zn concentrations in the four rice genotypes, the transfer fraction of Cd from root tissues to stem and leaf tissues increased. The authors noted that the underlying physiological mechanisms for this phenomenon, in which increased amounts of Cd are translocated to stem and leaf tissues from the roots in the presence of high Zn concentrations are still not well understood, and that further scientific investigations are required to understand this phenomenon [21]. Moreover, there are still gaps in understanding how plant species translocate Cd and Zn to their different organs, and how different concentrations of these metals influence underlying physiological mechanisms responsible for translocation.

3.5. Overview of the biochemical, molecular, and physiological mechanisms for regulating Zn and Cd in plants

The prolonged exposure to toxic heavy metals such as Cd (or Zn at elevated concentrations) of a plant cell results in DNA and RNA degradation, ion leakage, cell membrane damage, and eventually cell death [20, 27]. Therefore, in the presence of trace heavy metals, notably toxic heavy metals, plants have developed two primary strategies to resist or cope with these metals: (1) the excluder strategy and (2) the tolerance strategy [20,27,28]. As part of these two strategies, plants employ one or more mechanisms to limit or tolerate trace heavy metals. For the excluder strategy, plants either decrease soil metal bioavailability or control metal influx [27, 28]. In the tolerance strategy, plants either promote metal efflux or sequester and immobilise metals [20,27,28]. Regardless of the strategy the plant uses to limit the adverse impacts from excess trace heavy metals, the plant's response also needs to ensure that there is homeostasis of essential micronutrient

elements. The strategies used by the plants are dependent on the specific trace heavy metal and the plant species [27].

3.5.1. *Excluder strategy*

The first line of defence for most plant species in soils with unusually high concentrations of Cd or Zn is to employ the excluder strategy [27]. This strategy tries to limit trace heavy metals from entering the plant's roots and to keep their concentrations in the roots low, despite elevated trace heavy metals concentrations in the soil. The plant implements the excluder strategy primarily through either reducing soil metal bioavailability or reducing the expression of metal membrane transport proteins responsible for metal uptake [27].

3.5.1.1. Reducing soil metal bioavailability

Soil metal bioavailability determines how readily metals are accessible for uptake by plants, and it is predominately determined by the rhizosphere, the soil area surrounding a plant's roots [27,30]. The rhizosphere includes a set of soil microorganisms and microbes that can regulate metal availability, solubility, mobility, and precipitation through changing soil pH and by secreting metal chelators [27,30,31]. Certain rhizosphere microorganisms, such as mycorrhiza fungi, can work symbiotically with plants to decrease metal solubility and availability in the soil, through processes such as biosorption, extracellular sequestration, bioprecipitation and selective chelation [27, 32]. In the rhizosphere, plant root cells can also actively or passively excrete compounds (e.g., amino acids, organic acids, sugars, phenolics, polysaccharides and proteins), known as root exudates [27]. Root exudates, through metal chelation and complexation, can form complexes with Cd or Zn in the rhizosphere to prevent these metals from entering the plant's root cells, or root

exudates can enhance soil metal availability and uptake through the acidification of the rhizosphere and reducing these elements [27].

3.5.1.2. Controlling of metal influx

Trace heavy metals can enter the plant root cell's symplast through three primary ways: (1) simple diffusion, (2) passive transport via channel proteins, and (3) active transport via carrier proteins [27, 33, 34, 35]. For regulating the influx of metals, notably toxic metals, active transport via carrier proteins (also known as transport carrier proteins) play a crucial role [27, 34, 35, 36]. These transport carrier proteins have different levels of affinity for different metals, which allows them to discriminate at the root cell's plasma membrane between essential micronutrients and non-essential elements [27]. When plants restrict the excessive uptake and influx of a specific metal, they downregulate relevant transport carrier proteins to restrict them from taking up the specific metal [27, 34, 35, 36]. It is believed, for example, that Cd and Zn, notably as free ions, are crossing the root cell's plasma membrane via a set of different transport carrier proteins such as Zn- and Iron- regulated transporter-like proteins (ZIP), Zn^{2+} transporter (ZNT1), iron-regulated transporter 1 (IRT1) and natural resistance-associated macrophage protein 1 and 5 (NRAMP1, NRAMP5) [27, 34, 36]. Therefore, a plant's root cell can, in part, regulate the excessive uptake of Cd or Zn in contaminated soils via transport carrier proteins such as ZIP [19, 24, 27, 34, 36]. When there is too much Cd and Zn present, the plant can signal to these transport carrier proteins to restrict the uptake of these metals [24, 27, 34, 36].

3.5.2. Tolerance strategy

When soils are highly contaminated with trace heavy metals, notably toxic metals, and it is not possible to exclude these metals from the plant's roots due to high concentration levels in the soil, the tolerance strategy is employed by plants [27]. The tolerance strategy tries to cope with metals by having plant root cell's either efflux the metals or to immobilise and sequester them in a controlled manner [20, 27].

3.5.2.1. Promoting metal efflux

One way in which plants try to handle the high amounts of metals entering their root cells is to try to efflux or extrude these metals from inside of the cells. This process is known as metal efflux [17, 27]. Through promoting metal efflux, metals can either be returned into the soil of the rhizosphere by root efflux transport carrier proteins or be loaded into the xylem and translocated to aerial organ tissues [17, 27]. The direction of whether metals are extruded from a plant's root cell or are translocated to and accumulated in other plant organ tissues, depends on the plant species' genotype [27]. Plant species known as metal-tolerant hyperaccumulators, have metal accumulation genotypes that allow them to store metals, and therefore their efflux system directs the metals, in particular free ions, to be translocated to other plant organ tissues via the xylem, notably the leaves. Plant species with non-metal accumulation genotypes, known as metal-intolerant, non-hyperaccumulators, usually expel the metals into the soils via root efflux transport carrier proteins [27].

Plants also have transport carrier proteins for metals, such as Zn, that help to ensure Zn homeostasis. An important Zn transport carrier protein is from the P1B-type ATPase family,

known as Heavy Metal ATPase 4 or HMA4, which is responsible for loading Zn into the xylem [17, 27, 28, 36]. It is implied that, in plants, Cd uses transport carrier proteins that have higher affinities for other essential elements. Thus, during transport, Cd likely accompanies other essential elements such as Zn by using their specific transport carrier proteins such as NRAMP3 and NRAMP4 [27].

3.5.2.2. Sequestering and immobilising metals

If a plant root cell is unable to prevent entry or efflux of a trace heavy metal, the cell will have to allow symplastic entry of the metal [27]. Said another way, the plant root cell will have to allow the metal(s) to enter the cell and it will have to sequester the metal in a non-detrimental site in the cell such as in specific organelles or storage tissues [27, 35]. Once metals get past the plasma membrane of a plant's root cell, largely as free ions, they first need to be chelated by different ligands (i.e., oligopeptides, organic acids, amino acids, or proteins), forming a metal–ligand complex, to decrease any adverse interactions with other cellular compounds [17, 21, 27, 34, 35, 36, 37]. Common Zn and Cd ligand chelators are nicotianamine (NA), which forms Zn-nicotianamine (Zn-NA) complexes, and metallothioneins (Mt) or phytochelatins (PCs), which form Mt-Cd or PC-Cd complexes, respectively [21, 27, 33, 34, 35, 36, 37]. Once metal-ligand complexes such as PC-Cd are formed, the root cell either sequesters them in vacuoles or it confines and immobilises them in the cell's root wall (i.e., apoplast) [19,27]. There are a series of transport carrier proteins involved in the sequestration and immobilisation of Zn and Cd in root cells. For example, metal tolerance protein 1 (MTP1) is an important Zn vacuolar sequestration transport carrier protein in plants [27, 34, 36, 37,38]. ATP-binding cassette (ABC) transporters 1 and 2

(ABCC1, ABCC2) and Heavy metal ATPase 3 (HMA3) are both hypothesized Cd vacuolar sequestration transport carrier protein in plant species [27, 39].

If toxic heavy metals are translocated from root to aerial plant organ tissues, via xylem, the metals are usually sequestrated and immobilised in photosynthetically inactive tissues, such as the epidermis, or in storage tissues, such as the trichomes, bark and old leaves. It should be noted that metal-intolerant, non-hyperaccumulator plant species generally tend to sequester toxic heavy metals in their root cells' vacuoles, preventing them from translocating to photosynthetic active tissues where these metals could be more detrimental than in the plant's roots. On the other hand, metal-tolerant, hyperaccumulator plant species that have a greater ability to sequester toxic heavy metals in stem and leaf tissues generally tend to reduce their root vacuolar sequestration and store metals in aerial plant organs [27].

3.6.Application of stable isotope analyses to vascular plant systems

Stable isotope compositions of individual plant organs provide insight into the physiological processes that control a given element's journey from its 'source' (e.g., soil, soil solution) to different 'sinks' or plant organs (i.e., roots, stems, leaves, fruit/seeds) [33, 40]. Furthermore, stable isotope fractionation is the partitioning of stable isotopes between two chemical species or physical phases, which is due to either the separation of isotopes in equilibrium systems (i.e., equilibrium isotope fractionation) or during rate-controlled (bio)chemical or physical processes such as biological metabolism or diffusion occurring in soil solutions (i.e. kinetic isotope fractionation) [40, 41]. In plant systems, physiological processes that can lead to stable isotope fractionation include root uptake, short- and long- distance transport, storage, metabolic

functionalisation, compartmentalisation, and remobilisation, which are largely regulated by physico-chemical processes such as water mass flow, sorption, ligand exchange, redox changes, precipitation, dissolution, and diffusion [30,40]. Additionally, stable isotope compositions can be used to define the primary binding forms for the metals that have entered vascular plants, and stable isotope compositions of different metals in the same plant sample can provide information on competitive interactions among metals having similar physico-chemical properties [30]. Similarly, in soil systems, chemical and physical processes can also lead to stable isotope fractionation such as evaporation/condensation, dissolution/precipitation, redox processes, adsorption/desorption, and biological cycling [41]. These processes subsequently influence the chemical speciation of a metal that is taken up by a vascular plant [30].

In this Ph.D. thesis, Chapter 4 applies stable isotope analyses to understand how Cd availability can influence how chemically similar Zn is taken up by plants and translocated to aerial plant organs in different cacao cultivars. Further, no previous reviews have critically examined exclusively the relationship between Zn and Cd stable isotope fractionation in vascular plant systems. An in-depth examination of Zn and Cd stable isotope fractionation in vascular plant systems is discussed in Chapter 6 of this Ph.D. thesis.

3.7. Elements in cacao plants

This section will outline Cd and other element concentrations observed in cacao plants. Furthermore, existing research and knowledge gaps for the uptake and transport of metals in cacao-soil systems are briefly discussed.

3.7.1. *Cd concentrations in cacao*

With the exception of Engbersen et al. [42], no other studies have attempted to examine Cd concentrations of all different plant parts encompassing a mature cacao system: roots, branches/stems/scions, bark, leaf, and entire fruit (i.e., pod husk, mucilage and beans). In fact, most studies have predominately examined Cd concentrations in the leaves and fruit of the cacao tree exclusively (Table 3.3) [6,8,943,44,45,46,47,48,49,50,51,52]. For example, Cd concentrations in leaves, pod husk, mucilage and bean range from 0.02 to 8.1 mg kg^{-1}, respectively. As such, the limited information and research available on the full cacao system has directly influenced the understanding of the uptake and transport of Cd.

Table 3.3. Summary of Cd concentrations (mg kg^{-1}) for different cacao plant tissues.

Cd concentration (mg kg^{-1})					Reference
Bean	**Pod husk**	**Leaves**	**Bark/branch/scion**	**Root/rootstock**	
0.03-7.1	0.1-10.2	0.1-28.0	-	-	Gramlich et al. [43]
0.09-3.51	0.08- 4.09	0.19-7.87	-	-	Barraza et al. [6]
1.26-3.92	0.99-2.14	1.95-3.63			Barraza et al. [44]
2.05	2.76	1.75-3.49	6.12	3.21	Blommaert et al. [45]
0.08-1.45	-	-	-	-	Gil et al. [46]
0.17-1.78	-	-	-	-	Arévalo-Gardini et al. [47]
1.89 - 3.46	1.99-3.72	2.19-2.85	2.21-6.34	2.31-4.27	Engbersen et al. [42]
0.03- 10.4	-	-	-	-	Argüello et al., 2019
0.02 - 3.00	-	-	-	-	Chavez et al. [9]
0.99	-	2.15	-	-	Lewis et al. [51]
0.544-1.388	-	-	-	-	Bertoldi et al. [49]
0.267-1.715	-	-	-	-	Romero-Estévez et al. [50]
0.18-0.23	0.38-0.73	0.78-0.99	-	-	Gramlich et al. [52]
-	-	0.4-8.08	-	0.03-8.95	Oliva et al. [48]

3.7.2. Cd uptake and transport in cacao

At present, there are still many knowledge and research gaps in understanding the uptake and translocation of Cd in cacao trees. For root uptake, it is suggested that Cd likely enters the

cacao root system as free Cd^{2+} ions via transport carrier proteins. After entering the root system, free Cd^{2+} ions can be chelated with donor ligands of different molecules to produce Cd-ligand complexes. In Cd-ligand complexes, the precise ligands responsible for the chelation of Cd in cacao remains unknown [53]. A portion of free Cd^{2+} ions and/or Cd-ligand complexes are likely transported into root cells' vacuoles for sequestration, to reduce the mobility and possible harmful effects of Cd to aerial cacao organs. The precise transport carrier proteins responsible for vacuolar sequestration in cacao, and notably cacao root cells, remains largely unknown. In the root, available free Cd^{2+} ions and possibly Cd-complexes in the cytosol are usually transported radially across the root cell and loaded onto the xylem, most likely via transporter carrier proteins. Subsequently, after loading of Cd onto the xylem, there is long-distance transport of Cd via xylem-phloem transfer into aerial cacao organs. However, the precise pathway and mechanisms responsible for transport from root-to-shoot, and more specifically to fruit, remains not well understood [53].

3.7.3. Other element uptake and transport in cacao

Almost all previous studies have exclusively reported elemental concentrations of other trace elements such as Zn, Fe, and Mn (Table 3.4) [43,47,49,50,51,52,54], without fully examining existing relationships between these elements. Previous examinations have largely focused on employing correlations to understand possible shared relationships between elements across different cacao plant organs. Furthermore, previous studies largely looked at aerial cacao organs, notably leaves and beans. As such, there is limited understanding of whether other trace and major elements share similar nutrient pathways and mechanisms as Cd, or how these elements are transported throughout the entire mature cacao tree. One study by Barraza et al. [54], for example,

suggested there were strong positive correlation between Zn and Cd in the bean and leaves for the CCN-51 cacao variety, respectively, indicating possible shared transport mechanisms within these organs. Thus, at present, no studies have attempted to fully understand the uptake and transport of other elements, notably Zn, and their relationship or possible shared mechanisms with Cd in cacao-soil system. Several proceeding Chapters of this Ph.D. thesis, notably Chapter 4 and 5, aim to address several of the existing knowledge and research gaps that exist for Cd and other metal uptake and translocation in cacao, both in juvenile and mature plants.

Table 3.4. Summary of element concentrations (mg kg^{-1}) for different cacao plant tissues.

Element	Tissue concentration (mg kg^{-1})			References
	Bean	Pod husk	Leaves	
Al	41.1-90.2	-	-	Bertoldi et al. [49]
As	0.039-0.041	-	-	Bertoldi et al. [49]
Co	0.039-0.048	-	-	Bertoldi et al. [49]
Cu	5.6-34.1	3.3-21.1	2.9-23.7	Barraza et al. [54]
	18.8-30.4	-	7.2-10.3	Arévalo-Gardini et al. [47]
	20.1 - 20.8	-	-	Bertoldi et al. [49]
Fe	5- 47	20-269	24 - 444	Gramlich et al. [43]
	34.0-53.6	-	50.5-275.8	Arévalo-Gardini et al. [47]
	65.6-90.4	-		Bertoldi et al. [49]
	221.5-244.7	43.1-57.4	173-274	Gramlich et al. [52]
Mn	10 – 99	5 – 217	12 - 1960	Barraza et al. [54]
	12.3-28.5	-	88.2 - 347.4	Arévalo-Gardini et al. [47]
	51.9	-	832	Lewis et al. [51]
Mo	24.1-24.7	-	-	Bertoldi et al. [49]
	0.06-2.9	0.04-3.1	0.05-8.44	Barraza et al. [54]
Ni	1.0-11.5	0.4-32.3	0.7-40	Barraza et al. [54]
	3.5-9.3	-	2.3-12.2	Arévalo-Gardini et al. [47]
	14	-	36.9	Lewis et al. [51]
	1.46-8.53	-	-	Romero-Estévez et al. [50]
Zn	19-59	21- 136	17 - 381	Gramlich et al. [43]
	46.5-93.8	19.1-91.4	17-263	Barraza et al. [54]
	37.3-59.2	-	43-104	Arévalo-Gardini et al. [47]
	40.6	-	161	Lewis et al. [51]
	41.31-46.6	40.4-45.1	36.9-48.8	Gramlich et al. [52]

3.8. References

1. Sposito, G. The chemistry of Soils. (Ed) *Oxford University Press, Oxford, New York* (2008).
2. Mertens, J., & Smolders, E. Zinc. In: Alloway, B. (Eds) Heavy Metals in Soils: Trace Metals and Metalloids in Soils and Their Bioavailability. Environmental Pollution, *Springer, Dordrecht* **22** (2013).
3. Smolders, E., Mertens, J. (2013). Cadmium. In: Alloway, B. (Eds) Heavy Metals in Soils: Trace Metals and Metalloids in Soils and Their Bioavailability. Environmental Pollution, *Springer, Dordrecht* **22** (2013).
4. Kubier, A., Wilkin, R. T., & Pichler, T. Cadmium in soils and groundwater: A review. *Applied geochemistry: Journal of the International Association of Geochemistry and Cosmochemistry* **108**, 1–16 (2019).
5. Barraza, F. *et al.* Distribution, contents and health risk assessment of metal(loid)s in small-scale farms in the Ecuadorian Amazon: An insight into impacts of oil activities. *The Science of the Total Environment* **622-623**, 106-120 (2018).
6. Barraza, F. *et al*. Cadmium bioaccumulation and gastric bioaccessibility in cacao: A field study in areas impacted by oil activities in Ecuador. *Environmental Pollution* **229**, 950–963 (2017).
7. Chavez, E. *et al.* Chemical speciation of cadmium: An approach to evaluate plant-available cadmium in Ecuadorian soils under cacao production. *Chemosphere* **150**, 57-62 (2016).

8. Argüello, D. *et al.* Soil properties and agronomic factors affecting cadmium concentrations in cacao beans: A nationwide survey in Ecuador. *The Science of the Total Environment* **649**,120–127 (2019).
9. Chavez, E. *et al.* Concentration of cadmium in cacao beans and its relationship with soil cadmium in southern Ecuador. *The Science of the Total Environment* **533**, 205–214 (2015).
10. Stumm, W. & Morgan, J.J. Aquatic Chemistry, Chemical Equilibria and Rates in Natural Waters (Eds), *John Wiley & Sons, Inc., New York* (1996).
11. Khanna, K. *et al.* Agroecotoxicological Aspect of Cd in Soil-Plant System: Uptake, Translocation and Amelioration Strategies. *Environmental Science and Pollution Research International* **29(21)**, 30908–30934 (2022).
12. Buekers, J., Degryse, F., Maes, A., & Smolders, E. Modelling the effects of ageing on Cd, Zn, Ni and Cu solubility in soils using an assemblage model. *European Journal of Soil Science* **59** (2008).
13. Sharma, R. and Agrawal, M. Single and Combined Effects of Cadmium and Zinc on Carrots: Uptake and Bioaccumulation. *Journal of Plant Nutrition* **29(10)**, 1791-1804 (2006).
14. Hart, J., Welch, R., Norvell, W. & Kochian, L. Transport interactions between cadmium and zinc in roots of bread and durum wheat seedlings. *Physiologia Plantarum* **116(1)**, 73-78 (2002).
15. Green, C., Chaney, R. & Bouwkamp, J. Increased zinc supply does not inhibit cadmium accumulation by rice (Oryza sativa L.). *Journal of Plant Nutrition* **40(6)**, 869-877 (2016).

16. Cheng, M. *et al.* Cadmium reduces zinc uptake but enhances its translocation in the cadmium-accumulator, *Carpobrotus rossii,* without affecting speciation. *Plant and Soil* **430(1-2)**, 219-231 (2018).

17. Du, J. *et al.* The presence of zinc reduced cadmium uptake and translocation in Cosmos bipinnatus seedlings under cadmium/zinc combined stress. *Plant Physiology and Biochemistry* **151**, 223-232 (2020).

18. Rizwan, M., Ali, S., Rehman, M., & Maqbool, A. A critical review on the effects of zinc at toxic levels of cadmium in plants. *Environmental Science and Pollution Research International* **26(7)**, 6279–6289 (2019).

19. Sanaeiostovar, A., Khoshgoftarmanesh, A. & Shariatmadari, H. Effects of zinc activity in nutrient solution on uptake, translocation, and root export of cadmium and zinc in three wheat genotypes with different zinc efficiencies. *Soil Science and Plant Nutrition* **57(5)**, 681-690 (2011).

20. dos Santos, M. L. S. *et al.* Mitigation of cadmium toxicity by zinc in juvenile cacao: Physiological, biochemical, molecular and micromorphological responses, *Environmental and Experimental Botany* **179**, 104201 (2020).

21. Cai, Y. *et al.* Mechanisms and uncertainties of Zn supply on regulating rice Cd uptake. *Environmental Pollution* **253**, 959-965 (2019).

22. Tavarez, M., Macri, A. & Sankaran, R. Cadmium and zinc partitioning and accumulation during grain filling in two near isogenic lines of durum wheat. *Plant Physiology and Biochemistry* **97**, 461-469 (2015).

23. Qaswar, M., Hussain, S. & Rengel, Z. Zinc fertilisation increases grain zinc and reduces grain lead and cadmium concentrations more in zinc-biofortified than

standard wheat cultivar. *The Science of The Total Environment* **605-606**, 454-460 (2017).

24. Laporte, M. *et al.* Variability in cadmium and zinc shoot concentration in 14 cultivars of sunflower (Helianthus annuus L.) as related to metal uptake and partitioning. *Environmental and Experimental Botany* **109**, 45-53 (2015).
25. Nan, Z., Li, J., Zhang, J. & Cheng, G. Cadmium and zinc interactions and their transfer in soil-crop system under actual field conditions. *Science of The Total Environment* **285(1-3)**, 187-195 (2002).
26. Wiggenhauser, M. *et al.* isotope fractionation during grain filling of wheat and a comparison of zinc and cadmium isotope ratios in identical soil-plant systems. *The New Phytologist,* **219(1)**, 195– 205 (2018).
27. Lin, Y. & Aarts, M. The molecular mechanism of zinc and cadmium stress response in plants. *Cellular and Molecular Life Sciences* **69(19)**, 3187-3206 (2012).
28. Broadley, M. *et al*. Zinc in plants. *New Phytologist* **173(4)**, 677-702 (2007).
29. Liu, H.J., Zhang, J.L., Christie, P. & Zhang, F.S. Influence of external zinc and phosphorus supply on Cd uptake by rice (Oryza sativa L.) seedlings with root surface iron plaque. *Plant Soil* **300**, 105e115 (2007).
30. von Blanckenburg, F. *et al.* Fractionation of Metal Stable Isotopes by Higher Plants. *Elements* **5(6)**, 375-380 (2009).
31. Schweizer, S. *et al.* Impact of organic and conventional farming systems on wheat grain uptake and soil bioavailability of zinc and cadmium. *Science of The Total Environment* **639**, 608-616 (2018).

32. Haferburg, G. & Kothe E. Microbes and metals: interactions in the environment. *Journal of Basic Microbiology* **47(6)**, 453–467 (2007).

33. Caldelas, C. & Weiss, D. J. Zinc homeostasis and isotopic fractionation in plants: a review. *Plant Soil* **411 (1−2)**, 17−46 (2017).

34. Clemens, S. Toxic metal accumulation, responses to exposure and mechanisms of tolerance in plants. *Biochimie* **88 (11)**, 1707–1719 (2006).

35. Clemens S. Metal ligands in micronutrient acquisition and homeostasis. *Plant,Cell Environment* **42(10)**, 2902–2912 (2019).

36. Clemens S. The cell biology of zinc. *Journal of Experimental Botany* **73(6)**, 1688–1698 (2022).

37. Clemens, S. *et al.* Nicotianamine is a major player in plant Zn homeostasis. *Biometals* **26(4),** 623–632 (2013).

38. Desbrosses-Fonrouge, A.G. *et al.* *Arabidopsis thaliana* MTP1 is a Zn transporter in the vacuolar membrane which mediates Zn detoxification and drives leaf Zn accumulation. *FEBS Letters* **579(19)**, 4165–4174 (2005).

39. Ueno, D. *et al.* Gene limiting cadmium accumulation in rice. *The Proceedings of the National Academy of Science* **107(38)**, 16500–16505 (2010).

40. Wiggenhauser, M. *et al.* Stable Isotope Fractionation of Metals and Metalloids in Plants: A Review. *Frontiers in plant science* **13**, 840941 (2022).

41. Wang, L. *et al.* Possible application of stable isotope compositions for the identification of metal sources in soil. *Journal of Hazardous Materials* **407**, 124812 (2021).

42. Engbersen, N. *et al.* Cadmium accumulation and allocation in different cacao cultivars. *Science of the Total Environment* **678**, 660–670 (2019).

43. Gramlich, A. *et al.* Soil cadmium uptake by cocoa in Honduras. *Science of the Total Environment*, **612**, 370– 378 (2018).

44. Barraza, F. *et al*. Cadmium isotope fractionation in the soil – cacao systems of Ecuador: A pilot field study. *RSC Advances* **58(9)**, 34011-34022 (2019).

45. Blommaert, H. *et al.* From soil to cacao bean: Unravelling the pathways of cadmium translocation in a high Cd accumulating cultivar of *Theobroma cacao* L. *Frontier in Plant Sciences* **13**, 1055912 (2022).

46. Gil, J.P. *et al.* Cadmium distribution in soils, soil litter and cacao beans: a case study from Colombia. *International Journal of Environmental Science and Technology* **19(4),** 2455–2476 (2022).

47. Arévalo-Gardini, E., Arévalo-Hernández, C. O., Baligar, V. C., & He, Z. L. Heavy metal accumulation in leaves and beans of cacao (*Theobroma cacao L.*) in major cacao growing regions in Peru. *The Science of the Total Environment* **605-606**, 792–800 (2017).

48. Oliva, M. *et al.* Cadmium Uptake in Native Cacao Trees in Agricultural Lands of Bagua, Peru. *Agronomy* **10(10)**, 1551 (2020).

49. Bertoldi, D. *et al.* Multielemental fingerprinting and geographic traceability of Theobroma cacao beans and cocoa products. *Food control* **65**, 46–53 (2016).

50. Romero-Estévez, D., Yánez-Jácome, G. S., Simbaña-Farinango, K. & Navarrete, H. Content and the relationship between cadmium, nickel, and lead concentrations in Ecuadorian cocoa beans from nine provinces. *Food Control* **106**, 106750 (2019).

51. Lewis, C., Lennon, A.M., Eudoxie, G. & Umaharan, P. Genetic variation in bioaccumulation and partitioning of cadmium in Theobroma cacao L. *The Science of the Total Environment* **640–641**, 696–703 (2018).

52. Gramlich, A. *et al.* Cadmium uptake by cocoa trees in agroforestry and monoculture systems under conventional and organic management. *The Science of the Total Environment* **580,** 677-686 (2017).

53. Vanderschueren, R. *et al.* Mitigating the level of cadmium in cacao products: Reviewing the transfer of cadmium from soil to chocolate bar. *The Science of the Total Environment* **781**, 146779 (2021).

54. Barraza, F. *et al.* Beyond cadmium accumulation: Distribution of other trace elements in soils and cacao beans in Ecuador. *Environmental Research* **192**, 110241 (2021).

Chapter 4

An investigation of zinc isotope fractionation in cacao (*Theobroma cacao* L.) and a comparison of zinc and cadmium isotope compositions in hydroponic plant systems under high cadmium stress

4.1. Declaration of research contributions

Elnaz Barati (Imperial College London) collected, analysed and interpreted all Zn stable isotope composition and concentration data for cacao and hydroponic solution samples. Professor Jim Dunwell and Dr. Ihsan Ullah (University of Reading) grew and harvested juvenile cacao samples. Dr. Katharina Kreissig and Mr. Barry J. Coles provided technical support and assistance at the MAGIC Laboratories, Imperial College London.

4.2. Introduction

Zinc is one of the most abundant essential micronutrients in organisms, and the only trace metal required for all the six major enzyme classes [1,2]. As a co-factor for over 300 enzymes [3], Zn is involved in enzyme activity regulation, transcriptional and translational control functions, protein-binding, and signal transduction [4,5,6]. Due to it playing a vital role in plant physiology and plant cell growth and development, Zn needs to be maintained at homeostasis in plant cells [4,6]. This process involves Zn concentrations in plant cells being maintained within a narrow and specific range to avoid deficiency or toxicity effects during changing conditions [4,6,7].

Understanding the uptake and translocation of Zn can provide invaluable insights into the physiological mechanisms that are vital for plant growth and development [4,5,6,8]. Previous studies that examined metal hyperaccumulators and metal tolerant plants [9,10,11,12,13,14,15,16,17], fruit, vegetable and cereal crops [18,19,20,21], and other plant species [22,23,24] have shown that stable isotope analyses can provide insight into the mechanisms

employed by plants to regulate the uptake of Zn and its translocation from the roots to the aerial plant organs [25]. Differences in Zn stable isotope compositions between plant species and internal organs occur due to variations in physiological mechanisms that are responsible for the uptake of a metal from its source (e.g., hydroponic solution or soil) and its distribution and accumulation in different plant organs (e.g., roots, stems, leaves and seeds/fruits) [25, 26]. Physiological mechanisms such as root uptake, short- and long-distance transport, metal storage and compartmentalisation, and metabolic functionalisation are controlled by mechanisms such as sorption, ligand exchange, redox changes, precipitation, and diffusion [25]. As such, through stable isotope analyses, inferences can be made about mechanisms, including the primary binding form in which Zn is retained in a particular plant organ [25,26,27]. Most previous studies have shown, for example, that isotopically heavy Zn is retained in plant roots, whilst isotopically light Zn is preferentially translocated to and stored in aerial plant organs [25]. In addition, stable isotope analyses of different metals in plant samples can provide insights into interactions among metals with similar physical and chemical properties [26].

As a trace heavy metals of group 12 of the periodic table, Zn and Cd share similar chemical and physical properties. Due to this similarity, plant species may use similar mechanisms for regulating the uptake and translocation of Zn and Cd [4,7, 31,32, 33]. However, the underlying mechanisms responsible for regulating Zn and Cd in different plant species are not fully understood and it is hence unclear if different plant species share similar uptake and translocation mechanisms [4, 28, 29, 30, 31, 32, 33, 34]. For example, previous studies have shown that the application of Zn to hydroponic solutions or soils can either reduce or increase the uptake and translocation of Cd, depending on the plant species [28, 29,30,31,32,33,34]. In comparison to the

essential micronutrient Zn, Cd is a known enzyme inhibitor in plants, and in plant cells it can cause mitochondrial damage, cell proliferation and cell division inhibition, lipid peroxidation, DNA and RNA degradation, ion leakage and cell membrane damage [4, 33]. Damage to cell organelles in plants is related to exposure to high Cd concentrations (e.g., 50-100 mg kg^{-1}) in nutrient growth media (e.g., hydroponic solutions and soils), but the specific Cd concentration threshold above which damage occurs is highly dependent on the plant species [35]. In humans, progressive accumulation of Cd in the body through long-term exposure to higher Cd levels in air, water, soils, and food can lead to adverse health complications [36,37]. These well-documented complications include permanent damage to the urinary and skeletal systems and various cancers [36].

Irrespective of their age, cacao plants are considered as Cd "accumulators" because they have the capacity to accumulate high amounts of Cd without impacting their growth and development [38, 39, 40, 41, 42]. Barraza et al. [39], for instance, found that banana, pineapple, lemon and soursop grown alongside cacao in Ecuador had fruit with Cd concentrations of up to 0.022 μg g^{-1}, whilst the Cd levels in cacao beans were much higher at between 0.1-1.6 μg g^{-1}. Elsewhere in South and Central America, Cd concentrations of 1 to 10 μg g^{-1} are common for cacao beans [38, 39, 40, 41, 42, 43]. These high Cd concentrations make it increasingly challenging for cacao-based industries to meet the strict Cd concentration limits set by the EU in 2019 (maximum of 0.1 to 0.8 μg g^{-1} Cd) for final cacao-based products [37, 44].

Cadmium isotope analyses have helped to constrain and understand the underlying mechanisms responsible for the uptake of Cd and its translocation to cacao beans [45, 46]. In particular, previous Cd stable isotope studies suggest that cacao plants preferentially remove

isotopically light Cd from hydroponic solutions using membrane transporter proteins such as natural resistance-associated macrophage proteins (NRAMPs). In addition, it was shown that cacao plants retain isotopically light Cd in the roots, whilst translocating isotopically heavy Cd to aerial parts, possibly due to regulation by proteins such as heavy metal ATPases (HMAs) [46]. To date, however, no studies have directly determined the Zn stable isotope compositions of cacao plants. Such stable isotope data will not only provide insight into how Zn is regulated and translocated in cacao but can also reveal whether the physiological mechanisms of Zn regulation are impacted by Cd. In this study, juvenile cacao plants were used to investigate whether the overarching mechanisms responsible for Zn uptake and translocation are similar to those of Cd and whether these mechanisms change under high Cd conditions. This is the first step towards understanding the mechanisms responsible for the uptake of Zn and its translocation to cacao beans in mature cacao plants under field conditions. Subsequently, a better understanding of both metals can be used to inform future agricultural and land management practices that aim to reduce Cd accumulation in cacao, and particularly cacao beans, without disrupting Zn homeostasis. For example, if Cd and Zn share and possibly compete for the same physiological mechanisms responsible for root uptake, Zn applied through fertilisers could be used to reduce the overall uptake of Cd by the cacao plant and its subsequent translocation to cacao beans [47]. In contrast, if the metals do not share similar mechanisms, then this could also be used to design genetically distinct cultivars that allow sufficient Zn to reach the important organs but exclude Cd or sequester the metal in organs other than the beans [47, 48].

In this study, hydroponic systems were used to grow 19 genetically distinct varieties of cacao. Hydroponic plant studies uniquely allow the testing of plant responses to different nutrient

availability and exposure to toxic metals, through controlling the concentrations of the metal of interest, in this case, Zn and Cd. In addition, the systems also reduce confounding factors observed in soil studies from soil microenvironments [49,50]. This controlled setup enables direct analysis of how Cd concentrations in the hydroponic solution influence the uptake and translocation of Zn in cacao plants. Most importantly, hydroponic plant systems allow for root and shoot tissues to be easily harvested and separated for analyses of the entire plant system [49].

This study is focused on examining the uptake and translocation of Zn and its stable isotopes in Cd-stressed juvenile cacao plants grown under controlled hydroponic conditions. Stable isotope analyses were conducted on the leaves, stems and roots of 19 diverse cacao genotypes; the same plants previously analysed by Moore et al. [46] for Cd stable isotope compositions. The aims of the current investigation were to (1) examine the Zn stable isotope fractionation among the plant organs across the 19 genotypes to investigate overarching mechanisms for Zn uptake and translocation; (2) compare Zn and Cd stable isotope fractionation to identify shared or distinct physiological mechanisms for the uptake and translocation of these metals across the 19 genotypes; and (3) examine whether the availability of Cd influences the uptake of Zn by cacao plants and its translocation to aerial plants organs.

4.3. Methods

4.3.1. Samples

4.3.1.1. Cultivation of cacao plants

Juvenile cacao plants representing 19 different genotypes were obtained from the International Cocoa Quarantine Centre at the University of Reading, UK (Appendices Table A4.1). These plants were identical to those analysed in the study of Moore et al. [46]. The planting, growing, and harvesting period of the juvenile cacao plants encompassed a total of 8 weeks. All cacao plants were grown under controlled environmental conditions, with temperatures of 28 °C during the day and 20 °C at night with a 16-hour photoperiod at a 60% relative humidity. The cacao seeds (nibs) first had their coats (testa) removed and then were placed in seed compost for germination. After two weeks, as part of the hydroponic system, the seedlings were transferred into food grade polyethylene containers (Clas Ohlson) with a hydroponic solution comprising 3 L of half-strength Hoagland solution with a pH of 5.2 (Appendices Table A4.2). A sufficient amount (0.38 μmol L^{-1}) of zinc sulfate ($ZnSO_4 \cdot 7H_2O$) was added as part of the half-strength Hoagland solution. In each container, there were four cacao seedlings of the same genotype. The hydroponic solution was aerated for 15 min every 2 hours and renewed every 7 days.

After 28 days, the nutrient solutions were continued to be renewed for a further 14 days, but with the addition of 20 μmol L^{-1} $CdCl_2$ (Sigma-Aldrich, 99.99% trace metals basis). To assess to what extent different Cd concentrations influenced plant growth and the uptake and translocation of Zn, additional seedlings of one genotype (NA702) were grown under the same conditions as the other seedlings, but only 0 and 5 μmol L^{-1} $CdCl_2$ were added to the nutrient solutions for the final 14 days. The NA 702 genotype, part of Nanay family, was selected for the additional Cd conditions as it is one of the most widely used and traditionally grown cacao genotypes in South and Central America [51].

After 14 days of Cd stress, the plants were harvested and separated into leaves, stems and roots. To remove any residual Zn, Cd and other metals that were apoplastically bound to the roots, the roots were bathed in a solution of 20 mmol L^{-1} Na_2EDTA for 15 mins and then rinsed with deionised water. The leaves and stems were washed with deionised water. After cleaning, the different plant organs were oven-dried at 70 °C and ground using a plastic grinder. Between each sample grinding, the grinder was cleaned with 18.2 MΩ cm^{-1} grade (Milli-Q) H_2O and ethanol.

4.3.1.2. Plastic leaching experiment

Part of the experimental conditions by which the cacao plants were grown was replicated to understand the contribution of Zn from plastic leaching to the total concentration of Zn in the hydroponic solutions. Two additional hydroponic containers were filled with 3 L solutions of 0.25 µg L^{-1} Zn with a pH of about 6. These solutions were prepared using the same $ZnSO_4$ as used in the plant experiments and Milli-Q H_2O. The plastic tubing, foam stopper and vials used to hold and grow the cacao seedlings, were also placed in the containers. A lower Zn concentration (0.25 µg L^{-1}) than present in the hydroponic solutions was used here, so that any Zn addition, particularly from leaching of plastics, would be easy to detect and quantify. To replicate the hydroponic systems, the solutions were renewed each week for 6 weeks and before each renewal, a 15 mL aliquot was taken from each solution and stored in a Savillex Teflon vial. The aliquots from each week were combined, dried down on a hotplate and then treated with 6 mol L^{-1} HCl to convert Zn into the chloride form.

4.3.2. Sample preparation

Sample preparation was performed in the clean room facilities of the MAGIC Laboratories, Imperial College London. The mineral acids used in this study, 15.4 mol L^{-1} HNO_3, 5.8 mol L^{-1} HCl and 28 mol L^{-1} HF, were prepared by sub-boiling distillation in Teflon or quartz glass stills from AnalaR grade stock acids. All acid dilutions used Milli-Q H_2O from a Millipore purification system. Samples were stored in acid-cleaned Savillex Teflon vials.

4.3.2.1. Digestion

Between 50 and 550 mg of the leaf, stem and root samples alongside the reference material NIST spinach leaf SRM 1570a, were digested in 100 mL PTFE vessels with 7 mL of 15.4 mol L^{-1} HNO_3 and 3 mL of 30–32% Optima grade H_2O_2 (Romil) using a Milestone Ethos EZ microwave system. The treated samples of NIST SRM 1570a were matched to the sample weights of the different plant organs that were digested for analysis. The digestion protocol consisted of heating at 90°C for 15 min and then at 180°C for 30 min. After completion, the samples were transferred to 15 mL Savillex Teflon vials and dried on a hotplate. Then, 700 µL of 15.4 mol L^{-1} HNO_3, 300 µL of H_2O_2 and 20 to 50 µL of 28 mol L^{-1} HF were added and the digestion continued at 120°C on a hotplate for approximately 48 hours, until all residual organic materials and silica were completely dissolved.

Digestions were carried out for biological and analytical replicates of plants to determine their homogeneity and biological variability. These constituted single leaf, stem, and root samples

of three separate plants of genotypes GU 207/H and CC 41, and duplicate analyses of leaf, stem, and root samples from a single plant of Matina 1-7.

4.3.2.2. Zinc separation chemistry

Following digestion, appropriate aliquots of the sample solutions were further treated for subsequent Zn stable isotope measurements. For each set of eight sample digestions, a procedural blank was prepared. For the stable isotope measurements, sample aliquots with about 250 ng Zn were mixed with an appropriate volume of a ^{64}Zn–^{67}Zn double spike (DS) solution to obtain a ratio of DS-derived to natural Zn (S/N) of about 1 to 1.2, and then equilibrated overnight at 120 °C [52,53]. To optimise the S/N ratio, the Zn concentrations of the samples were determined by a MC-ICP-MS prior to this step using a ~10% aliquot of the sample solutions. Once equilibrated with the DS, anion exchange chromatography was utilized to prepare purified Zn fractions from the samples [52]. This procedure consisted of filling shrink-fit Teflon columns with 3 mL acid reservoirs with 250 µL of the anion-exchange resin (AG MP-1M, 100–200 mesh). After cleaning with 8 mL of 0.1 mol L^{-1} HNO_3 and 0.5 mL of MQ H_2O, the resin was converted to Cl^- form using 3.5 mL of 6 mol L^{-1} HCl. Following this, 2 mL of 1 mol L^{-1} HCl was added. The samples, as well as a procedural blank and a column blank, were then loaded onto the resin columns as solutions in 1 mL of 1 mol L^{-1} HCl. The sample matrix was eluted with 8 mL of 1 mol L^{-1} HCl, whilst the Zn fractions were then stripped from the resin by adding 6 mL of 0.01 mol L^{-1} HCl. Once the Zn fractions were isolated, they were dried, dissolved in a few drops of 15.4 mol L^{-1} HNO_3 and re-dried, twice, to remove Cl^-. Finally, the samples were dissolved in 0.1 mol L^{-1} HNO_3 to make solutions of 100 ng mL^{-1} Zn, for analyses via MC-ICP-MS.

4.3.3. Zinc concentration and stable isotope measurements

The Zn stable isotope compositions of the samples were determined in the MAGIC Laboratories using a Nu Instruments Nu Plasma HR MC-ICP-MS. Sample introduction to the MC-ICP-MS was performed with a Cetac autosampler and Cetac Aridus II desolvation system fitted with a glass nebuliser that had nominal uptake rates of 100 μL min^{-1}. A Faraday collector configuration that employed the L5, L3, Ax, H2, H3 and H4 cups was used for the analyses, with all collectors fitted with 10^{11} Ω resistors. Faraday collectors L3, Ax, H2 and H4 were employed to measure the ion beams of ^{64}Zn, ^{66}Zn, ^{67}Zn and ^{68}Zn, while L5 and H3 were used to monitor ^{62}Ni and $^{135}Ba^{2+}$ to allow for spectral interference corrections of isobaric Ni^{+} and Ba^{2+} ions on the different Zn isotopes. Each sample measurement entailed three blocks of twenty 5 second integration cycles, with electronic baselines measured for 15 seconds prior to each block, during which the ion beam was deflected in the electrostatic analyser [52]. For sample measurements, the instrumental sensitivity for Zn was typically between 120 and 150 V/(μg/mL).

As MC-ICP-MS is prone to instrumental drift, the sample runs were bracketed by analyses of the AA-ETH Zn isotope standard [54]. The AA-ETH Zn solutions had S/N values and Zn concentrations that matched the values of the samples to within 10%. The analytical precision of the Zn stable isotope data for samples was determined from the precision of the bracketing analyses of the AA-ETH Zn isotope standard that were conducted in the same measurement session. Such analyses yielded analytical precisions that were typically between ±0.02‰ and ±0.09‰ (Table

4.1). The secondary London Zn isotope standard and spinach leaf reference material NIST SRM 1570a, were also analysed alongside samples to further monitor data quality.

Following data acquisition, the raw measured isotope ratios were treated offline to correct for both spectral interferences and any instrumental and laboratory-induced mass bias using an iterative double spike data reduction method [53, 55, 56]. The Zn concentrations of the samples were determined with the isotope dilution technique from the mass bias corrected isotope data.

4.3.4. Calculations and data analysis

The Zn stable isotope compositions of the samples are reported in δ notation (‰). The δ values were originally determined relative to data obtained in the same measurement session for bracketing runs of the AA-ETH Zn isotope standard:

$$\delta^{66}\mathrm{Zn} = \left[\left(\frac{(^{66}\mathrm{Zn}/^{64}\mathrm{Zn})_{\mathrm{sample}}}{(^{66}\mathrm{Zn}/^{64}\mathrm{Zn})_{\mathrm{AA-ETH\ Zn}}} \right) - 1 \right] \mathrm{x}\ 1000 \qquad \text{(Equation 4.1)}$$

In the following, all δ^{66}Zn values are reported relative to the JMC-Lyon Zn isotope standard. To this end, the initial results were corrected for a δ^{66}Zn offset of +0.28‰ for AA-ETH Zn relative to JMC-Lyon Zn [54].

For the comparison of Zn stable isotope compositions, the apparent isotope fractionation or difference between two samples or reservoirs, denoted A and B, was calculated as:

$$\Delta^{66}\mathrm{Zn}_{\mathrm{A\text{-}B}} = \delta^{66}\mathrm{Zn}_{\mathrm{A}} - \delta^{66}\mathrm{Zn}_{\mathrm{B}} \qquad \text{(Equation 4.2)}$$

A one-way analysis of variance (ANOVA) was conducted for the Zn stable isotope fractionations that were determined for cacao plants treated with different concentrations of $CdCl_2$ (0, 5 and 20 µmol L^{-1}). The level of significance for the ANOVA test was set at $p < 0.05$. Further ANOVA and Kruskal-Wallis tests were conducted for the dry biomass (g), Zn concentrations (mg kg^{-1}) and $\delta^{66}Zn$ values of the cacao organs from the 19 genotypes, with the level of significance also set at $p < 0.05$. The coefficient of determination (R^2) was calculated for the dry biomass (g), Zn concentrations (mg kg^{-1}) and $\delta^{66}Zn$ values of the 19 cacao genotypes.

4.4.Results

4.4.1. Quality control

4.4.1.1. Blank contributions and reference materials

The total procedural Zn blank during the study was between 1 and 10 ng (n = 41). This corresponds to mean and maximum blank contributions of 0.6% and 1.9%, respectively, to the total Zn mass of the cacao samples. All Zn concentrations were blank corrected to account for exogenous Zn contributions, but no corrections were applied to the $\delta^{66}Zn$ data as the stable isotope composition of the blank is not well defined. For the full 6-week growing period of the hydroponic experiment, the total contribution of exogenous Zn from plastic leaching to the Zn concentration of the hydroponic solution accounted to 2.0%. The $\delta^{66}Zn$ value of the solution in the hydroponic setup (+0.47±0.03‰, 2SD, n = 2) was, furthermore, identical (within analytical precision) to that of the $ZnSO_4$ reagent (+0.51±0.06‰, 2SD, n = 7). Given these findings, the hydroponic solutions

were assigned a stable isotope composition of $\delta^{66}Zn$ = +0.51±0.06‰, as there were more analyses for the $ZnSO_4$ reagent.

The Zn stable isotope and concentration data obtained for the secondary isotope standard and NIST spinach leaf SRM 1570a showed excellent reproducibility and agreed with the published literature values (Appendices Table A4.3). In detail, replicate runs of the secondary London Zn isotope standard yielded a mean $\delta^{66}Zn$ of +0.10 ± 0.06‰ (2SD; *n* = 30) whilst multiple analyses of SRM 1570a defined a mean result of $\delta^{66}Zn$ = +0.41 ± 0.06‰ (2SD; *n* = 19).

4.4.1.2. Zinc data for biological and analytical replicates of cacao plant samples

Zinc concentrations, [Zn], were determined for samples from three different plants of the CC 41 and GU 207/H genotypes and duplicate samples from a single Matina 1-7 plant. These replicates displayed limited variability with coefficients of variation (CV) of 17%, 12% and 7% for the whole plant Zn concentrations of CC 41, GU 207/H and Matina 1-7, respectively (Tables 4.1, 4.2 and Appendices Table A4.4). Considering the stable isotope data, with one exception, all $\delta^{66}Zn$ values determined for replicate leaf, stem and root samples of the CC 41, GU 207/H and Matina 1-7 plants were identical, within uncertainty, with one another (Tables 4.1, 4.2 and Appendices Table A4.4). The exception is a single leaf aliquot from the CC 41 genotype, which was isotopically heavier by about 0.35‰ compared to the other two CC 41 leaf aliquots (Appendices Table A4.4). These findings are in accord with the results of previous studies that employed plants grown in hydroponic systems under controlled conditions and which demonstrate

that such experiments typically produce plants that yield reproducible results for metal uptake and translocation [11,12,18]. These previous and our current results thus indicate that additional replicate analyses for the different cacao genotypes of this study are not needed to arrive at robust conclusions, also considering that the stable isotope measurements are particularly time-consuming and expensive.

4.4.2. Zinc data for the 19 cacao genotypes

The dry plant masses are summarized in Appendices Table A4.5. The cacao seedlings grew to a total dry mass (root, stem, leaves) of between 0.40 g and 2.16 g, with roots, stems and leaves accounting for 14-17%, 21-26%, and 62-64%, respectively. For all 19 cacao genotypes, the Zn contents of the plant organs (Zn_{leaf}, $Zn_{stem,}$ and Zn_{root}) and the mass fractions of Zn in each organ relative to the total plant Zn inventory (f_{leaf}, f_{stem} and f_{root}) followed the pattern leaf>stem>root (Tables 4.1, 4.2, Figure 4.1 and Appendices Figure A4.1). The mean Zn mass fractions were $f_{leaf} = 66.3\%$, $f_{stem} = 23.3\%$, and $f_{root} = 10.4\%$ (Table 4.1), and the total Zn inventory of the plants, $Zn_{total\ plant}$, was positively correlated with total biomass ($R^2=0.78$, $p<0.05$).

The $[Zn]_{total\ plant}$ data ranged between 14 and 50 mg kg^{-1} (Table 4.2) and these show a strong positive correlation with $[Zn]_{leaf}$ ($R^2=0.93$, $p<0.05$; Appendices Figure A4.2), which indicates that $[Zn]_{total\ plant}$ is controlled by $[Zn]_{leaf}$. The Zn concentrations for the cacao plant organs of the 19 genotypes were variable. For 17 genotypes, $[Zn]_{leaf}$ exceeded $[Zn]_{root}$, whilst only for 9 genotypes $[Zn]_{leaf}$ exceeded $[Zn]_{stem}$. Furthermore, for all but two of the 19 genotypes, $[Zn]_{stems}$ exceeded $[Zn]_{root}$. The Zn concentrations ranged from 14 to 63 mg kg^{-1} for $[Zn]_{leaf}$, 14 to 62 mg kg^{-1} for

$[Zn]_{stem}$, and 10 to 23 mg kg^{-1} for $[Zn]_{root}$. The $[Zn]_{leaf}$ values were in accord with literature data for mature leaves from cacao plants grown in the field, and this indicates that the cacao plants of our study received sufficient Zn from the hydroponic solutions (Appendices Table A4.6). The cacao genotype U70 [PER] had the highest $[Zn]_{leaf}$ and $[Zn]_{root}$ (tied with SCA 9 for highest $[Zn]_{root}$), whereas genotype CL 19/10 had the highest $[Zn]_{stem}$. The cacao genotypes CL 19/10 had lowest $[Zn]_{leaf}$ and PNG 340 had the lowest $[Zn]_{stem}$ and $[Zn]_{root}$. Overall, $[Zn]_{root}$ had the lowest variability, with a CV of 20%, whereas $[Zn]_{leaf}$ and $[Zn]_{stem}$ were more variable and had similar concentration ranges, with CVs of 42% and 38%, respectively (Table 4.1 and Appendices Figure A4.1). No strong relationships ($R^2>0.5$, $p<0.05$) were observed between the Zn concentrations of the different organs or with the dry biomass of the different organs.

Over the course of the full 6-week growing period of the hydroponic experiment, the four cacao plants in each hydroponic setup depleted the $ZnSO_4$ added to the hydroponic solution by, on average, 21% (Table 4.2). This depletion factor was determined from the total Zn inventory of the plants in each hydroponic setup relative to the total amount of Zn that was available to the plants via the provided hydroponic solutions (see Appendices Note A4.1). For all 19 genotypes, the $\delta^{66}Zn$ values of the plant organs decreased in the order root > stem > leaf. In detail, $\delta^{66}Zn$ data obtained for the organs ranged between –1.11‰ and –0.43‰ for leaves, between –0.67‰ and +0.25‰ for stems and between –0.28‰ and +0.68‰ for roots (Table 4.1). The $\delta^{66}Zn$ values for the total plants ranged between −0.22‰ and −0.70‰ (Table 4.2). There were no strong correlations ($R^2>0.5$, $p<0.05$) between $\delta^{66}Zn$ values and the Zn concentrations of leaves, stems, roots and total plants.

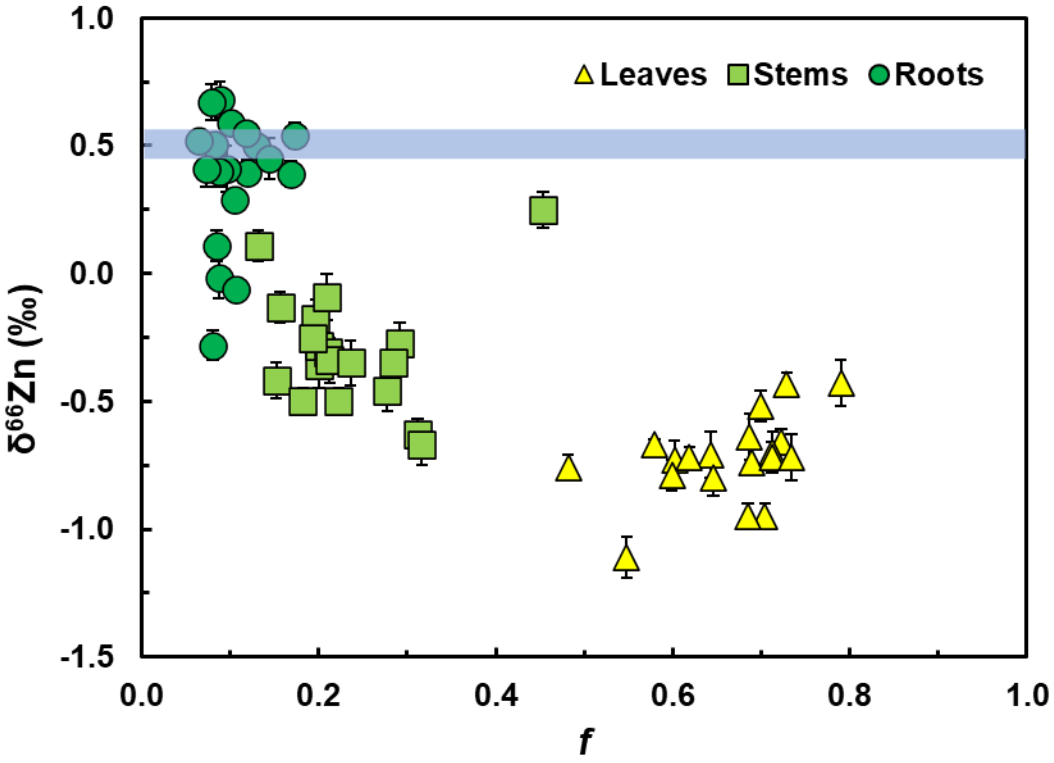


Figure 4.1. Zinc stable isotope compositions (δ^{66}Zn) of leaves, stems and roots versus mass fractions (*f*) of Zn in leaves, stems and roots for the 19 cacao genotypes treated with 20 µmol L^{-1} $CdCl_2$. The error bars denote the 2SD precision determined for multiple analyses of the Zn isotope standard that bracketed the sample runs. The blue line denotes the δ^{66}Zn value of +0.51±0.06‰ for the $ZnSO_4$ that was added to the hydroponic solutions.

4.4.3. Zinc data for plants treated with 0, 5 and 20 µmol L^{-1} $CdCl_2$

The total dry masses of the NA 702 seedlings treated with different concentrations of $CdCl_2$ (0, 5 and 20µmol L^{-1}) were similar at 1.83 g, 1.70 g, and 1.72 g, respectively (Appendices Table A4.7 and Appendices Figures A4.3 a, b). In comparison, the 18 remaining genotypes that were treated only with 20 µmol L^{-1} $CdCl_2$ produced seedlings with total dry masses that varied between

0.40 g and 2.16 g. These 18 genotypes hence encompass plants that were very similar to the NA 702 seedlings in leaf, stem, root and total plant biomass and others which produced more or less biomass.

For the NA 702 seedlings treated with 0, 5 and 20 μmol L^{-1} Cd, the Zn distribution in the organs followed the same pattern seen in the seedlings of different genotypes treated with 20 μmol L^{-1} Cd, with higher Zn concentrations in the stems and leaves compared to the roots (Figure 4.2 and Appendices Table A4.7, Figure A4.4). The NA 702 plants cultured with different Cd treatments (0, 5, and 20 μmol L^{-1}) showed no substantial differences in biomass and the distribution and concentration of Zn in the plant organs. The Zn concentration data for the leaves, stems, and roots thereby showed CV values of 13%, 27%, and 33%, respectively. The mean Zn mass fractions present in the organs relative to the total plants were $f_{leaf} = 66\%$, $f_{stem} = 22\%$, and $f_{root} = 12\%$ (Appendices Table A4.7). Considering the Zn stable isotope data, the δ^{66}Zn values of the organs decreased in the same order that was identified for the seedlings of all other genotypes, with root > stem > leaf. The δ^{66} Zn values determined for the cacao organs varied between –0.70‰ and –0.43‰ for leaves, between –0.52‰ and –0.28‰ for stems, and between +0.21‰ and +0.40‰ for roots (Figure 4.2, Table 4.2 and Appendices Table A4.7, Figure A4.4).

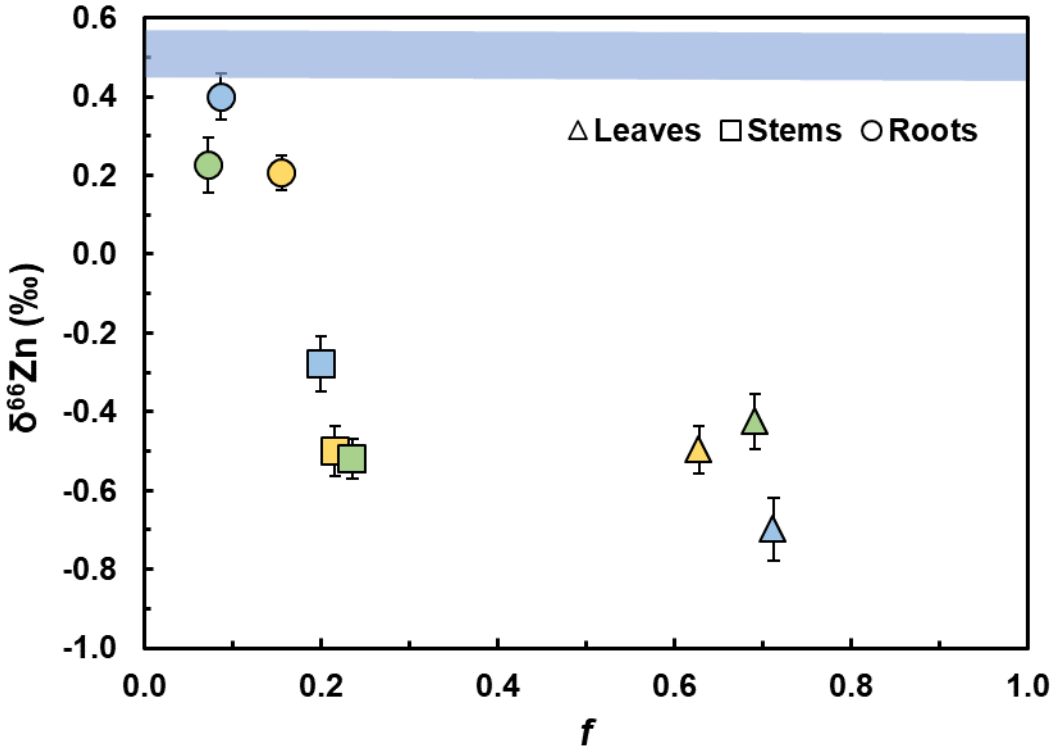


Figure 4.2. Mean Zn stable isotope compositions (δ^{66}Zn) versus mean mass fractions (*f*) of Zn in leaves, stems and roots relative to the total plant Zn inventory for NA 702 plants treated with 0 µmol L^{-1} (yellow, *n*=3), 5 µmol L^{-1} (green, *n*= 2), and 20 µmol L^{-1} (blue, *n*=1) $CdCl_2$. The error bars denote the 2SD precision determined for multiple analyses of the Zn isotope standard that bracketed the sample runs. The blue line denotes the δ^{66}Zn value of +0.51±0.06‰ for the $ZnSO_4$ that was added to the hydroponic solutions.

Table 4.1. Zinc mass fractions (*f*), concentrations (mg kg^{-1}) and stable isotope compositions ($\delta^{66}Zn$) of leaves, stems and roots for 19 cacao genotypes grown with 20 µmol L^{-1} $CdCl_2$.

Cacao Clones (Genotype)	Leaf				Stem				Root			
	f	[Zn] (mg kg^{-1})	$\delta^{66}Zn$ (‰)	2SD (‰)	*f*	[Zn] (mg kg^{-1})	$\delta^{66}Zn$ (‰)	2SD (‰)	*f*	[Zn] (mg kg^{-1})	$\delta^{66}Zn$ (‰)	2SD (‰)
B 5/7 [POU]	0.69	21	−0.74	0.05	0.22	15	−0.50	0.05	0.09	16	0.68	0.07
Catie 1000	0.58	28	−0.67	0.02	0.29	35	−0.27	0.08	0.13	15	0.50	0.04
CC 41[a]	0.72	27	−0.66	0.05	0.20	19	−0.18	0.07	0.08	14	0.51	0.04
CL 19/10	0.48	14	−0.76	0.05	0.45	62	0.25	0.07	0.06	16	0.52	0.02
GU 207/H[a]	0.73	32	−0.43	0.04	0.15	28	−0.42	0.07	0.12	16	0.40	0.05
GU 236/V	0.70	34	−0.52	0.06	0.16	28	−0.13	0.06	0.14	16	0.45	0.08
IMC 27	0.70	43	−0.95	0.05	0.20	25	−0.36	0.09	0.10	13	0.41	0.09
LP 1/41 [POU]	0.64	22	−0.71	0.09	0.28	23	−0.46	0.08	0.08	17	−0.28	0.06
Matina 1-7[b]	0.60	20	−0.73	0.08	0.31	28	−0.63	0.06	0.09	15	−0.02	0.08
NA 702	0.71	16	−0.70	0.08	0.20	16	−0.28	0.07	0.09	12	0.40	0.06
PNG 340	0.60	16	−0.79	0.06	0.32	14	−0.67	0.08	0.08	10	0.11	0.06
Pound 12/A [POU]	0.68	26	−0.95	0.05	0.21	30	−0.31	0.07	0.10	17	0.29	0.00
RB46	0.55	15	−1.11	0.08	0.28	29	−0.35	0.08	0.17	18	0.39	0.05
RIM 179	0.71	23	−0.72	0.06	0.18	23	−0.50	0.05	0.11	15	−0.06	0.02
SCA 9	0.69	28	−0.64	0.09	0.21	22	−0.34	0.09	0.10	23	0.59	0.02
SPA 9 [COL]	0.65	25	−0.80	0.07	0.24	23	−0.35	0.09	0.12	19	0.55	0.02
TARS 31	0.62	30	−0.72	0.04	0.21	30	−0.09	0.09	0.17	16	0.54	0.05
TSA 654	0.73	31	−0.72	0.09	0.19	33	−0.25	0.01	0.07	14	0.41	0.07
U 70 [PER]	0.79	63	−0.43	0.09	0.13	31	0.11	0.06	0.08	23	0.67	0.07
Min	0.48	14	−1.11	0.02	0.13	14	−0.67	0.01	0.06	10	−0.28	0.00
Max	0.79	63	−0.43	0.09	0.45	62	0.25	0.09	0.17	23	0.68	0.09
Mean	0.66	27	-0.72	-	0.23	27	−0.30	-	0.10	16	0.37	-
1SD	0.07	11	-	-	0.07	10	-	-	0.03	3	-	-
2SD	-	-	0.32	-	-	-	0.44	-	-	-	0.50	-

[a] Mean values for the leaf, stem, and root aliquots from three separate plants of the CC 41 and GU 207/H genotypes ($n = 3$). [b] Mean value for the duplicate leaf, stem, and root aliquots from a single plant of the Matina 1-7 genotype ($n = 1$). *f* represents the mass fraction of Zn in leaves, stems, and roots relative to the Zn inventory of the total plant. SD represents the standard deviation. 2SD for individual samples represents the analytical precision of the Zn stable isotope data determined from multiple analyses of the Zn isotope standard that bracketed the sample runs.

Table 4.2. Zinc masses (μg), concentrations (mg kg $^{-1}$) and stable isotope compositions (δ^{66}Zn) for total plants and Zn stable isotope differences (Δ^{66}Zn) and fractionation factors (ε^{66}Zn).

Cacao Clones (Genotype)	Total Plant					Isotopic Differences[d]			Fractionation Factors	
	Zn (μg)	[Zn] (mg kg $^{-1}$)	δ^{66}Zn (‰)	2SD (‰)	Zn Uptake[c] (%)	$\Delta^{66}Zn_{total-sol}$[d] (‰)	$\Delta^{66}Zn_{leaf-total}$[d] (‰)	$\Delta^{66}Zn_{shoot-total}$[d] (‰)	$\varepsilon^{66}Zn_{uptake}$[e] (‰)	$\varepsilon^{66}Zn_{seq-mob}$[f] (‰)
B5/7 [POU]	17	19	−0.56	0.04	14.7	−1.07	−0.18	−0.06	−1.16	0.48
Catie 1000	15	27	−0.40	0.03	12.8	−0.91	−0.27	−0.06	−0.98	0.49
CC 41[a]	21	23	−0.46	0.04	18.7	−0.98	−0.19	−0.04	−1.09	0.58
CL 19/10	39	22	−0.22	0.04	34.4	−0.73	−0.54	−0.03	−0.91	0.74
GU 207/H[a]	18	29	−0.33	0.03	15.3	−0.84	−0.10	−0.05	−0.92	0.32
GU 236/V	16	28	−0.32	0.04	13.9	−0.83	−0.20	−0.06	−0.89	0.56
IMC 27	19	32	−0.70	0.04	16.2	−1.21	−0.25	−0.04	−1.33	0.71
LP 1/41 [POU]	21	22	−0.61	0.06	18.7	−1.12	−0.10	0.02	−1.24	0.23
Matina 1-7[b]	45	21	−0.63	0.05	39.4	−1.15	−0.09	0.00	−1.49	0.18
NA 702	27	16	−0.52	0.06	23.7	−1.03	−0.18	−0.03	−1.18	0.53
PNG 340	24	14	−0.68	0.04	21.2	−1.19	−0.11	−0.01	−1.34	0.22
Pound 12/A [POU]	20	25	−0.69	0.04	17.3	−1.20	−0.26	−0.03	−1.32	0.70
RB46	14	18	−0.64	0.05	12.5	−1.15	−0.47	−0.07	−1.23	0.78
RIM 179	42	22	−0.61	0.04	36.8	−1.12	−0.11	0.01	−1.42	0.32
SCA 9	27	26	−0.45	0.06	23.7	−0.96	−0.19	−0.06	−1.10	0.50
SPA 9 [COL]	21	24	−0.53	0.05	18.2	−1.04	−0.27	−0.06	−1.16	0.61
TARS 31	26	26	−0.37	0.03	22.3	−0.88	−0.35	−0.09	−1.00	0.73
TSA 654	26	29	−0.55	0.07	22.8	−1.06	−0.17	−0.03	−1.21	0.56
U70 [PER]	20	50	−0.27	0.07	17.2	− 0.78	−0.16	−0.05	−0.86	0.67
Min	14	14	−0.70	-	12.5	−1.21	−0.54	−0.09	−1.49	0.18
Max	45	50	−0.22		39.4	−0.73	−0.09	0.02	−0.86	0.78
Mean	24	25	−0.50	-	21.0	−1.01	−0.22	−0.04	−1.15	0.52
1SD	8.8	7.4	-	-	7.7	-	-	-	-	-
2SD	-	-	0.29	-	-	0.15	0.24	0.06	0.36	0.36
NA702 (0 μmol L^{-1} $CdCl_2$)[g]	30	16	−0.38	0.04	26.0	−0.89	−0.12	-0.04	−1.04	0.25
NA702 (5 μmol L^{-1} $CdCl_2$)[g]	26	15	−0.39	0.05	22.8	−0.90	−0.03	-0.02	−1.03	0.09
NA702 (20 μmol L^{-1} $CdCl_2$)[g]	27	16	−0.52	0.06	23.7	−1.03	−0.18	-0.03	−1.18	0.53
Mean	28	16	−0.43	-	24.5	−0.92	−0.10	-0.03	−1.06	0.29
1SD	2	1	-	-	3.12	-	-	-	-	-
2SD	-	-	0.12	-	-	0.18	0.14	0.04	0.20	0.37

[a] Mean values for the leaf, stem, and root aliquots of three separate CC 41 and GU 207/H plants (n = 3). [b] Mean value for the duplicate leaf, stem, and root aliquots of a single Matina 1-7 plant (n = 1). [c] Fraction of Zn (in %) taken up from the nutrient solutions by the 4 cacao plants of the same genotype cultured in the same hydroponic container. [d] Isotopic differences between total plants and the $ZnSO_4$ added to the hydroponic solutions ($\Delta^{66}Zn_{total-sol}$), between leaves and total plants ($\Delta^{66}Zn_{leaf-total}$), and between shoots and total plants ($\Delta^{66}Zn_{shoot-total}$). SD represents the standard deviation. 2SD for individual

samples represents the analytical precision of the Zn stable isotope data determined from multiple analyses of the Zn isotope standard that bracketed the sample runs. [e] $\varepsilon^{66}Zn_{uptake}$ denotes isotope fractionation factor for the uptake of Zn by the cacao plants from the hydroponic solutions. [f] $\varepsilon^{66}Zn_{seq\text{-}mob}$ represents the Zn stable isotope fractionation between the sequestered and mobile Zn in cacao plant. [g] The NA 702 genotypes treated with different $CdCl_2$ concentrations had different samples sizes: 0 µmol L^{-1} $CdCl_2$, n=3; 5 µmol L^{-1} $CdCl_2$, n=2; 20 µmol L^{-1} Cl_2, n=1.

4.5. Discussion

4.5.1. Stable isotope fractionation during Zn uptake

In this study, the hydroponic plant systems were assumed to be unidirectional, with no efflux of Zn from the plant back to the hydroponic solution. The stable isotope fractionation that occurs during root uptake of Zn can be determined using the following Rayleigh mass-balance equation:

$$\Delta^{66}\mathrm{Zn}_{\mathrm{final-initial}} = \varepsilon^{66}\mathrm{Zn}_{\mathrm{uptake}} * In(f_{\mathrm{remaining}}) \qquad \text{(Equation 4.3)}$$

where $\Delta^{66}Zn_{final\text{-}initial}$ represents the isotope difference between the initial and final Zn in the hydroponic solution, $\varepsilon^{66}Zn_{uptake}$ denotes the isotope fractionation factor associated with the uptake of Zn by the cacao plants, and $f_{remaining}$ represents the mass fraction of Zn from the hydroponic solution not taken up by the cacao plants. The mean $\varepsilon^{66}Zn_{uptake}$ for all 19 genotypes was –1.15±0.36‰ (2SD; Table 4.2), indicating that the cacao plants preferentially took up isotopically light Zn. These similarities in $\varepsilon^{66}Zn_{uptake}$ across 19 cacao genotypes indicate that the plants of the different genotypes likely employ similar physiological mechanisms to take up Zn from the hydroponic solutions.

Previous studies also noted preferential uptake of light Zn isotopes in both plant-hydroponic [10, 11, 12, 57] and plant-soil systems [9, 13, 16, 18, 19, 24, 57]. In detail, $\Delta^{66}Zn$ values for fruit and cereal crops, as well as hyperaccumulator plant species, were between –0.60‰ and –0.01‰ [9,10, 11, 12, 13,16, 18, 19, 24, 57]. This preferential uptake of isotopically light Zn has been ascribed to low-affinity transport of free Zn^{2+} ions under Zn

sufficient or excess conditions, via ion channels and electrogenic pumps or a combination of both high- and low-affinity transport of Zn [9, 11, 18]. There are exceptions to this observed pattern, where Δ^{66}Zn values were positive (as high as +0.63‰) for *Thlaspi arvense*, *Alyssum murale, Agrostis capillaris* L.*, Noccaea caerulescens*, *Arabidopsis helleri*, and wheat [9, 11, 12, 16, 18]. In these cases, Zn uptake may be mediated by high-affinity transport, under Zn deficient conditions, via membrane transporter proteins such as zinc-regulated, iron-regulated transporter-like proteins (ZIPs) [9,11]. However, the specific conditions at which plants switch between high- and low-affinity transport of Zn have yet to be fully characterised and understood [5,9].

The cacao plants of the current study were grown under Zn sufficient conditions. The low-affinity transport hypothesis may therefore explain the negative $\varepsilon^{66}Zn_{uptake}$ values of the cacao seedlings. In comparison to all other investigated plants, however, cacao plants show the largest Zn stable isotope fractionation during Zn uptake, regardless of genotype (Appendices Table A4.8). This suggests that cacao plants may have a different or more pronounced dominant physiological mechanism for Zn uptake compared to other plant species, which is not fully encapsulated by the low-affinity transport hypothesis. A possible reason may be the presence of membrane transporter proteins such as NRAMPs that mediate the uptake of free Zn^{2+} ions into cacao roots, a similar uptake mechanism as hypothesised for free Cd^{2+} ions [58]. It is also not yet clear whether the uptake mechanisms would change under Zn deficient or excess conditions, and this could be investigated in future hydroponic plant studies.

4.5.2. Stable isotope fractionation during Zn translocation

Partial sequestration (seq) of Zn in roots and stems during unidirectional Zn mobilisation (mob) to the leaves, can produce an isotope fractionation that follows a Rayleigh mass balance equation:

$$\delta^{66}\mathrm{Zn}_{\mathrm{mob}} = \delta^{66}\mathrm{Zn}_{\mathrm{total}} + \varepsilon^{66}\mathrm{Zn}_{\mathrm{seq-mob}} * \mathrm{In}(f_{mob}) \qquad \text{(Equation 4.4)}$$

where $\delta^{66}Zn_{mob}$ and $\delta^{66}Zn_{total}$ denote the Zn stable isotope compositions of mobilized Zn in the leaves, and the total plant, respectively, $\varepsilon^{66}Zn_{seq\text{-}mob}$ represents the isotope fractionation factor that characterizes the retention and translocation of Zn, and f_{mob} represents the mass fraction of mobilised Zn in the leaves relative to the total Zn inventory of the plant. The isotope fractionation factor $\varepsilon^{66}Zn_{seq\text{-}mob}$ of the cacao plants is a result of processes that store isotopically heavy Zn in the plant roots and stems and the mobilisation of isotopically light Zn to the leaves. A logarithmic best fit curve for the data in a plot of $\Delta^{66}Zn_{mob\text{-}total\ plant}$ versus f_{leaf}, when forced through $f_{leaf} = 1$ at $\Delta^{66}Zn_{mob\text{-}total\ plant} = 0$, yields a mean $\varepsilon^{66}Zn_{seq\text{-}mob}$ of +0.54‰ (Figure 4.3). The rationale for fixing the fit through $f = 1$ at $\Delta 66Zn_{mob\text{-}total\ plant}$ is the following: if 100% of the Zn is mobilised to the leaves, then the $\Delta 66Zn_{mob\text{-}total\ plant}$ must be 0 by definition, as the total plant isotope composition would be equal to the leaf composition. Furthermore, when arithmetically derived using Equation 4.4, the mean $\varepsilon^{66}Zn_{seq\text{-}mob}$ value is +0.52±0.36‰ (2SD; Table 4.2). When compared, both the logarithmic best fit curve (Figure 4.3) and arithmetically derived mean $\varepsilon^{66}Zn_{seq\text{-}mob}$ values are within excellent agreement with one another. The $\varepsilon^{66}Zn_{seq\text{-}mob}$ values for individual genotypes are listed in Table 4.2. Therefore, a single well-defined fractionation factor is hence able to fully capture all 19 cacao genotypes, indicating that there are likely only minor differences in the mechanisms that are utilized by the different genotypes

to mobilize and retain Zn. The mean $\varepsilon^{66}Zn_{seq\text{-}mob}$ from this study is consistent with previous studies examining Zn translocation in both metal hyperaccumulators and non-hyperaccumulators, in which isotopically light Zn is transferred to aerial parts of the plant [9,11,12]. In examining root-to-shoot isotope fractionation of Zn, *Thlaspi arvense*, *Noccaea caerulescens* and *Alyssum murale* [11], *Noccaea caerulescens* and *Silene vulgaris* [9], and *Arabidopsis halleri* and *Arabidopsis petraea* [12], had $\varepsilon^{66}Zn_{seq\text{-}mob}$ values of +0.32‰, +0.39‰ and +0.37‰, respectively. This suggests that cacao plants have a mean $\varepsilon^{66}Zn_{seq\text{-}mob}$ value that is identical, within 2SD, to the previous results, in accord with similar partitioning of isotopically light Zn to the aerial parts of the plant. Given the similarity in $\varepsilon^{66}Zn_{seq\text{-}mob}$ values, it is likely that cacao and other plant species employ similar mechanisms to regulate sequestration and translocation of Zn within the plants.

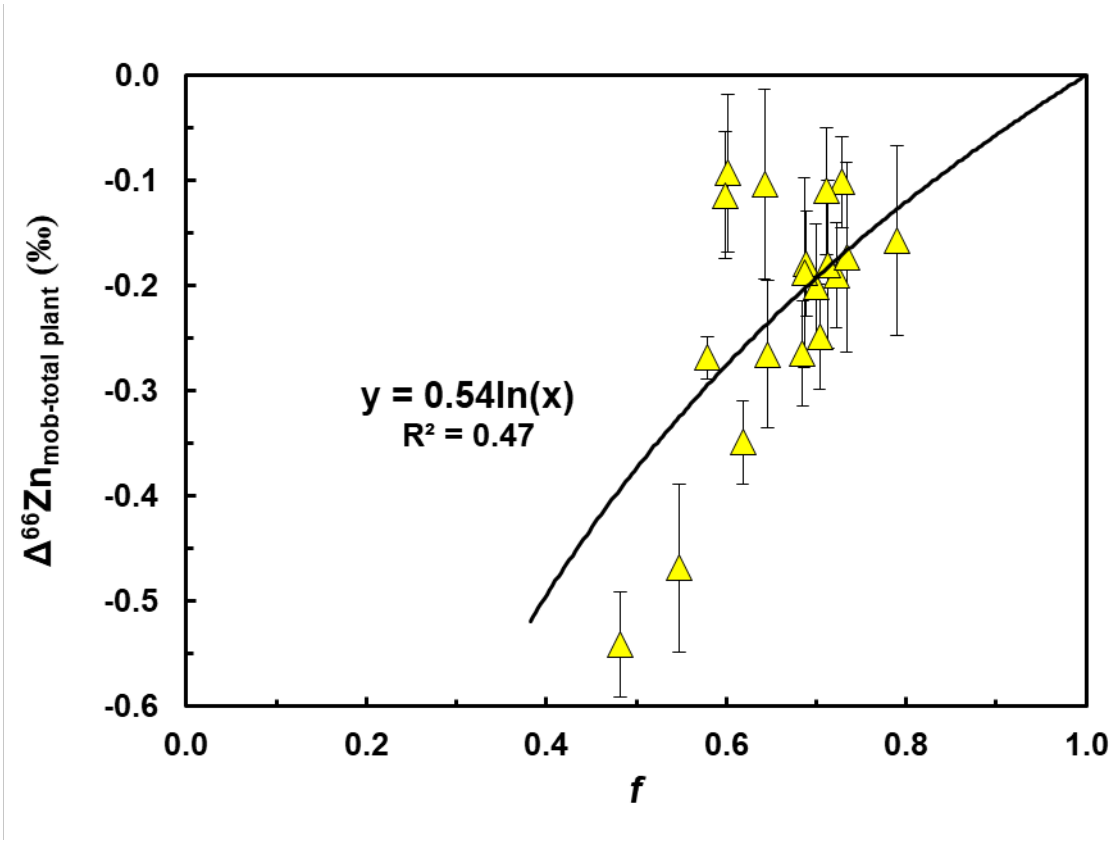


Figure 4.3. Zinc stable isotope difference ($\Delta^{66}Zn_{mob\text{-}total\ plant}$) between mobilised Zn in cacao leaves (mob) and total plant Zn inventory versus mass fraction (*f*) of Zn present in cacao leaves

for the 19 cacao genotypes treated with 20 µmol L^{-1} $CdCl_2$. The solid line is a logarithmic best-fit Rayleigh fractionation trend for the sample data, which is forced through $\Delta^{66}Zn_{mob\text{-}total\ plant}$ at $f = 1$. This yields an isotope fractionation factor of $\varepsilon^{66}Zn_{seq\text{-}mob} = +0.54‰$ between sequestered Zn and Zn mobilised to leaves.

The $\varepsilon^{66}Zn_{seq\text{-}mob}$ values determined in this study indicate that root-to-shoot translocation of Zn in cacao plants is mediated by mechanisms that favour isotopically light Zn, as was previously discussed for other plant species [5, 9, 17, 18, 24]. In cacao plants, as with other plant species, it is likely that once external Zn^{2+} ions have entered the root, the isotopically heavy Zn^{2+} ions in the cytosol preferentially bind with ligands that contain nitrogen- and oxygen-donors [27, 59], such as nicotianamine and histidine, to form Zn-ligand complexes [60, 61]. This complexed Zn either remains in the cytosol of the cacao roots or is further transferred by membrane transporter proteins, such as metal tolerance proteins (MTPs) on the tonoplast, to vacuoles for storage [5, 9, 17, 18, 24]. As examined in previous plant studies, this likely leads to the enrichment of isotopically light Zn^{2+} ions in the cytosol of cacao roots, which can subsequently be loaded into the xylem by membrane transporter proteins, such as HMAs, for translocation to the cacao stems and leaves [9,17].

4.5.3. Comparison of Zn and Cd stable isotope fractionation in cacao plants

Regardless of the $CdCl_2$ concentration added to the hydroponic solutions, the cacao plants preferentially removed isotopically light Zn from the nutrient media. For the NA 702 genotype treated with 0, 5 and 20 µmol L^{-1} $CdCl_2$, the mean $\varepsilon^{66}Zn_{uptake}$ was –1.06±0.20‰ (2SD; Table 4.2). The small observed differences in $\varepsilon^{66}Zn_{uptake}$ values for the different treatments and the similarity of the mean value to that obtained for the 19 genotypes treated with 20 µmol L^{-1} $CdCl_2$, (–1.15±0.36‰, 2SD; Table 4.2) suggests that the Zn uptake mechanism is not substantially impacted when Cd availability changes. In contrast, the NA 702 plants treated

with 0 and 5 μmol L^{-1} $CdCl_2$ yielded significantly lower $\varepsilon^{66}Zn_{seq\text{-}mob}$ values than the 19 cacao genotypes that were treated with 20 μmol L^{-1} $CdCl_2$, including NA 702 ($p < 0.05$, Table 4.2). In detail, the $\varepsilon^{66}Zn_{seq\text{-}mob}$ values for the two low-Cd treatments were +0.25‰ and +0.09‰, compared to +0.53‰ for NA702 and +0.52±0.36‰ (2SD) for the other 18 genotypes treated with 20 μmol L^{-1} $CdCl_2$. However, irrespective of the $CdCl_2$ concentration of the hydroponic solutions, the cacao leaves retained isotopically light Zn compared to the roots.

The $\varepsilon^{66}Zn_{seq\text{-}mob}$ values for the different Cd treatments demonstrate that while cacao plants can maintain Zn homeostasis under different Cd stress conditions, there appear to be differences in the mechanisms that the plants employ to mediate the translocation of Zn when they are exposed to different levels of Cd stress. One possible explanation for this observation is the presence of metallochaperones that maintain Zn homeostasis. Metallochaperones are metal-binding-proteins, which likely preferentially bind with cytosolic Zn^{2+}, Cu^{2+}, Ni^{2+} [62] and Cd^{2+} ions [63,64], and that coordinate with membrane transporter proteins to transfer these heavy metals to different intracellular compartments and plant tissues [65,66,67]. It is plausible that in cacao plants Zn and Cd share an individual or a series of metallochaperones that are activated together and participate in a *linked* response to heavy metal stress as part of an internal tolerance strategy. The findings of this study may suggest that when excess Cd is introduced and taken up by the plant, in order to maintain Zn homeostasis to ensure plant growth under Cd stress, cacao plants upregulate and activate metallochaperones to chelate free Zn^{2+} ions in the roots and transfer these to aerial plant organs via membrane transporter proteins [65, 67]. In the absence of or under limited Cd stress, these metallochaperones may be downregulated or deactivated. This explanation is in accord with the findings on the formation and sequestration of isotopically heavy ligand-Zn complexes in the cytosol and vacuoles, as metallochaperones could preferentially bind with free cytosolic Zn^{2+} ions that are likely

isotopically light and are then transferred to aerial plant organs. However, given the small number of cacao plants grown under low Cd conditions, further work is required to confirm if the inferred differences in $\varepsilon^{66}Zn_{seq\text{-}mob}$ values for cacao plants cultured with different Cd concentrations in the hydroponic solutions are indeed significant. Biological studies are also required to confirm the presence and functionality of metallochaperones that regulate Zn and Cd homeostasis in cacao plants, and the genes that encode them.

When the Zn stable isotope compositions of this study are compared to previously published Cd stable isotope data for the same 19 hydroponically-grown cacao genotypes [46], inverse stable isotope fractionation dynamics are observed for the translocation of Zn and Cd (Appendices Figure A4.5). During uptake, however, the 19 cacao genotypes preferentially removed *both* isotopically light Zn and Cd from the hydroponic solutions, indicating there may be similar physiological mechanisms for the uptake of both metals. Moore et al. [46] determined through stable isotope analyses that the light Cd isotope compositions of the plants relative to the hydroponic solutions may reflect, at least in part, Cd uptake via NRAMP5 membrane transporters. This inference was based on the finding that transgenic yeast encoded with the cacao *TcNRAMP5* gene took up more and isotopically lighter Cd than yeast controls without this gene [46]. Furthermore, Ullah et al. [58] found in examining the role of NRAMPs in the uptake of Cd and nutritionally vital divalent cations (Fe^{2+}, Mn^{2+}, Zn^{2+}) by cacao, that transgenic yeast strains modified with *TcNRAMP5* genes showed substantial Zn^{2+} transport activity. Hence, it is plausible that cacao plants also utilise similar NRAMP transporters, and in particular NRAMP5, to preferentially take up isotopically light Zn. However, further studies are required to confirm the importance of NRAMP transporters for Zn and Cd uptake by cacao plants.

Once Zn and Cd make their way into the cacao plants, an inverse relationship in stable isotope fractionation was observed, whereby isotopically light Zn and heavy Cd are mobilized to the leaves. This is consistent with the observed isotope fractionation for translocation of Zn and Cd in durum wheat and is likely a result of differences in ligand environments [18]. In the cytosol of cacao roots, the isotopically heavy Zn^{2+} ions likely bind with ligands containing oxygen- and nitrogen-donor groups [27, 59], whereas the isotopically light Cd^{2+} ions likely bind with ligands containing sulphur-donor groups [18, 68]. Given that the heavy and light isotopes of both Zn and Cd preferentially bind to the oxygen- and nitrogen- versus the sulphur-donor groups of ligands, respectively [27,70], the observed difference is likely due to the two metals binding to distinct enzymes and/or proteins that contain ligands with the respective electron donors. For instance, isotopically heavy Zn^{2+} ions may bind with ligands attached to organic molecules such as nicotianamine and histidine [27,59,60,61]. In contrast, the isotopically light Cd^{2+} ions may bind with the ligands of organic molecules such as glutathione or phytochelatins [18,68,69]. The metal-ligand complexes that are formed in such reactions are subsequently immobilized and stored in the cacao roots. The remaining unbound pool of isotopically light Zn^{2+} ions and isotopically heavy Cd^{2+} ions in the cytosol of the root cells are then preferentially loaded into the xylem and transferred to the cacao stems and leaves. The root-to-shoot translocation of isotopically light Zn^{2+} ions and isotopically heavy Cd^{2+} ions could be mediated by similar membrane proteins such as HMAs [9,17, 46, 70]. However, it is also conceivable that the two metals utilise distinct membrane transporters for root-to-shoot translocation in cacao plants. During root-to-shoot translocation of Zn, in order to maintain homeostasis, it is also likely that under high-Cd stress, additional regulation such as the activation of metallochaperones is necessary. This may explain the stronger preference for the transfer of isotopically light Zn to aerial plant organs under high Cd conditions. Further studies

are required to better understand the dynamics of the interaction of Zn and Cd in cacao plants, in particular concerning the mechanisms involved in their root-to-shoot translocation.

4.6. Conclusion

All 19 cacao genotypes analysed in this study preferentially removed isotopically light Zn from the hydroponic solutions, with a mean fractionation factor of $\varepsilon^{66}Zn_{uptake}$ = –1.15±0.36‰ (2SD). The uptake of Zn by the cacao plants was not noticeably impacted by exposure to different Cd concentrations (0, 5 and 20 µmol L^{-1} $CdCl_2$) in the hydroponic solutions during the growing period. The exposure to different Cd concentrations, however, influenced the translocation of Zn, whereby the isotope fractionation was enhanced when the plants were exposed to higher Cd concentrations. In detail, the Zn isotope fractionation factor for translocation from roots to shoots, $\varepsilon^{66}Zn_{seq\text{-}mob}$, was +0.17±0.13‰ (2SD) for plants grown with 0 and 5 µmol L^{-1} $CdCl_2$ in the hydroponic solution, but +0.52±0.36‰ (2SD) for cacao grown in hydroponic solutions with 20 µmol L^{-1} $CdCl_2$. These findings indicate that cacao plants most likely use similar physiological mechanisms for the uptake of both metals but distinct mechanisms for translocation. These interpretations are supported by published Cd isotope data for the same cacao plants that were analysed in the current study for Zn [46]. In detail, there is a concurrent enrichment of isotopically light Zn and Cd in the cacao plants in comparison to the hydroponic solutions. In contrast, cacao leaves revealed an inverse isotope fractionation pattern for the two metals, with light Zn isotopes and heavy Cd isotopes enriched in leaves relative to the roots. These systematics may reflect that Zn and Cd share the same membrane transporter proteins for uptake, but that the sequestration and translocation of the two metals is regulated by distinct organic molecules in the cacao roots. Furthermore, the root-

to-shoot translocation of Zn may be impacted by metallochaperones when elevated Cd concentrations are present in the plants.

Based on the findings of this study, there are broader implications for Cd isotope investigations of cacao plants. An important next step would be to examine the Cd isotope compositions of cacao plants cultured at different Zn conditions. Of particular interest is whether higher Zn concentrations in the nutrient media alter the uptake and translocation of Cd, both in hydroponics- and soil-plant systems, including for mature cacao plants. Such experiments may help to elucidate whether similar or distinct mechanisms are responsible for Zn and Cd homeostasis in cacao plants. In particular, if such work confirms that Zn and Cd share similar uptake mechanisms, this may enable the use of Zn amendments to soils to reduce the overall Cd uptake of cacao by a competition mechanism. Furthermore, the contrasting isotope systematics of the two metals within the plants suggest it may be possible to mitigate the high Cd concentrations of cacao beans without affecting essential Zn, via knock-out or overexpression of genes responsible for encoding proteins that assist in the translocation of Cd to above-ground parts or in the sequestration in roots, respectively. Also desirable are XAS studies to further constrain Zn and Cd speciation and ligand binding environments in different cacao plant organs and investigations of genes that are likely to play a role in the uptake, sequestration and mobilisation of the two metals.

4.7. References

1. Vallee, B. L. & Auld, D. S. Functional zinc-binding motifs in enzymes and DNA-binding proteins. *Faraday Discussions* **93**, 47-65 (1992).
2. Coleman, J. E. Zinc Proteins: Enzymes, Storage Proteins, Transcription Factors, and Replication Proteins. *Annual Review of Biochemistry* **61**, 897-946 (1992).
3. Coleman, J.E. Zinc enzymes. *Current Opinion in Chemical Biology* **2**, 222–234 (1998).
4. Lin, Y. F. & Aarts, M. G. M. The molecular mechanism of zinc and cadmium stress response in plants. *Cellular and Molecular Life Sciences* **69**, 3187-3206 (2012).
5. Caldelas, C. & Weiss, D. J. Zinc Homeostasis and isotopic fractionation in plants: a review. *Plant Soil* **411**, 17-46 (2017).
6. Broadley, M. R., White, P. J., Hammond, J. P., Zelko, I. & Lux, A. Zinc in plants. *The New Phytologist* **173**, 677-702 (2007).
7. Cai, Y. *et al*. Mechanisms and uncertainties of Zn supply on regulating rice Cd uptake. *Environmental Pollution* **253**, 959-965 (2019).
8. Gupta, N., Ram, H. & Kumar, B. Mechanism of Zinc absorption in plants: uptake, transport, translocation and accumulation. *Reviews in Environmental Science and Bio/Technology* **15**, 89-109 (2016).
9. Tang, Y. *et al*. Fractionation of Stable Zinc Isotopes in the Field-Grown Zinc Hyperaccumulator *Noccaea caerulescens* and the Zinc-Tolerant Plant *Silene vulgaris*. *Environmental Science & Technology* **46**, 9972-9979 (2012).
10. Tang, Y. *et al*. Zinc Isotope Fractionation in the Hyperaccumulator *Noccaea caerulescens* and the Nonaccumulating Plant *Thlaspi arvense* at Low and High Zn Supply. *Environmental Science & Technology* **50**, 8020-8027 (2016).

11. Deng, T. *et al*. Nickel and Zinc Isotope Fractionation in Hyperaccumulating and Nonaccumulating Plants. *Environmental Science & Technology* **48**, 11926 (2014).
12. Aucour, A. M., Pichat, S., Macnair, M. R. & Oger, P. Fractionation of Stable Zinc Isotopes in the Zinc Hyperaccumulator *Arabidopsis halleri* and Nonaccumulator *Arabidopsis petraea. Environmental Science & Technology* **45**, 9212-9217 (2011).
13. Aucour, A. *et al*. Zn Speciation and Stable Isotope Fractionation in a Contaminated Urban Wetland Soil–*Typha latifolia* System. *Environmental Science & Technology* **51**, 8350-8358 (2017).
14. Zhou, J. *et al*. Zinc uptake and replenishment mechanisms during repeated phytoextraction using *Sedum plumbizincicola* revealed by stable isotope fractionation. *The Science of the Total Environment* **806**, 151306 (2022).
15. Li, S., Zhu, X., Wu, L. & Luo, Y. Zinc, iron, and copper isotopic fractionation in *Elsholtzia splendens* Nakai: A study of elemental uptake and (re)translocation mechanisms. *Journal of Asian Earth Sciences* **192**, 104227 (2020).
16. Houben, D. *et al*. Impact of Root-Induced Mobilization of Zinc on Stable Zn Isotope Variation in the Soil–Plant System. *Environmental Science & Technology* **48**, 7866 (2014).
17. van der Ent, A. *et al*. Isotopic signatures reveal zinc cycling in the natural habitat of hyperaccumulator *Dichapetalum gelonioides* subspecies from Malaysian Borneo. *BMC Plant Biology* **21**, 1-437 (2021).
18. Wiggenhauser, M. *et al*. Zinc isotope fractionation during grain filling of wheat and a comparison of zinc and cadmium isotope ratios in identical soil–plant systems. *The New Phytologist* **219**, 195-205 (2018).

19. Arnold, T. *et al*. Iron and zinc isotope fractionation during uptake and translocation in rice (Oryza sativa) grown in oxic and anoxic soils. *Comptes Rendus Geoscience* **347**, 397-404 (2015).
20. Jouvin, D. *et al*. Stable Isotopes of Cu and Zn in Higher Plants: Evidence for Cu Reduction at the Root Surface and Two Conceptual Models for Isotopic Fractionation Processes. *Environmental Science & Technology* **46**, 2652-2660 (2012).
21. Weiss, D. J. *et al*. Isotopic Discrimination of Zinc in Higher Plants. *The New Phytologist* **165**, 703-710 (2005).
22. Viers, J. *et al*. Evidence of Zn isotopic fractionation in a soil–plant system of a pristine tropical watershed (Nsimi, Cameroon). *Chemical Geology* **239**, 124-137 (2007).
23. Moynier, F. *et al*. Isotopic fractionation and transport mechanisms of Zn in plants. *Chemical Geology* **267**, 125-130 (2009).
24. Aucour, A. *et al*. Dynamics of Zn in an urban wetland soil–plant system: Coupling isotopic and EXAFS approaches. *Geochimica et Cosmochimica Acta* **160**, 55-69 (2015).
25. Wiggenhauser, M. *et al*. Stable Isotope Fractionation of Metals and Metalloids in Plants: A Review. *Frontiers in Plant Science* **13**, 840941 (2022).
26. von Blanckenburg, F., von Wirén, N., Guelke, M., Weiss, D. J. & Bullen, T. D. Fractionation of metal stable isotopes by higher plants. *Elements* **5**, 375-380 (2009).
27. Fujii, T., Moynier, F., Blichert-Toft, J. & Albarède, F. Density functional theory estimation of isotope fractionation of Fe, Ni, Cu, and Zn among species relevant to geochemical and biological environments. *Geochimica et Cosmochimica Acta* **140**, 553-576 (2014).

28. Rizwan, M., Ali, S., Rehman, M. Z. u. & Maqbool, A. A critical review on the effects of zinc at toxic levels of cadmium in plants. *Environmental Science and Pollution Research* **26**, 6279-6289 (2019).

29. Sanaeiostovar, A., Khoshgoftarmanesh, A. H. & Shariatmadari, H. Effects of zinc activity in nutrient solution on uptake, translocation, and root export of cadmium and zinc in three wheat genotypes with different zinc efficiencies. *Soil Science and Plant Nutrition* **57**, 681-690 (2011).

30. Hart, J. J., Welch, R. M., Norvell, W. A. & Kochian, L. V. Transport interactions between cadmium and zinc in roots of bread and durum wheat seedlings. *Physiologia Plantarum* **116**, 73-78 (2002).

31. Du, J. *et al*. The presence of zinc reduced cadmium uptake and translocation in *Cosmos bipinnatus* seedlings under cadmium/zinc combined stress. *Plant Physiology and Biochemistry* **151**, 223-232 (2020).

32. Cheng, M., Kopittke, P. M., Wang, A., Sale, P. W. G. & Tang, C. Cadmium reduces zinc uptake but enhances its translocation in the cadmium-accumulator, *Carpobrotus rossii*, without affecting speciation. *Plant Soil* **430**, 219-231 (2018).

33. dos Santos, M. L. S. *et al*. Mitigation of cadmium toxicity by zinc in juvenile cacao: Physiological, biochemical, molecular and micromorphological responses. *Environmental and Experimental Botany* **179**, 104201 (2020).

34. Sharma, R. K. & Agrawal, M. Single and Combined Effects of Cadmium and Zinc on Carrots: Uptake and Bioaccumulation. *Journal of Plant Nutrition* **29**, 1791-1804 (2006).

35. El Rasafi, T. *et al*. Cadmium stress in plants: A critical review of the effects, mechanisms, and tolerance strategies. *Critical Reviews in Environmental Science and Technology* **52**, 675 (2020).

36. Rahimzadeh, R. M., Rafati Rahimzadeh, M., Kazemi, S., & Moghadamnia, A. A. Review Article Cadmium toxicity and treatment: An update. *Caspian Journal of Internal Medicine* **8**, 135 (2017).
37. Maddela, N. R. *et al*. Cocoa-laden cadmium threatens human health and cacao economy: A critical view. *The Science of the Total Environment* **720**, 137645 (2020).
38. Engbersen, N. *et al*. Cadmium accumulation and allocation in different cacao cultivars. *The Science of the Total Environment* **678**, 660-670 (2019).
39. Barraza, F. *et al*. Distribution, contents and health risk assessment of metal(loid)s in small-scale farms in the Ecuadorian Amazon: An insight into impacts of oil activities. *The Science of the Total Environment* **622-623**, 106-120 (2018).
40. Barraza, F. *et al*. Cadmium bioaccumulation and gastric bioaccessibility in cacao: A field study in areas impacted by oil activities in Ecuador. *Environmental Pollution* **229**, 950-963 (2017).
41. Argüello, D. *et al*. Soil properties and agronomic factors affecting cadmium concentrations in cacao beans: A nationwide survey in Ecuador. *Science of the Total Environment* **649**, 120-127 (2019).
42. Gramlich, A. *et al*. Soil cadmium uptake by cocoa in Honduras. *The Science of the Total Environment* **612**, 370-378 (2018).
43. Chavez, E. *et al*. Concentration of cadmium in cacao beans and its relationship with soil cadmium in southern Ecuador. *The Science of the Total Environment* **533**, 205-214 (2015).
44. The European Commission. Commission Regulation (EU) No 488/ 2014 of 12 May 2014 Amending Regulation (EC) No. 1881/2006 as regards maximum levels of cadmium in foodstuffs. *Official Journal of European Union* **138**, 75–79 (2014).

45. Barraza, F. *et al*. Cadmium isotope fractionation in the soil - cacao systems of Ecuador: a pilot field study. *RSC Advances* **9**, 3411-3422 (2019).
46. Moore, R. E. T. *et al*. Cadmium isotope fractionation reveals genetic variation in Cd uptake and translocation by *Theobroma cacao* and role of natural resistance-associated macrophage protein 5 and heavy metal ATPase-family transporters. *Horticulture Research* **7**, 71 (2020).
47. Vanderschueren, R. *et al*. Mitigating the level of cadmium in cacao products: Reviewing the transfer of cadmium from soil to chocolate bar. *The Science of the Total Environment* **781**, 146779 (2021).
48. Hamdan, M., Chou Khai Soong Karlson, Ee Yang Teoh, Su-Ee Lau & Boon Chin Tan. Genome Editing for Sustainable Crop Improvement and Mitigation of Biotic and Abiotic Stresses. *Plants* **11**, 2625 (2022).
49. Nguyen, N. T., McInturf, S. A. & Mendoza-Cózatl, D. G. Hydroponics: A Versatile System to Study Nutrient Allocation and Plant Responses to Nutrient Availability and Exposure to Toxic Elements *Journal of Visualized Experiments* **113**, 54317 (2016).
50. Monte-Bello, C. *et al*. A Flexible Low-Cost Hydroponic System for Assessing Plant Responses to Small Molecules in Sterile Conditions. *Journal of Visualized Experiments* **138**, 57800 (2018).
51. Cornejo, O. E. *et al*. Population genomic analyses of the chocolate tree, *Theobroma cacao* L.*,* provide insights into its domestication process. *Communications Biology* **1** (2018).
52. Moore, R. E. T., Larner, F., Coles, B. J. & Rehkämper, M. High Precision Zinc Stable Isotope Measurement of Certified Biological Reference Materials Using the Double Spike Technique and Multiple Collector-ICP-MS. *Analytical and Bioanalytical Chemistry* **409**, 2941-2950 (2017).

53. Arnold, T. *et al*. Measurement of zinc stable isotope ratios in biogeochemical matrices by double-spike MC-ICPMS and determination of the isotope ratio pool available for plants from soil. *Analytical and Bioanalytical Chemistry* **398**, 3115-3125 (2010).

54. Archer, C. *et al*. Inter-calibration of a proposed new primary reference standard AA-ETH Zn for zinc isotopic analysis. *Journal of Analytical Atomic Spectrometry* **32**, 415-419 (2017).

55. Siebert, C., Nägler, T. F. & Kramers, J. D. Determination of molybdenum isotope fractionation by double-spike multicollector inductively coupled plasma mass spectrometry. *Geochemistry, Geophysics, Geosystems* **2,** 2000GC000124 (2001).

56. Bridgestock, L. J. *et al*. Unlocking the zinc isotope systematics of iron meteorites. *Earth and Planetary Science Letters* **400**, 153-164 (2014).

57. Smolders, E. *et al*. Isotopic fractionation of Zn in tomato plants suggests the role of root exudates on Zn uptake. *Plant Soil* **370**, 605-613 (2013).

58. Ullah, I., Wang, Y., Eide, D. J. & Dunwell, J. M. Evolution, and functional analysis of Natural Resistance-Associated Macrophage Proteins (NRAMPs) from Theobroma cacao and their role in cadmium accumulation. *Scientific Reports* **8**, 14412-15 (2018).

59. Moynier, F., Vance, D., Fujii, T. & Savage, P. The isotope geochemistry of zinc and copper. *Reviews in Mineralogy and Geochemistry* **82**, 543-600 (2017).

60. Haydon, M. J. & Cobbett, C. S. Transporters of Ligands for Essential Metal Ions in Plants. *The New Phytologist* **174**, 499-506 (2007).

61. Clemens, S., Deinlein, U., Ahmadi, H., Höreth, S. & Uraguchi, S. Nicotianamine is a major player in plant Zn homeostasis. *Biometals* **26**, 623-632 (2013).

62. Dykema, P.E. *et al*. A new class of proteins capable of binding transition metals. *Plant Molecular Biology* **41**,139–150 (1999).

63. Suzuki, N., Yamaguchi, Y., Koizumi, N. & Sano, H. Functional characterization of a heavy metal binding protein CdI19 from *Arabidopsis*. *The Plant Journal* **32**, 165-173 (2002).

64. Tehseen, M., Cairns, N., Sherson, S. & Cobbett, C. S. Metallochaperone-like genes in *Arabidopsis thaliana*. *Metallomics* **2**, 556-564 (2010).

65. Rono, J. K., Sun, D. & Yang, Z. M. Metallochaperones: A critical regulator of metal homeostasis and beyond. *Gene* **822**, 146352 (2022).

66. Cao, H.W., Li, C., Zhang, Q. B., R, J. K., & Yang, Z. M. A metallochaperone Hipp33 is required for rice zinc and iron homeostasis and productivity. *Agronomy* **12**, 488 (2022).

67. Khan, I. U. *et al*. Identification of novel rice (Oryza sativa) HPP and HIPP genes tolerant to heavy metal toxicity. *Ecotoxicology and Environmental Safety* **175**, 8-18 (2019).

68. Wiggenhauser, M. *et al*. Cadmium transfer in contaminated soil-rice systems: Insights from solid-state speciation analysis and stable isotope fractionation. *Environmental Pollution* **269**, 115934 (2021).

69. Zhao, Y. *et al*. Theoretical isotope fractionation of cadmium during complexation with organic ligands. *Chemical Geology* **571**, 120178 (2021).

70. Zhong, S. *et al*. Cadmium uptake and transport processes in rice revealed by stable isotope fractionation and Cd-related gene expression. *The Science of the Total Environment* **806**, 150633 (2022).

71. Barraza, F. *et al.* Beyond cadmium accumulation: Distribution of other trace elements in soils and cacao beans in Ecuador. *Environmental research* **192**, 110241 (2021).

72. Gramlich, A. *et al.* Cadmium uptake by cocoa trees in agroforestry and monoculture systems under conventional and organic management. *The Science of the Total Environment* **580,** 677-686 (2017).

Chapter 5

Uptake and translocation of essential and non-essential elements in cacao (*Theobroma cacao* L.): An Ecuador field study

5.1. Declaration of research contributions

Elnaz Barati (Imperial College London) collected multi-elemental data for cacao samples from Ecuador as well as analysed and interpreted all the data for cacao, soil leachate and bulk soil samples. Dr. Rebekah E. T. Moore (Imperial College London) collected Cd data for cacao and bulk soil samples from Ecuador. Mr. James Weeks (King's College London) collected multi-elemental data for soil leachates from Ecuador. Ms. Laudine Marchive (Géosciences Environnement Toulouse) collected multi-elemental and physico-chemical data for bulk soil samples from Ecuador. Dr. Eve Schreck provided technical assistance at the Géosciences Environnement Toulouse Laboratory facilities, and Dr. Alex Griffiths, Ms. Renata Magueta and Dr. Alex Morrell provided technical assistance at the London Metallomics Facility, King's College London.

5.2. Introduction

In tropical countries, cacao (*Theobroma cacao* L.) is one of the most important agricultural commodities. Between 7 and 8 million smallholder farmers worldwide produce more than 80% of global cacao supply [1]. Ecuador is the third largest producer of cacao [2], and is the largest producer of fine flavour cacao, accounting for roughly 65% of the global supply [1]. More than 10 traditionally grown cacao genotypes are cultivated in South America, including Amelonado, Contamana, Criollo, Curaray, Guianna, Iquitos, Marañon, Nacional, Nanay, and Purús [3]. In Ecuador, two common types are grown, Nacional and a Nacional hybrid called CCN-51 [1,2,4,5]. The Nacional genotype produces the fine flavoured cacao beans, whereas CCN-51 produces beans that are more sour and bitter tasting [2,4,5]. A growing

number of Ecuadorian farmers are using CCN-51, as it is perceived as more productive and disease-resistant than the Nacional genotype [1,2,4,5].

Smallholder farmers throughout Ecuador depend on the production, sale and export of cacao beans and cocoa-based products (e.g., cacao liquor or butter) for their subsistence [1,5]. However, cacao beans and cocoa-based products from South and Central American countries such as Ecuador commonly have problematically high Cd concentrations [6,7]. For instance, cacao beans from Ecuador have up to about 10 μg g^{-1} of Cd [8, 9, 10, 11], whilst other crop tree species, such as banana, pineapple, lemon and soursop, have fruit with Cd concentrations up to three orders of magnitude lower than cacao from the same plantation [11]. The high Cd concentrations of cacao beans pose health risks, as Cd is a recognized group 1 human carcinogen and linked to a variety of health conditions such as kidney and musculoskeletal diseases and various cancers [7,12,13]. Therefore, in 2019, the European Union (EU) imposed stricter limits on Cd concentrations in final cocoa-based products of between 0.1 to 0.8 μg g^{-1} [14]. The EU is one of the largest importers of cacao beans from South America, and these stringent regulations have ramifications for the subsistence and livelihoods of smallholder farmers that produce and export cacao beans [7].

Through understanding the distribution of Cd across different plant organs of the cacao tree, insights can be inferred about the underlying physiological mechanisms and pathways responsible for Cd uptake and its subsequent translocation to the beans [8,11,15]. These mechanisms include, for example, root uptake and short- and long-distance transport facilitated by membrane transporter proteins [6,15,16,17]. In addition, investigating other essential or non-essential elements in cacao trees can provide insights into whether Cd uses similar uptake and translocation mechanisms, such as the same membrane transporter proteins [6, 17, 18, 19].

Previous studies have looked at correlations between Cd and other trace elements, including Fe, Mg, Mn, Ni and Zn in aerial cacao organs like leaves, pod husks and beans [10,19, 20, 21, 22, 23]. For example, Romero-Estévez et al. [23] found no direct linear correlation between Ni and Cd in cacao beans and suggested that these two elements likely have distinct mechanisms for their uptake and translocation. To date, however, no studies have examined the mass distribution of both essential and non-essential elements in a full cacao tree-soil system. Additionally, no studies have examined the bioaccumulation and translocation factors for multiple elements for a full cacao-soil system. By understanding the overarching distribution relationships between different essential and non-essential elements in full cacao-soil systems, there may be opportunities to identify shared physiological mechanisms and subsequently identify possible mitigation strategies to reduce the accumulation of Cd in cacao beans. In particular, previous studies have suggested that Zn and Cd may share and compete for similar mechanisms during root uptake by cacao plants [24, 25], such that the addition of Zn supplements, through fertilisers added to soils (or hydroponic solutions), may help to reduce Cd uptake by and translocation in cacao trees [6].

This field study aims to examine the full cacao-soil systems across six smallholder cacao farms in Ecuador. The aims are to (1) understand the mass distribution of Cd, the essential metals Cu, Fe, Mg, Mn, Mo, Ni and Zn and the additional non-essential elements Al, As, and Co in (i) soil and the bioavailable soil pool, and (ii) total cacao trees (cacao fruit, leaves, woody biomass and roots) of the two most common Ecuadorian genotypes (Nacional and CCN-51); (2) assess how these elements bioaccumulate in and translocate within the trees; and (3) compare element bioaccumulation findings to previous studies. Other factors such as genotype effects, tree age effects, soil properties and farming practices are not directly examined or compared due the limited sample size considered in this pilot field study.

5.3. Samples

5.3.1. Cacao farms

Mature, fruit-producing cacao tree and soil samples were collected from 6 smallholder farms in March 2020. Farms 1 and 2 are near Mompiche, Esmeraldas, Farm 3 is near Atacames, Esmeraldas, and Farms 4 to 6 are near Puerto Inca, Guayas (Appendices Figure A5.1). These farms were primarily selected due to previously reported high Cd concentrations in cacao beans in the Ecuadorian localities these farms are situated in and their selection of the most commonly grown cacao species in Ecuador (Nacional or CCN-51) [10]. Farms 1 to 5 are members of the agricultural cooperative *Ethiquable*. These farms strictly adhere to organic farming practices, whereby plant litter is used as a soil conditioner, and they do not apply agrichemicals such as P-fertilisers and herbicides. Farm 6 is a conventional farm that applies P-fertilisers once a year and herbicides three times a year.

5.3.2. Sample collection and initial preparation

Between one and four cacao trees of either the Nacional or CCN-51 variety were sampled at each farm, with tree ages ranging between 4 and 50 years old (Appendices Table A5.1). Cacao fruit (including pod husks, mucilage, and beans), leaves, branches, bark and lateral roots were sampled to characterise the distribution of the elements within each tree. Ten mature and young leaves were taken from each tree, from different branches. In addition, both ripe and unripe cacao fruits were collected. Leaf litter was also collected from around the base of each tree. Topsoil samples were collected at a depth of 0-20 cm about 50 cm away from the tree trunks, where the lateral roots are predominately found [26, 27].

Ten beans were sampled from each fruit pod on the day of collection and the mucilage was separated using a ceramic knife. The mucilage, bean and pod husk samples were kept in a cool box and the leaf, branch, bark, root and soil samples were airdried before transportation to the Géosciences Environnement Toulouse (GET) laboratories for further preparation. The leaf and root samples were cleaned with deionised water and a soft plastic brush, and any lichen attached to the bark was carefully removed, using a ceramic knife. All plant samples were then dried at 60°C prior to shipping to the MAGIC Laboratories at Imperial College London (ICL) for further processing. The dried samples were ground using an agate pestle and mortar or a clear plastic tobacco grinder (leaves). Between samples, the grinding apparatuses were cleaned with 18.2 MΩ cm grade H_2O and ethanol.

5.4. Analytical methods

5.4.1. Laboratories and reagents

The analyses for this project were carried out in three different laboratories. Most work was done at the London Metallomics Facility (LMF) at Kings College London. Further analyses were also completed in the MAGIC Laboratories at ICL and in France, at the GET Laboratories and at the Plateforme d'Analyses Physico-Chimiques (PAPC) of the Laboratoire d'Écologie Fonctionnelle et Environnement, both in Toulouse.

At the LMF, the reagents used were 15.8 mol L^{-1} trace metal grade HNO_3 and 99% acetic acid (both from Fisher Scientific), ammonium fluoride and ammonium acetate (from Supelco), 99.4-100.6% ethylenediaminetetraacetic acid (EDTA) and ammonium nitrate (both

from Sigma-Aldrich), and ≥18.2 MΩ cm Milli-Q H_2O from a Millipore Ultra purification system.

At the GET and MAGIC Laboratories purified ~5.8 mol L^{-1} HCl, 15.4 mol L^{-1} HNO_3, and 28 mol L^{-1} HF were used, which were prepared by sub-boiling distillation of analytical grade mineral acids in quartz or Teflon stills. All acid dilutions were made with ≥18.2 MΩ cm Milli-Q H_2O from Millipore purification systems.

5.4.2. Analyses at the LMF

Most of the cacao and all soil leachate samples were prepared for analysis at the LMF. Except for the Cd data for the cacao plant parts, all elemental concentrations for these samples were determined by a single collector quadrupole ICP-MS (ICP-Q-MS) at the LMF. This encompasses the determination of Al, As, Cu, Co, Fe, Mg, Mn, Mo, Ni and Zn in cacao samples and Cd, Cu, Mn and Zn in the soil leachates.

5.4.2.1. Digestion of cacao samples

Between 150 and 300 mg of the various cacao plant samples were digested with a Milestone ultraWAVE microwave system at the LMF using a digestion protocol detailed in Appendices Note A5.1. For quality control, the NIST reference materials, spinach leaf SRM 1570a and baking chocolate SRM 2384, were digested alongside cacao samples, using masses that were matched to the latter. After digestion, the samples were dried on a hotplate and treated with 15.4 mol L^{-1} HNO_3 for conversion to the nitrate form. The samples were then dissolved in 1 mL of 2 mol L^{-1} HNO_3 and transferred to acid-cleaned trace metal free centrifuge tubes

(Elkay), in preparation for the concentration measurements. Analytical replicates of cacao samples (root, leaf litter, leaf, pod husk, mucilage and bean) from different trees were digested to determine their homogeneity and evaluate reproducibility.

5.4.2.2. Preparation of soil leachates

Leaching experiments were performed on aliquots of the soil samples to approximate the bioavailable pool, using published extraction protocols that apply different reagents: Mehlich-3, ammonium acetate (AA), and EDTA-ammonium acetate (EDTA-AA) [9, 28, 29]. Between 0.25 g and 1 g of soil were extracted using these protocols, which are further outlined in Appendices Note A5.2. After extraction, the solutions were dried, treated with 15.4 mol L^{-1} HNO_3 and dried again, and then taken up in 1 mL of 1 mol L^{-1} HNO_3, in preparation for concentration measurements. For quality control, 3 analytical replicate extractions were carried out with the different extraction methods on a homogenized soil sample from Farm 4.

5.4.2.3. Elemental concentration measurements by ICP-Q-MS

In preparation for the elemental concentration measurements, appropriate aliquots of the reference materials (NIST SRM 1570a, NIST SRM 2384) and cacao sample solutions were diluted by a factor of 10x for trace elements and 1000x for major elements, whilst the soil leachates were diluted by a factor of 10x, all using 0.2 mol L^{-1} HNO_3. For internal standardisation, the cacao samples, reference materials and procedural blanks were doped to 50 µg L^{-1} with standard solutions of Ga, In, Ir, Sc and Y prepared from Sigma Aldrich and Teledyne Leeman Labs standard solutions. As part of further quality control, an additional reference material, drinking water CRM-TMDW-500, and acid blanks were also prepared by

doping them with the internal standard solution to 50 µg L^{-1}. The soil leachates were doped with the same internal standard elements but only to 40 µg L^{-1}. External calibration standards with concentrations of between 0.1 and 5000 µg L^{-1} for the elements of interest were also prepared from Sigma Aldrich and Teledyne Leeman Labs standard solutions.

The elemental concentrations were determined using a Perkin Elmer NexION 350 ICP -Q-MS. Samples were introduced to the ICP-Q-MS with a Cetac ASX-100 autosampler and a quartz cyclonic spray chamber fitted with a SeaSpray glass nebuliser. The instrumental conditions for the ICP-Q-MS were as follows: 1600 W RF power, 1.2 L min^{-1} Ar auxiliary gas flow, 18 L min^{-1} Ar plasma gas flow, and 0.95 L min^{-1} nebuliser gas flow. Depending on the major and trace element concentration being measured, one of two mode settings were selected for the ICP-Q-MS: dynamic reaction cell (DRC), which reduces isobaric ion interferences, or kinetic energy discrimination (KED), which reduces polyatomic ion interferences [30]. The DRC mode utilized a cell gas flow of NH_3 (0.6 mL min^{-1}), whereas the KED mode utilized a He cell gas flow. For measuring ^{27}Al, a DRC mode setting with a 100 ms dwell time was used. For measuring ^{24}Mg, ^{75}As and ^{111}Cd and ^{55}Mn, ^{56}Fe, ^{59}Co, ^{60}Ni, ^{63}Cu and ^{66}Zn, KED modes with a He cell gas flow of 4.5 mL min^{-1} and dwell times of 50 ms and 100 ms were used, respectively. For determination of ^{95}Mo, the KED mode with a He cell gas flow of 0.5 mL min^{-1} and a 100 ms dwell time were applied.

Repeat measurements of procedural and acid blanks, a calibration standard solution and reference materials were conducted, to ensure the accuracy and precision of the cacao and soil leachate analyses. For each sample, 5 replicate measurements were completed. To account for instrumental drift and matrix effects, sample measurements were normalised to the internal standard solution. Following data acquisition, sample measurements were blank corrected by

subtracting the average relevant ion beam intensities determined in repeat blank measurements. The blank-corrected ion beam intensities were then converted to concentration data by interpolation to the calibration curve. The quality of the interpolation was verified by the linearity of the latter.

5.4.3. Analyses at the GET and PAPC Laboratories

Initial processing of the topsoil samples (hereafter referred to as "bulk soil", to distinguish them from the soil leachates) was carried out at the GET and PAPC Laboratories in Toulouse, France. This included the determination of the physico-chemical properties and measurements of As, Cu, Fe, Mg, and Mn concentrations by ICP-Q-MS, after full digestion.

5.4.3.1. Determination of physico-chemical properties of soils

The soil texture, pH and CEC (cation exchange capacity) of the bulk soils (0-20 cm) were determined at the GET Laboratories, while the TOC (total organic carbon), C, N, H, S and P concentrations were measured at the PAPC Laboratories. The soil texture was determined using laser granulometry. The soil pH measurements were carried out in triplicate on 1:5 soil dilutions with Milli-Q water using a EUTECH Instruments pH meter. The CEC was determined by spectrocolorimetry using the cobalt hexammine chloride exchange method [31]. The TOC and N abundances and the C, H and S concentrations were measured with a total organic carbon and nitrogen analyser (Shimadzu) and a C, H, N, S Flash-2000 elemental analyser (ThermoFisher Scientific), respectively [32]. The P concentrations were determined using a UVI light XT 5 SECOMAM spectrophotometer. The OM (organic matter) content was

calculated from the TOC results (in % w/w) by multiplying by 1.72, based on the assumption that OM consists of 58% of the TOC [33].

5.4.3.2. Determination of elemental concentrations of soils

The bulk soil samples were first processed in an agate ball mill (Fisher Biobloc Scientific–Retsch) for 10 to 20 mins and then ground in an agate mortar (Pulverisette 2) for 6 to 10 mins, to break down the soil aggregates into a fine powder. Once ground, 0.1 g of the bulk soil and reference material San Joachim Soil NIST SRM 2709a were digested on a hotplate using a protocol outlined in Appendices Note A5.3. After digestion, the sample solutions were passed through 0.22 µm syringe filters, dried in Savillex Teflon vials and taken up in 0.37 mol L^{-1} HNO_3, in preparation for concentration measurements. For quality control, analytical replicates were prepared for 8 bulk soil samples.

For the ICP-Q-MS measurements of elemental concentrations, the bulk soil samples were diluted by a factor of 4000x for trace elements (As, Cd, Cu, Fe and Mn) and by 40000x for major elements (Mg) using 0.37 mol L^{-1} HNO_3. An internal standard solution containing In and Re was added to the bulk soil, reference material (NIST SRM 2709a), procedural and acid blank solutions to obtain concentrations of between 2.5 and 3.9 µg L^{-1}. The calibration standard solutions had concentrations of between 0.1 and 5000 µg L^{-1} for the elements of interest.

The element concentrations were determined using an iCAP ICP-Q-MS (Thermo Scientific) fitted with a quartz cyclonic spray chamber and glass nebuliser. Similar instrumental configurations were implemented for the determination of ^{24}Mg, ^{55}Mn, ^{56}Fe, ^{63}Cu and ^{75}As as

were employed for the cacao and soil leachate analyses at the LMF. Three repeat measurements were carried out for procedural and acid blanks, reference material (NIST SRM 2709a) and the bulk soil samples. Following data acquisition, sample measurements were blank corrected and subsequently converted into concentration data.

5.4.4. Analyses at the MAGIC Laboratories

A minority of the cacao samples, as well as some analytical replicates together with the reference materials (NIST SRM 1570a, NIST SRM 2384, BCR 679 (White Cabbage)), were digested at the MAGIC Laboratories with a Milestone Ethos EZ microwave system, using methods identical to those employed at the LMF. In addition, accurate Cd concentration data were obtained for all cacao and bulk soil samples, alongside the reference materials (NIST SRM 1570a, NIST SRM 2384, BCR 679, NIST SRM 2709a), using a multiple collector (MC)-ICP-MS.

For the analyses, 5% to 10% sample solution aliquots (with about 100 to 150 ng Cd) were equilibrated with a ^{111}Cd–^{113}Cd double spike solution to obtain a ratio of double spike-derived to natural Cd of about 1 to 3. Chromatographic procedures followed by a liquid-liquid extraction clean-up step were then used to separate Cd at high yield from the sample solutions [34]. The purified Cd fractions were dissolved in 0.1 mol L^{-1} HNO_3 and analysed with a Nu Plasma II MC-ICP-MS using a Cetac autosampler and a Cetac Aridus II desolvation system, fitted with quartz glass nebuliser. These analyses determined the Cd isotope compositions of the spike-sample mixtures. These isotope data were subsequently processed using isotope dilution techniques to determine the Cd concentrations of the samples [34, 35].

5.5. Data analysis and calculations

5.5.1. Elemental (mass) distribution calculation

In this investigation, the elemental (dry mass) distributions were calculated for six trees from four of the six farms (Farms 3, 4, 5 and 6). For the calculations, the cacao trees were assumed to be comprised of four major reservoirs: roots, woody biomass, leaves and cacao fruit. Based on published data for the dry biomass of cacao trees, the mass fractions of the root, woody biomass, leaf and cacao fruit reservoirs were estimated as 11%, 67%, 22% and 1% of the total tree, respectively [36, 37, 38]. To determine the elemental distributions, the elemental concentrations were first calculated for these reservoirs. For woody biomass, leaves and cacao fruit, average element concentrations were determined from the individual data measured for branches and bark, young and mature leaves, and ripe pod husks, mucilage, and beans, respectively. The elemental concentrations calculated for the four reservoirs and the mass fractions of these reservoirs (determined from the dry biomass) were then employed to calculate the total elemental concentrations of the cacao tree and the elemental (mass) distributions. Finally, the calculated median elemental distributions were adjusted (normalised) to obtain a sum of 100%.

5.5.2. Bioaccumulation and translocation factors

Bioaccumulation factors (BFs) were calculated to quantify the transfer of elements from the soils to the cacao plants [39, 40]:

$$BF = \frac{[Sink]}{[Source]} \qquad \text{(Equation 5.1)}$$

where [sink] is the element concentration in individual cacao organs or the total cacao tree and [source] is the element concentrations in bulk soil or soil leachates. Whether plants are element 'accumulators', 'indicators' or 'excluders' is determined by their BF. A BF of >1 indicates efficient enrichment (accumulator), BF ≈ 1 indicates neither enrichment nor exclusion (indicator), and BF < 1 indicates exclusion or inefficient uptake and/or transfer (excluder) [40,41].

The translocation of elements between two different plant organs was quantified by the translocation factor (TF) [42,43, 44]:

$$TF_{i-j} = \frac{[Cacao\ Organ_i]}{[Cacao\ Organ_j]} \qquad \text{(Equation 5.2)}$$

The notation [cacao organ] represents the element concentration of a given plant organ and the subscripts "i" and "j" denote two distinct organs. A TF > 1 indicates that the plant is efficient in transporting a given element from one organ to another, whilst a TF < 1 demonstrates inefficient element transport between the organs [44].

5.6.Results

5.6.1. Quality control

The limits of detection (LOD) and quantification (LOQ) for cacao, bulk soil and soil leachate samples were calculated as 3x and 10x the standard deviation determined for the 5, 3 and 2 relevant procedural blanks, respectively. The trueness of the concentration data was assessed based on the results obtained for the reference materials (Appendices Tables A5.2, A5.3, A5.4 and A5.5). The reproducibility of the concentration data, which can be affected by

both the analytical precision and the homogeneity of the samples were assessed by the analyses of the analytical replicates (Appendices Tables A5.6, A5.7 and A5.8).

5.6.1.1. Cacao samples

All cacao concentration data for As, Cd, Co, Cu, Fe, Mg, Mn, Mo, Ni and Zn were above the LOD and LOQ (Appendices Table A5.2 and A5.3). For Al, 6 of 16 samples, all ripe cacao beans, had concentrations below the LOD and LOQ and these data were excluded from further consideration. The average procedural blank contributions to the Al, Cd, Co, Cu, Fe, Mn, Ni and Zn inventories of the samples were 2.02%, 0.02%, 0.14%, 0.17%, 0.24%, 0.03%, 0.24%, 0.30%, respectively. The remaining elements, As, Mg, and Mo, had procedural blank contributions of <0.001%. Following blank correction, the bias of the measured concentration data was between 1% and 26% for the different reference materials (Appendices Table A5.2 and A5.3). For CRM-TMDW-500 (n=8), the bias for Al, As, Cu, Co, Fe, Mn, Mg, Mo, Ni and Zn was between 5% and 12%. For NIST SRM 2384 (n=2), the Cd, Cu, Fe, Mg, Mn, and Zn data had a bias of between 1% and 14%. Finally, for NIST SRM 1570a (n=3), the results for Al, As, Cd, Mn, and Zn had a bias of between 1% and 13%, whilst the bias was 21% and 26% for Cu, Co and Ni. For BCR 679 (n=2), the results for Cd had a bias of 2%. Together, these results demonstrate generally good to acceptable agreement between measured and published concentration data for the analysed reference materials (Appendices Table A5.2 and A5.3).

The 11 analytical replicates of mature leaves, leaf litter, pod husks, mucilage, beans and roots analysed by ICP-Q-MS yielded element concentrations with CVs that were mostly better than 25%, except for Mo (Appendices Table A5.6). For Mo, the analytical replicates of leaf litter, pod husks, mucilage and roots samples yielded CV values of between 55% and 90%

(Appendices Table A5.6). For the Cd concentration measurements by isotope dilution and MC-ICP-MS, the 7 analytical replicates yielded CVs between 0.5% and 17% (Appendices Table A5.6). Overall, the analytical replicates indicate excellent to acceptable reproducibility, and hence sample homogeneity, for the cacao samples.

5.6.1.2. Bulk soil samples

All bulk soil concentration data for Cd, Cu, Mn, and Zn were above the LOD and LOQ (Appendices Table A5.4). The bulk soil concentrations of As, Cd, Cu, Fe, Mg and Mn were corrected for small blank contributions, with average procedural blank contributions of 0.88%,0.06%,0.39%, 0.02%, 0.15% and 0.03%, respectively. For the NIST SRM 2709a (n=2) reference material, the measured As, Cd, Cu, Fe and Mn concentrations had a bias of between 0.3% and 6% but for Mg this was 19%. Thus, the reference material data show good to acceptable agreement with the published literature (Appendices Table A5.4). The analytical replicates yielded concentrations with CV values of better than 9% for As, Cu, Fe, Mg and Mn, indicating good reproducibility and homogeneity for the bulk soil samples (Appendices Table A5.7).

5.6.1.3. Soil leachate samples

The soil leachate concentration data for Cd, Cu, Mn and Zn were all above the LOD and LOQ (Appendices Table A5.5). The average exogenous blank contributions for Cd, Cu, Mn and Zn were 0.02%, 0.40%, 0.30% and 0.56%, respectively. Analyses of the matching reference material, CRM-TMDW-500 (n=15), gave Cd, Cu, Mn and Zn results with a bias of between 2% and 12%, and were therefore in good agreement with the literature (Appendices Table A5.5).

The three analytical replicates that were analysed for the soil leachates obtained using Mehlich-3, AA and EDTA-AA had CV values of better than 7%, 7%, 13%, and 23% for Cd, Cu, Mn, and Zn, respectively. This indicates good to acceptable analytical reproducibility and sample homogeneity (Appendices Table A5.8).

5.6.2. Cacao samples

5.6.2.1. Elemental concentrations of cacao organs

For essential elements, the range of concentrations determined for the cacao tree parts were 1–56 μg g^{-1} for Cu, 3–7280 μg g^{-1} for Fe, 314–9611 μg g^{-1} for Mg, 1–662 μg g^{-1} for Mn, 0.1–7 μg g^{-1} for Mo, 0.2–30 μg $g^{-1}$for Ni and 2–233 μg g^{-1} for Zn. For non-essential elements, the cacao organ concentrations had ranges of 0.022–11135 μg g^{-1} for Al, 0.002-2 μg g^{-1} for As, 0.5–11 μg g^{-1} for Cd and 0.03-18 μg g^{-1} for Co (Figure 5.1 and Appendices Table A5.9 and A5.10).

Almost all elements had high concentrations in the leaf litter. Excluding the leaf litter, the organs which showed the highest and lowest concentrations for particular elements were variable (Figure 5.1 and Appendices Table A5.9 and A5.10). Copper, Mo and Ni were most enriched in unripe and ripe beans (with 16–56 μg g^{-1} Cu), in ripe pod husks (with 0.2 –7 μg g^{-1} Mo) and unripe beans (with 7–26 μg g^{-1} Ni), respectively. Three elements were most concentrated in the mature leaves: Mn (60–656 μg g^{-1}), Co (1–7 μg g^{-1}) and Zn (31–155 μg g^{-1}). Two elements had their highest concentrations in the bark: Cd (4 –11 μg g^{-1}) and Mg (3668–

9611 μg g^{-1}). For three elements, the roots had the highest concentrations: Al (127–2351 μg g^{-1}), As (0.02 –0.6 μg g^{-1}) and Fe (21–630 μg g^{-1}).

Eight elements had the lowest concentrations in the cacao fruit organs: Al (0.022–5.1 μg g^{-1} in ripe and unripe beans), As (0.005–0.02 μg g^{-1} in unripe beans), Cd (0.7–0.9 μg g^{-1} in unripe mucilage and pod husk), Co (0.03–2 μg g^{-1} in ripe pod husk and ripe mucilage), Fe (7–27 μg g^{-1} in ripe pod husk), Mg (314–2014 μg g^{-1} in ripe mucilage), Mn (1–17 μg g^{-1} in ripe mucilage) and Mo (0.1–0.5 μg g^{-1} in unripe beans). For Co, in addition to having low concentrations in the cacao fruit parts, equally low levels were observed in the bark with results of 0.1–1 μg g^{-1}. Two other essential elements also had the lowest concentrations in the bark: Cu (2.0–4.3 μg g^{-1}) and Ni (0.2–2.2 μg g^{-1}). Zinc was the only element which was most depleted in the roots with concentrations of 3 –51 μg g^{-1}.

For essential elements, the range of concentrations determined for the total cacao tree were 3–9 μg g^{-1} for Cu, 81–192 μg g^{-1} for Fe, 4341–7141 μg g^{-1} for Mg, 30–317 μg g^{-1} for Mn, 0.5–1.2 μg g^{-1} for Mo, 0.8–6.3 μg $g^{-1}$for Ni and 37–118 μg g^{-1} for Zn (Appendices Table A5.9). For non-essential elements, the total cacao tree concentrations had ranges of 95–376 μg g^{-1} for Al, 0.03-0.09 μg g^{-1} for As, 2.7–8.9 μg g^{-1} for Cd and 0.4–1.6 μg g^{-1} for Co.

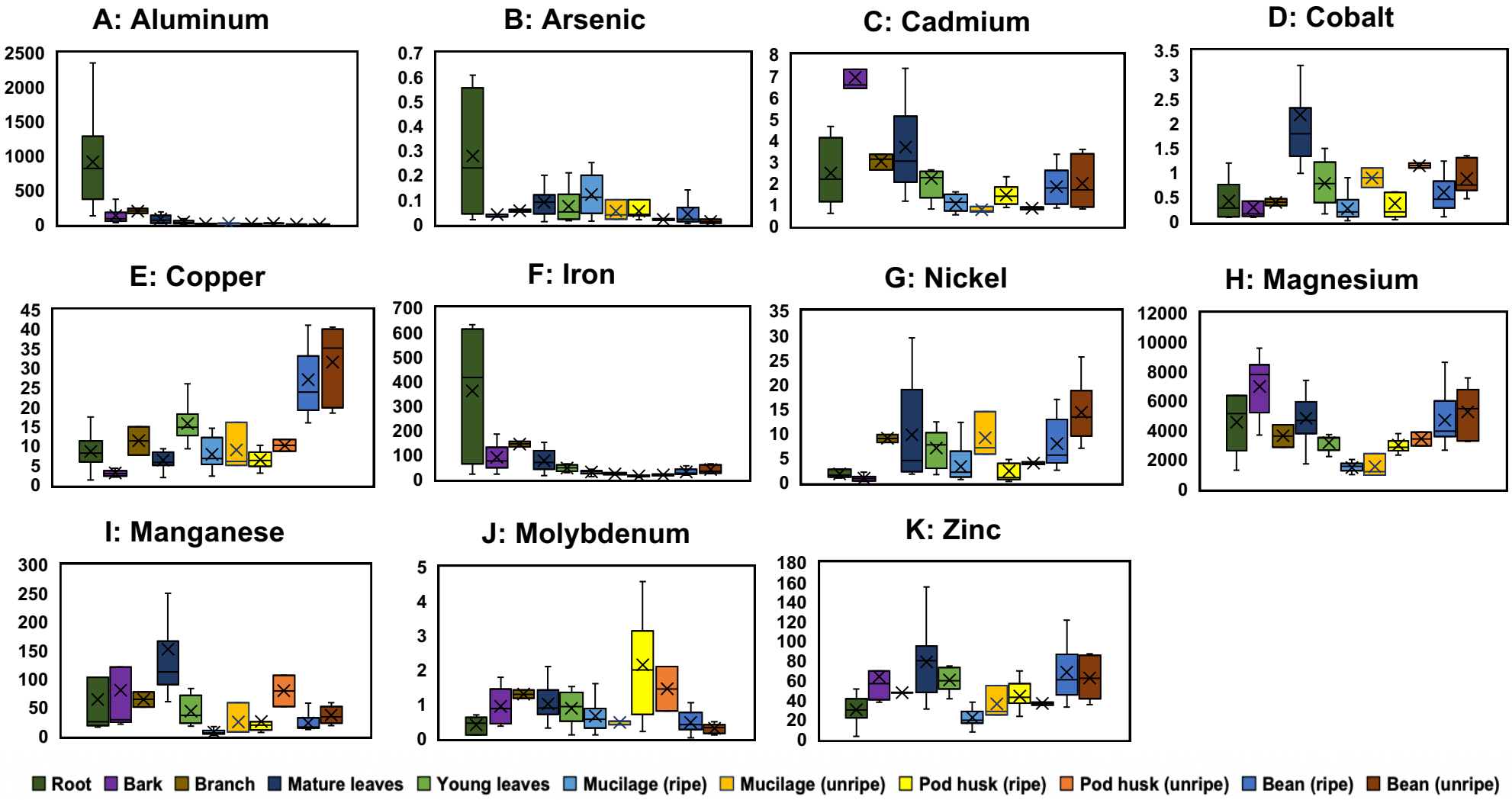


Figure 5.1. Element concentrations (μg g^{-1}) of cacao plant organs from the six farms.

5.6.2.2. Elemental distributions in the total cacao tree

The concentration data for six trees from four farms were employed to estimate the elemental (mass) distributions in the four major reservoirs of the cacao trees, namely roots, woody biomass, leaves, and fruit (Figure 5.2 and Appendices Figure A5.2, Table A5.11). For all elements, only a small mass fraction (median values <2%) was present in the cacao fruit. Considering the other reservoirs, the elements fall into four broad groups. (1) Particularly high mass fractions of Al, As and Fe are stored in the roots (median values between 25% and 52%), with similar or slightly lower mass fractions present in the woody biomass (median values between 36% and 60%). (2) For Zn, Cd and Mg the woody biomass was the primary reservoir, with median mass fractions of between 69% and 85%, whereas only a smaller fraction was stored in the leaves, with median results of 10% to 26%. (3) Copper, Mn and Mo are primarily stored to roughly equal amounts in woody biomass and leaves, with median mass fractions of 43%–63% and 32%–46%, respectively. (4) For Co and Ni, exceptionally high mass fractions were stored in the leaves, with median values of 69% and 71%, respectively.

Notably, there was significant variability for the elemental (mass) distributions, with most CV values determined from the data obtained for the six trees falling between 10% and 50% (Appendices Figure A5.2 and Table A5.11). Despite of this variability, however, the assignment of the elements to the four distinct distribution groups is robust, but there are two notable exceptions (Figure 5.2 and Appendices Figure A5.2). For Cu, the relatively large median mass fraction of 19% present in the roots combined with a CV of 39% implies that this element also has a distribution which is similar to that of Al, Fe and As. Similarly, for Mo the

high and variable median mass fraction of 63 ± 23% (CV) stored in the woody biomass implies that the elemental distribution is also akin to that of Zn, Cd and Mg.

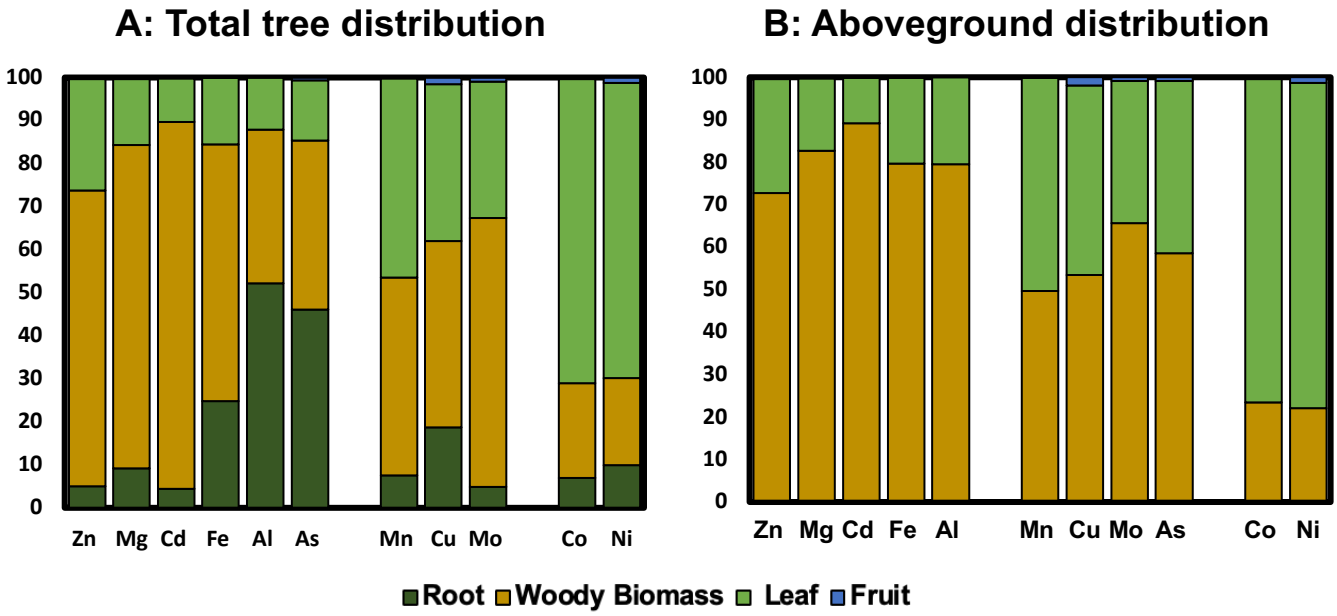


Figure 5.2. Median elemental (mass) distributions (%) determined for (a) total trees with root, woody biomass, leaf and fruit reservoirs and (b) aboveground tree parts with woody biomass, leaf and fruit reservoirs. The data are for six trees from Farms 3 to 6.

5.6.3. Soils

5.6.3.1. Physico-chemical properties of soils

All the bulk soil samples had similar textures, as they were of silty, silt-loam and silty-clay-loam type, with more than 60% of the soil consisting of silt particles and less than 40% of clay and sand particles. For the bulk soil samples from the 6 farms, the results ranged from 5–8 for the pH, 5–36 cmol+ kg^{-1} for the CEC, 1.2–5.4% for OM content, 0.7–2.8% for TOC, 0.7–3.2% for the C concentration, 0.1–0.3% for the N abundance, 8–12 for the C/N ratio, ≤0.1% for the S abundance, and 0.05–0.2% for the P concentration (Appendices Table A5.12).

5.6.3.2. Element Concentrations of bulk soils

The range of concentrations across the 6 farms for bulk soil were 1–23 μg g^{-1} for As, 0.3–2 μg g^{-1} for Cd, 35–70 μg g^{-1} for Cu, 28400–46400 μg g^{-1} for Fe, 6360–12100 μg g^{-1} for Mg and 320–1380 μg g^{-1} for Mn (Appendices Table A5.12).

5.6.3.3.Element concentrations of the soil leachates

Across the 6 farms, the Cd, Cu, Mn and Zn concentrations of soil leachates extracted using Mehlich-3 were 0.1–0.6 μg g^{-1}, 2.6–7.1 μg g^{-1}, 15–179 μg g^{-1} and 0.7–8 μg g^{-1}, respectively (Figure 5.3 and Appendices Table A5.13). Similar element concentrations were extracted from soil leachates using EDTA-AA, with Cd, Cu, Mn and Zn concentration of 0.08–0.7 μg g^{-1}, 2.7–10 μg g^{-1}, 10–191 μg g^{-1}, and 0.09–5.1 μg g^{-1}, respectively. The lowest element concentrations extracted from bulk soils were for leachates obtained using AA, which had Cd,

Cu, Mn and Zn concentrations of 0.04–0.2 μg g^{-1}, 0.03–0.2 μg g^{-1}, 0.05–139 μg g^{-1}, and 0.05–0.7 μg g^{-1}, respectively.

Together, bulk soil and leachate element concentration data can be used to calculate extraction efficiencies (%), which denote the fraction of elements extracted from the bulk soils using different reagents. For the soil leachate samples, the range of mass fractions of Cd, Cu and Mn that were extracted from bulk soils using Mehlich-3 were 19%–60%, 5%–12% and 2%–27%, respectively (Appendices Table A5.14). When EDTA-AA was used for soil extraction, the range of fractions extracted for Cd, Cu and Mn were 21%–59%, 5%–17% and 2%–14%, respectively. A somewhat lower extraction efficiency was observed for AA, with extracted range of mass fractions for Cd, Cu and Mn of 7%–31%, 0.1%–0.3% and 0.01%–10%, respectively. In detail, these results revealed similarities and statistically significant differences ($p < 0.05$) in extraction efficiencies. In particular, Mehlich-3 (with pH ≈ 2.5) and EDTA-AA (with pH ≈ 4.6–5.3) extracted higher concentrations of Cd, Cu, Zn and Mn than the less acidic AA (pH ≈ 7; Figure 5.3 and Appendices Table A5.14). Furthermore, Mehlich-3 and EDTA-AA extracted similar amounts of Cd and Mn from bulk soils. However, there was a statistically significant difference between Mehlich-3 and EDTA-AA for the extraction of Cu. The findings of this study for the Mehlich-3 soil leachates are, therefore, consistent with the results of Chavez et al. [9], who also found that Mehlich-3 is better able to extract Cd from soils in comparison to AA.

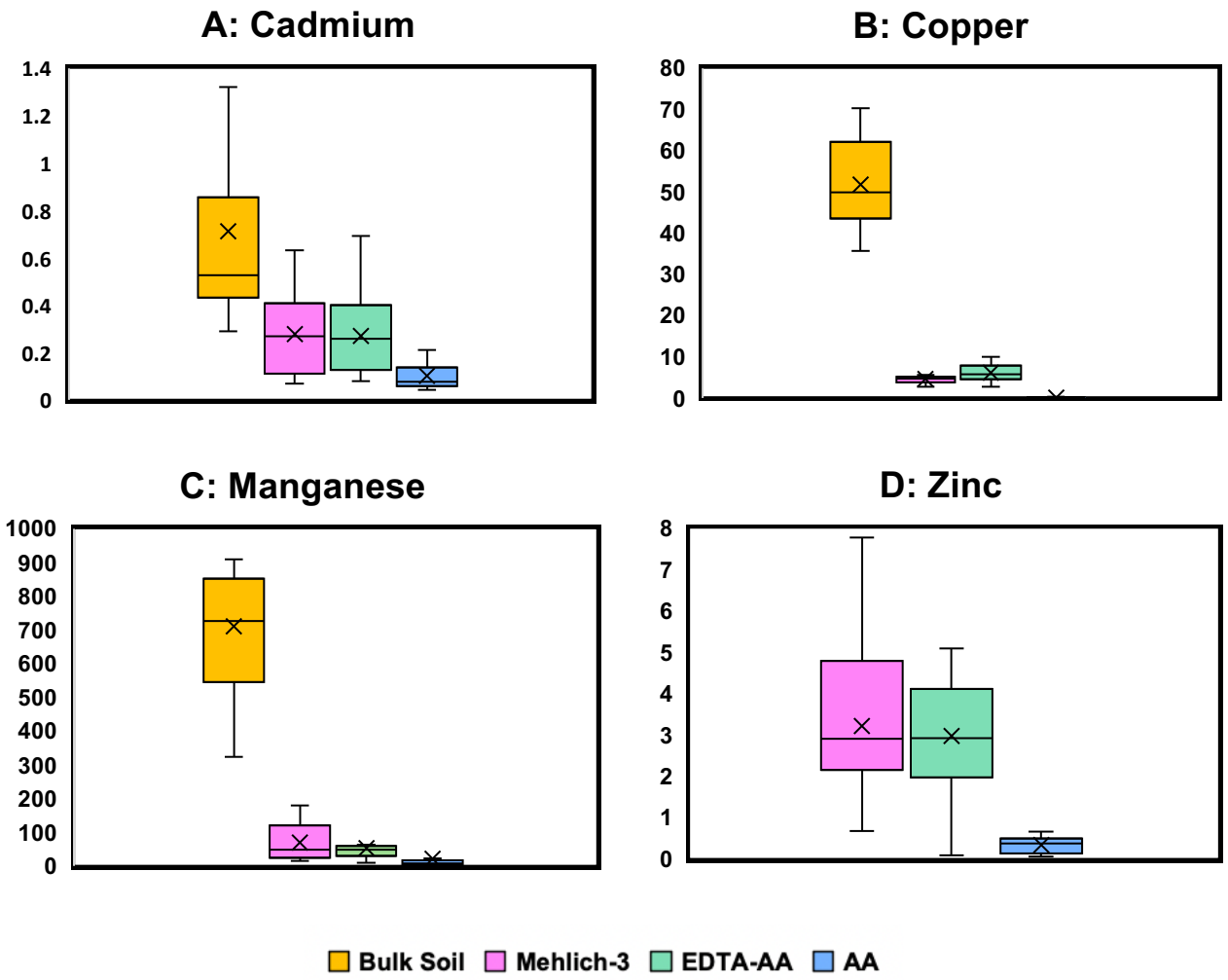


Figure 5.3. Element concentrations (µg g-1) for bulk soil samples and the Mehlich-3, EDTA-AA and AA soil leachates from the six farms.

5.7. Discussion

5.7.1. Element uptake and bioaccumulation by cacao trees

5.7.1.1. Bioaccumulation factors between total plants and bulk soils

Bioaccumulation factors provide deeper insights into elemental transfers within plant-soil systems. Firstly, if total tree mass balances can be applied, BF values demonstrate the overall ability of an entire plant to take up efficiently elements from soils, or more specifically, the elemental uptake capabilities of a particular plant species. Secondly, BF values can also elucidate the elemental accumulation efficiencies of an individual plant organ. In particular, BF values can demonstrate how efficiently a particular organ such as the leaves or bean is able to transfer an element from the soils.

The current findings demonstrate for the first time the elemental uptake capabilities of cacao trees for different elements. Notably, the median BF values for As, Cu, Fe, Mg and Mn between total cacao trees and bulk soils ($BF_{\text{total plant-bulk soil}}$; $n = 6$) were consistently less than 1 (Figure 5.4 and Appendices Table A5.15). These findings suggest that cacao trees do not readily remove or accumulate these elements from soils. For Cd, in contrast to the other elements, the data yielded a median $BF_{\text{total plant-bulk soil}}$ value of 11±4 (median absolute deviation; MAD, $n = 6$). These results, hence, indicate that total cacao trees take up Cd from soils much more efficiently than other elements. To date, however, no previous studies have attempted to examine $BF_{\text{total plant-bulk soil}}$ values for different elements in cacao trees, as such it is difficult to confirm the findings of this research with previous investigations. Nonetheless, these initial

findings provide compelling evidence that cacao trees, as a plant species, are most likely 'Cd accumulators'.

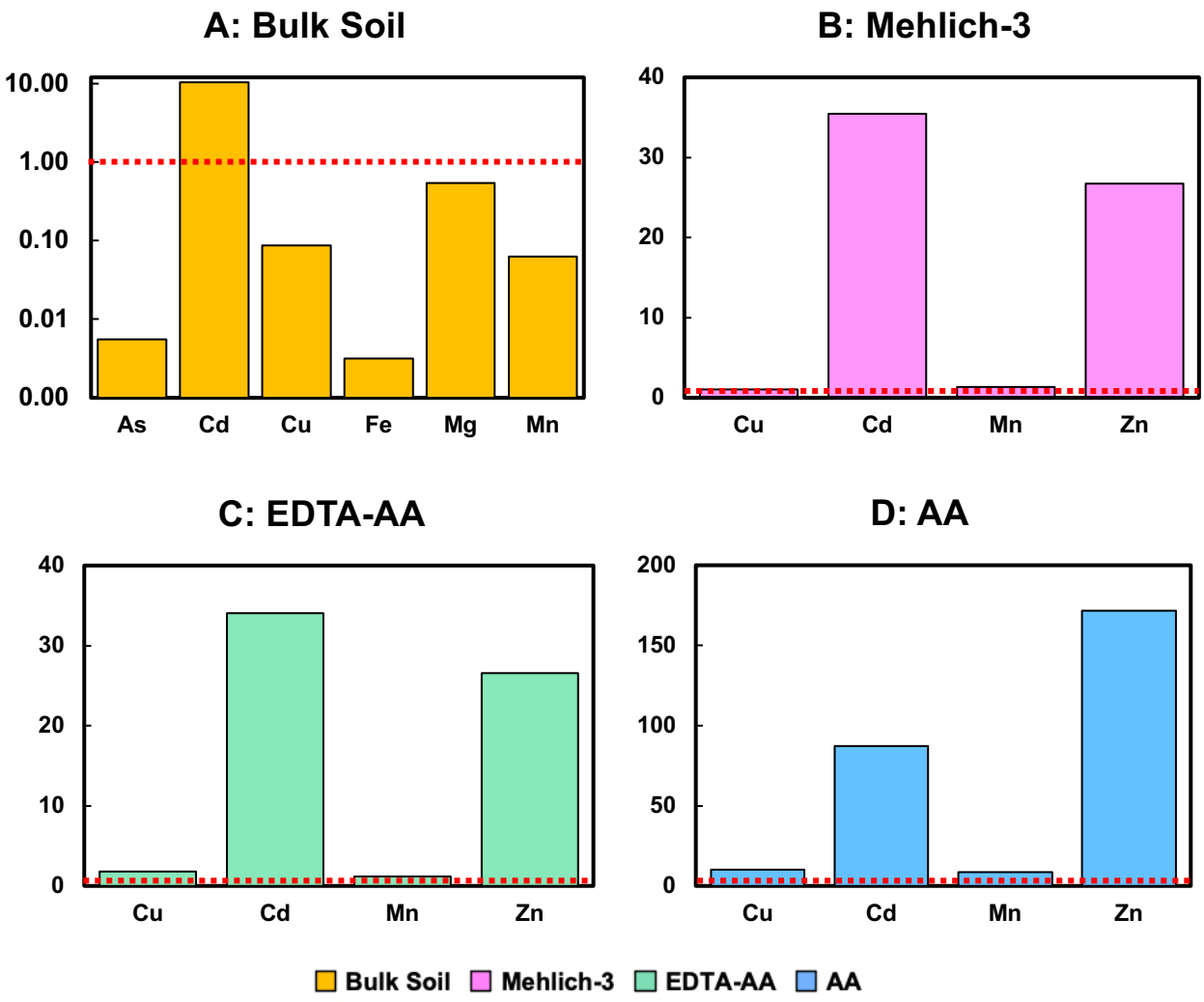


Figure 5.4. Median BF values for elements between six total cacao trees from Farms 3 to 6 and (a) bulk soils, and the (b) Mehlich-3, (c) EDTA-AA and (d) AA soil leachates. The red dotted line denotes BF values of 1. A logarithmic scale is used in panel A, whilst linear scales are used in panels B, C and D.

Most previous studies report BF values that examine uptake efficiencies for aerial plant parts, notably beans and leaves. On the one hand, this focus is likely associated with the simplicity of sampling leaves and beans. On the other hand, it also most likely reflects that the beans are the primary commodity of cacao plantations and therefore the most economically important organ to investigate. However, as cacao trees only produce fruit (i.e. beans) during

specific time periods, cacao leaves can be used as a proxy organ to the fruit/beans, when the latter are not available for sampling [45].

A previous investigation by Barraza et al. [19] determined BF values between cacao organs (beans, leaves) and soils from farms in Ecuador for Mn and Cu, which were generally less than 1, indicating inefficient transfer of these elements into these plant parts. Similar to Barraza et al. [19], this current study found median BF values between cacao organs (ripe beans, mature leaves) and bulk soils for As, Cu, Fe, Mg and Mn (n = 6) that were consistently less than 1. Taken together, these cacao organs appear to not efficiently accumulate in these elements.

In contrast, unlike other elements, Cd is efficiently taken up into aerial plant parts. The BF values for Cd between cacao organs (ripe beans, mature leaves) and bulk soils varied between values of about 1 and 13 (n=6; Figure 5.5). Similarly, in their examination of Cd in cacao-soil systems, Arguello et al. [10] and Gramlich et al. [22] determined BF values for Cd between cacao organs (beans, leaves) and bulk soils of between 0.13 and 12.5 (median values greater than 1; n = 580) and 0.1 and 46 (median values greater than 1; n = 108), respectively (Figure 5.5). In addition, though not directly examined by Barraza et al. [8], Engbersen et al. [25] and Oliva et al. [46], the estimated BF values for Cd between beans or leaves and bulk soils in these studies are between 0.3 and 30 (with median values all greater than 1; n = 29 to 60; Figure 5.5). Together, the current and previous findings indicate efficient accumulation of Cd in individual cacao organs. Additionally, and most importantly, the BF values for Cd between beans and leaves versus bulk soils are similar across different studies (Figure 5.5). This illustrates that it is feasible to use BF values between cacao leaves and bulk soils as an approximation for BF values between cacao beans and bulk soils, notably during time periods

that cacao trees are not producing fruit. Furthermore, since aerial organs such as leaves and beans account for a minor repository of Cd (and other elements) in cacao trees, the overall elemental uptake capabilities must be evaluated using $BF_{\text{total plant-bulk soils}}$. Any inferences made solely based on BF values between leaves and fruit and bulk soils may lead to incorrect conclusions on overall elemental uptake capabilities. Thus, the use of $BF_{\text{total plant-bulk soils}}$ can provide better insights into the overall elemental uptake capabilities for the entire cacao tree, as opposed to using BF values for individual organs, which may overestimate or possibly underestimate elemental uptake capabilities in comparison, as shown with the BF values for Cd (Figure 5.5). As shown by the findings of this investigation, future studies should integrate and use $BF_{\text{total plant-bulk soil}}$ values to determine and better understand the overall elemental uptake capabilities of cacao trees for Cd and other elements.

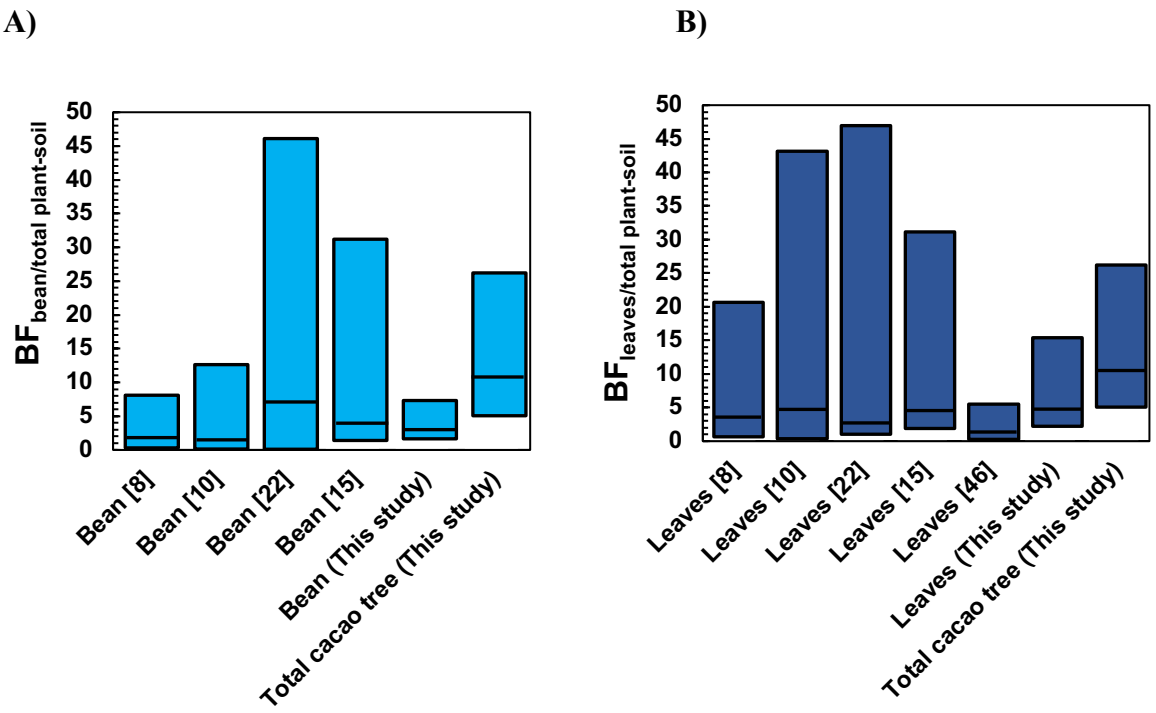


Figure 5.5. The range of BF values A) between (i) cacao beans and bulk (top)soils from previously published literature compared to this study's BF values for (ii) ripe cacao beans and (iii) total cacao trees versus bulk soils; and range of BF values B) between (i) cacao leaves and bulk (top)soils from previously published literature compared to this study's BF values between (ii) mature leaves and (iii) total cacao trees and bulk soils. The solid black bars denote the median values.

5.7.1.2. Bioaccumulation values between total plants and bioavailable pools

The soil leachates provide insights into the bioavailable pool of trace elements that cacao trees can readily access for uptake, and may be indicative of soil conditions in Ecuador, as the topsoils from this region are typically acidic [9, 47]. As such, to understand the uptake efficiencies of different elements by cacao trees from the bioavailable pools, the BF values

between full cacao trees and different bioavailable pools (Mehlich-3, AA and EDTA-AA soil leachates) were determined. The median BF values determined for the total plants relative to the Mehlich-3, AA and EDTA-AA soil leachates were all above 1 for Cd, Cu, Mn, and Zn, which suggests that cacao trees efficiently took up these trace elements from the bioavailable pool (Figure 5.4 and Appendices Table A5.15). Similar to $BF_{\text{total plant-bulk soil}}$, no previous studies have examined BF values between full cacao trees and bioavailable pools, and therefore it is not possible to do direct comparisons on elemental uptake capabilities of the entire cacao-bioavailable soil system.

As similar elemental BF values were observed for the Mehlich-3 and EDTA-AA leachates, the following discussion will focus primarily on the results obtained for the Mehlich-3 and AA soil extractions. The median BF values between total plants and soil leachates obtained by Mehlich-3 ($BF_{\text{total plant-Mehlich-3}}$; $n = 6$) and AA ($BF_{\text{total plant-AA}}$; $n = 6$) for Zn and Cd were well above 1 and similar (Figure 5.4 and Appendices Table A5.15). In particular, the median results of Zn and Cd for $BF_{\text{total plant-Mehlich-3}}$ were 27±15 and 36±24 (MAD), respectively, and for $BF_{\text{total plant-AA}}$ they were 172±69 and 87±24 (MAD), respectively. Further, the median BF(Zn)/BF(Cd) ratio were similar for Mehlich-3 (ratio of 0.75) and for AA (ratio of 2) but slightly lower for the former. Together, this demonstrates that cacao trees have similar uptake efficiencies for Zn and Cd from bioavailable pools which are likely characterised by variable Zn and Cd concentrations, but with Zn/Cd concentration ratios that are ubiquitously >>1. The latter conclusion is supported by the observation of high median Zn/Cd ratios for both the Mehlich-3 (Zn/Cd ≈ 15±6, MAD) and the AA soil leachates (Zn/Cd ≈ 6±3, MAD) of this investigation. The finding of similarly high BF values for Zn and Cd, and the comparable chemical properties of the two elements, are in accord with the conclusion that Cd and Zn share and possibly compete for similar physiological uptake mechanisms. This interpretation is in

line with evidence from several previous investigations. For example, in addition to uptake of Zn^{2+} and Cd^{2+} ions through diffusion via ion channels and electrogenic pumps, previous studies have suggested that membrane transporter proteins such as natural resistance-associated macrophage proteins (NRAMPs), namely cacao *TcNRAMP5*, may be partly responsible for the uptake of Cd^{2+} and Zn^{2+} ions in cacao [25, 34, 48]. For instance, Ullah et al. [48] found that transgenic yeast encoded with the cacao *TcNRAMP5* had increased transport activity for Zn^{2+} and Cd^{2+} ions, suggesting NRAMP5 may be a vital membrane transporter protein in cacao. Alternatively, as suggested for other plant species, cacao trees may use iron regulated transporters (IRT), zinc-regulated, iron-regulated transporter-like proteins (ZIPs), and Zn transporter (ZnT) proteins to mediate the uptake of Zn^{2+} and Cd^{2+} ions and complexes [49, 50, 51, 52]. As such, it is highly plausible that the cacao tree likely employs closely related mechanism for the uptake of Zn and Cd. Furthermore, given these similarities in uptake mechanisms for Zn and Cd, there is an opportunity to utilise Zn amendments added to soils in cacao-soil systems, to reduce the uptake of Cd in cacao trees and their subsequent translocation to the cacao fruit.

Focusing on Mn and Cu, the median $BF_{total\ plant\text{-}Mehlich\text{-}3}$ values of these elements were lower than those of Zn and Cd, with results of 1.4±0.6 and 1.1±0.2 (MAD; $n = 6$), respectively (Figure 5.4 and Appendices Table A5.15). The median $BF_{total\ plant\text{-}AA}$ values for Mn and Cu were 9±6 and 10±3 (MAD) values, respectively. Unlike the BF ratios for Zn and Cd, the median BF(Mn)/BF(Cu) ratio were similar for Mehlich-3 (ratio of 1.3) than AA (ratio of 0.9), and only slightly higher for the former. Taken together, these results suggest that Mn and Cu are taken up with similar efficiencies by cacao trees from bioavailable pools, which likely resemble the soil leachates of this study. The latter were found to have Mn/Cu ratios clearly exceeding 1, with median results of about 13±7 and 51±35 (MAD) for the Mehlich-3 and AA leachates,

respectively, and variable absolute Mn and Cu concentrations. Similar to Zn and Cd, it is hence also plausible that Mn and Cu use similar mechanisms for uptake by cacao trees. However, the distinct chemical properties of the two elements as well as evidence from plant studies argues against the latter conclusion. Currently, no studies have directly examined Cu uptake into cacao plants and the role of membrane transporter proteins facilitating this uptake. However, many plant species employ distinct copper transport proteins (COPT/CRT) for root uptake of Cu^{+} ions [52, 53,54] and cacao trees may also have such transporters. In contrast, previous studies have demonstrated that uptake of Mn^{2+} ions by cacao trees appears to be facilitated by NRAMP proteins, specifically cacao *TcNRAMP3* [48]. Further studies are still required to confirm the role of these membrane transporter proteins in cacao.

5.7.2. Element translocation in cacao trees

To further examine the transport of elements within entire cacao trees, internal elemental distributions were determined, whereby the cacao trees were divided into the four major reservoirs of roots, woody biomass, leaves, and fruit. Considering these reservoirs, the elements were found to display four broad types of distributions: (1) Al, Fe and As were primarily hosted in similar fractions in roots and woody biomass; (2) Zn, Cd, and Mg were predominantly hosted in the woody biomass; (3) Cu, Mn and Mo were mainly hosted in about equal fractions in woody biomass and leaves; and (4) Ni and Co were primarily present in the leaves (Figure 5.2 and Appendices Figure A5.2). The observed distributions are of interest as they can be used to evaluate possible shared or distinct transport pathways of elements within cacao trees and, in particular, to the edible cacao fruit. It is notable, however, that elements with different biological roles and chemical properties can exhibit similar elemental distributions. Hence, it is important that the elemental distributions are evaluated with care,

considering independent constraints on the nutrient supply, translocation and biological use of these elements. In turn, this will avoid unjustified conclusions that are based only on correlated elemental behaviour.

5.7.2.1. Element enrichments in the roots

The elements Fe, Al and As have high concentrations in the roots, with more than 24% (median values) of their total tree budgets concentrated in the roots (Figure 5.2 and Appendices Table A5.11). To a lesser extent this is also true for Cu (with a median value ≈ 19%). Notably, these elements are known to either readily form precipitates in soil environments and/or strongly adsorb to natural substrates such as root surfaces [18, 55, 56, 57,58]. Given this, it is likely that the considerable mass fractions of these elements in the roots reflect, in large part, adsorption to the external root surfaces, instead of these elements being taken up into the roots for subsequent internal sequestration and translocation to aerial plant parts. This conclusion is further supported by the observation of high concentrations of these elements in the leaf litter relative to young and mature leaves (Appendices Table A5.9 and A5.10). These high leaf litter concentrations most likely also reflect elemental adsorption from the soil to the leaf surfaces after the leaves were shed from the cacao tree.

5.7.2.2. Element enrichments in the woody biomass

The woody biomass serves as the predominant reservoir for Zn, Cd and Mg in cacao trees, whereby more than 68% (median values) of these metals were sequestered in this reservoir (Figure 5.2 and Appendices Table A5.11). Furthermore, when examining only the aboveground plant parts, disregarding the impact of elemental adsorption to the root surfaces,

Al and Fe have a similar distribution as Zn, Cd, and Mg. In the aerial plant parts, Al and Fe are also largely sequestered in the woody biomass (median values >75%; Figure 5.2 and Appendices Figure A5.2 and Table A5.16). In addition, significant mass fractions, with median values between about 43% and 63%, were present in the woody biomass for the elements Cu, Mn and Mo. When discounting elemental adsorption to the root surfaces, As also had a similar fraction in the woody biomass (median ≈ 59%) as Cu, Mn and Mo. It is furthermore notable, except for Cu, all the elements had efficient transport from the cacao roots to different woody plant parts (branches, bark), with fairly high median TF values (TF>1; Figure 5.6; Appendices Table A5.17). Together, this demonstrates that the woody biomass is a key reservoir for many elements and plays a central role in regulating the abundances of these elements, and presumably for further essential and non-essential elements, in cacao trees.

For the non-essential elements, such as Al, As and Cd the woody biomass can serve as a sequestration reservoir. The woody biomass can sequester and reduce the transport of these elements to cacao leaves and fruit, where they are not needed and can possibly generate adverse effects in these organs. Previous investigations, in part, also support the findings from this study and have suggested that the woody biomass, notably branches and bark, is a large sequestration reservoir for Cd in cacao trees and may play an important role in distribution of Cd to the leaves and fruit [15, 16]. This inference is made due to studies finding elevated Cd concentrations in the woody biomass tissue samples as compared to other organs. For instance, though not completing an elemental (mass) distribution of an entire cacao tree, Engbersen et al. [25] found elevated Cd concentrations of predominately in scions, branches and bark (2.21-6.34 mg kg^{-1}), compared to other organs such as the cacao beans, leaves, and roots (1.89-4.27 mg kg^{-1}), suggesting the woody biomass is a key sequestration reservoir.

For the essential elements, Cu, Fe, Mg, Mn, Mo and Zn, the woody biomass can serve as an intermediary storage reservoir that can help to regulate the abundances of elements in the cacao trees. The woody biomass can maintain the development and growth of the trees and prevent toxic effects from excessive elemental concentrations in the cacao leaves and fruit. Previous investigations have also found that the woody biomass, notably the bark, is an important storage reservoir for essential elements [59, 60]. Therefore, the large mass fractions in the woody biomass are not unexpected for essential elements, which can be taken up in sufficient quantities from soils relative to the requirements of the cacao tree. In particular, the uptake will be governed by the concentrations of the elements in the bioavailable pools, and the availability of efficient uptake pathways via ion channels and electrogenic pumps and membrane transporter proteins. An example of this is Mg, which is needed for the synthesis of chlorophyll and is present primarily in leaves. Magnesium is also available in ample quantities for uptake by cacao trees, as it is a major element in rocks and soils and is readily soluble in soil solutions (Appendices Table A5.13) [52, 61, 62]. Therefore, the transport of Mg to cacao leaves likely occurs primarily through the woody biomass, with some fraction of the Mg being temporarily stored that can be released as needed, via either the xylem or phloem transfer pathway or possibly through a combination of both pathways. Furthermore, in woody biomass tissues, the xylem parenchyma temporarily stores water and nutrients such as carbohydrates, lipids and essential elements and redistributes the water and nutrients during times of need [63,64]. However, less is known about the phloem parenchyma and its ability to store and redistribute nutrients in the woody biomass. It is plausible that elements are temporarily stored and redistributed in the woody biomass via the xylem and/or phloem in cacao trees. Additional research examining xylem and phloem sap and tissue are required to further understand the specific pathway(s) that preferentially transport different elements. Similarly, Zn is an essential micronutrient for plant species, and serves a critical role in metabolic processes and enzymatic

functions and is also required to produce chlorophyll [65]. Zinc is also readily available for uptake by cacao trees to meet its nutritional requirements, as Zn is present in sufficient quantities in tropical soils [10,11, 65]. As with Mg, Zn is likely translocated to cacao leaves mainly through the woody biomass via xylem or phloem transfer and/or a combination of the two.

The similar enrichments that are observed in the woody biomass for the essential metals Cu, Fe, Mg, Mn, Mo and Zn does not directly imply that these elements all largely share the same uptake and translocation pathways and regulation mechanisms within cacao trees. This reflects that the chemical properties and biological roles of the elements that are primarily stored in the woody biomass are too diverse to render this feasible. Nonetheless, shared mechanisms are possible and even likely for certain groups of chemically similar essential elements. It is plausible that cacao trees utilise similar mechanisms, in particular membrane transporter proteins, to transport some chemically similar essential elements throughout different organs. For instance, Ullah et al. [48] showed using transgenic yeast strains modified with cacao *TcNRAMP6* genes, that *TcNRAMP6* had mild sensitivity towards nutritionally vital divalent cations $Zn^{2+}$and Fe^{2+} ions and it is plausibly an intracellular metal transporter for these metals in cacao. However, no studies to date have examined closely the relationship between these elements, notably Cu, Mg, and Mo, in cacao trees, and therefore further studies are required to understand the various mechanisms and membrane transporter proteins responsible for these similar elemental distributions.

5.7.2.3. Element enrichments in the leaves and fruit

For Cu, Mn and Mo, between about 32% and 46% (median values) of a tree's elemental budget were present in the leaves, and this fraction rises to about 69% and 71% (median values) for Ni and Co, respectively (Figure 5.2 and Appendices Table A5.11). When disregarding root adsorption, As had a similar mass fraction (median ≈ 41%) in the leaves as Cu, Mn and Mo. In addition, except for As, all of these elements were efficiently transported from the cacao roots to the leaves, with relatively high median TF values (TF>1; Figure 5.6; Appendices Table A5.17). The smaller mass fractions stored for these elements in the woody biomass (median values <63%), as compared to elements such as Mg, Fe and Zn (median values >68%), presumably reflects a lower overall availability of these elements in the nutrient source for uptake, to meet the requirements of the tree and sufficiently deliver these elements to the cacao leaves and fruit. It is furthermore notable that the highest elemental mass fractions present in cacao fruit (relative to the total trees) were observed for essential Cu, Mo, and Ni, with median values >0.9%. In comparison, for all other elements in this study except for As, less than 0.4% of the total elemental budgets were stored in the cacao fruit. Taken together, these systematics indicate that many of these elements, and in particular essential elements, are translocated to the fruit primarily from the leaves via phloem transfer.

The above observations and inferences are supported by several independent findings. Notably, Mn is stored to a large extent in the leaves (median ≈ 46%) but only a small fraction is present in the cacao fruit (median ≈ 0.2%). This most likely reflects that Mn is stored in the leaves and is not readily transported over longer distances from leaves to other organs via the phloem, as was found in studies of other plant species such as the white lupin and wheat [18, 66, 67, 68]. In contrast, Ni was found to be a highly phloem-mobile element in multiple plant

species, and therefore can be readily remobilised from leaves to the fruit [18, 66, 67, 68, 69]. Molybdenum and Cu were also found to be moderately phloem-mobile in different plant species such as oilseed rape, black gram and dappled willow [70, 71, 72]. In addition, the essential elements Cu, Mo and Ni are known to play important roles in *both* the leaves and fruit of plant species, namely as cofactors for various enzymes [18, 49, 54, 69, 73]. For example, Cu and Mo are both involved in chlorophyll production and photosynthetic reactions in the leaves, and Ni is required for key enzymatic processes in the leaves [49, 54, 69, 73, 74]. Copper, Mo and Ni are also involved in seed and fruit production and development in plant species [69, 54, 74]. Thus, it is plausible given the greater fraction of Cu, Mo and Ni in both leaves and fruit, their phloem mobility, and biological roles in seed and fruit development, these elements are transported to the cacao fruit, in large part, from the leaves through phloem transfer.

Whilst substantial mass fractions of essential Cu, Mn, Mo and Ni are stored in the leaves, there are small but noteworthy differences in mass distributions of these elements. For example, compared to Cu, Mn and Mo, a higher fraction of Ni is stored in the leaves (median ≈ 69%; Figure 5.2 and Appendices Table A5.11 and Figure A5.2). The distinct elemental distributions, chemical properties and biological roles of these elements, indicate that there are clear differences in the mechanisms of storage and transport. Given these conclusions, cacao trees most likely have disparate underlying physiological mechanisms for the transport of these elements. Further biological studies are required to understand the specific mechanisms, notably the membrane transporter proteins, responsible for the transport of these elements in cacao trees and the genes that encode them.

5.7.2.4. Hitchhiker elements and their rides: Cd–Zn and Co-Ni

In plant sciences, ‘hitchhiker elements’ are typically non-essential elements that use transport mechanisms, notably membrane transporter proteins, originally intended for the use of essential micronutrients [6]. Whilst Zn and Ni are essential micronutrients in plants, Cd and Co are non-essential elements that are largely toxic to plants, particularly at higher concentrations [17, 18, 49]. The elemental distributions that are observed for Cd and Co are in accord with the conclusion that they are hitchhiker elements in cacao plants to Zn and Ni, respectively.

Zinc and Cd are both transition metals of Group 12 of the periodic table, with broadly comparable chemical behaviours and distributions in silicate rocks and soil environments [75, 65]. The findings of this research show that both elements have high and remarkably similar BF values in the trees relative to soil leachates. In addition, both elements have similar internal distributions in the cacao tree (Figure 5.2 and Appendices A5.11), with high mass fractions concentrated in the woody biomass, and high median TF values for cacao beans, leaves, and bark from the roots (Figure 5.6 and Appendices Table A5.17). This suggests that the high levels of Cd which are present in cacao organs are a consequence of the requirement for the efficient uptake and translocation of essential Zn, whereby Cd is taken up and transported with a similar efficiency inadvertently.

Previously, coupled stable isotope investigations of Cd and Zn in plant species such as in wheat and cacao have shown distinct isotope fractionation signatures for both elements [25, 76]. In detail, juvenile cacao plants preferentially sequestered isotopically heavy Zn and light Cd in the roots, whilst isotopically light Zn and heavy Cd were transported to the leaves [25, 34]. Additionally, previous Cd stable isotope studies have found that the woody biomass of mature cacao trees sequestered isotopically light Cd as compared to the leaves [16]. The data

from this current research suggest that in cacao, and possibly other plants, these distinct fractionation signatures between Zn and Cd may reflect, in part, the substantial sequestration of Cd in the woody biomass. This reservoir, and in particular the bark, is a more significant reservoir for Cd (median ≈ 85%) than for Zn (median ≈ 69%; Figure 5.2). As such, the sequestration of isotopically light Cd in the bark may hence be responsible for the observed Cd isotope fractionation in aboveground cacao organs. This reflects that large fractions of isotopically light Cd are likely preferentially removed and sequestered in the bark, thereby depleting the available pool of isotopically light Cd. In turn, the remaining pool of Cd available for transport to the cacao leaves and fruit will be isotopically heavy. Therefore, whilst Cd is taken up and transported with a similar efficiency as Zn, it is sequestered more readily in the woody biomass and is less mobile than Zn in the cacao tree, likely as part of an internal tolerance strategy. Furthermore, from their bulk XANES results, Blommaert et al. [16] found that isotopically heavy Cd sequestered in the woody biomass (i.e. branches) and in cacao fruit parts (i.e. nibs) of mature trees were both bound to O-containing donor ligands. This also supports previous hypotheses on observed isotopic fractionation signatures in juvenile cacao plants that suggest isotopically heavy Cd is bound to O-containing donor ligands in aerial plant parts, whilst isotopically light Cd is bound to S-containing donor ligands in the belowground parts [25]. As a result, there may also be differences in binding preferences for specific donor ligands attached to different molecules, which also contribute to isotopic fractionation signatures. Another hypothesis for differences in sequestration patterns between Cd and Zn, put forth by Blommaert et al. [16] from their findings using LA-ICP-MS and microscopy imaging, is that in the woody parts Cd may be partially separated from nutrients and translocated to aerial cacao organs through phloem rays, whereas Zn is translocated more readily by the xylem rays to the foliage. It is plausible that differences in transport pathways in woody biomass explain differences seen in sequestration patterns for these elements, whereby

Cd is sequestered at a higher fraction as compared to Zn. Nonetheless, given the overall similarities in elemental distributions, efficiencies in their transport, and chemical behaviours, it is plausible that Zn and Cd share similar physiological mechanisms for their transport in cacao trees, notably similar membrane transporter proteins such as HMAs or NRAMPs [25, 34, 48].

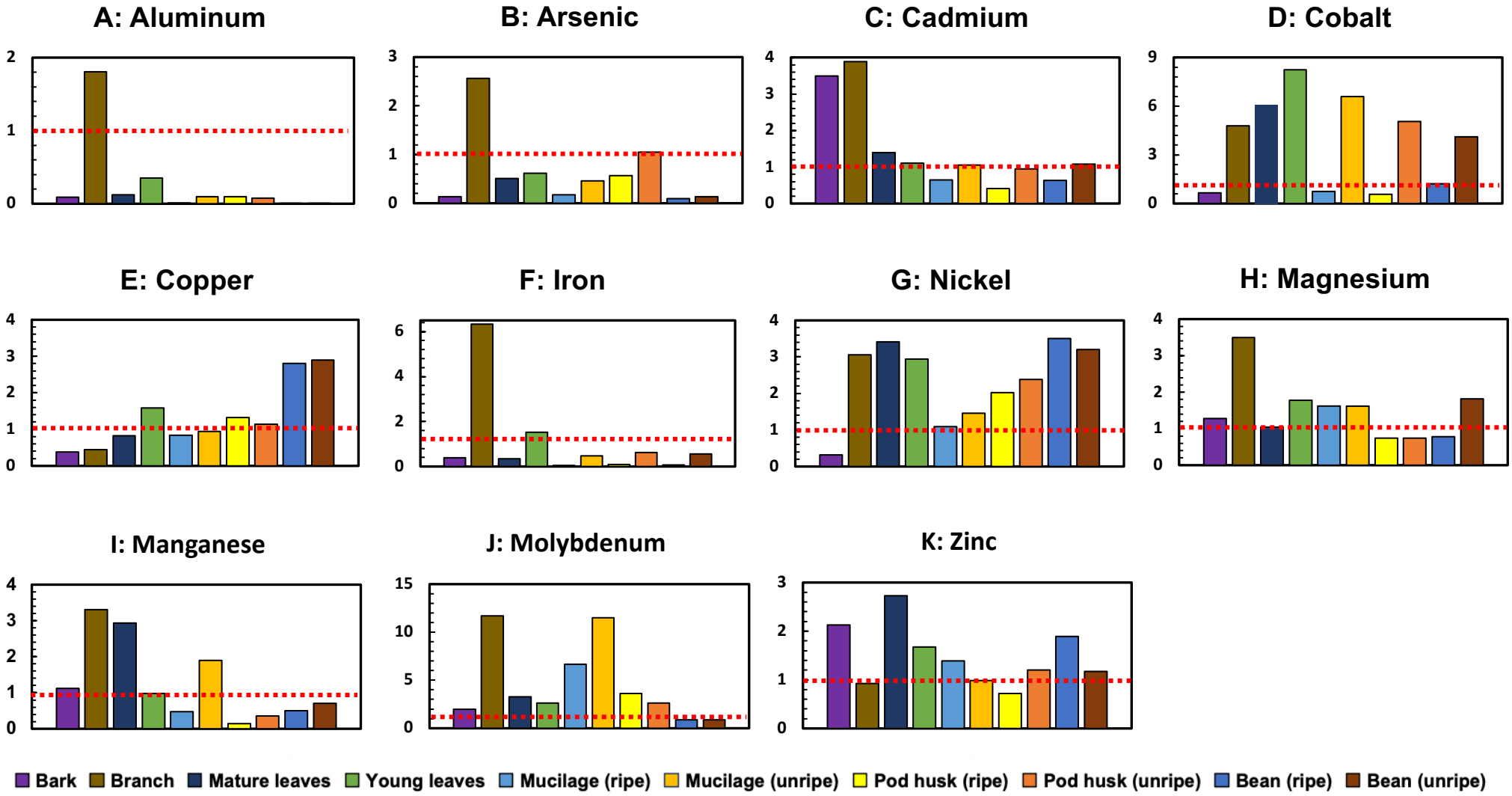


Figure 5.6. Median TF values for elements between plant organs and roots. The red dotted line denotes TF values of 1.

Nickel and cobalt are both transition metals of the iron triad and in many respects, they have comparable chemical properties. Consequently, the elements also share broadly similar distributions in silicate rocks and soil environments [82, 83]. Nickel and Co are distinct from other elements studied here, as more than 69% (median values) of these metals are stored in the leaves (Figure 5.2 and Appendices A5.11). Both Co and Ni also have similar efficiencies for their translocation from cacao roots to leaves and beans, with relatively high median TF values (TF>1; Figure 5.6 and Appendices Table A5.17). These similarities in elemental distributions and transport efficiencies, and considering that Co is non-essential in plants, are in accord with the conclusion that in cacao trees Co is a hitchhiker element which follows Ni. Further, there are limited studies directly examining the role of possible shared mechanisms for these elements, in particular the membrane transporter proteins responsible for both Co and Ni storage and transport in plant species [84, 85]. As such, whilst cacao trees may utilise similar mechanisms and pathways for Ni and Co storage and transport in different organs, the specific underlying mechanisms remain not well understood in plant species including in cacao.

5.8. Conclusions

This investigation attempted for the first time to determine the uptake and transport of selected essential and non-essential elements in full cacao-soil systems. This included understanding the extent to which cacao trees efficiently took up metals from the bioavailable portion of soils. A key finding is that cacao trees are most likely an accumulator of Cd (median $BF_{\text{total plant-bulk soil}}$ of 11±4; MAD, n=6), but not of other elements in this study, such as As, Cu, Fe,

Mg, and Mn (median $BF_{\text{total plant-bulk soil}}$ values <1; *n*=6). In addition, the similar BF values for Zn and Cd between total plant and soil leachates (denoting the bioavailable pools), with median $BF_{\text{total plant-soil leachate}}$ values exceeding 27 (*n*=6), indicate that these metals may share similar physiological mechanisms such as membrane transporter proteins (e.g., NRAMPs) during uptake by cacao trees. Furthermore, Zn and Cd are found to share physiological mechanisms for uptake, there is a possible opportunity to utilise Zn amendments added to soils in cacao-soil systems, to reduce the uptake of Cd in cacao trees and their subsequent translocation to the edible cacao fruit. Similar findings were also observed for Mn and Cu, as they shared similar BF values between total plant and soil leachates (median $BF_{\text{total plant-bulk soil}}$ values >1; *n*=6), though it is less likely these elements share uptake mechanisms due to differences in their chemical behaviours.

To examine the elemental accumulation efficiencies of different cacao organs, a comparison of BF values for Cd between beans and leaves versus bulk soils demonstrate that these two values can be used interchangeably. In particular, this implies that BF values determined for leaves versus bulk soils can be used to estimate the accumulation efficiency of Cd in the economically important beans, even when fruit are not available for sampling. Additionally, the use of $BF_{\text{total plant-bulk soils}}$ can elucidate the overall elemental uptake capabilities for the entire cacao tree. Furthermore, simply examining BF values between beans and leaves and soils may overestimate or possibly underestimate overall elemental uptake capabilities. Thus, further studies that examine the bioaccumulation of elements, notably Cd, in full cacao-soil systems using $BF_{\text{total plant-bulk soil}}$ values are required to better understand the overall extent to which cacao trees accumulate elements.

The elemental (mass) distributions of the entire cacao tree demonstrated that the tree may utilise similar mechanisms for the sequestration and translocation of certain elements across different plant parts. In particular, the cacao roots retained high fractions (median values >19%) of Al, Fe and As and to a lesser extent Cu, likely due to adsorption of these elements onto the root surfaces. Further, apart from Co and Ni, the woody biomass serves as an important storage and sequestration reservoir for non-essential and essential elements, whereby the fraction of elements in the woody biomass exceeded 40% (median values) with high TF values (median TF values >1) for most elements from roots to branches and bark. From the woody biomass, essential elements are likely transported to other organs such as the leaves through xylem or phloem transfer, to meet the nutritional requirements of the cacao tree. Additionally, the cacao leaves retained a high fraction (median values > 30%) of As, Cu, Co, Mn, Mo and Ni, with high TF values from roots to leaves (median TF values >1), indicating that leaves are also an important storage and sequestration reservoir. From the leaves, a limited quantity of these elements, in particular the essential elements Cu, Ni and Mo, are most likely transported to the edible fruit via the phloem. Only a minor fraction of all elements reached the cacao fruit (median values < 2%). The precise physiological mechanisms used in the cacao tree to transport an element between different organs is highly dependent on the specific element, its biological role and its chemical behaviour. Non-essential Cd and Co are likely 'hitchhiker' elements, whereby they likely use transport pathways and membrane transporter proteins designated for the essential elements Zn and Ni, respectively. Further biological studies are required to understand the specific mechanisms and membrane transporter proteins responsible for the transport of these elements in cacao trees.

Although this investigation provides novel and promising insights into the uptake and transport of elements in the cacao-soil system, there are important limitations on the findings. As this study did not fully extract any of the cacao trees sampled in Ecuador, all dry biomass weights were estimated using previously published data for cacao trees to determine the elemental (mass) distributions and BF values. Furthermore, the sample size considered in this investigation is relatively small. As such, further research is required to confirm the findings of this small pilot study. Additionally, given the small sample size, other important factors were not directly examined such as genotype and tree age effects, and how they may impact elemental distributions of cacao trees. In the future, researchers should consider and include these factors alongside soil properties and farming practices in their experimental design.

5.9. References

1. Díaz-Montenegro, J., Varela, E. & Gil, J.M. Livelihood strategies of cacao producers in Ecuador: Effects of national policies to support cacao farmers and specialty cacao landraces. *Journal of Rural Studies* **63**, 141–156 (2018).
2. Rottiers, H. *et al.* A multipronged flavor comparison of Ecuadorian CCN51 and Nacional cocoa cultivars. *European Food Research and Technology* **245(11),** 2459-2478 (2019).
3. Cornejo, O. E. *et al.* Population genomic analyses of the chocolate tree, *Theobroma cacao* L., provide insights into its domestication process. *Communications Biology* **1(1)**, 167–167 (2018).
4. Jaimez, R. E. *et al.* Theobroma cacao L. cultivar CCN 51: a comprehensive review on origin, genetics, sensory properties, production dynamics, and physiological aspects. *PeerJ* **10**, e12676–e12676 (2022).
5. Middendorp, R. S., Boever, O., Rueda, X. X. & Lambin, E. F. Improving smallholder livelihoods and ecosystems through direct trade relations: High-quality cocoa producers in Ecuador. *Business Strategy & Development* **3(2)**, 165–184 (2020).
6. Vanderschueren, R. *et al.* Mitigating the level of cadmium in cacao products: Reviewing the transfer of cadmium from soil to chocolate bar. *The Science of the Total Environment* **781**, 146779 (2021).
7. Maddela, N. R. *et al.* Cocoa-laden cadmium threatens human health and cacao economy: A critical view. *The Science of the Total Environment* **720,** 137645 (2020).

8. Barraza, F. *et al.* Cadmium bioaccumulation and gastric bioaccessibility in cacao: A field study in areas impacted by oil activities in Ecuador. *Environmental Pollution* **229**, 950-963 (2017).
9. Chavez, E. *et al.* Concentration of cadmium in cacao beans and its relationship with soil cadmium in southern Ecuador. *The Science of the Total Environment* **533,** 205-214 (2015).
10. Argüello, D. *et al.* Soil properties and agronomic factors affecting cadmium concentrations in cacao beans: A nationwide survey in Ecuador. *Science of the Total Environment* **649**, 120-127 (2019).
11. Barraza, F. *et al.* Distribution, contents and health risk assessment of metal(loid)s in small-scale farms in the Ecuadorian Amazon: An insight into impacts of oil activities. *The Science of the Total Environment* **622-623**, 106-120 (2018).
12. International Agency for Research on Cancer (IARC). Cadmium and cadmium compounds. In Beryllium, Cadmium, Mercury and Exposures in the Glass Manufacturing Industry. *IARC Monographs on the Evaluation of Carcinogenic Risk of Chemicals to Humans* **58**,119-239 (1993).
13. Rahimzadeh, R. M., Rafati Rahimzadeh, M., Kazemi, S., & Moghadamnia, A. A., Review Article Cadmium toxicity and treatment: An update. *Caspian Journal of Internal Medicine* **8**, 135 (2017).
14. The European Commission. Commission Regulation (EU) No 488/ 2014 of 12 May 2014 Amending Regulation (EC) No. 1881/2006 as regards maximum levels of cadmium in foodstuffs. *Official Journal of European Union* **138**, 75–79 (2014).

15. Engbersen, N. *et al.*Cadmium accumulation and allocation in different cacao cultivars. *The Science of the Total Environment* **678**, 660-670 (2019).
16. Blommaert, H. *et al.* From soil to cacao bean: Unravelling the pathways of cadmium translocation in a high Cd accumulating cultivar of *Theobroma cacao* L. *Frontier in Plant Sciences* **13**, 1055912 (2022).
17. Jogawat, A., Yadav, B., Chhaya & Narayan, O.P. Metal transporters in organelles and their roles in heavy metal transportation and sequestration mechanisms in plants. *Physiologia Plantarum* **173(1)**, 259–275 (2021).
18. Page, V. & Feller, U. Heavy Metals in Crop Plants: Transport and Redistribution Processes on the Whole Plant Level. *Agronomy* **5(3)**, 447-463 (2015).
19. Barraza, F. *et al.* Beyond cadmium accumulation: Distribution of other trace elements in soils and cacao beans in Ecuador. *Environmental Research* **192**, 110241 (2021).
20. Arévalo-Gardini, E., Arévalo-Hernández, C. O., Baligar, V. C. & He, Z. L. Heavy metal accumulation in leaves and beans of cacao (*Theobroma cacao* L.) in major cacao growing regions in Peru. *The Science of the Total Environment* **605-606**, 792-800 (2017).
21. Gramlich, A. *et al.* Cadmium uptake by cocoa trees in agroforestry and monoculture systems under conventional and organic management. *The Science of the Total Environment* **580**, 677-686 (2017).
22. Gramlich, A. *et al*. Soil cadmium uptake by cocoa in Honduras. *The Science of the Total Environment* **612**, 370-378 (2018).
23. Romero-Estévez, D., Yánez-Jácome, G. S., Simbaña-Farinango, K. & Navarrete, H. Content and the relationship between cadmium, nickel, and lead concentrations in Ecuadorian cocoa beans from nine provinces. *Food Control* **106**, 106750 (2019).

24. dos Santos, M. L. S. *et al*. Mitigation of cadmium toxicity by zinc in juvenile cacao: Physiological, biochemical, molecular and micromorphological responses. *Environmental and Experimental Botany* **179**, 104201 (2020).

25. Barati, E. *et al.* An investigation of zinc isotope fractionation in cacao (*Theobroma cacao* L.) and comparison of zinc and cadmium isotope compositions in hydroponic plant systems under high cadmium stress. *Scientific Reports* **13** (1), 4682–4682 (2023).

26. Moser, G. *et al.* Response of cocoa trees (Theobroma cacao) to a 13-month desiccation period in Sulawesi, Indonesia. *Agroforestry Systems* **79(2)**, 171-187 (2010).

27. Nygren, P., Leblanc, H.A., Lu, M. & Gómez Luciano, C.A. Distribution of coarse and fine roots of Theobroma cacao and shade tree Inga edulis in a cocoa plantation. Annals of forest science **70(3)**, 229–239 (2013).

28. Lewis, C. *et al.* Plant metal concentrations in Theobroma cacao as affected by soil metal availability in different soil types. *Chemosphere* **262**, 127749–127749 (2021).

29. Rauret, G. *et al.* Improvement of the BCR three step sequential extraction procedure prior to the certification of new sediment and soil reference materials. *Journal of Environmental Monitoring* **1(1)**, 57–61 (1999).

30. Pröfrock, D. & Prange, A. Inductively Coupled Plasma–Mass Spectrometry (ICP-MS) for Quantitative Analysis in Environmental and Life Sciences: A Review of Challenges, Solutions, and Trends. *Applied Spectroscopy* **66**, 843-868 (2012).

31. Fallavier, P., Babre, D. & Breysse, M. Détermination de la capacité d'échange cationique des sols tropicaux acides. *Agronomy Tropical* **40** (4), 298–308 (1985).

32. Nelson, D.W. & Sommers, L.E. Total carbon, organic carbon, and organic matter. In Sparks, D.L., et al., Eds., Methods of Soil Analysis. Part 3, SSSA Book Series, Madison **961-1010** (1996).

33. Shamrikova, E.V. *et al.* Transferability between soil organic matter measurement methods for database harmonization. *Geoderma* **412**, 115547 (2022).

34. Moore, R. E. T. *et al.* Cadmium isotope fractionation reveals genetic variation in Cd uptake and translocation by Theobroma cacao and role of natural resistance-associated macrophage protein 5 and heavy metal ATPase-family transporters. *Horticulture Research* **7(1)** (2020).

35. Xue, Z. *et al.* A new methodology for precise cadmium isotope analyses of seawater. *Analytical and Bioanalytical Chemistry* **402**, 883–893 (2012).

36. Andrade, H. J., Segura, M. & Somarriba, E. Above-ground biomass models for dominant trees species in cacao agroforestry systems in Talamanca, Costa Rica. *Agroforestry Systems* **96(4),** 787-797 (2022).

37. Siswanto, Sumanto, Hartati, R. S. & Prastowo, B. Biomass of cocoa and sugarcane. *IOP Conference Series. Earth and Environmental Science* **65(1)**, 12009 (2017).

38. Calvo Romero, F. Biomass and nutrient distribution in cacao trees (Theobroma cacao): A case study in Ivory Coast., MSc Thesis Wageningen University (2018).

39. Usman, K., Al-Ghouti, M.A. & Abu-Dieyeh, M.H. The assessment of cadmium, chromium, copper, and nickel tolerance and bioaccumulation by shrub plant *Tetraena qataranse*. *Scientific Reports* **9(1)**, 5658 (2019).

40. Mingorance, M.D., Valdés, B. & Oliva, S.R. Strategies of heavy metal uptake by plants growing under industrial emissions. *Environment International* **33(4)**, 514–520 (2007).

41. Baker, A. J. M. Accumulators and excluders-strategies in the response of plants to heavy metals, *Journal of Plant Nutrition* **3(1-4)**, 643-654 (1981).

42. de Oliveira Mesquita, F., Pedrosa, T. D., Batista, R. O. & de Andrade, E. M. Translocation factor of heavy metals by elephant grass grown with varying concentrations of landfill leachate. *Environmental Science and Pollution Research International* **28(32)**, 43831-43841 (2021).

43. Rezapour, S. *et al.* Cadmium accumulation, translocation factor, and health risk potential in a wastewater-irrigated soil-wheat (Triticum aestivum L.) system. *Chemosphere* **231**, 579-587 (2019).

44. Islam, M. D. *et al.* Translocation and bioaccumulation of trace metals from industrial effluent to locally grown vegetables and assessment of human health risk in Bangladesh. *SN Applied Sciences* **2(8)**, 1315 (2020).

45. de Souza, P. A., Moreira, L. F., Sarmento, D. H., & da Costa, F. B. (2018). Cacao—Theobroma cacao. In *Exotic fruits* (pp. 69-76). Academic Press.

46. Oliva, M. *et al.* Cadmium Uptake in Native Cacao Trees in Agricultural Lands of Bagua, Peru. *Agronomy* **10(10)**, 1551 (2020).

47. Chavez, E. *et al.* Chemical speciation of cadmium: An approach to evaluate plant-available cadmium in Ecuadorian soils under cacao production. *Chemosphere* **150**, 57-62 (2016).

48. Ullah, I., Wang, Y., Eide, D.J. & Dunwell, J.M. Evolution, and functional analysis of Natural Resistance-Associated Macrophage Proteins (NRAMPs) from Theobroma cacao and their role in cadmium accumulation. *Scientific Reports* **8(1)**, 14412–14415 (2018).

49. Arif, N. *et al*. Influence of High and Low Levels of Plant-Beneficial Heavy Metal Ions on Plant Growth and Development. *Frontiers of Environmental Sciences* **4(69)**, (2016).

50. Fox, T.C. & Guerinot, M.L. Molecular Biology of Cation Transport in Plants. *Annual Review of Plant Physiology and Plant Molecular Biology* **49(1)**, 669–696 (1998).

51. Colangelo, E.P. & Guerinot, M.L. Put the metal to the petal: metal uptake and transport throughout plants. *Current Opinion in Plant Biology* **9(3)**, 322–330 (2006).

52. Pinto, E. & Ferreira, I.M.P.L.V.O. Cation transporters/channels in plants: Tools for nutrient biofortification. *Journal of Plant Physiology* **179**, 64–82 (2015).

53. Vatansever, R., Ozyigit, I.I. & Filiz, E. Genome-Wide Identification and Comparative Analysis of Copper Transporter Genes in Plants. *Interdisciplinary Sciences: Computational Life Sciences* **9(2)**, 278–291 (2017).

54. Burkhead, J.L. *et al.* Copper homeostasis. *The New phytologist* **182(4)**, 799–816 (2009).

55. Zhang, H. *et al.* The aluminum distribution and translocation in two citrus species differing in aluminum tolerance. *BMC Plant Biology* **22(1)**, 93–93 (2022).

56. Zheng, S. *et al.* kinetics of aluminum adsorption and desorption by root cell walls of an aluminum resistant wheat (*Triticum aestivum* L.) cultivar. *Plant and Soil* **261(1-2)**, 85–90 (2004).

57. Bravin, M.N. *et al.* Oxygen input controls the spatial and temporal dynamics of arsenic at the surface of a flooded paddy soil and in the rhizosphere of lowland rice (Oryza sativa L.): a microcosm study. *Plant and Soil* **312(1/2)**, 207–218 (2008).

58. Kosegarten, H., Giessen, U. & Koyro, H.W. Apoplastic accumulation of iron in the epidermis of maize (Zea mays) roots grown in calcareous soil. *Physiologia Plantarum* **113(4)**, 515–522 (2001).

59. Ponette-González, A.G. Accumulator, Transporter, Substrate, and Reactor: Multidimensional Perspectives and Approaches to the Study of Bark. *Frontiers in Forests and Global Change* **4** (2021).

60. Jones, J.M., Heineman, K.D. & Dalling, J.W. Soil and species effects on bark nutrient storage in a premontane tropical forest. *Plant and Soil* **438(1/2)**, 347–360 (2019).

61. Berezin, I. *et al.* Overexpression of *AtMHX* in tobacco causes increased sensitivity to Mg^{2+}, Zn^{2+}, and Cd^{2+} ions, induction of V-ATPase expression, and a reduction in plant size. *Plant Cell Reports* **27(5)**, 939-949 (2008).

62. Hermans, C. *et al.* An update on magnesium homeostasis mechanisms in plants. *Metallomics* **5(9)**, 117–1183 (2013).

63. Kotowska, M. M., Wright, I. J., & Westoby, M. Parenchyma Abundance in Wood of Evergreen Trees Varies Independently of Nutrients. *Frontiers in Plant Science* **11**, 86 (2020).

64. Słupianek, A., Dolzblasz, A., & Sokołowska, K. Xylem Parenchyma-Role and Relevance in Wood Functioning in Trees. *Plants* **10(6)**, 1247 (2021).

65. Broadley, M. *et al.* Zinc in plants. *New Phytologist* **173(4)**, 677-702 (2007).

66. Riesen, O. & Feller, U. Redistribution of nickel, cobalt, manganese, zinc, and cadmium via the phloem in young and maturing wheat. *Journal of Plant Nutrition* **28(3)**, 421–430 (2005).

67. Page, V. & Feller, U. Selective transport of zinc, manganese, nickel, cobalt and cadmium in the root system and transfer to the leaves in young wheat plants. *Annals of Botany* **96(3)**, 425–434 (2005).

68. Page, V., Weisskopf, L. & Feller, U. Heavy Metals in White Lupin: Uptake, Root-to-Shoot Transfer and Redistribution within the Plant. *The New Phytologist* **171(2)**, 329–341 (2006).

69. Yusuf, M., Fariduddin, Q., Hayat, S. & Ahmad, A. Nickel: An Overview of Uptake, Essentiality and Toxicity in Plants. *Bulletin of Environmental Contamination and Toxicology* **86(1)**, 1–17 (2011).

70. Qin, S. Y. *et al.* Uptake, transport and distribution of molybdenum in two oilseed rape (Brassica napus L.) cultivars under different nitrate/ammonium ratios. *Journal of Zhejiang University. Science. B* ***18*****(6)**, 512–521 (2017).

71. Cao, Y. *et al.* Xylem-based long-distance transport and phloem remobilization of copper in Salix integra Thunb. *Journal of Hazardous Materials* **392**, 122428 (2020).

72. Jongruaysup, S., Dell, B. & Bell, R.W.. Distribution and redistribution of molybdenum in black gram (*Vigna mungo* L. Hepper) in relation to molybdenum supply. *Annals of Botany* **73(2)**, 161–167 (1994).

73. Chen, G. *et al.* Physiological and Molecular Mechanisms of Plant Responses to Copper Stress. *International Journal of Molecular Sciences* **23(21)**, 12950 (2022).

74. Mendel, R. & Schwarz, G. Molybdoenzymes and molybdenum cofactor in plants. *Critical Reviews in Plant Sciences* **18(1)**, 33–69 (1999).

75. Kubier, A., Wilkin, R.T. & Pichler, T. Cadmium in soils and groundwater: A review. *Applied Geochemistry* **108**, 1–16 (2019).

76. Wiggenhauser, M. *et al.* Zinc isotope fractionation during grain filling of wheat and a comparison of zinc and cadmium isotope ratios in identical soil–plant systems, *The New Phytologist* **219(1)**, 195-205 (2018).

77. Google Earth. Modified Map of Ecuador. Google Maps [online]. Available from: https://earth.google.com/ (2023).

Chapter 6

A critical review of zinc and cadmium stable isotope fractionation in vascular plant systems

6.1. Introduction

As a toxic and non-essential metal, Cd competes with other divalent cations that are essential micronutrients in plants such as Cu, Fe, Mn and Zn for sorption sites in soils as well for carrier and channel proteins responsible for these metals' uptake and translocation in plant species [1,2,3]. Of these elements, Zn is the most chemically similar to Cd (Chapter 3). Zinc is the only element to be present in all six enzyme classes [4]. As an essential element and enzyme co-factor, Zn plays an important role in plant growth, development and homeostasis [5, 6]. It is suggested that the application of Zn to a nutrient medium (e.g., hydroponic solution or soil) may help to either reduce or increase the uptake and translocation of Cd across plant organs such as roots, stems and leaves [1,3,7, 8,9,10,11,12]. Previous research findings demonstrate that the ability for Zn to either inhibit or promote the uptake, translocation and accumulation of Cd in plants is a complex, interconnected and multi-faceted phenomenon [8], and is dependent on the doses and concentrations of Cd and Zn [1,3,7,8,9,10,11,12], the timing and duration of exposure [11], and the plant species and genotype [10,13,14]. This phenomenon also requires understanding the environmental and soil conditions and plant-soil interactions that influence Zn and Cd uptake and transport [14,15]. Moreover, by understanding if Zn uses similar mechanisms as Cd in plant species, and in particular for uptake, mitigation strategies such as Zn amendments added to a nutrient medium could be implemented to reduce the uptake and subsequent translocation of Cd in plant species. Alternatively, if Cd and Zn do not share similar mechanisms, genetic interventions could be implemented to design genetically distinct plant species that allow sufficient Zn to reach the important organs for plant development and growth, but exclude or sequester Cd in organs that

limit any toxic effects [16]. In turn, these mitigation strategies can help to reduce Cd in plant species.

The development and application of Cd and Zn stable isotope analysis techniques, using MC-ICP-MS, to biological samples have provided insights into the underlying physiological mechanisms responsible for their uptake and translocation in vascular plant species [17, 18, 19, 20]. This critical review provides novel insights into the relationship between Zn and Cd stable isotope compositions and fractionations in vascular plant systems not previously examined in other non-traditional stable isotope plant reviews. Firstly, this review aims to unravel complexation processes and adsorption onto soil components by comparing Zn and Cd stable isotope fractionation between bulk soils and soil solutions; this can provide insights into the metal species readily accessed and taken up by vascular plants. Secondly, this review provides a comprehensive comparative examination of the processes, patterns and mechanisms that are similar or different for Zn and Cd stable isotope fractionation during uptake and translocation in vascular plant systems, from 'source' (e.g., soils) to 'sink' (i.e. different plant organs). Furthermore, this review focuses on the similarities and/or differences in Zn and Cd stable isotope fractionation specifically in vascular plant species. Vascular plant species also known as 'higher plants' are defined and characterised by the presence of vascular tissues, which are made up of the xylem and phloem. As such, non-vascular plant species such as lichen or fungi are not examined. Thirdly, this review highlights key research gaps within the existing body of research on Zn and Cd stable isotope fractionation in vascular plant systems, and provides possible avenues to address these gaps moving forwards. Fourthly, the review provides novel insights into the state of quality control and assurance in Zn and Cd stable isotope studies for vascular plant systems, not discussed previously

in other reviews. Finally, the influence of plant height on Zn and Cd stable isotope fractionation during translocation, and influence of plant genotype on Zn and Cd stable isotope fractionation during uptake and translocation in vascular plants will also be briefly discussed. This critical review is inclusive of and examines all published literature released up until March 10, 2023.

6.2. Stable isotope ratio notation

Cadmium stable isotope compositions are commonly expressed using a delta notation (δ), whereby the sample isotope data are expressed as a ratio (e.g., $^{114}Cd/^{110}Cd$) relative to a standard, namely the certified Cd reference material NIST SRM 3108, and expressed in parts per thousand (‰). The following equation is used:

$$\delta^{114}\mathrm{Cd} = \left[\left(\frac{(^{114}\mathrm{Cd}/^{110}\mathrm{Cd})_{\mathrm{sample}}}{(^{114}\mathrm{Cd}/^{110}\mathrm{Zn})_{\mathrm{Standard}}} \right) - 1 \right] \text{ x } 1000 \qquad \text{(Equation 6.1)}$$

Similarly, Zn stable isotope compositions for samples are commonly expressed using an isotope ratio relative to a standard, namely JMC-Lyon Zn, also with a δ notation:

$$\delta^{66}\mathrm{Zn} = \left[\left(\frac{(^{66}\mathrm{Zn}/^{64}\mathrm{Zn})_{\mathrm{sample}}}{(^{66}\mathrm{Zn}/^{64}\mathrm{Zn})_{\mathrm{Standard}}} \right) - 1 \right] \text{ x } 1000 \qquad \text{(Equation 6.2)}$$

For comparison of Cd or Zn stable isotope compositions, the apparent isotope fractionation between two samples or reservoirs, denoted by A and B, are calculated as:

$$\Delta^{114}\mathrm{Cd}_{\text{A-B}} = \delta^{114}\mathrm{Cd}_{\mathrm{A}} - \delta^{114}\mathrm{Cd}_{\mathrm{B}} \qquad \text{(Equation 6.3)}$$

$$\Delta^{66}\mathrm{Zn}_{\text{A-B}} = \delta^{66}\mathrm{Zn}_{\mathrm{A}} - \delta^{66}\mathrm{Zn}_{\mathrm{B}} \qquad \text{(Equation 6.4)}$$

All values summarized and discussed in this review are reported relative to JMC-Lyon Zn or NIST SRM 3108 Cd, respectively, and, where appropriate, values are converted for the purposes of comparison of stable isotope data to the respective isotope standard solutions [19,20,21,22,23].

In contrast to apparent fractionation values (Δ), isotope fractionation factors, often denoted by ε, describe the isotope fractionation that occurs over time during uptake and/or translocation due to chemical reactions and/or physical processes. Interestingly, many studies cited in this critical review use apparent fractionation and isotope fractionation interchangeably, whereby they are treated as being fundamentally the same, which may not be appropriate or suitable in the context of the research. In many cases, the two values describe two different phenomena and observations. However, in certain cases, when the reservoir size is essentially infinite, the Δ and ε values are the same and can describe the same phenomena. Furthermore, only about a quarter (15/55) of the Zn and Cd stable isotope studies determined the isotope fractionation factors either for uptake [24, 25, 26], translocation [27, 28, 29, 30, 31, 32, 33] or both [34, 35, 36, 37, 38]. This omission of isotope fractionation factors for most of the studies, in particular for translocation, is largely due to the fact that many of these papers do not have full mass balances for the plant species in the study. With that said, given that the vast majority of the studies in this critical review do not use isotope fractionation factors, especially for *both* uptake and translocation, apparent isotope fractionation values will be used for comparison purposes.

For comparison of literature in this review, the apparent isotope fractionation between the total plant and nutrient medium is denoted by $\Delta^{66}Zn_{\text{total plant-medium}}$ and $\Delta^{114}Cd_{\text{total plant-medium}}$, respectively, whereby the medium can represent a soil extract or solution, bulk soil, or a

hydroponic solution. It is important to note that $\Delta^{66}Zn_{\text{total plant-medium}}$ and $\Delta^{114}Cd_{\text{total plant-medium}}$ describe the Zn and Cd isotope differences between two reservoirs, and not the isotope fractionation factor.

Similarly, for comparison of literature in this review, to understand the transport of Zn and Cd stable isotopes from source to sink organs, the apparent isotope fractionation between the shoot and total plant for Zn and Cd is denoted by $\Delta^{66}Zn_{\text{shoot-total plant}}$ and $\Delta^{114}Cd_{\text{shoot-total plant}}$. In this case, the $\Delta^{66}Zn_{\text{shoot-total plant}}$ and $\Delta^{114}Cd_{\text{shoot-total plant}}$ values help show how Zn and Cd stable isotopes are fractionated during transport to the shoot (sink) relative to total plant (source). In instances that studies do not consider $\Delta^{66}Zn_{\text{shoot-total plant}}$ and $\Delta^{114}Cd_{\text{shoot-total plant}}$, alternative apparent isotope fractionation notations will be introduced and discussed.

Table 6.1. Summary of glossary terms important to understanding isotope fractionation in vascular plant systems.

Term	Definition
Apoplast	Comprises the space outside the cell membrane in plants, including the intercellular space and the cell wall, which allows for the transport of free metal ions.
Bioavailable pool	The amount of an element or mineral and organic compound accessible to plant species for uptake.
Bulk soil	Consists of the soil outside and around the rhizosphere that can largely be reached by plant roots.
Carrier protein	A type of membrane transporter protein that binds to a molecule or ion on one side of the cell membrane and transports it to the other side through a change in conformation, often requiring energy to complete the transport.
Channel protein	A type of membrane transporter protein that allows for molecules and small ions to move across the cell membrane without using energy.
Diffusion	The movement of molecules and ions along a concentration gradient from an area of higher concentration to an area of lower concentration.
Essential micronutrients	One of the major groups of nutrients a plant needs to grow and develop, these include B, Ca, Cl, Cu, Fe, Mg, Mn, Mo, Ni, N, P, K, S, and Zn.
High- and low-affinity transport	High-affinity transport is the transport of essential and non-essential elements via carrier proteins when there are limited availabilities of these elements in nutrient sources, whereas low-affinity transport is the transport of these elements via channel proteins under sufficient or excess availabilities of these elements in the nutrient sources.
Hyperaccumulator plant species	Hyperaccumulators can grow on metalliferous soils and accumulate extremely high quantities of heavy metals in the aerial plant parts without suffering from any toxic effects, as compared to most other plant species.
Ligand	A molecule or an ion that coordinates and binds to a central metal atom or molecule to form a complex.
Phloem	Plant vascular tissue responsible for transporting organic compounds such as sucrose and amino acids produced during photosynthesis to all plant parts, namely through remobilisation in any direction.
Rhizosphere	The soil surrounding the plant root that is inhabited by microorganisms and is influenced by root activity.
Senescence	The process of halting permanent cell growth, inducing cell death, whereby cells stop dividing.
Transpiration stream	The stream is the movement of water and solutes into the roots and then into the xylem towards aerial plant parts, in particular the leaves.
Xylem	Plant vascular tissue responsible for transporting water and dissolved mineral salts from the roots to the aerial plant parts in an upward and unidirectional manner.

6.3. Quality control in Zn and Cd stable isotope studies of vascular plant species

Quality control materials are typically certified reference materials with known concentrations and/or stable isotope compositions, which are used to determine the precision and accuracy of sample measurements by a specific instrument such as an MC-ICP-MS. Ideal quality control materials are homogenous, have similar matrices, concentrations and/or isotope compositions as the samples being analysed in the research study. In this critical review, most of the vascular plant studies (50/55) use certified reference materials with reported concentration and/or stable isotope values (Appendices Table A6.1 and A6.2). This is important for monitoring the effectiveness of sample preparation techniques, and the accuracy and precision of concentration and stable isotope measurements of study samples. Most of the studies that omitted such analyses are over 10 years old and primarily applied Zn stable isotope data. The majority of the 50 studies from the last 5 to 10 years integrated at least two types of certified reference materials to ensure robust concentration and stable isotope measurements. Together, this suggests that vascular plant studies are moving towards greater use of certified reference materials, and that the more contemporary studies are likely reporting more robust Zn and Cd stable isotope data. In addition, across studies that used the same certified reference materials, the reported isotopic compositions agreed well. This is particularly important as manufacturers *usually* only report certified concentrations of reference materials, not stable isotope compositions, so there is a reliance on cross-institute comparison. For instance, whilst there are no certified values for δ^{66}Zn (± 2SD) for the BCR-482 (lichen) reference material, seven studies reported δ^{66}Zn (± 2SD) values that were in close agreement with each other (δ^{66}Zn values of between 0.03‰ to 0.14‰ ± 2SD;

Appendices Table A6.1) [27, 37, 39, 40, 41, 42, 43]. As such, these reported δ^{66}Zn values for BCR-482, as well as for other reference materials, enable future studies to monitor the accuracy and precision of their study's stable isotope measurements.

A few studies, whilst stating that they used certified reference materials, did not disclose the values in either their main research paper or supplementary information. Moreover, these studies were lacking a level of transparency in the quality of their measurements [25, 26, 31, 44, 45]. In order to determine and compare the accuracy and precision of the study's stable isotope measurements, future studies should strive to integrate and report values for multiple certified reference materials.

6.4. Brief overview of kinetic and equilibrium isotope effects and high- and low-affinity transport systems in vascular plant species

Both kinetic and equilibrium isotope effects likely explain the Zn and Cd stable isotope fractionation that occurs during uptake and translocation in vascular plant species. Kinetic isotope effects represent the fractionation of Zn or Cd stable isotopes due primarily to unidirectional or incomplete processes, in particular disassociation or biologically-mediated chemical reactions [46,47], such as the interaction exchange between Zn stable isotopes and carrier and channel proteins [46]. Equilibrium isotope effects represent the fractionation of Zn or Cd stable isotopes due primarily to bonding and non-bonding interactions with chemical structures of molecules during chemical reactions, which are dependent largely on energy changes (i.e. vibrational energies) [48]. One illustrative example of equilibrium isotope effects in plant species is the

preferential binding of isotopically heavy Zn^{2+} ions to phytosiderophores forming Zn-phytosiderophores complexes in the soil solution. These complexes are then likely taken up via carrier proteins in Strategy II plants such as grasses and rice [28, 49, 50, 51]. Additionally, physical processes such as diffusion also induce stable isotope fractionation, whereby during diffusion the heavy isotopes move slower than light isotopes of the same element along a concentration gradient [48, 52]. The dominant isotope effect responsible for observed isotope fractionation during uptake and translocation in vascular plant species remains to be explored, with many of the studies unable to clearly ascertain which is the most critical to Zn and Cd isotope fractionation in vascular plant systems [26, 28, 33, 37, 38, 42, 49, 50, 53, 54, 55,56].

It is suggested that high- and low-affinity transport systems are employed for both Zn and Cd transport via membrane transporter proteins, with corresponding kinetic and equilibrium isotope effects [24, 25, 26, 27, 28, 30, 33, 34, 37, 38, 39, 40, 42, 43, 49, 50, 51, 53, 54, 55, 57, 58, 59, 60, 61, 62, 63, 64]. Previous studies have stipulated that high-affinity transport systems favour covalent binding with isotopically heavy Zn and Cd to carrier proteins, whereas low-affinity transport systems appear to prefer transporting isotopically light Zn^{2+} and Cd^{2+} ions through ion channels/electrogenic pumps due, in part, to their greater diffusion coefficients [24, 25, 26, 29, 31, 36, 37, 38, 39, 49, 52, 54, 57, 58, 59, 60, 62, 65]. Caldelas et al. [65] reviewed the transport of Zn in plant species. The body of literature appears to support that Zn is handled by high- and low-affinity transport systems, which is likely controlled by Zn supply. At high concentrations of Zn (sufficient or excess levels), it is expected that low-affinity transport systems are predominately employed by plant species, while at low concentrations of Zn (deficient levels), high-affinity transport systems are likely employed [65]. The precise Zn concentration for the switch between

systems appears to be highly variable and dependent on the plant species [65]. Less is known about high-affinity and low-affinity model as it relates to Cd, but it is hypothesised to be similar to Zn [26, 38, 57, 58].

6.5. Isotopic fractionation of Zn and Cd during uptake by vascular plants

In this section a summary of Zn and Cd apparent isotope fractionation data for uptake in vascular plant species is reviewed. The succeeding section introduces possible processes and mechanisms responsible for the observed Zn and Cd isotope fractionations during uptake.

6.5.1. *Summary of apparent isotope fractionation for uptake of Zn in vascular plant species*

Most studies report the preferential uptake of light Zn isotopes in both plant-hydroponic (Figure 6.1 and Appendices Table A6.3) [24, 34, 36, 37, 39, 40, 63] and plant-soil systems [29, 54, 63, 66, 67, 68]. The $\Delta^{66}Zn_{\text{total plant-medium}}$ values reported for 8 different metal hyperaccumulator and tolerant plants are between –0.60‰ and +0.00‰ (Figure 6.1 and Appendices Table A6.3) [24, 29, 36, 37, 39, 40, 66]. For non-hyperaccumulators, the $\Delta^{66}Zn_{\text{total plant-medium}}$ are between −0.36‰ to −0.09‰ for *Arabidopsis halleri* and *Thlaspi arvense* [24, 36, 37]. For fruits, the $\Delta^{66}Zn_{\text{total plant-medium}}$ values for cacao and tomato are −1.21‰ to –0.06‰ [34, 63]. For cereal crops, the $\Delta^{66}Zn_{\text{total plant-medium}}$ values for maize, rice, and wheat are between −0.36‰ to −0.02‰ [28, 54, 68]. An unspecified tree species has a $\Delta^{66}Zn_{\text{total plant-medium}}$ value of −0.10‰ [67].

Although a large segment of the existing literature suggest that plant species preferentially remove isotopically light Zn, there are exceptions to the observed apparent isotope fractionation

pattern for uptake that favour isotopically heavy Zn. For both hyperaccumulator and non-hyperaccumulator plant species, *Thlaspi arvense*, *Alyssum murale, Agrostis capillaris* L.*, Noccaea caerulescens*, *Elsholtzia splendens, Phragmites australis*, *Elsholtzia splendens* N., *Arabidopsis helleri*, rice, wheat and trees (species not stated) have $\Delta^{66}Zn_{\text{total plant-medium}}$ values reported between +0.00‰ and +0.63‰ (Figure 6.1 and Appendices Table A6.3) [29,36, 37, 44, 49, 61, 66, 67, 68]. For all the plant species that had a positive isotope fractionation for uptake, all authors strongly suggest that the chemical composition and speciation of the nutrient source the plant accessed likely influenced the observed isotope fractionations (mechanisms discussed further in section 6.5.4) [29, 36, 37, 44, 49, 61, 66, 67, 68]. Furthermore, the authors elucidate that the positive isotope fractionation observed in plant-soil and plant-hydroponic studies are, in part, ascribed to total Zn supply and high- and low-affinity system phenomena, whereby high-affinity transport under Zn deficient conditions favours the uptake of isotopically heavy Zn from nutrient sources [29, 36, 37, 44, 49, 61, 66, 67, 68].

Previous studies have suggested that uptake of Zn by plants and its associated apparent isotope fractionation are likely influenced by the type of medium (e.g., bulk soil, soil extract) in which the plants are grown in, though these studies focus on the apparent isotope fractionation between individual plant parts (e.g., root, shoot) and bulk soil and soil extract or solution [25,27, 49, 50]. Only one study by Li et al. [44] examine the apparent fractionation between total plant and bulk soil ($\Delta^{66}Zn_{\text{total plant-bulk soil}}$=+0.41‰) and soil solution ($\Delta^{66}Zn_{\text{total plant-soil solution}}$=+0.43‰) for *Elsholtzia splendens* N.. Li et al. [44] highlight that their findings for the $\Delta^{66}Zn_{\text{total plant-soil solution}}$ are *not* consistent with previous studies on isotope fractionation for uptake of Zn, in particular from hydroponic systems. The authors assert that hydroponic systems likely emulate the bioavailable

pool of Zn that plants can readily access, and that isotopically light Zn is preferentially removed from the hydroponic solution by plants. Li et al. [44] state their findings for $\Delta^{66}Zn_{\text{total plant-soil solution}}$ being positive may be an outlier and not be consistent with previous research findings. Thus, given the limited studies that look at both $\Delta^{66}Zn_{\text{total plant-bulk soil}}$ and $\Delta^{66}Zn_{\text{total plant-soil solution}}$ in the *same study*, it is difficult to ascertain robust conclusions on how a plant's nutrient medium influences the apparent isotope fractionation for Zn uptake, namely whether there are significant differences between the bioavailable portion (e.g., soil solution or extract) and bulk soil (discussed further in section 6.5.4).

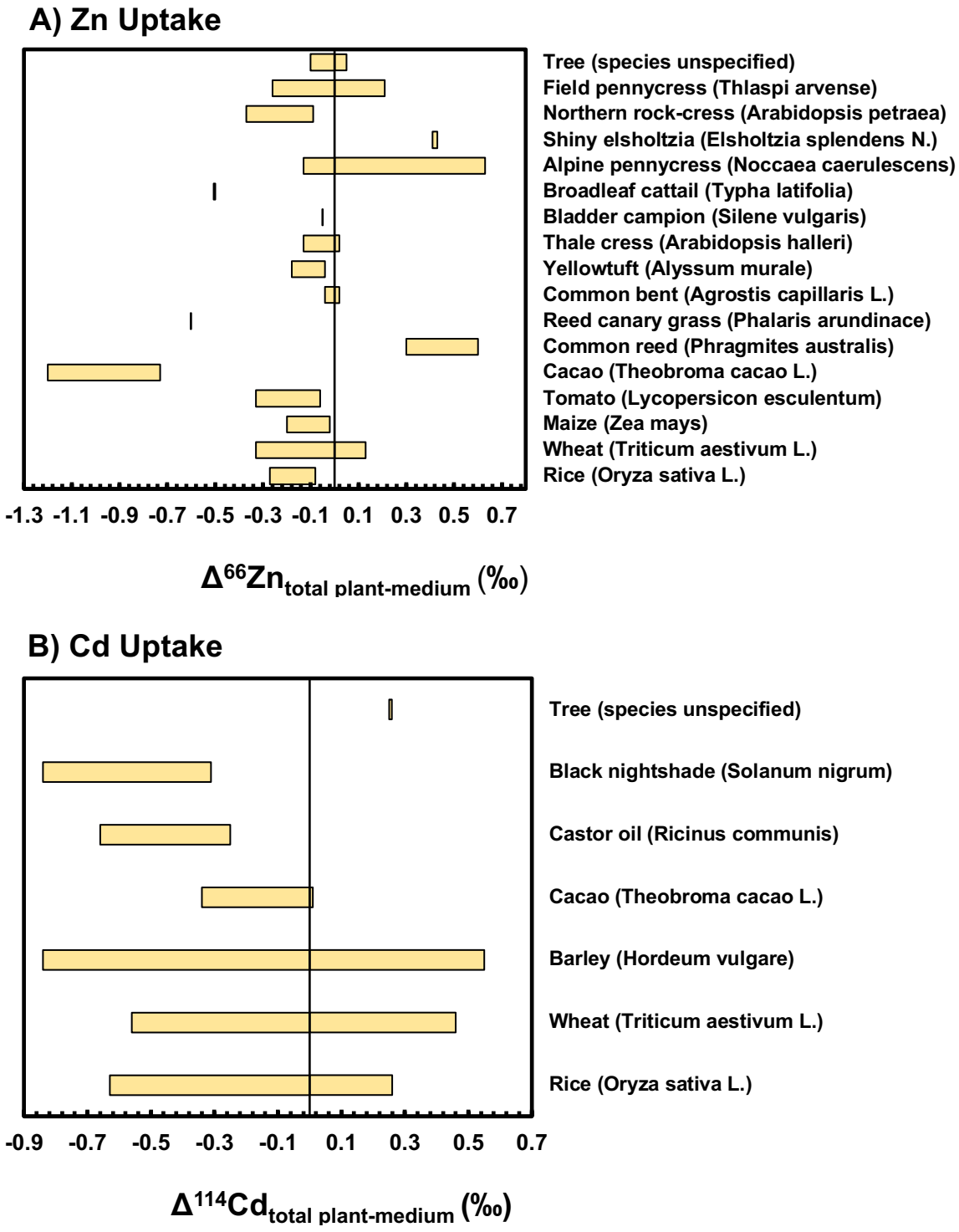


Figure 6.1. Zn and Cd uptake. Summary of apparent isotope fractionation values between total plant and medium (a) $\Delta^{66}Zn_{\text{total plant-medium}}$ and (b) $\Delta^{114}Cd_{\text{total plant-medium}}$ for different vascular plant species, whereby the

medium represents hydroponic solution, soil solution or extract, and/or bulk soil. For detailed information on values see Appendices Table A6.3 and A6.4.

6.5.2. *Summary of apparent isotope fractionation for uptake of Cd in vascular plant species*

Similar to Zn, most studies indicate that plant species preferentially removed isotopically light Cd in both plant-hydroponic systems (Figure 6.1 and Appendices Table A6.4) [35, 38, 57] and plant-soil systems [30, 32, 33, 53, 56, 69, 70, 71, 72, 73]. The $\Delta^{114}Cd_{\text{total plant-medium}}$ reported for Cd hyperaccumulators, *Ricinus communis* and *Solanum nigrum,* are between −0.84‰ and −0.27‰ [38, 57]. In cereal crops, the $\Delta^{114}Cd_{\text{total plant-medium}}$ for rice, wheat and barley are between –0.83‰ to −0.02‰ [30, 32, 33, 53, 69, 70, 56, 72]. For fruit crops, the $\Delta^{114}Cd_{\text{total plant-medium}}$ are between −0.34‰ to +0.01‰ for cacao [35].

One study found that trees (unspecified species) grown in soils preferentially remove isotopically heavy Cd ($\Delta^{114}Cd_{\text{total plant-medium}}$=+0.25‰) [70]. Furthermore, there are a few exceptions observed in the apparent isotope fractionation pattern that favours the removal of isotopically heavy Cd by plants. Notably, there are differences in $\Delta^{114}Cd$ values for total plant and bioavailable pool (i.e., soil extract and solution) and bulk soil (Figure 6.1, Table 6.2 and Appendices Table A6.4). Studies have reported that $\Delta^{114}Cd_{\text{total plant-bulk soil}}$ values are positive (+0.25‰ to +0.26‰, rice, [53]; +0.13‰ to +0.39‰, wheat, [30]; +0.31‰ to +0.55‰, wheat and barley, [32]; +0.05‰, cacao, [71]), whereas $\Delta^{114}Cd_{\text{total plant-bioavailable pool}}$ values are predominately negative (−0.47‰ to −0.41‰, rice, [53]; −0.21‰ to +0.03‰, wheat, [30]; −0.36‰ to −0.06‰, wheat and barley, [32]; −0.20‰, cacao, [71]). As such, it is likely that the nutrient medium

conditions impacts Cd speciation and the apparent isotope fractionation between the plant and its medium (discussed further in section 6.5.4).

This review shows for the first time, as shown by Zn and Cd stable isotope data (Table 6.2), it is also clear that the 'bioavailable' pool of the soil needs to be characterised isotopically to quantify isotope fractionation on uptake, as there are differences of between −0.63‰ and +0.72‰ between bulk soil and soil extract or solution (discussed further in section 6.5.4.).

Table 6.2. Summary of soil pH, $\delta^{114}Cd$ (‰) and $\delta^{66}Zn$ (‰) values for bulk soil, soil extract and/or solution and summary of $\Delta^{114}Cd$ (‰) and $\Delta^{66}Zn$ (‰) values.

Type of soil extract or solution	Soil pH	Bulk Soil $\delta^{114}Cd$ (‰)	Soil extract or solution $\delta^{114}Cd$ (‰)	$\Delta^{114}Cd_{\text{soil extract/solution-bulk soil}}$ (‰)	Reference
Porewater; 0.05 M $Ca(NO_3)_2$; 0.1 M HCl	7 to 7.2	+0.05[a]	+0.72 to +0.77[a]; +0.35 to +0.36[a]; +0.09 to +0.15[a]	+0.67 to +0.72[a]; +0.30 to +0.31[a]; +0.04 to +0.10[a]	Zhong et al. [53]
0.05 M $Ca(NO_3)_2$	5.2 to 7.1	−0.04 to +0.09[b]	+0.12 to +0.54[b]	+0.16 to +0.45[b]	Wiggenhauser et al. [30]
Seepage water	5.1 to 7.3	−0.18 to +0.11[b]	+0.47 to +0.79[b]	+0.59 to +0.69[b]	Imseng et al. [32, 70]
0.01 M $CaCl_2$	4.1	−0.32[c]	−0.17[c]	+0.15[c]	Blommaert et al. [71]
Porewater	~4.5 to ~5.7	−0.33 to +0.24[d]	−0.03 to +0.18[d]	+0.21 to +0.47[d]	Gao et al. [73]
1 M NH2OH·HOAc; 1 M $MgCl_2$	6.2	+0.05[e]	−0.01 to +0.12[d]; +0.02 to +0.16[e]	−0.06 to +0.07[d]; −0.03 to +0.11[e]	Zhong et al. [72]
Type of soil extract or solution	Soil pH	Bulk Soil $\delta^{66}Zn$ (‰)	Soil extract or solution $\delta^{66}Zn$ (‰)	$\Delta^{66}Zn_{\text{soil extract/solution-bulk soil}}$ (‰)	Reference
0.1 M HCl	6.4	+0.36[f]	+0.59[f]	+0.23[f]	Arnold et al. [28]
0.1 M HCl	7.0 to 7.8	+0.00 to +0.14[g]	−0.13 to +0.25[g]	−0.13 to +0.39[g]	Arnold et al. [49]
Porewater	6.7	+0.25 to +0.33[h]	+0.43 to +0.78[h]	+0.16 to +0.44[h]	Liu et al. [54]
Seepage water	5.2 to 6.6	+0.24 to +0.39[i]	−0.24 to +0.44[i]	−0.63 to +0.19[i]	Imseng et al. [67]
0.01 M $CaCl_2$	6.7 to 7.5	+0.09 to +0.32[j]	−0.06 to +0.19[j]	−0.22 to +0.04[j]	Houben et al. [66]
0.01 M $CaCl_2$	4.8 to 7.3	−0.05 to +0.26[k]	−0.18 to +0.14[k]	–0.13 to –0.12[k]	Couder et al. [27]
0.1 M DTPA; 0.1 M $CaCl_2$	~7.3	+0.14[l]	+0.25; +0.07[l]	+0.11;−0.07[l]	Aucour et al. [39,40]
0.1 M HCl	5.6 to 7.1	+0.16 to +0.18[m]	+0.37 to +0.60[m]	+0.21 to +0.42[m]	Wiggenhauser et al. [68]

All Cd and Zn stable isotope composition values are reported relative to NIST SRM 3108 and JMC lyon Zn, respectively. [a]represents mean values for flooded and non-flooded bulk soils and soil extracts and solution from soil sites in China. [b]represents range of mean values for bulk soil and soil extracts from three sites in Switzerland. [c]represents mean values of soils and soil extracts originating from soil sites in Trinidad. [d]represents range of mean values for soils and soil solutions under flooded and drained conditions from different soil sites in China. [e]represents mean values for soils and soil extracts collected from soil sites under flooded and drained conditions in China. [f]represents mean values of soils that were under aerobic and anaerobic conditions in soil pots at Rothamsted facility (Britain).[g]represents range of mean values for soils and soil extracts from soil sites in Philippines under both Zn deficient and Zn sufficient conditions. [h]represents the range of individual values for soils and soil solutions in three different treatments of native, disturbed, and reconditioned soils from Switzerland with and without maize planted in the soils. [i]represents range of individual values for bulk soils and soil solutions across three sites in Switzerland. [j]represents range of mean values for bulk soils and soil extracts from two soil sites in Belgium with and without plant species planted in the soil, soil leachates values are at weeks 3 and 6. [k]represents range of mean values for bulk soils and soil extracts from three soil sites in Belgium. [l]represents range of mean values for bulk soils and soil extracts from a soil site in France. [m]represents range of mean values for bulk soils and soil extracts across two sites in Switzerland.

6.5.3. *Comparison of apparent isotope fractionation for uptake of Zn and Cd in vascular plant species*

This review highlights fort the first time that preferential uptake of isotopically light Zn and Cd is more common than their heavy counterparts, especially for Cd. The magnitude in the negative shift for $\Delta^{66}Zn_{\text{total plant-medium}}$ and $\Delta^{114}Cd_{\text{total plant-medium}}$ in different plant systems is likely contingent on the plant species and their distinct underlying physiological mechanisms for uptake of these trace metals. There are a few exceptions to this observed pattern in apparent isotope fractionation, whereby isotopically heavy Zn and Cd are taken up by plants. Furthermore, a limited number of studies have directly attempted to compare Zn and Cd apparent isotope fractionation during uptake for the same plant species, notably within the same study. The findings from these limited studies support the overarching observation that isotopically light Zn and Cd are typically preferentially taken up by plant species (Figure 6.1 and Figure 6.2). For instance, Wiggenhauser et al. [68] conducted a Zn stable isotope follow-up study on durum wheat to a previous study the authors did on Cd stable isotopes for the same sample set [30]. The authors found that isotopically light Zn and Cd were preferentially taken up by wheat grown in one of the sites in Switzerland ($\Delta^{66}Zn_{\text{total plant-soil extract}}$=−0.33‰ and $\Delta^{114}Cd_{\text{total plant-soil extract}}$ = −0.21‰), whilst wheat grown at the other site preferentially removed isotopically heavy Zn and Cd ($\Delta^{66}Zn_{\text{total plant-soil extract}}$=+0.13‰ and $\Delta^{114}Cd_{\text{total plant-soil extract}}$ = +0.03‰), and this was attributed to soil conditions. In particular, Wiggenhauser et al. [68] hypothesise the site that preferentially removed isotopically heavy Zn had insufficient Zn in the soils, which led to a shift towards the uptake of heavier Zn isotopes. Furthermore, the authors suggest that due to the low Zn supply, the wheat enhanced the release of phytosiderophores to mobilize Zn from the soil, whereby the phytosiderophores preferentially

complexed with isotopically heavy Zn. These Zn-phytosiderophores complexes are then subsequently taken up by the wheat. In turn, the authors suggest this uptake of phytosiderophores complexes led to a stronger enrichment of heavy Zn isotopes observed between soil and wheat. The authors do not provide further explanation on why isotopically light Zn was preferentially taken up by wheat at the other soil site in Switzerland [68]. For Cd, Wiggenhauser et al. [30] do not explicitly explain the rationale for why isotopically heavy Cd is preferentially removed by wheat at one of the soil sites. Instead, the authors focus on and only discuss the preferential uptake of isotopically light Cd by wheat at one of the sites, which the authors suggest is likely due to this soil having a higher organic content and pH. Wiggenhauser et al. [30] hypothesise that isotopically heavy Cd is bound to ligands of organic molecules in the bioavailable pool and soil. In turn, the authors suggest the plant-available Cd^{2+} ions from the bioavailable pool should be isotopically light. The wheat, in turn, likely takes up the isotopically light Cd from the bioavailable pool, resulting in the enrichment of isotopically light Cd in the plant relative to the bioavailable pool [30]. However, this hypothesis on Cd may not be entirely accurate, as subsequent experimental studies have largely debunked this original hypothesis [74, 75, 76]. Notably, subsequent studies have shown that isotopically light Cd, not isotopically heavy Cd, is shown to preferentially bind to organic molecules in bioavailable pools and soils and adsorb to mineral compounds in soils [26,32,33,38,45,72,74,75,77]. The processes that influence isotope differences between soils and plants for both Zn and Cd are further discussed in section 6.5.4.

Similarly, a hydroponic study conducted by Barati et al. [34] on Zn stable isotopes of 19 genetically diverse juvenile cacao plants was a follow-up study on the same sample set from Moore et al. [35] in their study examining Cd stable isotopes. In comparing Zn and Cd stable isotope fractionations, Barati et al. [34] observe that isotopically light Zn and Cd are

preferentially removed by juvenile cacao plants from their hydroponic solution (Figure 6.2). Both Barati et al. [34] and Moore et al. [35] suggest that the observed uptake of isotopically light Zn and Cd by cacao plants is largely facilitated by specific membrane transporter proteins. Thus, whilst there are limited studies that examine Zn and Cd stable isotope fractionation for the same plant species within the same study, there is promising evidence to suggest that isotopically light Zn and Cd are taken up by vascular plants, which further support the overall findings of this review.

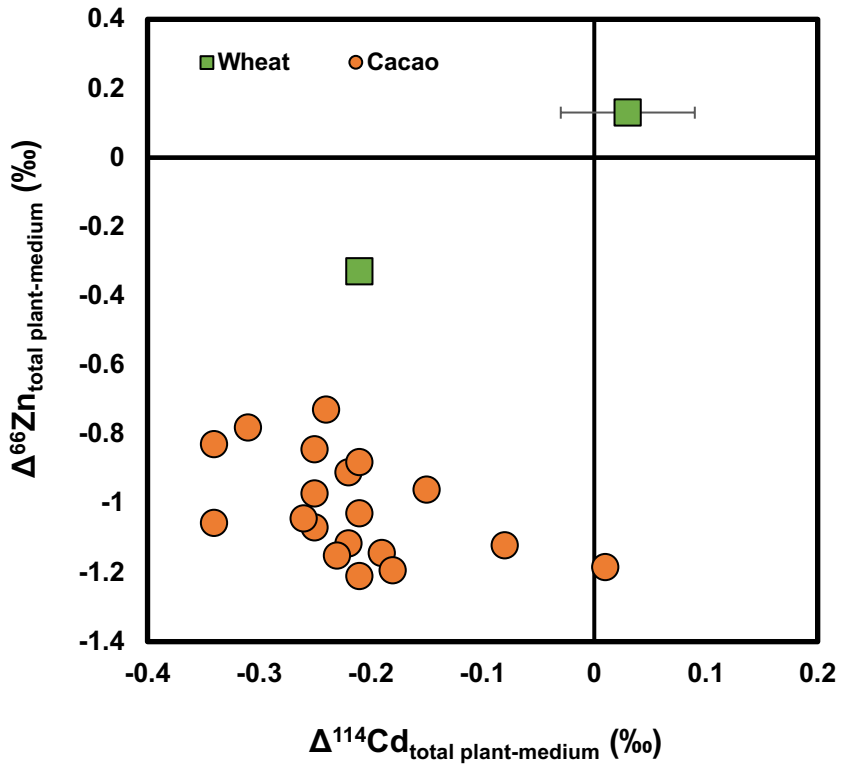


Figure 6.2. Summary of $\Delta^{66}Zn_{\text{total plant-medium}}$ (‰) and $\Delta^{114}Cd_{\text{total plant-medium}}$ (‰) values for cacao and wheat, whereby medium represents the nutrient medium such as a hydroponic solution or soil extract. Wheat isotope data which uses mean values +/- 2SD (n=3) is from Wiggenhauser al. [68] and Wiggenhauser et al. [30], and cacao isotope data which uses individual values is from Barati et al. [34] and Moore et al. [35].

6.5.4. *Understanding uptake mechanism(s) for Zn and Cd using stable isotope analyses*

Similar processes are reported to contribute to the isotopic differences between soils and plants for both Zn and Cd (Figure 6.3). The five key processes are: 1) desorption or dissolution from soils; 2) speciation in bioavailable pools; 3) adsorption to root surfaces; 4) diffusion during root uptake; and 5) uptake through membrane transporter proteins. The dominant processes vary across studies and depend on factors such as plant species, genotypes, soil properties, and Zn and Cd availability (corresponding to high- and low-affinity transport systems), though not all the processes equally contribute to the isotope fractionation observed during uptake. Furthermore, some of the studies simply list several possible dominant processes, without providing clear justifications or having limited discussions for their observations and conclusions. As such, it remains unclear which processes are likely of the most importance for stable isotope fractionation during uptake by vascular plant species. Below, the five processes are examined and discussed. It is important to note that some of these processes are responsible for the isotope composition of bulk and bioavailable pools (processes 1,2), whereas other processes are directly related to fractionation on uptake (processes 3,4,5).

Process 1: Desorption or dissolution of Zn and Cd from soils

Desorption or dissolution of Zn and Cd from solid (bulk soil) to liquid (bioavailable pool) phase influence the isotope fractionation observed during plant uptake, and can occur as a result of physical and chemical weathering or biochemical and biological processes [30,32, 43,45,50,54,66,67,70,72,73,78,79,80,81]. Bulk soils are reported as being enriched in isotopically heavy Zn and light Cd relative to the bioavailable pools that are enriched in free

isotopically light Zn^{2+} and heavy Cd^{2+} ions [25, 27, 30, 31, 32, 33, 39, 45, 49, 50, 55, 56, 53, 54, 66, 67, 70, 72, 73, 79, 80,81, 82].

Briefly on the underlying theory, the isotope fractionation observed between solid and liquid phases are, in part, determined by the number, length, and stiffness of the bonds in Zn and Cd complexes and sorbed species [25, 26, 30, 31, 32, 33, 43, 53, 55, 56, 64, 67]. Although both isotopically heavy and light $Zn^{2+}$and Cd^{2+} ions bond with O-, N- and S- donor groups of ligands attached to organic molecules, theoretically derived calculations have shown that isotopically heavy $Zn^{2+}$and Cd^{2+} ions tend to preferentially bind with O- and N-donor groups of ligands, whereas isotopically light Zn^{2+} and Cd^{2+} ions tend to preferentially bind with S-donor groups of ligands [83, 84, 85]. Cadmium is also suggested to have a higher affinity for thiols than Zn and is likely more stable in Cd-S ligand complexes than in Cd-O and Cd-N ligand complexes [55,68,85, 86]. Similarly, for calcite and Fe−Mn oxyhydroxides, isotopically heavy Zn and light Cd have been shown through experimental studies to preferentially adsorb to these mineral compounds [45, 64, 72, 73, 75, 76, 87,88].

In the context of vascular plant systems, at equilibrium conditions, previous studies have suggested that the isotopically heavier Zn isotope signatures in bulk soils are due to preferential bonding with O-containing donor groups (e.g., carboxyl or hydroxyl groups) of high molecular weight organic compounds (e.g., humic and fulvic acids), forming Zn-ligand complexes, and/or adsorb to silicates, calcites, and/or Fe−Mn oxyhydroxides in soils [25,27, 39,40,43,44,50,54,66,67,78,82], in particular forming tetrahedral Zn-ligand complexes and sorbed species [39, 40]. In turn, the remaining bioavailable pool is largely enriched in isotopically light Zn [25, 27,39, 40,43,44,50,54,66,67,78,82]. For example, Houben et al. [66] have examined isotope fractionation between bulk soils and soil leachates from two soil sites

in Belgium with and without plant species planted in the soils. The authors demonstrate that soil leachates from plant-free soils were systematically enriched in isotopically light Zn relative to the related bulk soil ($\Delta^{66}Zn_{\text{plant-free leachate – bulk soil}}$ = −0.21‰ to −0.12‰) [66]. This demonstrates that the spontaneous release of Zn from the soil solid phase to the soil solution phase favours light isotopes. In addition, the authors also found heavy Zn isotopes in leachates from planted soils compared to leachates from plant-free soils ($\Delta^{66}Zn_{\text{with plant leachate − plant-free leachate}}$ = +0.04‰ to +0.14‰) [66]. The authors conclude that the heavier Zn isotope composition of leachates from planted soils can be explained only by the release of Zn from a pool characterized by enrichment in heavy Zn isotopes compared to the pool that spontaneously supplied Zn to leachates in the absence of plants [66]. This helps, in part, explain the observed positive isotope fractionation Houben et al. [66] found for *Agrostis capillaris* ($\Delta^{66}Zn_{\text{total plant − with plant leachate}}$ = +0.02‰), whereby isotopically heavy Zn is preferentially taken up by the plant [66]. This shows the ability of plants to induce the mobilisation of Zn from a less soluble pool, such as bulk soils [66], and the importance of examining both bulk and bioavailable pools to understand how vascular plants are accessing their nutrient source(s).

In contrast to Zn, as mentioned earlier, most recent experimental studies have demonstrated that isotopically light Cd preferentially binds to organic molecules and adsorbs to mineral compounds in soils [45,72,73,74,75,76,77]. In vascular plant systems, at equilibrium, it is suggested that isotopically light Cd^{2+} ions likely preferentially bind with S-containing thiol groups of high molecular weight organic compounds and/or adsorb to calcite and Fe−Mn oxyhydroxides. In turn, the remaining bioavailable pool is enriched in isotopically heavy Cd [26, 31, 32, 33, 38, 45, 53, 55, 56, 72, 73, 89]. Zhong et al. [53], for instance, found a positive apparent fractionation between the porewater solution and bulk soil ($\Delta^{114}Cd_{\text{soil solution-bulk soil}}$ = +0.67‰ to +0.72‰). The authors report that when Cd is released from the soil into

solution, it can be expected that the soil solution is preferentially enriched in heavy Cd isotopes [53]. This difference in the isotope composition of bulk soil and soil solutions, in turn, also influences the fractionation observed during uptake. Zhong et al. [53] observe that the Cd isotope composition of a whole rice plant was heavier than those in bulk soils ($\Delta^{114}Cd_{\text{total plant-bulk soil}}$ = +0.25‰ to +0.26‰) and lighter than those in the soil solution ($\Delta^{114}Cd_{\text{total plant-soil solution}}$ = −0.47‰ to −0.41‰). Thus, differences in Cd stable isotope compositions between bulk soil and bioavailable pools effect the Cd readily taken up by plant species and should be carefully considered. Additionally, in plant systems, the desorption and dissolution of ZnS or CdS in bulk soils will also likely result in the enrichment of isotopically light Zn or Cd in the bioavailable pool [33, 40]. In contrast, the precipitation of CdS likely promotes the enrichment of isotopically heavy Cd in the bioavailable pool [31, 33, 55].

Based on the findings from this review, it appears to be consistent that isotopically light Cd is bound to bulk soils and isotopically heavy Cd is present in the bioavailable pools, with $\Delta^{114}Cd_{\text{soil extract/solution-bulk soil}}$ value being between −0.06‰ to +0.72‰ (Table 6.2). This is notable as irrespective of the reagent used (e.g., $Ca(NO_3)_2$, $MgCl_2$, $CaCl_2$), the bioavailable pool was predominately enriched in isotopically heavy Cd (Table 6.2). In contrast, however, there are broad differences between the Zn stable isotope compositions of bulk soil and bioavailable pools, with $\Delta^{66}Zn_{\text{soil extract/solution-bulk soil}}$ ranging from −0.63‰ to +0.44‰ (Table 6.2). It is hence less clear whether isotopically heavy Zn is adsorbed to the bulk soil and isotopically light Zn is present in the bioavailable pools. Based on general observations, one possible explanation for these discrepancies could be due to the specific reagents used to extract Zn from the bulk soils, whereby the stronger acids (i.e. HCl) with a lower pH tended to have bioavailable pools enriched in isotopically heavy Zn relative to bulk soil. In contrast, weaker reagents (e.g., $CaCl_2$) with a higher pH tended to have bioavailable pools enriched in isotopically light Zn. As such,

perhaps, the stronger acids are stripping the bulk soils of isotopically heavy Zn to a far greater degree than the weaker reagents. It is notable that weaker reagents such as $CaCl_2$ are generally thought to mimic soil solutions observed in 'nature' and under most field conditions as compared to stronger reagents such as HCl [27, 90]. With that said, these differences between strong and weak reagents could also be illustrative of different soil conditions. In detail, when Zn is not readily bioavailable, the plant's root could release strong exudates to access the vital micronutrient, releasing adsorbed isotopically heavy Zn into the bioavailable pools. In instances where Zn is abundant and readily bioavailable, and the plant does not need to release (or releases very little) exudates to solubilise Zn from bulk soils, then the bioavailable pools could be enriched in isotopically light Zn.

As part of a further discussion on plant root exudates, the desorption of the Zn and Cd sorbed species in bulk soils that are less soluble can occur through biochemical and biological processes from soil microorganisms and plant roots. In particular, through root-induced acidification in the plant's rhizosphere, which may release Zn and Cd from these mineral compounds in bulk soils and enrich the bioavailable pool in isotopically heavy Zn or light Cd [25, 26, 49, 50, 54, 66, 67, 80]. For instance, Liu et al. [54] found that the soil solution (porewater) was enriched in isotopically heavy Zn isotopes ($\delta^{66}Zn$ = +0.43‰ to +0.78‰) relative to bulk soils ($\delta^{66}Zn$ =+0.25‰ to +0.33‰). The authors found that the porewater from the soils that had maize growing in them had heavier Zn isotope compositions relative to soils without maize growing in them. This is likely ascribed to plant root exudates that solubilised heavy Zn isotopes from the soils into the porewater. In addition, the maize in this study tended to take up isotopically light Zn isotopes from the porewater (over the course of 5 months). In turn, this ongoing removal of light Zn isotopes from the porewater by the maize subsequently led to its depletion in the porewater [54]. In contrast, certain biochemical and biological

processes between soil microorganism and plant roots whilst facilitating desorption of isotopically heavy Zn or light Cd from bulk soil retain the bioavailable pool with isotopically light Zn and heavy Cd [26, 50]. For instance, isotopically heavy Zn^{2+} ions adsorbed to mineral compounds in bulk soil may be removed and immediately complexed with ligand-containing organic compounds exuded by bacteria or fungi in the plant's rhizosphere, which keep the bioavailable pool with isotopically light Zn^{2+} ions [50]. For most plant species, namely non-Strategy II species, the plants can then remove isotopically light Zn^{2+} ions from the bioavailable pool. Therefore, though difficult to accurately quantify and measure, it is likely that biochemical and biological interactions from within soil microenvironments, which can be unique to specific plant species, influence the dissolution and dissociation of Zn and Cd from bulk soils and the corresponding isotopic composition of these metals in the nutrient medium. However, a limited number of stable isotope studies directly look at the role of biochemical and biological processes in the context of plant-soil systems, of which all of them focus on Zn [49, 50, 54, 66].

The pH of the plant medium also likely contributes to isotope fractionation observed during uptake by plant species, notably the desorption of isotopically light Cd and heavy Zn [25, 26, 29, 30, 32, 42, 45, 50, 53, 66, 67, 70, 71, 72, 73, 80]. It is suggested at a higher pH (e.g. pH>6.5) isotopically heavy Zn^{2+} and light Cd^{2+} ions are likely chelated to ligands of organic compounds or adsorbed to mineral compounds, namely in soils, leaving the bioavailable pool of free, isotopically light Zn^{2+} and heavy Cd^{2+} ions [25, 26, 32, 45, 66, 67, 72, 73]. At a lower pH (e.g., pH<6.5), however, isotopically heavy Zn^{2+} and light Cd^{2+} ions are likely preferentially desorbed and present in the liquid phase as free ions, enriching the bioavailable pool in isotopically heavy Zn^{2+} and light Cd^{2+} ions [32, 45, 53, 67, 70, 72, 73]. For instance, Imseng et al. [67] found in their study of three soil sites in Switzerland that the soil

pH greatly influenced the desorption of Zn from bulk soils into the bioavailable pools, and its corresponding speciation. In particular, one of the study sites (Ebikon) had soils with a lower pH (5.3-5.7) and had seepage water that was enriched in largely isotopically heavy Zn (δ^{66}Zn= +0.29‰ to +0.44‰; measurements taken over the course of about a year) relative to the bulk soil (δ^{66}Zn = +0.25‰). In contrast, at another soil site (Tanikon) with a higher soil pH (6.3-6.6), the seepage water was enriched in isotopically light Zn (δ^{66}Zn= −0.24‰ to −0.18‰; measurements taken over the course of about a year) relative to the bulk soil (δ^{66}Zn = +0.37‰). Thus, it is likely that soil pH plays an important role for desorption and dissolution of metals from bulk soils into bioavailable pools. However, it is not explicitly examined in almost all the vascular plant studies as a key study parameter.

In summary, the isotope composition of the bioavailable pool is affected by: (1) the initial isotopic composition and make-up of the solid (bulk soil); (2) the complicated interactions between solid and liquid phases in the soil and the associated isotope effects; (3) the biochemical and biological interactions between plant species and the soil ; and (4) the pH of the soil or nutrient medium. It is not entirely clear, however, to what extent these factors impact and contribute to the species of Zn and Cd taken up by vascular plants and the observed apparent isotope fractionations. With that said, the differences in Zn and Cd stable isotope compositions between bulk soil and bioavailable pools influence the Zn and Cd taken up by plant species, and these differences provide insights into the medium that plant species readily access.

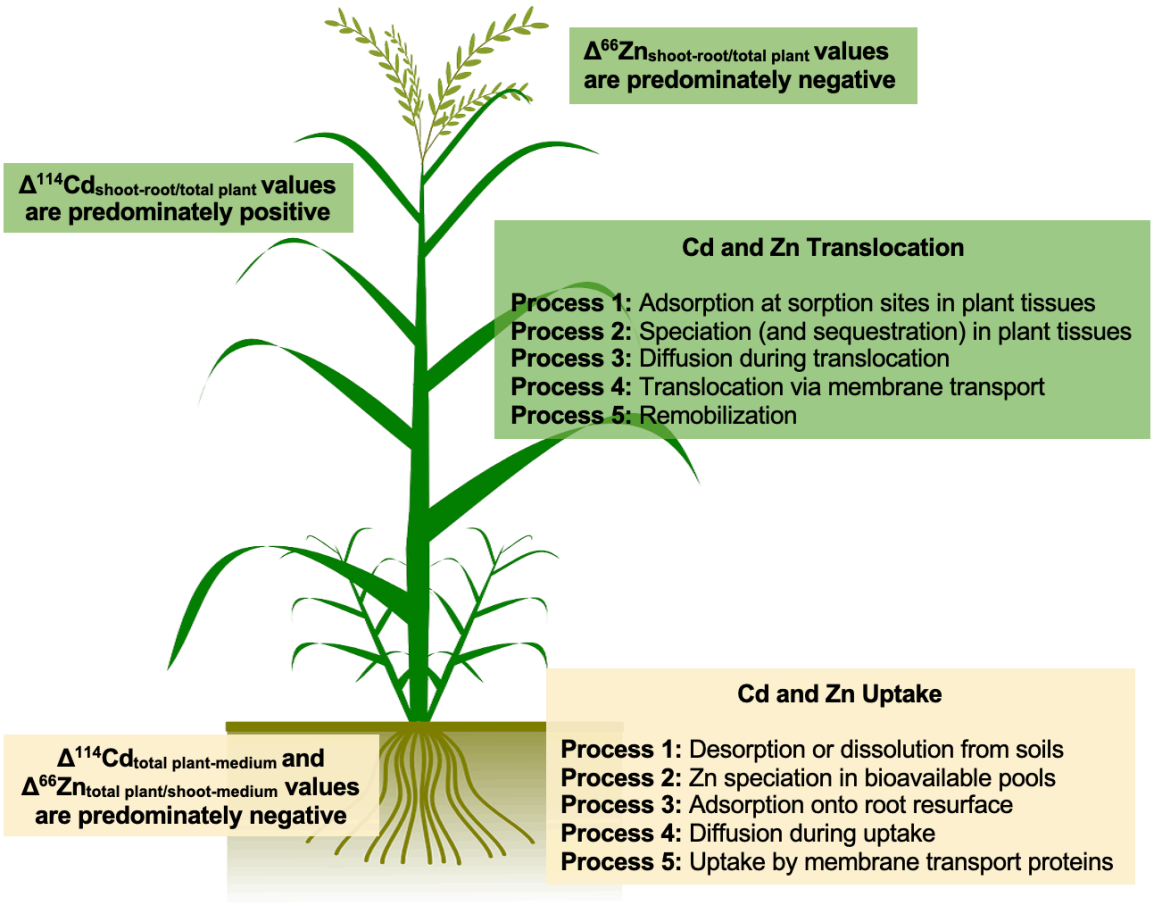


Figure 6.3. Summary of apparent isotope fractionations (Δ^{114}Cd and Δ^{66}Zn) between total plant and medium and between aerial plant parts, and processes responsible for Zn and Cd isotope fractionation during uptake and translocation. Figure modified from Pixibay (creative commons,n.d.).

Process 2: Speciation in bioavailable pools

In bioavailable pools such as soil solutions and extracts, the equilibrium between free ions and those bound to small inorganic and organic ligands also contribute to isotope fractionation observed during plant uptake [24, 26, 28, 32, 33, 37, 38, 49, 50, 51, 89, 91]. At equilibrium, it is suggested that isotopically heavy Zn^{2+} ions in the bioavailable pools preferentially bind to O- and N- donor groups of ligands attached to low molecular weight

organic molecules (e.g., phosphate, citrate and oxalate), to inorganic molecules (e.g., bicarbonate and chloride) or to phytosiderophores forming Zn-ligand complexes [24, 28, 37, 49, 50, 51, 68, 91]. Consequently, the remaining bioavailable pool is enriched in free Zn^{2+} ions that are isotopically light compared to Zn-ligand complexes [37, 49, 60, 51, 91]. Markovic et al. [51], for example, found phytosiderophore 2′-deoxymugeneic acid (DMA) preferentially partitioned isotopically heavy Zn in the complexed form (Zn-DMA) as opposed to in the free ion form (with $\Delta^{66}Zn_{DMA\text{-}Zn^{2+}}$ =+0.26‰ to +0.36‰). Similarly, at equilibrium, it is suggested that isotopically light Cd^{2+} ions in bioavailable pools preferentially bind to S-donor groups of ligands attached to low molecular weight organic and inorganic molecules, forming Cd-ligand complexes, with the remaining bioavailable pool being enriched in free, isotopically heavy Cd^{2+} ions [26, 32, 33, 38, 45, 72]. Thus, the Zn and Cd speciation in the bioavailable pool may provide insights into which metal form is being preferentially taken up by a given plant species. The extent by which the equilibrium isotope effects, due to equilibrium between free ions and those bound to small inorganic and organic ligands in bioavailable pools, contribute to the fractionation of these metals during uptake is still not fully understood.

Process 3: Adsorption to roots

Adsorption of Zn and Cd to root surface or cell wall components is hypothesised to, in part, contribute to isotope fractionation during plant uptake [25, 26, 27, 29, 30, 31, 32, 33, 36, 37, 38, 39, 40, 42, 49, 53, 56, 57, 59, 60, 64, 66, 72, 78, 89, 92]. Previous studies have found that the isotopically heavy Zn adsorbs and binds to carboxylate moieties located in proteins side chains or external polysaccharidic layers of the cell wall [75]. Free, isotopically heavy Zn^{2+} ions are suggested to preferentially bind to hydroxyl or carboxyl groups of polysaccharides and pectin in root's cell walls, to Fe plaque present on root surfaces or to

phosphates on the root surface and in the apoplast (forming Zn-phosphate precipitates), leaving the remaining bioavailable pool with free isotopically light Zn^{2+} ions [24, 27, 29, 36, 42, 49, 50, 59, 60, 66, 78, 83, 92]. However, Aucour et al. [40] found that for *Typha latifolia* isotopically light Zn is bound to Fe plaque ($\Delta^{66}Zn_{Fe\ plaque\text{-}soil}$ = −0.3‰ to −0.1‰). The authors suggested the dissolution of ZnS (enriched in light isotopes) in the rhizosphere led to the enrichment of isotopically light Zn^{2+} ions that subsequently adsorbed onto Fe plaque [40]. In contrast to Zn, it is suggested that isotopically light Cd^{2+} ions preferentially bind to Fe or Mn plaque on root surfaces, to phosphates on the root surface and in the apoplast (forming Cd-phosphate precipitates), and to negatively charged sorption sites on root surfaces and cell walls, enriching the bioavailable pool in isotopically heavy Cd^{2+} ions [26, 30, 31, 32, 33, 38, 45, 53, 56, 64, 72, 89]. For instance, Zhong et al. [72] found that Cd in Fe plaque was isotopically light as compared to the Cd in the soil solution ($\Delta^{114}Cd_{Fe\ plaque\text{-}soil\ solution}$ = −0.78‰ to −0.54‰). A few studies have suggested that isotopically heavy Cd^{2+} ions preferentially bind with carboxyl groups of polysaccharides and pectin of root cell walls, which subsequently enrich the bioavailable pool in isotopically light Cd^{2+} ions [31,33]. The mechanisms by which isotopically heavy and light Zn and Cd adsorb onto Fe plaque and root surfaces are not well understood with discrepancies in findings between studies. Nevertheless, most study observations suggest that adsorption to root surfaces and cell wall components appears to *usually* favour isotopically heavy Zn and light Cd.

Process 4: Zn and Cd diffusion during uptake

Ion diffusion is also hypothesised to contribute to isotope fractionation during uptake in plant species. Isotopically light Zn^{2+} and Cd^{2+} ions likely diffuse faster than their heavy isotope counterparts and complexed ions across the bioavailable pool to root surfaces and cell

walls, and subsequently to membrane transporter proteins for uptake. Isotope fractionation due to ion diffusion is associated with a diffusion gradient, which is controlled by the plant Zn and Cd uptake rates and the concentration of Zn and Cd in the rhizosphere [24, 25, 26, 27, 29, 31, 32, 34, 37, 38, 44,45,49, 50, 52, 53, 56, 57, 59, 60, 63, 64, 73, 92, 93]. Although previous studies list diffusion as an important process for fractionation that occurs during uptake, none of the studies experimentally attempt to confirm this finding. In particular, whilst experiments such as Rodushkin et al. [52], which is often cited as the primary literature in previous studies, demonstrate isotopically light Zn^{2+} (and Fe^{2+}) ions diffuse faster than their heavy isotope counterparts and complexed ions in aqueous solutions, it is unclear how these findings fully translate to complex plant systems.

Process 5: Zn and Cd uptake through membrane transport proteins

Membrane transporter proteins, both carrier and channel proteins, likely contribute to isotope fractionation as they transport Zn and Cd into root cells [24, 25, 26, 27, 29, 31, 32, 33, 34, 35, 36, 37, 38, 53, 54, 56, 57, 59, 60, 71, 92]. However, almost all the previous studies infer the membrane transporter proteins without using additional biological studies to support their hypotheses [31, 35, 53]. Channel proteins such as ion channels and electrogenic pumps are suggested as preferentially taking up isotopically light Zn^{2+} and Cd^{2+} ions, as part of low-affinity transport under Zn sufficient and excess conditions, though no studies have experimentally confirmed this hypothesis [24, 25, 26, 29, 32, 38, 59, 60, 92]. In contrast to channel proteins, carrier proteins such as yellow Stripe1-Like transporters (YSL) are hypothesised to be an important transporter for Zn in strategy II plants (i.e. grasses) and may take up Zn-phytosiderophore complexes from the nutrient source, which are likely isotopically heavy [28,49,51,59,60]. Other carrier proteins such as Zinc-regulated, Iron-regulated

transporter-like proteins (ZIP) and Zinc transporter 1 (ZNT1) are also hypothesised to preferentially take up isotopically heavy Zn^{2+} ions [24, 25, 27, 29, 36, 60]. Wei et al. [57] hypothesised that ZIP transporters could also participate in preferentially take up isotopically light Cd from the nutrient source during uptake. This may, in part, be due to isotopically light Cd being complexed to S-containing ligands attached to organic molecules, and these complexes are then subsequently taken up by plant species [85]. For Cd, additional carrier proteins suggested as being responsible for the uptake of isotopically light Cd^{2+} ions are NRAMP, namely NRAMP5 in cacao crops [35] and rice [33, 53, 56, 72], and NRAMP1 in rice [53, 56, 72]. For instance, Moore et al. [35] found that transgenic yeast encoded with the cacao *TcNRAMP5* gene took up more and isotopically lighter Cd than yeast controls without this gene, suggesting that NRAMP5 carrier proteins, in part, may play a role in the uptake of isotopically light Cd in plant species such as cacao. However, Zhang et al. [31] suggest that NRAMP5 transporters in rice likely prefer the uptake of isotopically heavy Cd, in contrast to previous studies. It is plausible that Zhang et al. [31] may be an outlier, as Wiggenhauser et al. [86] suggest this discrepancy seen in Zhang et al. [31] may be primarily due to a variety of factors such as differences in the initial soil properties (e.g., pH, soil Cd concentration). Barati et al. [34] found similar uptake dynamics for both Zn and Cd in cacao and, based on the yeast results of Moore et al. [35], attributed this partly to sharing similar transporters (NRAMP5). Thus, while it is possible that Zn and Cd may share similar channel proteins, it is unclear whether Zn and Cd share or use distinct carrier proteins, and what preferences for specific Zn and Cd stable isotopes these proteins have in plant species, and what implications they have on Zn and Cd stable isotope fractionation during uptake in plant systems. These carrier proteins may also be part of plant species-specific uptake strategies and influenced by metal concentrations, as part of high- and low-affinity transport systems, as previously discussed. Most importantly, only a few studies such as Zhong et al. [53] and Moore et al. [35] employ

biological studies to help identify genes that encode for possible membrane transporter proteins responsible for the uptake of these metal isotopes.

6.5.5. *Key takeaways on the uptake of Zn and Cd stable isotopes in vascular plants*

Together, this review provides novel insights into the key processes responsible for the observed Zn and Cd isotope fractionation during uptake across different plant species. Furthermore, for the first time, this review demonstrates the importance of closely examining Zn and Cd isotope compositions of bulk soils and bioavailable pools, to understand how plants are accessing their nutrient sources. Interestingly, it appears that the distribution of heavy and light Zn and Cd isotopes are not the same across bulk soils and bioavailable pools, in so far as heavy Zn and light Cd isotopes appear to be adsorbed to mineral compounds and bound to organic matter in bulk soils, whilst light Zn^{2+} and heavy Cd^{2+} ions are present in bioavailable pools. The review also highlighted the importance of Fe-Mn plaque and phosphates on the root surface on influencing both Cd and Zn isotope fractionation during uptake in plant species. Furthermore, Zn and Cd possibly share membrane transporter proteins, though as pointed out in this review further experimental studies that combine biological studies to help identify key membrane transporter proteins are still required.

The comparison between Zn and Cd stable isotopes within the same plant species also demonstrate similar isotope fractionation patterns for uptake. Barati et al. [34] suggest that similarities in preferential uptake of isotopically Zn and Cd are likely due to selective uptake by membrane transporter proteins, notably NRAMP5. Wiggenhauser et al [30, 68] observe both isotopically light and heavy Zn and Cd isotopes being taken up from nutrient sources by wheat, depending largely on the soil conditions. Furthermore, the driving processes for Zn and

Cd isotope fractionation during uptake may differ across plant species and soil conditions. Thus, now that the key processes are identified in this review, further controlled, systematic experimental studies are required. These studies are required to determine the dominant or prevailing process(es) most vital for both Zn and Cd isotope fractionation during uptake by vascular plants, and whether the process(es) are shared among different plant species.

6.6. Isotopic fractionation of Zn and Cd translocation in Plants

In this section, Zn and Cd apparent isotope fractionation data for translocation in plant species is reviewed and discussed. The subsequent section introduces the processes attributed to the fractionations.

6.6.1. *Summary of apparent isotope fractionation for the translocation of Zn in vascular plant species*

Studies primarily report the preferential translocation of light Zn stable isotopes from below ground plant organs to aerial plant organs in both plant-hydroponic (Figure 6.4 and Appendices Table A6.3) [24, 34, 36, 37, 59, 60, 61, 62, 92] and plant-soil systems [25, 27, 29, 40,54,66]. The $\Delta^{66}Zn_{\text{shoot-total plant}}$ values are between –0.29‰ and +0.00‰ for 3 hyperaccumulators, *Noccaea aerulescens*, *Arabidopsis helleri* and *Silene vulgaris* [24, 29, 36]. For non-hyperaccumulators, the $\Delta^{66}Zn_{\text{shoot-total plant}}$ values are –0.59‰ to –0.21‰ for *Arabidopsis petraea* and *Thlaspi arvense* [24, 36]. Similarly, for the cacao plant, the apparent fractionation between leaves and total plants ($\Delta^{66}Zn_{\text{leaf-total plant}}$) are between −0.54‰ and −0.09‰ [34]. The apparent isotope fractionation between shoot and root ($\Delta^{66}Zn_{\text{shoot-root}}$) values are between −1.00‰ and +0.02‰ for the 7 hyperaccumulators *Typha latifolia, Brassica napus*

L., *Lolium multiflorum* L., *Phragmites australis*, *Alyssum murale*, *Noccaea caerulescens*, and *Agrostis capillaris L.* [27, 37, 40, 61, 66, 92]. For the non-hyperaccumulator, *Thlaspi arvense*, the $\Delta^{66}Zn_{shoot\text{-}root}$ values are between −0.70‰ to −0.61‰ [37]. The $\Delta^{66}Zn_{shoot\text{-}root}$ values for tomato are between −0.51‰ and −0.30‰ and for lettuce between −0.49‰ and −0.35‰ [59, 60]. For cereal crops, the $\Delta^{66}Zn_{shoot\text{-}root}$ values are between −0.51‰ to −0.25‰ for rice, wheat and maize [54, 59, 60]. Similarly, Moynier et al. [62] report an apparent isotope fractionation between the leaves and stem/rhizome of bamboo ($\Delta^{66}Zn_{leaves\text{-}\ rhizome/stem}$) of –1.07‰ to –0.71‰, and Arnold et al. [28] found an apparent isotope fractionation between shoot and grain ($\Delta^{66}Zn_{grain\text{-}shoot}$) of −0.67‰ and −0.79‰ for rice. There is an exception to the observed apparent isotope fractionation pattern for translocation that favoured isotopically heavy Zn, notably reported for *Elsholtzia splendens* N. ($\Delta^{66}Zn_{aboveground\ tissue\text{-}root}$ = +0.47‰) [44]. Similarly, Wiggenhauser et al. [68] found that the apparent isotope fractionation between straw and root of wheat ($\Delta^{66}Zn_{straw\text{-}root}$) are between –0.14‰ and +0.10‰.

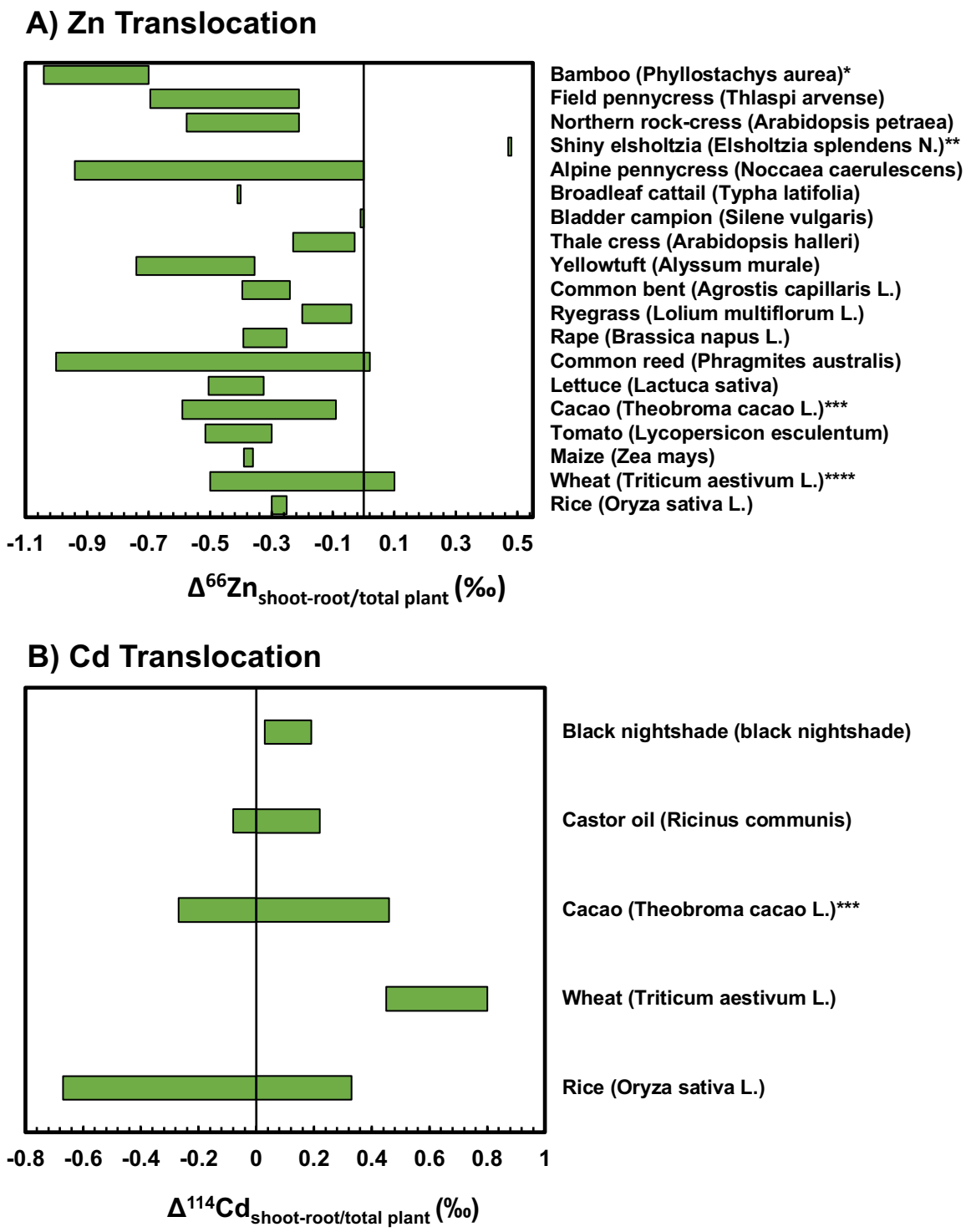


Figure 6.4. Zn and Cd translocation. Summary of apparent isotope fractionation values between shoot and root or total plant (a) $\Delta^{66}Zn_{shoot-\ root/total\ plant}$ and (b) $\Delta^{114}Cd_{\ shoot-\ root/total\ plant}$ for different vascular plant species. For detailed information on values see Appendices Table A6.3 and A6.4. *Apparent fractionation between leaves and rhizome/stem. **Apparent fractionation between aboveground tissues and root. ***Apparent fractionation between leaf and total plant. ****Apparent fractionation between straw and root.

6.6.2. *Summary of apparent isotope fractionation for the translocation of Cd in vascular plant species*

In contrast to Zn, most studies report that isotopically heavy Cd was translocated to aerial plant organs from below ground plant organs in both plant-hydroponic (Figure 6.4 and Appendices Table A6.4) [35, 38] and plant-soil systems [30, 32, 33, 45, 53, 55, 56, 64, 69, 71, 72, 73]. The $\Delta^{114}Cd_{shoot\text{-}total\ plant}$ values are between −0.08‰ to +0.22‰ for hyperaccumulators *Ricinus communis* and *Solanum nigrum* [38], and the apparent isotope fractionation between leaf and total plant ($\Delta^{114}Cd_{leaf\text{-}total\ plant}$) values are between −0.04‰ and +0.46‰ for cacao [35]. Similarly, for the cacao plant, the apparent isotope fractionation between shoot and root ($\Delta^{114}Cd_{shoot\text{-}root}$) is +0.27‰ [71]. For cereal crops, the apparent $\Delta^{114}Cd_{shoot\text{-}root}$ values are between −0.67‰ to +0.45‰ for wheat and rice [45, 53, 55, 56, 69, 72, 73]. The apparent isotope fractionation between straw and roots ($\Delta^{114}Cd_{straw\text{-}root}$) is reported for wheat with values between +0.21‰ to +0.41‰ [30]. Other studies also report positive values for the apparent isotope fractionation between leaf and root ($\Delta^{114}Cd_{leaf\text{-}root}$ = +0.17‰, [64]) and grain and root ($\Delta^{114}Cd_{grain\text{-}root}$=+0.93‰, [33]) for rice. For cacao crops, Barraza et al. [80] report an apparent isotope fractionation between beans and leaves ($\Delta^{114}Cd_{bean\text{-}leaves}$) of between −0.40‰ and −0.08‰. This study, however, did not directly examine the translocation of Cd isotopes from belowground to aerial plant organs.

6.6.3. *Comparison of apparent isotope fractionation for uptake of Zn and Cd in vascular plant species*

In comparing both Zn and Cd published literature, as clearly shown by Figure 6.4, plant species appear to mostly translocate Zn and Cd in an inverse manner, in which isotopically

light Zn and heavy Cd are translocated from belowground to aboveground organs. There are a few exceptions to this pattern, however, whereby plant species translocate isotopically heavy Zn (e.g., *Elsholtzia splendens* N.) or light Cd (e.g., in cacao, rice and *Ricinus communis*). The magnitude of apparent isotope fractionations shift, either a negative shift or positive shift, appears to be plant species-specific. Furthermore, similar to examining the Zn and Cd apparent fractionations during uptake in plant systems, few studies have examined the apparent isotope fractionation during translocation for both Zn and Cd in the same plant species (Figure 6.5). However, the findings of these few studies support the overall observations made in this review, as can be seen by Figure 6.4. As previously mentioned, Wiggenhauser et al. [68] and Wiggenhauser et al. [30] examine Zn and Cd stable isotope compositions, for the same sample set of durum wheat. The authors conclude there is largely an inverse relationship between Zn and Cd isotopes in wheat, whereby isotopically heavy Zn and light Cd were sequestered in the roots whilst isotopically light Zn and heavy Cd were translocated to the aerial plant organs [30, 68]. Barati et al. [34] make a similar observation for 19 genetically diverse juvenile cacao plants (Figure 6.5). Both Wiggenhauser et al. [68] and Barati et al. [34] suggest that the inversed isotopic fractionation patterns observed for Zn and Cd may be explained by complexation of the two elements with different ligands, with isotopically heavy Zn^{2+} binding with O- and N-donors of ligands and isotopically light Cd^{2+} binding with S-donors of ligands. This reflects that different organic molecules with distinct metal binding ligands likely control the sequestration and mobilisation of Cd and Zn. As such, there is evidence to suggest an inverse relationship for the translocation of Zn and Cd stable isotopes within different plant species, though further empirical evidence is required to support these studies' findings.

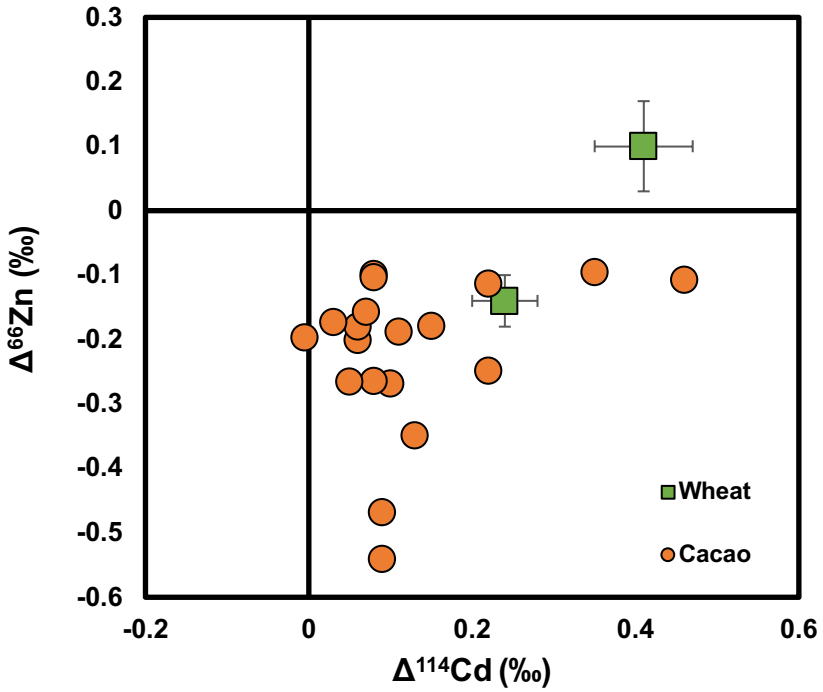


Figure 6.5. Plot shows the $\Delta^{66}Zn$ (‰) and $\Delta^{114}Cd$ (‰) during translocation for wheat and cacao. The $\Delta^{66}Zn_{straw\text{-}root}$ (‰) and $\Delta^{114}Cd_{straw\text{-}root}$ (‰) values are mean values +/- 2SD (*n*=3) used for durum wheat [68, 30], and $\Delta^{66}Zn_{leaf\text{-}total\ plant}$ (‰) and $\Delta^{114}Cd_{leaf\text{-}total\ plant}$ (‰) values are individual values for 19 genetically diverse cacao plants [34, 35].

6.6.4. *Understanding translocation mechanism(s) for Zn and Cd using stable isotope analyses*

There is an overall observed pattern demonstrating the belowground-aboveground translocation of isotopically light Zn and heavy Cd in plant species (Figure 6.3) [24, 30, 32, 33, 34, 35, 36, 37, 38, 40, 45, 53, 54, 55, 56, 59, 60, 61, 62, 66, 67, 68, 71, 72, 73, 92]. The belowground-aboveground translocation of Zn and Cd consists largely of an upward flowing system, whereby the transfer of Zn and Cd within and between the individual cells and plant parts can induce isotope fractionation. The upward flow of Zn and Cd in plants usually includes

these metals undergoing these steps: (1) entering the root where they bind to sorption sites of cell walls, precipitate in intercellular spaces or are sequestered in the vacuole; (2) transferring from the root to aerial plant parts such as stems, branches and leaves via the xylem; (3) transferring from the xylem to phloem; (4) remobilising from mature leaves to young leaves, seeds, stems and roots via the phloem [24, 27, 28, 29, 30, 34, 36, 37, 38, 39, 42, 44, 53, 55, 56, 61, 66, 68, 71, 78, 80, 93]. For both Zn and Cd, less is known about the transport of Zn and Cd from phloem to leaves and reproductive organs (e.g., seeds and grains), and the associated isotope fractionation possibly occurring during these transport processes. Throughout this upward flowing system, five key processes have been linked to Zn and Cd isotope fractionation observed within plants: 1) adsorption at sorption sites in plant tissues; 2) speciation and sequestration in plant tissues; 3) diffusion during translocation; 4) translocation via membrane transport; and 5) remobilization (Figure 6.3). As with uptake, it is unclear which process or processes are the most dominant or important contributor to observed isotope fractionations for translocation in vascular plant species.

Process 1: Adsorption at sorption sites in plant tissues

The interactions between Zn and Cd at sorption sites of the cell walls are hypothesised to influence stable isotope fractionation observed in the different plant parts [24, 27, 30, 31, 36, 37, 38, 40, 42, 43, 59, 60, 61, 78, 89, 92, 93]. Isotopically heavy Zn is suggested to preferentially adsorb onto negatively charged sites of the cell wall of tissues and in the apoplast surrounding the xylem, stems and leaves, enriching the xylem sap and stem and leaf cells in isotopically light Zn^{2+} ions [27,39,40]. For Cd, Wiggenhauser et al. [55] suggest that isotopically heavy Cd observed in rice shoots may be, in part, ascribed to isotopically light Cd being bound to cell walls in the apoplast of the root while isotopically heavy Cd is transported

to the shoots. As previously mentioned, a considerable number of studies examine the role of adsorption of Zn and Cd on root surfaces and sorption sites on cell walls and its contribution to isotope fractionation. However, limited studies have examined the role of Zn and Cd binding to sorption sites of cell wall and apoplast of aerial organs in plant species, and its impact on the isotope fractionation [27, 39, 40, 55]. It appears that isotopically heavy Zn binds to the cell wall and apoplast of root, xylem, stem and leaves, whereas isotopically light Cd binds to cell wall and apoplast of root and shoot (i.e., grain, straw and leaves) [27, 39, 40, 55]. There is no Zn or Cd stable isotope data or explanations for cell wall binding preferences for either metal in the phloem. Thus, given the limited studies, it is difficult to make a robust comparison between the Zn and Cd isotope binding preferences in these vascular tissues (i.e., phloem and xylem), and whether these few observations and explanations are indicative of a wider pattern seen throughout different plant species.

Process 2: Speciation and sequestration in plant tissues

The equilibrium dynamics between free ions of Zn and Cd and those bound to ligands attached to organic molecules such as organic acids, amino acids or peptides is also likely to induce fractionation that will contribute to the overall stable isotope composition differences observed between plant parts [24, 27, 29, 34, 35, 36, 38, 43, 44, 50, 57, 60, 61, 66, 68, 71, 72, 89, 91, 92, 93, 94]. Notably, Zn and Cd binding to cysteine-rich organic molecules such as glutathione, phytochelatins (PC; a glutathione oligomer), and metallothioneins, which play an important role in plant detoxification, tolerance and accumulation strategies, likely influence isotope fractionation [5,30,34,38,40,55,57,61, 66, 72, 93]. As will be discussed in the following paragraphs, the current literature has examined, at least in part, Zn and Cd speciation and its

related isotope fractionation for plant roots, xylem, phloem, stem, leaves and seeds (i.e., grains).

Based on the findings of this review, plant roots are consistently enriched in isotopically heavy Zn relative to aerial plant organs (e.g., shoot, leaves, grain) (Appendices Table A6.3). For example, the roots are enriched in heavy Zn isotopes for rice (δ^{66}Zn= −0.03‰ to +0.18‰, [50]), tomato (δ^{66}Zn =+0.16‰ to +0.33‰, [63]) and *Phragmites australis* (δ^{66}Zn=+0.17‰ to +0.43‰, [61]), relative to the shoots (δ^{66}Zn =−0.25‰ to −0.06‰, rice, [50]; δ^{66}Zn =−0.36‰to +0.24‰, tomato, [63]; δ^{66}Zn = −0.55‰ to +0.26‰, *Phragmites australis*, [61]). In plant cells, Zn^{2+} ions are likely complexed with ligands, in order to keep the concentrations of free ions and Zn toxicity low [5, 61, 68]. Isotopically heavy Zn^{2+} ions are suggested to preferentially bind with O- and N- donor groups of ligands attached to organic acids and amino acids such as histidine and nicotianamine (NA), forming Zn-ligand complexes [24, 34, 39, 40, 66, 68], which likely remain in the root cytosol or are further stored in root cell vacuoles [24, 32, 34, 36, 37, 60, 61, 66, 78, 92, 93]. This would enrich the cytosol with light Zn^{2+} ions and isotopically heavy Zn-ligand complexes [24,34,66,68,78]. Studies looking at hyperaccumulators *Phalaris arundinacea* and *Typha latifolia* found that the roots are enriched in isotopically heavy Zn (δ^{66}Zn =+0.24‰ and +0.03‰, respectively; [39, 40]). In the case of *Typha latifolia*, however, Aucour et al. [40] report that Zn in the roots in addition to being bound to organic acids was also bound to thiols, forming Zn-thiol complexes, which accounted for approximately 20% of Zn species found in the roots. The authors conclude that isotopically light Zn was preferentially bound to the S-donor containing thiol groups likely attached to molecules such as glutathione or PCs, which may explain why the roots of *Typha latifolia* were isotopically lighter than those of *Phalaris arundinacea* [40]. Furthermore, it is possible in a plant's root that isotopically heavy Zn binds to O- and N- donor containing ligands and isotopically light Zn binds to S-

containing donor groups of ligands, which are both attached to distinct organic molecules. Thus, the extent to which a plant species is enriched in isotopically heavy Zn in the roots is due to the presence and relative amount of distinct organic molecules present in the roots, and the binding preferences of heavy and light Zn isotopes to the ligands of these distinct organic molecules. This explains, in part, the observed differenced in Zn stable isotope values for Typha *latifolia* and *Phalaris arundinacea.*

In contrast to Zn, most studies have found that the plant roots were largely enriched in isotopically light Cd relative to aerial organs (Appendices Table A6.4). For example, Wiggenhauser et al. [55] found that rice roots are enriched in isotopically light Cd ($\delta^{114}Cd$ = −0.47‰ to +0.03‰) relative to the shoots ($\delta^{114}Cd$ = −0.31‰ to +0.14‰). Studies of rice using X-ray absorption spectroscopy (XAS) report that Cd present in the root is almost exclusively bound to S-donor containing ligands, forming Cd-ligand complexes, as opposed to being free Cd^{2+} ions or bound to O- and N- donor containing ligands [33,55]. It is suggested that isotopically light Cd^{2+} ions are likely preferentially bound to S-containing thiol groups of proteins such as CAL1 and cysteine-rich organic molecules to form Cd-ligand complexes in the root cytosol [30, 31, 32, 33, 35, 38, 53, 55, 56, 57, 58, 64, 68, 80, 89]. These Cd-ligand complexes are less toxic than free Cd^{2+} ions and once formed in the root cytosol can be further sequestered in the root cell's vacuole [30, 31, 32, 33, 45, 55, 56, 72].

In comparing Cd and Zn stable isotope findings, it appears that isotopically heavy Zn and light Cd are complexed in the plant root, and likely both are further stored in root cell vacuoles.

From the plant root cell, Zn is loaded onto the xylem and directed to the aerial plant parts, in particular to the leaves, and Zn speciation in the xylem sap is hypothesised to influence Zn isotope fractionation [24, 27, 28, 29, 30, 39, 40, 42, 60, 66, 93]. The xylem-to-phloem transfer of Zn and the speciation in the phloem sap is likely to also influence Zn isotope fractionation [44]. The xylem sap is suggested to be enriched in isotopically light Zn^{2+} ions and isotopically heavy Zn bound to ligands of organic molecules [24, 27, 29, 30, 39, 40, 42, 60, 66, 93]. In xylem sap, the specific ligand containing organic molecules involved have still not been fully characterized [29], possible suggestions of organic molecules include phytosiderophore and organic molecules such as NA [30, 39, 40, 60]. Nicotianamine is thought to be the primary molecule responsible for complexing with 50% of Zn in the xylem and all the Zn in the phloem, with NA preferring to bind to isotopically heavy Zn [40,60]. Wiggenhauser et al. [68] hypothesise that in the phloem sap an incomplete complexation between NA and Zn may leave the pool enriched in isotopically light Zn^{2+} ions that could be transported to other plant parts, in particular to reproductive organs such as grains. The authors assert, however, it is not clear whether Zn is transferred to the grain as isotopically light Zn^{2+} ions or as Zn-ligand complexes [30, 68]. In plant stems and leaves, isotopically light Zn is also likely bound to organic acids and amino acids such as NA, citrates and malates [39, 40,91]. Overall, there are limited findings on the speciation of Zn in both xylem and phloem sap and in plant stems and leaves.

As with Zn, Cd is loaded onto the xylem and directed to the aerial plant parts. Cd speciation in both the xylem and phloem sap are hypothesised to influence Cd isotope fractionation [30, 38, 53, 55, 56, 72]. In the xylem sap, it is suggested that Cd is primarily present as isotopically heavy Cd^{2+} ions that are transported to leaves [30, 38,53, 55, 56]. In the phloem sap, Cd may be present as either isotopically heavy Cd^{2+} ions or as isotopically light Cd bound to S-donor containing thiol groups of ligands attached to organic molecules such as

PCs and CAL1 [30, 53, 56, 72]. The plant stem, leaves and grains are suggested to be enriched in isotopically light Cd that is primarily bound to organic molecules as opposed to free ions [30,53,55,56,71,72]. It is unlikely, however, that aerial plant parts are enriched *solely* in isotopically light Cd bound to thiol containing organic molecules such as PCs or metallothionein [30, 53, 55, 56, 71, 72]. Wiggenhauser et al. [55] found, using XAS, that Cd is bound to both S- and O- donor containing ligands in the rice shoots. The authors conclude that in addition to isotopically light Cd being bound to S-donor containing thiol ligands in plant shoots, isotopically heavy Cd is also bound to O-donor containing organic acids in the vacuoles of aerial plant parts or bound to cell walls in the apoplast [55]. This mixture of both isotopically heavy Cd-O ligand complexes and isotopically light Cd-S ligand complexes would account, in part, for why aerial plant parts may be enriched in isotopically heavy Cd compared to the plant roots that are enriched entirely in isotopically light Cd bound to S-containing organic molecules. Furthermore, as mentioned, since the roots sequester isotopically light Cd relative to the total plant, the aerial plant parts will by nature of mass balance be enriched in isotopically heavy Cd. The precise Cd speciation in xylem and phloem sap and aerial plant parts, however, remains not well understood and whether the Cd speciation varies between plant species, as it pertains to plant species-specific physiological mechanisms.

In comparing Zn and Cd stable isotope data for aerial plant parts, both metals are hypothesised to be travelling in xylem sap to other plant parts as free ions, namely as isotopically light Zn and heavy Cd. There is less information, however, on Zn and Cd speciation in phloem sap, stems, leaves and reproductive organs (e.g., seeds, fruits and grains).

Process 3: Diffusion

Passive ion diffusion may also, in part, contribute to isotope fractionation during translocation. Free Zn^{2+} and Cd^{2+} ions are likely transported long distance from roots to aerial plant parts following the transpiration stream within the xylem, with lighter isotopes travelling faster than their heavier counterparts or complexed ions, which prefer binding to isotopically heavy Zn and light Cd [27, 30, 34, 42, 43, 44, 52, 56, 61, 64, 68]. As a plants roots store isotopically light Cd and heavy Zn, notably in vacuoles, free isotopically light Zn^{2+} and heavy Cd^{2+} ions are readily available in the cytosol to be transported to aerial plant parts [27, 42, 43,52, 56, 60, 61, 62, 64, 68, 92]. Based on the findings from this review, it is plausible that diffusion could explain why aerial plant parts are systemically enriched in isotopically heavy Cd and light Zn as compared to the roots, due to free isotopically light Zn^{2+} and heavy Cd^{2+} ions that are not complexed to organic molecules being transported faster than complexed counterparts to aerial plant parts (Appendices Tables A6.3 and A6.4). As such, in part, this is in accord with the hypothesis on the role of diffusion in isotope fractionation during translocation.

Process 4: Translocation via membrane transport

The translocation and sequestration of Zn and Cd, as either free ions or metal-complexes, through membrane transporter proteins also contribute to isotope fractionation, as certain carrier proteins that tightly regulate metal transport may demonstrate preferences for certain Zn and Cd stable isotopes [24,29,30,31,33,35,36,39,40,44,45,53,55,56,61,66, 71,72,78]. Previous studies infer that free isotopically light Zn^{2+} ions likely travel to aerial plant parts using channel proteins, though few studies directly discuss the role of these proteins

in translocation [27, 60]. No studies on Cd stable isotopes in plant systems explicitly discuss the role of channel proteins in the isotope fractionations observed during translocation.

Several carrier proteins have been hypothesised as potentially being responsible for the translocation of Zn and Cd in plant species. The carrier proteins metal tolerance proteins (MTP) such as MTP1 and zinc-induced facilitator proteins (ZIF) such as ZIF1, both located on the tonoplast of the vacuole, are believed to participate in the storage of isotopically heavy Zn in roots [24,36, 61]. The YSL family of proteins are hypothesised to be responsible for the translocation of isotopically heavy Zn throughout aboveground plant parts, by loading and unloading Zn onto the xylem and phloem, in *Phalaris arundinacea* and *Typha latifolia* [39, 40]. The HMA carrier proteins may be involved in the translocation and sequestration of Zn and Cd [29, 31, 34,35,53,55,56,72,78]. Heavy metal ATPases are hypothesised to participate in the translocation of isotopically light Zn [29, 78]. In *Noccaea caerulescens*, for examples, HMA4 is suggested to transport isotopically light Zn from the root to aerial plant parts via the xylem using an electrochemical gradient that is supplied energy by ATP hydrolysis [29]. The carrier protein HMA3 is suggested to preferentially sequester isotopically light Cd in rice [31, 33, 55, 56, 72] and in cacao [35]. Zhang et al. [31], for instance, suggested that HMA3 may have an important role in translocation of Cd to the rice grain from roots. In detail, the authors found that rice containing a non-functional (downregulated) *HMA3* gene were enriched in isotopically light Cd (δ^{114}Cd = −0.23‰ for rice grains), whereas rice with a functional (upregulated) HMA3 was enriched in isotopically heavy Cd (δ^{114}Cd = +0.13‰ for rice grains) [31]. Similarly, HMA2 and LCT1 may also be involved in the transport of isotopically heavy Cd from roots to aerial plant parts, namely in rice [53, 56, 72]. Overall, it is unclear whether the carrier proteins identified for the translocation and storage of Zn and Cd are plant-species specific or potentially ascribed to all plant species, and whether Zn and Cd share carrier proteins

such as HMAs. For example, carrier proteins, could explain, in part, the large range of isotope fractionation during translocation of Zn for 7 hyperaccumulators ($\Delta^{66}Zn_{shoot\text{-}root}$ =−1.00‰ and +0.02‰) (Figure 6.4). As part of plant-specific strategies, different carrier proteins could be employed to regulate Zn transport, and therefore influence isotope fractionation during translocation.

Process 5: Remobilisation

Remobilisation of Zn and Cd from mature plant tissues (e.g., mature leaves) to young tissues and reproductive organs (e.g., seeds, grains) influence isotope fractionation observed in plant systems, notably during senescence [32,39,40,43,44,55,61,68,71, 72, 78]. Remobilisation of isotopically light Zn from mature to young tissues and reproductive organs, depletes the mature plant tissues of isotopically light Zn [39, 40, 43, 61, 68, 78]. Aucour et al. [39, 40] found, for instance, a remobilisation via the phloem of isotopically light Zn to stems from the leaves in *Typha latifolia* ($\Delta^{66}Zn_{stem\text{-}leaves}$ = −0.20‰) and *Phalaris arundinacea* ($\Delta^{66}Zn_{stem\text{-}leaves}$ = −0.40‰), and thus depleting the leaves of isotopically light Zn. Similarly, Imseng et al. [32] infer that the differences observed in the translocation of Cd stable isotopes in barley and wheat may be, in part, explained by remobilisation processes. The authors, however, do not explicitly quantify contributions of remobilisation to stable isotope fractionation. Barraza et al. [80] found, for cacao trees, the leaves are enriched in isotopically heavy Cd ($\delta^{114}Cd$ =+0.28‰ to +0.42‰) relative to beans ($\delta^{114}Cd$ =−0.11‰ to +0.34‰), with an apparent isotope fractionation between beans and leaves of −0.40‰ to −0.08‰. Though not directly discussed by the authors, this isotope fractionation between beans and leaves suggests that there is likely Cd transport from cacao leaves to beans possibly through remobilisation, which may impart a different isotope signature then translocation from roots to shoots or leaves. The authors did

not examine roots in this study, so a direct comparison cannot be made for isotope fractionation during translocation from root to shoot [80]. However, a subsequent investigation by Blommaert et al. [71] does find different isotope fractionations between shoot and root ($\Delta^{114/110}Cd_{\text{shoot-root}}$ = +0.27‰) as compared to between cacao beans (nibs) and leaves ($\Delta^{114}Cd_{\text{nibs-leaves}}$ = −0.25‰). This study's findings further support remobilisation from cacao leaves to beans induces a distinct Cd isotope fractionation. Previous studies have noted that the contributions of remobilisation to Cd and Zn isotope fractionation as likely being negligible, with most of Zn and Cd following a unidirectional process from belowground to aboveground plant parts [27, 28, 29]. However, in the case of Cd, few studies have directly examined the role and implications of remobilisation in isotope fractionation. Therefore, it is difficult to compare how Zn and Cd isotope fractionation may explain remobilisation-related physiological mechanisms in plant species.

6.6.5. *Key takeaways on the translocation of Zn and Cd stable isotopes in vascular plants*

This review demonstrates new understandings into the primary processes driving Zn and Cd stable isotope fractionation in vascular plants. In particular, this review found the importance of elemental adsorption and speciation throughout different plant tissues and elemental sequestration in inducing Zn and Cd stable isotope fractionation. In comparing Zn and Cd isotope fractionation within the same sample set of wheat and cacao, Wiggenhauser et al. [68] and Barati et al. [34], respectively, both found inversed isotopic fractionation patterns observed for Zn and Cd during translocation. These authors largely ascribe the inversed isotopic fractionation patterns to complexation of the two elements to distinct organic molecules with different metal binding ligands, which likely mediates the sequestration and

mobilisation of Cd and Zn in wheat and cacao. This explanation is highly plausible for other vascular plant species beyond cacao and wheat. Furthermore, whilst not examined in most studies, remobilisation is identified in this review as likely an important process that influences both Zn and Cd isotope fractionation in plant species and requires further investigation in future studies.

6.7. Influence of plant height on Zn and Cd isotope fractionation during translocation

Besides the five key processes influencing apparent isotope fractionation during translocation, other factors that may influence Zn and Cd isotope fractionation include plant height. A few studies have directly examined how differences in plant height and length may influence Zn stable isotope fractionation [29, 42, 44, 61, 62], and no studies directly examine this relationship in plants for Cd stable isotope fractionation. For instance, theoretical calculations demonstrated that isotope fractionation per distance for Zn was −0.005‰ cm^{-1} in *Phragmites australis* and −0.005‰ to −0.025‰ cm^{-1} in *Noccaea caerulescens* [29, 61]. The findings are also confounded. For instance, multiple studies report that observed Zn isotope fractionation may be associated with changes in plant height [29, 42, 61, 62]. However, Li et al. [44] found no correlation between plant height and Zn isotope fractionation, with the apparent isotope fractionation between stem and branches, leaves, flowers combined at 0-20 cm and 20-40 cm both being +0.17‰. On the other hand, for Cd, Zhong et al. [53] observed in rice that Cd stable isotopes were heavier in the lower leaves, namely in the fifth and bottom leaves, compared to the upper leaves, namely the flag and second leaves, indicating isotopically heavy Cd is preferentially sequestered in the lower leaves. The authors highlighted a possible relationship in plant height and the distribution of Cd stable isotopes, though the influence of plant height on isotope fractionation was not directly discussed nor the focus of the study. As

such, it remains unclear the contributions of plant height to stable isotope fractionation during translocation within and across plant species.

6.8. Genotype-specific influences on Zn and Cd isotope fractionation during uptake and translocation

Another contributing factor that likely affects Zn and Cd apparent isotope fractionation for both uptake and translocation in plant species may be genotype-specific variations in physiological mechanisms [28,34,35,49,50,57]. For instance, previous Zn stable isotope studies examining rice have reported relationships between genotype and Zn isotope fractionation, with certain genotypes largely having either no or positive isotope fractionation between the plant parts such as shoot and its nutrient source [50]. These differences in fractionation were attributed to both nutrient medium conditions, namely whether the rice was grown in Zn deficient or sufficient conditions, and genotype-specific uptake strategies. Additionally, Moore et al. [35] and Barati et al. [34] examined Cd and Zn isotope fractionation, respectively, for the same 19 diverse genotypes of cacao grown under high Cd stress. The authors determined that all 19 genotypes followed an overall similar physiological mechanism for uptake and translocation for either Zn or Cd, respectively, with differences in these mechanisms depending on the specific genotype. In part, this may explain, for example, the noteworthy differences in apparent isotope fractionation during translocation for Cd ($\Delta^{114}Cd_{leaf\text{-}total\ plant}$ =−0.04‰ and +0.46‰) and Zn ($\Delta^{66}Zn_{leaf\text{-}total\ plant}$ =−0.54‰ and −0.09‰), whereby isotopically heavy Zn and light Cd are stored in the plant roots and stems and isotopically light Zn and heavy Cd are mobilised to the leaves [34, 35]. Thus, with limited studies, it appears that genotype-specific strategies influence Zn and Cd isotope fractionation. However, further

studies are required to understand the extent to which genotype-specific strategies influence isotope fractionations during both uptake and translocation.

6.9. Conclusion and recommendations

In this review, most studies demonstrated that plant species preferentially take up isotopically light Zn and Cd from the nutrient medium. Once in the plant, isotopically heavy Zn and light Cd are likely sequestered in the root, while isotopically light Zn and heavy Cd are preferentially translocated from the root to the aerial plant parts. The body of literature suggests that both Zn and Cd isotope fractionation in plant systems are likely driven by biotic and abiotic processes, namely: (1) desorption or dissolution of Zn and Cd from soils influencing uptake fractionation; (2) Zn and Cd speciation in bioavailable pools for uptake and speciation and sequestration in plant tissues; (3) Zn and Cd adsorbed to root surfaces and plant tissues; (4) Zn and Cd diffusion during uptake and translocation; (5) Zn and Cd uptake and translocation through membrane transporter proteins; and (6) Zn and Cd remobilisation during translocation. In addition, during uptake and translocation, factors such as plant height, plant species and genotypes, and total Zn and Cd supply may influence the magnitude of Zn and Cd isotope fractionation during uptake and translocation. Now that these key processes likely responsible for Zn and Cd isotope fractionation in vascular plant species are determined, further studies are required to systematically identify which processes are the most dominant regarding fractionation and are they of similar importance for both metals.

6.9.1. *Key recommendations:*

While progress has been made in understanding Zn and Cd uptake and translocation mechanisms in plants using stable isotope analyses, there are still many research knowledge gaps. Wiggenhauser et al. [86] outlined a detailed set of recommendations for future research on metal and metalloids using stable isotope analyses. The findings of this critical review support their recommendations, in particular the need for studies to examine the apparent isotope fractionation for uptake using the whole plant, including roots and nutrient medium, and not just aerial plant parts. A similar recommendation applies to identifying the apparent isotope fractionation during translocation. Additional new recommendations include the following:

1. When possible, studies should aim to examine the isotope fractionation factors to demonstrate fractionation occurring over time due to biological processes and chemical reactions within plant species during Zn and Cd uptake and translocation. This would require conducting a full mass balance of the plant species being analysed.
2. Studies should strive to employ the use of and report the values for certified reference materials to ensure robust stable isotope measurements.
3. Future studies should also examine whether high- and low-affinity transport systems are an appropriate model for understanding Zn and Cd stable isotope fractionation in vascular plants. In particular, as there are limited studies on Cd, investigations on plant species are required to determine whether it is a suitable model for the experimental findings, including whether isotope fractionation for Cd transport changes under different concentrations (e.g., 0, 5, 20 mg kg^{-1}). Furthermore, future studies should examine, if high-and low-affinity transport systems are used by both these elements, and whether these findings have shared patterns across different types of plant species.

4. The influence and role of soil pH on desorption and adsorption of these metals should be actively considered in future Zn and Cd stable isotope analyses in plant systems. More importantly, changes in soil pH should be studied to evaluate changes in elemental bioavailability and any impact on plant uptake, whereby stable isotope data (e.g., for soil leachates) can provide further constraints on changes in elemental speciation. As such, this will allow for a full understanding of how soil pH impacts apparent isotope fractionation for uptake and will help to encapsulate the complexities of the entire plant system.
5. It is likely that soil microorganisms and plant roots play an important role in the desorption and dissolution of Zn and Cd in soils. Only a small handful of studies have explored the contribution of biological and biochemical processes in the rhizosphere to the desorption of isotopically heavy or light Zn and Cd, and how these processes influence the uptake of these metals by plant species. As such, future studies should actively aim to examine the soil microenvironments and how activities occurring in the rhizosphere impact the uptake of Zn and Cd stable isotopes in plant systems. Ideally, field studies examining plant-soil systems should be employed to capture the complexity of soil microenvironments and biodiversity seen in the natural world. Stable isotope data can help to further constrain the role of biological processes in soils.
6. Future studies should also strive to not just examine the bulk soil portion of the plant-soil system, but also examine the bioavailable pools, as they provide substantial insights into what plant species may be readily accessing.
7. Studies should also utilise XAS in combination with isotope analyses to better understand the Zn and Cd speciation in the bioavailable pools [77]. Further, future XAS studies combined with isotope analyses can provide insight into the binding conditions and Zn and Cd speciation in plant organs (i.e., roots, xylem, phloem, stems, leaves and

reproductive organs), potentially identifying physiological differences for metal storage between plant species. These studies are required to better understand and characterise whether enrichments in isotopically light and heavy Zn are related to the presence of free ions or binding to distinct ligands, and whether Zn and Cd speciation are plant species-specific. In turn, this would help elucidate the Zn and Cd species that are readily transported across plant cells and tissues.

8. There also remains substantial knowledge gaps in the processes and related physiological mechanisms responsible for the uptake and translocation of Zn and Cd, which need to further be examined such as membrane transporter proteins responsible for transport of these metals and their speciation within different organs. In detail, an additional useful tool that can help stable isotope analyses are genetic studies to help triangulate genes responsible for proteins that transport Zn and Cd. As demonstrated by Zhang et al. [31], genes encoding for key proteins that are likely responsible for the transport of metals can be upregulated or downregulated, and stable isotope analyses can determine whether changes in key genes alter observed Zn and Cd isotope fractionation patterns for uptake and/or translocation. In turn, this provides further insights into the underlying processes and mechanisms responsible for the transport of these metals in plant species.
9. Future studies should strive to better understand whether (and how) different genotypes influence stable isotope fractionation for both Zn and Cd during uptake and translocation across different plant species. This, in turn, may provide insights into genotype-specific physiological mechanisms.
10. There is also an opportunity to include in future studies other key study parameters such as plant height, which may influence Zn and Cd stable isotope fractionations in plant-soil and plant-hydroponic systems.

Through applying stable isotope analyses, greater insights have been obtained on the underlying physiological mechanisms responsible for Zn and Cd uptake and translocation, and how these mechanisms change under different environmental conditions. Moreover, by understanding whether Zn and Cd share similar mechanisms, future mitigation strategies may be able to use Zn to reduce the uptake and translocation of Cd in plant-hydroponic and plant-soil systems. In particular, given that in this review many plant species removed isotopically light Zn and Cd preferentially from a nutrient medium, this indicates that similar physiological mechanisms may be employed for Zn and Cd uptake such as membrane transporter proteins. As such, there is a promising opportunity to use Zn amendments to reduce or inhibit entirely the uptake of Cd in plant species.

6.10. References

1. Sharma, R. and Agrawal, M. Single and Combined Effects of Cadmium and Zinc on Carrots: Uptake and Bioaccumulation. *Journal of Plant Nutrition* **29(10)**, 1791-1804 (2006).

2. Haider, F.U. *et al.* Cadmium toxicity in plants: Impacts and remediation strategies. *Ecotoxicology and Environmental Safety* **211**, 111887 (2021).

3. Hart, J., Welch, R., Norvell, W. and Kochian, L. Transport interactions between cadmium and zinc in roots of bread and durum wheat seedlings. *Physiologia Plantarum* **116(1)**, 73-78 (2002).

4. Coleman, J. E. Zinc Proteins: Enzymes, Storage Proteins, Transcription Factors, and Replication Proteins. *Annual Review of Biochemistry* **61**, 897-946 (1992).

5. Lin, Y. and Aarts, M. The molecular mechanism of zinc and cadmium stress response in plants. *Cellular and Molecular Life Sciences* **69(19)**, 3187-3206 (2012).

6. Broadley, M. *et al.* Zinc in plants. *New Phytologist* **173(4)**, 677-702 (2007).

7. Cheng, M., *et al.* Cadmium reduces zinc uptake but enhances its translocation in the cadmium-accumulator, *Carpobrotus rossii*, without affecting speciation. *Plant and Soil* **430(1-2)**, 219-231 (2018).

8. Rizwan, M., Ali, S., Rehman, M., & Maqbool, A. A critical review on the effects of zinc at toxic levels of cadmium in plants. *Environmental Science and Pollution Research International* **26(7)**, 6279–6289 (2019).

9. dos Santos, M. L. S. *et al*. Mitigation of cadmium toxicity by zinc in juvenile cacao: Physiological, biochemical, molecular and micromorphological responses, *Environmental and Experimental Botany* **179**, 104201 (2020).

10. Sanaeiostovar, A., Khoshgoftarmanesh, A. and Shariatmadari, H. Effects of zinc activity in nutrient solution on uptake, translocation, and root export of cadmium and zinc in three wheat genotypes with different zinc efficiencies. *Soil Science and Plant Nutrition* **57(5)**, 681-690 (2011).

11. Cai, Y. *et al*. Mechanisms and uncertainties of Zn supply on regulating rice Cd uptake. *Environmental Pollution* **253**, 959-965 (2019).

12. Du, J. *et al.* The presence of zinc reduced cadmium uptake and translocation in *Cosmos bipinnatus* seedlings under cadmium/zinc combined stress. *Plant Physiology and Biochemistry* **151**, 223-232 (2020).

13. Laporte, M. *et al.* Variability in cadmium and zinc shoot concentration in 14 cultivars of sunflower (*Helianthus annuus* L.) as related to metal uptake and partitioning. *Environmental and Experimental Botany* **109**, 45-53 (2015).

14. Qaswar, M., Hussain, S. and Rengel, Z. Zinc fertilisation increases grain zinc and reduces grain lead and cadmium concentrations more in zinc-biofortified than standard wheat cultivar. *Science of The Total Environment* **605-606**, 454-460 (2017).

15. Nan, Z., Li, J., Zhang, J. and Cheng, G. Cadmium and zinc interactions and their transfer in soil-crop system under actual field conditions. *Science of The Total Environment* **285(1-3)**,187-195 (2002).

16. Hamdan, M. *et al.* Genome editing for sustainable crop improvement and mitigation of biotic and abiotic stresses. *Plants* **11**, 2625 (2022).

17. Wei, R. *et al.* Chromatographic Separation of Cd from Plants via Anion-Exchange Resin for an Isotope Determination by Multiple Collector ICP-MS. *Analytical Sciences* **33(3)**, 335–341 (2017).

18. Wei, R. *et al.* An analytical method for precise determination of the cadmium isotopic composition in plant samples using multiple collector inductively coupled plasma mass spectrometry. *Analytical methods* **7(6)**, 2479–2487 (2015).

19. Moore, R.E.T., Larner, F., Coles, B.J. & Rehkämper, M. High Precision Zinc Stable Isotope Measurement of Certified Biological Reference Materials Using the Double Spike Technique and Multiple Collector-ICP-MS. *Analytical and bioanalytical Chemistry* **409(11)**, 2941–2950 (2017).

20. Arnold, T. *et al.* Measurement of zinc stable isotope ratios in biogeochemical matrices by double-spike MC-ICPMS and determination of the isotope ratio pool available for plants from soil. *Analytical and Bioanalytical Chemistry* **398(7-8)**, 3115–3125 (2010a).

21. Li, D. *et al.* Cadmium Isotope Ratios of Standard Solutions and Geological Reference Materials Measured by MC-ICP-MS. *Geostandards and Geoanalytical Research* **42(4)**, 593–605 (2018).

22. Abouchami, W. *et al.* A Common Reference Material for Cadmium Isotope Studies - NIST SRM 3108. *Geostandards and Geoanalytical Research* **37** (1), 5–17 (2013).

23. Archer, C. *et al.* Inter-calibration of a proposed new primary reference standard AA-ETH Zn for zinc isotopic analysis. *Journal of Analytical Atomic Spectrometry* **32(2)**, 415–419 (2017).

24. Tang, Y. *et al.* Zinc Isotope Fractionation in the Hyperaccumulator *Noccaea caerulescens* and the Nonaccumulating Plant *Thlaspi arvense* at Low and High Zn Supply. *Environmental Science & Technology* **50(15)**, 8020-8027 (2016).

25. Zhou, J. *et al.* Zinc uptake and replenishment mechanisms during repeated phytoextraction using *Sedum plumbizincicola* revealed by stable isotope fractionation. *The Science of the Total Environment* **806(3)**,15130 (2022).

26. Zhou, J. *et al.* Cadmium Isotopic Fractionation in the Soil–Plant System during Repeated Phytoextraction with a Cadmium Hyperaccumulating Plant Species. *Environmental Science & Technology* **54(21)**, 13598-13609 (2020).

27. Couder, E. *et al.* Transpiration flow controls Zn transport in *Brassica napus* and *Lolium multiflorum* under toxic levels as evidenced from isotopic fractionation. *Comptes rendus Geoscience* **347(7-8)**, 386-396 (2015).

28. Arnold, T. *et al.* Iron and zinc isotope fractionation during uptake and translocation in rice (*Oryza sativa*) grown in oxic and anoxic soils. *Comptes rendus Geoscience* **347(7-8)**, 397-404 (2015).

29. Tang, Y. *et al.* Fractionation of Stable Zinc Isotopes in the Field-Grown Zinc Hyperaccumulator *Noccaea caerulescens* and the Zinc-Tolerant Plant *Silene vulgaris*. *Environmental Science & Technology* **46(18)**, 9972-9979 (2012).

30. Wiggenhauser, M. *et al.* Cadmium Isotope Fractionation in Soil–Wheat Systems. *Environmental Science & Technology* **50(17)**, 9223-9231 (2016).

31. Zhang, S. *et al.* Stable isotope fractionation of cadmium in the soil-rice-human continuum. *The Science of the Total Environment* **761**, 143262 (2021).

32. Imseng, M. *et al.* Towards an understanding of the Cd isotope fractionation during transfer from the soil to the cereal grain. *Environmental Pollution* **244**, 834-844 (2019).

33. Wiggenhauser, M. *et al.* Cadmium transfer in contaminated soil-rice systems: Insights from solid-state speciation analysis and stable isotope fractionation. *Environmental Pollution* **269**, 115934 (2021).

34. Barati, E. *et al.* An investigation of zinc isotope fractionation in cacao (*Theobroma cacao* L.) and comparison of zinc and cadmium isotope compositions in hydroponic plant systems under high cadmium stress. *Scientific Reports* **13(1)**, 4682–4682 (2023).

35. Moore, R.E.T. *et al.* Cadmium isotope fractionation reveals genetic variation in Cd uptake and translocation by Theobroma cacao and role of natural resistance-associated macrophage protein 5 and heavy metal ATPase-family transporters. *Horticulture Research* **7(1)**, 71 (2020).

36. Aucour, A.M., Pichat, S., Macnair, M.R. & Oger, P. Fractionation of Stable Zinc Isotopes in the Zinc Hyperaccumulator *Arabidopsis halleri* and Nonaccumulator *Arabidopsis petraea*. *Environmental Science & Technology* **45(21)**, 9212-9217 (2011).

37. Deng, T. *et al.* Nickel and Zinc Isotope Fractionation in Hyperaccumulating and Nonaccumulating Plants. *Environmental Science & Technology* **48(20)**, 11926-11933 (2014).

38. Wei, R. *et al.* Stable isotope fractionation during uptake and translocation of cadmium by tolerant *Ricinus communis* and hyperaccumulator *Solanum nigrum* as influenced by EDTA, *Environmental Pollution* **236**, 634-644 (2018).

39. Aucour, A. *et al.* Dynamics of Zn in an urban wetland soil–plant system: Coupling isotopic and EXAFS approaches, *Geochimica et Cosmochimica Acta* **160**, 55-69 (2015).

40. Aucour, A. *et al.* Zn Speciation and Stable Isotope Fractionation in a Contaminated Urban Wetland Soil–*Typha latifolia* System. *Environmental Science & Technology*, **51(15)**, 8350-8358 (2017).

41. Dinis, L. *et al.* Puzzling Zn isotopes in spruce tree-ring series, *Chemical Geology* **476**, 171-179 (2018).

42. Viers, J. *et al.* Evidence of Zn isotopic fractionation in a soil–plant system of a pristine tropical watershed (Nsimi, Cameroon). *Chemical Geology* **239(1)**, 124-137 (2007).

43. Viers, J. *et al.* Zn isotope fractionation in a pristine larch forest on permafrost-dominated soils in Central Siberia. *Geochemical Transactions* **16(1)**, 3-3 (2015).

44. Li, S., Zhu, X., Wu, L. & Luo, Y. Zinc, iron, and copper isotopic fractionation in *Elsholtzia splendens* Nakai: A study of elemental uptake and (re)translocation mechanisms. *Journal of Asian Earth Sciences* **192**, 104227 (2020).

45. Wang, M., Chen, S., Shi, H. & Liu, Y. Redox dependence of manganese controls cadmium isotope fractionation in a paddy soil-rice system under unsteady pe + pH conditions. *The Science of the Total Environment* **806(2)**, 150675 (2022).

46. Köbberich, M. & Vance, D. Kinetic control on Zn isotope signatures recorded in marine diatoms. *Geochimica et Cosmochimica Acta* **210**, 97-113 (2017).

47. Köbberich, M. & Vance, D. Zn isotope fractionation during uptake into marine phytoplankton: Implications for oceanic zinc isotopes. *Chemical Geology* **523**, 154-161 (2019).

48. Vanhaecke, F., Balcaen, L. & Malinovsky, D. Use of single-collector and multi-collector ICP-mass spectrometry for isotopic analysis. *Journal of Analytical Atomic Spectrometry* **24**, 863 (2009).

49. Arnold, T. *et al.* Evidence for the mechanisms of zinc uptake by rice using isotope fractionation. *Plant, Cell and Environment* **33(3)**, 370-381 (2010).

50. Weiss, D. *et al.* Isotope fractionation of zinc in the paddy rice soil-water environment and the role of 2'deoxymugineic acid (DMA) as zincophore under Zn limiting conditions. *Chemical Geology* **577**, 120271 (2021).

51. Marković, T. *et al.* Experimental Determination of Zinc Isotope Fractionation in Complexes with the Phytosiderophore 2′-Deoxymugeneic Acid (DMA) and Its Structural Analogues, and Implications for Plant Uptake Mechanisms. *Environmental Science & Technology* **51(1)**, 98-107 (2017).

52. Rodushkin, I. *et al.* Isotopic Fractionation during Diffusion of Transition Metal Ions in Solution. *Analytical Chemistry* **76(7)**, 2148–2151 (2004).

53. Zhong, S. *et al.* Water Management Alters Cadmium Isotope Fractionation between Shoots and Nodes/Leaves in a Soil-Rice System. *Environmental Science & Technology* **55(19)**, 12902-12913 (2021).

54. Liu, X. *et al.* Soil (microbial) disturbance affect the zinc isotope biogeochemistry but has little effect on plant zinc uptake. *The Science of the Total Environment* **162490** (2023).

55. Wiggenhauser, M. *et al.* Changes of Cadmium Storage Forms and Isotope Ratios in Rice During Grain Filling. *Frontiers in Plant Science* **12**, 645150-645150 (2021).

56. Zhong, S. *et al.* Cadmium uptake and transport processes in rice revealed by stable isotope fractionation and Cd-related gene expression. *The Science of the Total Environment* **806(2)**, 150633 (2022).

57. Wei, R. *et al.* Fractionation of Stable Cadmium Isotopes in the Cadmium Tolerant *Ricinus communis* and Hyperaccumulator *Solanum nigrum*. *Scientific Reports* **6(1),** 24309-24309 (2016).

58. Wei, R. *et al.* Characteristics of cadmium accumulation and isotope fractionation in higher plants. *Ecotoxicology and Environmental Safety* **174**, 1-11 (2019).

59. Weiss, D.J. *et al.* Isotopic discrimination of zinc in higher plants. *The New Phytologist* **165(3)**, 703-710 (2005).

60. Jouvin, D. *et al.* Stable Isotopes of Cu and Zn in Higher Plants: Evidence for Cu Reduction at the Root Surface and Two Conceptual Models for Isotopic Fractionation Processes. *Environmental Science & Technology* **46(5)**, 2652-2660 (2012).

61. Caldelas, C., Dong, S., Araus, J.L. & J. Weiss, D. Zinc isotopic fractionation in Phragmites australis in response to toxic levels of zinc. *Journal of Experimental Botany* **62(6)**, 2169-2178 (2011).

62. Moynier, F. *et al.* Isotopic fractionation and transport mechanisms of Zn in plants. *Chemical Geology* **267(3)**, 125-130 (2009).

63. Smolders, E. *et al.* Isotopic fractionation of Zn in tomato plants suggests the role of root exudates on Zn uptake. *Plant and Soil* **370(1-2)**, 605-613 (2013).

64. Yan, Y. *et al.* Source attributions of Cadmium contamination in rice grains by Cadmium isotope composition analysis*:* A field study. *Ecotoxicology and Environmental Safety* **210**, 111865 (2021).

65. Caldelas, C. & Weiss, D.J. Zinc Homeostasis and isotopic fractionation in plants: a review. *Plant and Soil* **411(1-2)**, 17-46 (2016).

66. Houben, D. *et al.* Impact of Root-Induced Mobilization of Zinc on Stable Zn Isotope Variation in the Soil–Plant System. *Environmental Science & Technology* **48(14)**, 7866-7873 (2014).

67. Imseng, M. *et al.* The Fate of Zn in Agricultural Soils: A Stable Isotope Approach to Anthropogenic Impact, Soil Formation, and Soil–Plant Cycling. *Environmental Science & Technology* **53(8),** 4140-4149 (2019).

68. Wiggenhauser, M. et al., Zinc isotope fractionation during grain filling of wheat and a comparison of zinc and cadmium isotope ratios in identical soil–plant systems. *The New Phytologist* **219(1)**, 195-205 (2018).

69. Wiggenhauser, M. *et al.* Using isotopes to trace freshly applied cadmium through mineral phosphorus fertilization in soil-fertilizer-plant systems. *The Science of the Total Environment* **648**, 779-786 (2019).

70. Imseng, M. *et al.* Fate of Cd in Agricultural Soils: A Stable Isotope Approach to Anthropogenic Impact, Soil Formation, and Soil-Plant Cycling. *Environmental Science & Technology* **52(4)**, 1919-1928 (2018).

71. Blommaert, H. *et al.* From soil to cacao bean: Unravelling the pathways of cadmium translocation in a high Cd accumulating cultivar of *Theobroma cacao* L. *Frontiers in Plant Science* **13** (2022).

72. Zhong, S. *et al.* Cadmium isotope fractionation and gene expression evidence for tracking sources of Cd in grains during grain filling in a soil-rice system. *The Science of the Total Environment* **873**, 162325–162325 (2023).

73. Gao, T. *et al.* Flooding-drainage alternations impact mobilization and isotope fractionation of cadmium in soil-rice systems. *Journal of Hazardous Materials* **436**, 129048–129048 (2022).

74. Ratié, G. *et al.* Cadmium Isotope Fractionation during Complexation with Humic Acid, *Environment, Science and Technology* **55(11),** 7430–7444 (2021).

75. Yan, X. *et al.* Cadmium Isotope Fractionation during Adsorption and Substitution with Iron (Oxyhydr)oxides. *Environment, Science and Technology* ***55*(17)**, 11601–11611 (2021).

76. Peng, H. *et al*. Cadmium isotope fractionation during adsorption onto calcite. *Chemical Geology* **620** (2023).

77. Aucour, A.M., Sarret, G., Blommaert, H. & Wiggenhauser, M. Coupling metal stable isotope compositions and X-ray absorption spectroscopy to study metal pathways in soil-plant systems: a mini review. *Metallomics* (2023).

78. van der Ent, A. *et al.* Isotopic signatures reveal zinc cycling in the natural habitat of hyperaccumulator *Dichapetalum gelonioides* subspecies from Malaysian Borneo. *BMC Plant Biology* **21(1)**, 1-437 (2021).

79. Pallavicini, N. *et al.* Cadmium isotope ratio measurements in environmental matrices by MC-ICP-MS. *Journal of Analytical Atomic Spectrometry* **29(9)**, 157-1584 (2014).

80. Barraza, F. *et al.* Cadmium isotope fractionation in the soil – cacao systems of Ecuador: a pilot field study. *RSC advances* **9(58)**, 3411-3422 (2019).

81. Zhang, Y. *et al.* Cd isotope fractionation during simulated and natural weathering. *Environmental Pollution* **216**, 9–17 (2016).

82. Jouvin, D. *et al.* Zinc Isotopic Fractionation: Why Organic Matters. *Environmental Science & Technology* **43(15),** 5747-5754 (2009).

83. Fujii, T., Moynier, F., Blichert-Toft, J. & Albarède, F. Density functional theory estimation of isotope fractionation of Fe, Ni, Cu, and Zn among species relevant to geochemical and biological environments. *Geochimica et Cosmochimica Acta* **140**, 553-576 (2014).

84. Moynier, F., Vance, D., Fujii, T. & Savage, P. The Isotope Geochemistry of Zinc and Copper. *Reviews in Mineralogy and Geochemistry* **82(1)**, 543-600 (2017).

85. Zhao, Y. *et al.* Theoretical isotope fractionation of cadmium during complexation with organic ligands. *Chemical Geology* **571**, 120178 (2021).

86. Wiggenhauser, *et al*. Stable Isotope Fractionation of Metals and Metalloids in Plants: A Review. *Frontiers in Plant Science* **13**, 840941–840941 (2022).

87. Dong, S. & Wasylenki, L.E. Zinc isotope fractionation during adsorption to calcite at high and low ionic strength. *Chemical Geology* **447**, 70-78 (2016).

88. Pokrovsky, O.S., Viers, J. & Freydier, R. Zinc stable isotope fractionation during its adsorption on oxides and hydroxides. *Journal of Colloid and Interface Science* **291(1)**, 192-200 (2005).

89. Wei, R., Guo, Q., Zhang, Q. & Ma, J. Characteristics of cadmium translocation and isotope fractionation in *Ricinus communis* seedlings: Effects from split/cut-root and limited nutrients. *The Science of the Total Environment* **819**, 152493 (2022).

90. Degryse F., Broos K., Smolders E. & Merckx R. Soil solution concentration of Cd and Zn can be predicted with a CaCl2 soil extract. *European Journal of Soil Science* **54**, 149- 158 (2003).

91. Fujii, T. & Albarède, F. Ab Initio Calculation of the Zn Isotope Effect in Phosphates, Citrates, and Malates and Applications to Plants and Soil. *PloS one* **7(2)**, e30726-e30726 (2012).

92. Caldelas, C., Poitrasson, F., Viers, J. & Araus, J.L. Stable Zn isotopes reveal the uptake and toxicity of zinc oxide engineered nanomaterials in *Phragmites australis*. *Environmental Science Nano* **7(7),** 1927-1941 (2020).

93. Araújo, D.F. *et al.,* Zinc isotopes as tracers of anthropogenic sources and biogeochemical processes in contaminated mangroves. *Applied Geochemistry* **95**, 25-32 (2018).

94. Lv, W. *et al.* Effect of the Dry Ashing Method on Cadmium Isotope Measurements in Soil and Plant Samples, *Geostandards and Geoanalytical Research* **45(1)**, 245-256 (2021).

95. Rodushkin, I. *et al.* Assessment of the natural variability of B, Cd, Cu, Fe, Pb, Sr, Tl and Zn concentrations and isotopic compositions in leaves, needles and mushrooms using single sample digestion and two-column matrix separation. *Journal of Analytical Atomic Spectrometry* **31(1)**, 220–233 (2015).

Chapter 7
Conclusion and Future Research Opportunities

7.1. Summary of Key Findings

The aim of this Ph.D. thesis has been to provide original contributions to the wider research on understanding and mitigating against the uptake and translocation of Cd in cacao plants, in particular the cacao fruit and beans. In Chapter 4, using MC-ICP-MS methodologies, Zn concentrations and stable isotope compositions were measured for genetically diverse, juvenile cacao samples under high Cd stress. In Chapter 5, using primarily ICP-Q-MS methodologies, Cd and other essential and non-essential element concentrations were measured for soil, soil leachate and cacao plant samples from diverse localities in Ecuador. In Chapter 6, a comprehensive critical review examined the current body of research on Cd and Zn isotope fractionation in vascular plant systems.

A key finding from Chapter 4 was that under high Cd stress, 19 genetically diverse, juvenile cacao plants preferentially removed isotopically light Zn from hydroponic solutions, and translocated isotopically light Zn from the roots to aerial plant parts (i.e. stem and leaves). Another key finding from Chapter 4 was that the juvenile cacao plants preferentially took up isotopically light Zn from the hydroponic solution under high Cd stress. In comparison, previously published data on the same juvenile cacao plants, grown under high Cd stress, preferentially removed isotopically light Cd from hydroponic solutions, and translocated isotopically heavy Cd from roots to aerial plant parts. Moreover, both isotopically light Zn and Cd were taken up by the 19 genetically diverse cacao plants under high Cd stress. As such, this indicates that it is highly likely that cacao plants share an overarching physiological mechanism for Cd and Zn uptake, namely that they likely utilise similar membrane transporter proteins. In contrast, the cacao roots and leaves revealed an inverse isotope fractionation pattern for the two metals, with isotopically heavy Zn and light Cd enriched in the roots and isotopically light Zn and heavy Cd enriched in the leaves. This systematic pattern may reflect that Zn and Cd

have different physiological mechanisms for the sequestration and translocation of the two metals, which are likely regulated by distinct organic molecules in the cacao roots.

In Chapter 5, full cacao-soil systems across six smallholder farms in Ecuador were examined to determine the distribution of essential and non-essential elements. The cacao trees examined in this Chapter were of the two most common Ecuadorian cacao genotypes (Nacional and CCN-51). This Chapter found irrespective of genotype or age, cacao trees only efficiently took up Cd from soils. However, when examining bioavailable pools, the cacao tree efficiently took up Cd, Cu, Mn and Zn. In particular, the cacao trees had similar distributions of BF values for Zn and Cd as well as for Mn and Cu between the cacao tree and bioavailable soil pools, which indicated that these metals may share similar physiological mechanisms for uptake. The elemental mass distributions demonstrated that cacao trees may utilise similar pathways and mechanisms for the transport of certain elements across different plant parts. One key finding from this Chapter, in particular, is that based on the similar elemental distributions, transport efficiencies and chemical behaviours, it is highly likely that Cd is a hitchhiker element to Zn, using similar pathways and underlying physiological mechanisms such as membrane transporter proteins. In addition, Chapter 5 proposed an additional explanation for the observed distinct isotopic signatures for Zn and Cd in cacao observed in Chapter 4, whereby the woody biomass serves as a large sequestration reservoir for Cd, more so than for Zn, likely as part of an internal tolerance strategy.

Based on the findings from Chapter 4 and 5, Zn and Cd more than likely share physiological mechanisms for their uptake in cacao. Both these studies examine Zn and Cd in environmentally controlled, cacao-hydroponic studies and in field conditions in Ecuador. Both Chapters support the hypothesis that as chemically similar elements, Zn and Cd are likely taken

up and transported through similar pathways and mechanisms. Therefore, the Ph.D. research strongly supports the possibility of Zn amendments and supplementation to reduce the uptake of Cd by cacao trees and its subsequent transport to cacao beans. However, further studies are required to confirm the efficacy of Zn amendments and supplementation as a mitigation strategy, particularly in field conditions in Ecuador and other South and Central American countries.

The findings from the comprehensive critical review (Chapter 6) strongly support the research findings from Chapter 4, with different vascular plant species following similar systematics for isotope fractionation as cacao plants for both Zn and Cd. In Chapter 6, most studies demonstrated that vascular plant species preferentially take up isotopically light Zn and Cd from nutrient mediums (i.e. bulk soils and soil extracts and solutions). Once Zn and Cd have entered a plant species, isotopically heavy Zn and light Cd are likely sequestered in the root, whereas isotopically light Zn and heavy Cd are preferentially translocated from the root to aerial plant parts. Through the body of literature, the primary processes and corresponding mechanisms likely responsible for both Zn and Cd isotope fractionation in vascular plant systems were identified. Furthermore, this Chapter identified knowledge gaps in the current research on Zn and Cd isotope fractionation observed across different plant species, which highlight opportunities to explore for future studies, to better understand the uptake and transport of these metals in plant systems, including in cacao.

7.2. Future Research Opportunities

As research into Cd and cacao is rapidly expanding, with most of the studies being conducted in the last 5 to 10 years, there are exciting future opportunities to explore. This Ph.D.

research found significant relationships between Zn and Cd both in environmentally controlled, hydroponic and field studies. In the future, there are opportunities in developing studies that examine the Cd isotope compositions of cacao plants cultivated in different Zn conditions. Of notable interest is whether higher Zn concentrations in the nutrient media (e.g., hydroponic solutions and soils) alter the uptake and translocation of Cd, including for mature cacao plants with ripe fruit and beans. These studies will help to highlight whether similar or distinct mechanisms are responsible for Zn and Cd homeostasis in cacao plants. If these future studies confirm that Zn and Cd do, in fact, share similar uptake mechanisms, this may enable the use of Zn amendments added to soils to reduce the overall Cd uptake of cacao plants grown in South and Central America through a competition mechanism. Similarly, there are opportunities to explore whether changes in concentration for other essential elements, such as Mg and Fe, alter the uptake and translocation of Cd. If these other elements and Cd also share and compete for physiological mechanisms for uptake and transport, there are further possibilities of utilising amendments or supplementation to nutrient medium (i.e. soils) to reduce Cd uptake, transport and accumulation in cacao fruit and beans.

There are additional opportunities to combine genetic studies with stable isotope and concentration (ionome) studies. The use of knockout or knockdown genes in conjunction with stable isotope and concentration measurements can help to isolate and identify genes responsible for membrane transporter proteins of essential and non-essential elements. In detail, for example, it may be possible to mitigate the high Cd concentrations of cacao beans without affecting essential elements such as Zn, Mg, and Fe, via knock-out of genes responsible for encoding proteins that assist in the translocation of Cd to aboveground parts or in sequestration in roots, respectively. In addition, the use of x-ray absorption spectroscopy studies can help to further constrain essential and non-essential elements, notably Zn and Cd,

speciation and ligand-binding environments in different cacao plant parts as well as supporting investigations into genes that likely participate in the uptake, sequestration and mobilisation of these metals. With that said, ionome and stable isotope studies of cacao have made great strides in helping to understand the underlying physiological mechanisms responsible for the transport of Cd, and more recently of other essential and non-essential elements. Future studies should continue to support understanding these mechanisms as well as trying to understand the efficacy of mitigation strategies aimed at combatting high Cd concentrations in cacao beans.

Chapter 8
Appendices

Appendix I:

Chapter 4

An investigation of zinc isotope fractionation in cacao (*Theobroma cacao* L.) and a comparison of zinc and cadmium isotope compositions in hydroponic plant systems under high cadmium stress

Table A4.1. Cacao clone names, accession numbers and donor organizations of the cacao germplasms used in this study.

Cacao Clones (Genotype) Name	Accession number (ICQC, R)	Donor Collection
B 5/7 [POU]	RUQ 522	ICG, T
Catie 1000	RUQ	CIRAD
CC 41	RUQ	ICG, T
CL 19/10	RUQ	ICG, T
GU 207/H	RUQ	CIRAD
GU 236/V	RUQ	CIRAD
IMC 27	RUQ	ICG, T
LP 1/41 [POU]	RUQ	ICG, T
Matina 1-7	RUQ	ICG, T
NA 702	RUQ	ICG, T
PNG 340	RUQ	CIRAD
Pound 12/A [POU]	RUQ	ICG, T
RB 46	RUQ	CATIE
RIM 179	RUQ	CATIE
SCA 9	RUQ	ICG, T
SPA 9 [COL]	RUQ	ICG, T
TARS 31	RUQ	USDA-TARS
TSA 654	RUQ	CEPLAC/CEPEC
U 70 [PER]	RUQ	UNAS

CATIE	Centro Agronómico Tropical de Investigión y Enseñanza (Costa Rica)
CEPLAC	Comissão Executiva do Plano da Lavoura Cacaueira (Brazil)
CIRAD	Centre de cooperation international en recherché agronomique pour le développement (France)
ICG, T	International Cocoa Genebank (Trinidad)
ICQC, R	International Cocoa Quarantine Centre, Reading (UK)
UNAS	Universidad Nacional Agraria de la Selva (Peru)
USDA-TARS	United States Department of Agriculture, Tropical Crops and Germplasm Research, Mayaguez (Puerto Rico)

Table A4.2. Composition of the half-strength Hoagland solution including additional $CdCl_2$.

Component	Species	Concentration	
		mg L^{-1}	µmol L^{-1}
Major nutrients			
KH_2PO_4	K^+	19.55	500
	PO_4^{2-}	47.49	500
	H^+	3.002	1500
KNO_3	K^+	97.75	2500
	NO_3^-	155.0	2500
$Ca(NO_3)_2 \cdot 4H_2O$	Ca_2^+	100.2	2500
	NO_3^-	310.0	5000
$MgSO_4 \cdot 7H_2O$	Mg^{2+}	24.31	1000
	SO_4^{2-}	96.07	1000
Micronutrients			
H_3BO_3	H_3BO_3	1.430	23.1
Fe-EDTA[a]	Fe^{3+}	2.383	42.7
	$EDTA^{4-}$	12.30	42.7
$MnCl_2 \cdot 4H_2O$	Mn^{2+}	0.253	4.6
	Cl^-	0.326	9.2
$ZnSO_4 \cdot 7H_2O$[a]	Zn^{2+}	0.025	0.38
	SO_4^{2-}	0.037	0.38
$CuSO_4 \cdot 5H_2O$	Cu^{2+}	0.010	0.2
	SO_4^{2-}	0.015	0.2
$Na_2MoO_4 \cdot 2H_2O$	Na^+	0.002	0.1
	MoO_4^{2-}	0.003	0.04
$CdCl_2$[b]	Cd^{2+}	2.248	20.0
	Cl-	1.418	20.0

[a]$C_{10}H_{12}FeN_2O_8$. [b]After 28 day growing period, $CdCl_2$ was introduced to the hydroponic solutions for an additional 14 days.

Table A4.3. Zinc concentrations ([Zn]; mg kg^{-1}) and stable isotope compositions ($\delta^{66}Zn$) for quality control materials.

			[Zn] ± SD mg kg^{-1}		δ^{66} Zn ± 2SD ‰	
Material	**Type**	**n**	**This study**	**Literature**	**This study**	**Literature**
London Zinc	Pure Zn solution	30	-	-	+0.10 ±0.06	+0.12 ± 0.06[a]
NIST SRM 1570a	Spinach leaf	19	79 ± 6	82 ± 4[b]	+0.41 ±0.06	-

All stable isotope compositions (δ^{66}) are reported relative to JMC-Lyon Zn. n represents the number of individual samples that were analysed. [a]The $\delta^{66}Zn$ ± 2SD (‰) is the mean value reported in Archer et al. [54]. [b] The Zn concentration data outlined in the original certificate. SD represents standard deviation. 2SD for individual samples represents the analytical precision of the Zn stable isotope data determined from multiple analyses of the Zn isotope standard (AA-ETH-Zn) that bracketed the sample runs.

Table A4.4. Summary of mass fractions (*f*), Zn concentrations ([Zn]; mg kg^{-1}) and Zn stable isotope compositions (δ^{66} Zn) for leaves, stems and roots determined for biological and analytical replicates.

Cacao Clones (Genotype)	Replicate	Leaf				Stem				Root				Total Plant
		f	[Zn] mg kg^{-1}	δ^{66}Zn ‰	2SD ‰	*f*	[Zn] mg kg^{-1}	δ^{66}Zn ‰	2SD ‰	*f*	[Zn] mg kg^{-1}	δ^{66}Zn ‰	2SD ‰	[Zn] mg kg^{-1}
CC 41[a]	1	0.66	24	−0.82	0.06	0.25	18	−0.19	0.06	0.10	16	0.58	0.06	21
	2	0.73	22	−0.75	0.02	0.18	19	−0.14	0.08	0.09	14	0.44	0.08	20
	3	0.77	35	−0.41	0.07	0.17	19	−0.20	0.08	0.06	11	0.50	0.08	27
Mean	**-**	**0.72**	**27**	**−0.66**	**-**	**0.20**	**19**	**-0.18**	**-**	**0.08**	**14**	**0.51**	**-**	**23**
1SD	**-**	**0.05**	**7**	**-**	**-**	**0.04**	**1**	**-**	**-**	**0.02**	**2**	**-**	**-**	**4**
2SD	**-**	**-**	**-**	**0.36**	**-**	**-**	**-**	**0.05**	**-**	**-**	**-**	**0.11**	**-**	**-**
GU 207/H[a]	1	0.68	27	−0.43	0.06	0.15	27	−0.44	0.06	0.17	18	0.33	0.03	25
	2	0.77	36	−0.43	0.03	0.16	32	−0.39	0.08	0.06	13	0.48	0.03	32
	3	0.73	33	−0.44	0.04	0.14	26	−0.42	0.07	0.12	18	0.38	0.08	29
Mean	**-**	**0.73**	**32**	**−0.43**	**-**	**0.15**	**28**	**−0.42**	**-**	**0.12**	**16**	**0.40**	**-**	**29**
1SD	**-**	**0.04**	**4**	**-**	**-**	**0.01**	**3**	**-**	**-**	**0.04**	**2**	**-**	**-**	**3**
2SD	**-**	**-**	**-**	**0.01**	**-**	**-**	**-**	**0.05**	**-**	**-**	**-**	**0.15**	**-**	**-**
Matina 1-7[b]	1	0.65	20	−0.68	0.09	0.27	23	−0.63	0.08	0.08	13	0.01	0.08	20
	1	0.55	19	−0.78	0.06	0.35	33	−0.63	0.04	0.09	16	−0.04	0.08	22
Mean	**-**	**0.60**	**20**	**−0.73**	**-**	**0.31**	**28**	**−0.63**	**-**	**0.09**	**15**	**−0.02**	**-**	**21**
1SD	**-**	**0.05**	**1**	**-**	**-**	**0.04**	**5**	**-**	**-**	**0.01**	**2**	**-**	**-**	**1**
2SD	**-**	**-**	**-**	**0.14**	**-**	**-**	**-**	**0**	**-**	**-**	**-**	**0.07**	**-**	**-**

[a] Biological replicates; single digests of leaf, stem and root samples from three separate plants of CC 41 and GU 207/H. [b] Analytical replicates; duplicate digests of leaf, stem and root samples from a single plant of Matina 1-7. SD represents the standard deviation; 1SD is used for *f* and Zn concentrations ([Zn]) and 2SD for Zn stable isotope compositions (δ^{66}Zn). 2SD for individual samples represents the analytical precision of the Zn stable isotope data determined from multiple analyses of the Zn isotope standard that bracketed the sample runs.

Table A4.5. Dry weights (g) of the organs from plants treated with 20 μmol L^{-1} $CdCl_2$.

Genotype	Leaf g	Stem g	Root g	Total Plant g
B 5/7 [POU]	0.554	0.246	0.092	0.892
Catie 1000	0.304	0.122	0.127	0.553
CC 41[a]	0.584	0.220	0.125	0.929
CL 19/10	1.361	0.289	0.159	1.809
GU 207/H[a]	0.393	0.094	0.115	0.602
GU 236/V	0.332	0.089	0.144	0.565
IMC 27	0.301	0.147	0.132	0.580
LP 1/41 [POU]	0.635	0.259	0.101	0.995
Matina 1-7	1.387	0.499	0.269	2.155
NA 702	1.181	0.341	0.198	1.720
PNG 340	0.940	0.551	0.206	1.697
Pound 12/A [POU]	0.525	0.139	0.121	0.785
RB 46	0.512	0.140	0.134	0.786
RIM 179	1.298	0.334	0.299	1.931
SCA 9	0.668	0.262	0.122	1.052
SPA 9 [COL]	0.535	0.218	0.127	0.880
TARS 31	0.534	0.181	0.280	0.995
TSA 654	0.616	0.153	0.138	0.907
U 70 [PER]	0.247	0.084	0.068	0.399
Mean	**0.679**	**0.230**	**0.156**	**1.065**
1SD	**0.370**	**0.131**	**0.065**	**0.527**

[a]Mean values for the single leaf, stem, and root aliquots of three separate plants of the CC 41 and GU 207/H genotypes (n = 3). SD represents the standard deviation.

Table A4.6. Summary of Zn concentration data (mg kg^{-1}) for cacao leaves from this study and the literature.

Reference	Country	Cacao leaf Zn concentrations (mg kg^{-1})
This Study	-	14 – 63
Gramlich et al. [42]	Honduras	17 – 381
Barraza et al. [71]	Ecuador	17 – 263
Gramlich et al. [72]	Bolivia	36.8 – 48.8

Table A4.7. Summary of mean dry weights (g), mass fractions (*f*), Zn concentrations ([Zn]; mg kg^{-1}) and Zn stable isotope compositions (δ^{66} Zn) of leaves, stems and roots and total plant dry weights (g) for seedlings of the NA 702 genotype treated with 0, 5, and 20 µmol L^{-1} $CdCl_2$.

$CdCl_2$ µmol L^{-1}	n	Leaf					Stem					Root					Total Plant
		Dry weight g	*f*	[Zn] mg kg^{-1}	δ^{66}Zn ‰	2SD ‰	Dry weight g	*f*	[Zn]mg kg^{-1}	δ^{66}Zn ‰	2SD ‰	Dry weight g	*f*	[Zn] mg kg^{-1}	δ^{66}Zn ‰	2SD ‰	Dry weight g
0	3	1.22	0.63	15	−0.50	0.06	0.38	0.22	18	−0.50	0.06	0.23	0.16	20	0.21	0.04	1.83
5	2	1.19	0.69	15	−0.43	0.07	0.31	0.24	21	−0.52	0.05	0.20	0.07	10	0.23	0.07	1.70
20	1	1.18	0.71	16	−0.70	0.08	0.34	0.20	16	−0.28	0.07	0.20	0.09	12	0.40	0.06	1.72
Mean		**1.20**	**0.66**	**16**	**−0.51**	**-**	**0.35**	**0.22**	**18**	**−0.46**	**-**	**0.21**	**0.12**	**15**	**0.25**	**-**	**1.77**
1SD		**0.06**	**0.05**	**2**	**-**	**-**	**0.06**	**0.03**	**5**	**-**	**-**	**0.03**	**0.05**	**5**	**-**	**-**	**0.09**
2SD		**-**	**-**	**-**	**0.29**	**-**	**-**	**-**	**-**	**0.21**	**-**	**-**	**-**	**-**	**0.14**	**-**	**-**

n represents the number of individual samples that were digested and analysed. SD represents standard deviation; 1SD is used for dry weight, *f* and Zn concentrations ([Zn]) and 2SD for Zn stable isotope compositions (δ^{66}Zn). 2SD for individual samples represents the analytical precision of the Zn stable isotope data determined from multiple analyses of the Zn isotope standard that bracketed the sample runs.

Table A4.8. Summary of Δ^{66}Zn for uptake, and Zn stable isotope compositions (δ^{66} Zn) for root, shoot and leaf published for different plant species.

Reference	Plant Species	Zn concentrations in nutrient sources	Δ^{66}Zn represents	Δ^{66}Zn ‰[a]	Root δ^{66}Zn ‰	Shoot δ^{66}Zn ‰	Leaves δ^{66}Zn ‰
This Study	*Theobroma cacao* L.	0.38 µmol L^{-1}	Total plant–hydroponic solution	−1.21 to −0.73 and *−1.49 to −0.86*	−0.28 to +0.68	-	−1.11 to −0.43
Aucour et al. [12]	*Arabidopsis halleri* and *Arabidopsis petraea*	10 and 250 µmol L^{-1}	Total plant–hydroponic solution	−0.36 to +0.00	+0.19 to +0.96	−0.54 to +0.16	-
Aucour et al. [13]	*Typha latifolia*	2089 mg kg^{-1}[g]	Total plant–soil	−0.50[b]	+0.03[b]	-	−0.32[b]
Aucour et al. [24]	*Phalaris arundinacea*	2129 mg kg^{-1}[g]	Total plant–soil	−0.60[b]	+0.24[b]	-	−0.19[b]
Deng et al. [48]	*Thlaspi arvense*, *Alyssum murale and Noccaea caerulescens*	2 and 50 µmol L^{-1}	Total plant–hydroponic solution	−0.23 to +0.20[b]	+0.17 to +1.12	−0.59 to +0.23	-
Tang et al. [10]	*Noccaea caerulescens* and *Thlaspi arvense*	0.02, 1, 5 and 50 µmol L^{-1}	Total plant–hydroponic solution	−0.26 to −0.06[b]	+0.14 to +0.82	−0.26 to +0.13	-
Houben et al. [16]	*Agrostis capillaris* L.	9470 and 56600 mg kg^{-1}[g]	Total plant–soil leachate	−0.04 and +0.02[f]	+0.17 to +0.36[f]	−0.10 to −0.05[f]	-
Tang et al. [9]	*Noccaea caerulescens and Silene vulgaris*	107, 115, 2220 and 2396 mg kg^{-1}[g]	Total plant–soil	−0.05 to +0.63[b]	+0.68 to +0.99[b]	-	+0.19 to +0.88[b]
Smolders et al. [57]	*Lycopersicon esculentum* L. (tomato)	<0.03, 0.9 and 1.0 µmol L^{-1}	Total plant–hydroponic solution	−0.33 to −0.06	+0.16 to +0.33[b]	−0.36 to +0.24[b]	-
Arnold et al. [19]	*Oryza sativa* L. (rice)	26 mg kg^{-1}[h]	Total plant above ground–soil leachate	−0.27 and −0.08[c]	-	+0.61 and +0.73[c]	-
Wiggenhauser et al. [18]	*Triticum aestivum* L. (wheat)	0.4 and 10.9 mg kg^{-1}[h]	Total plant–soil extract	−0.33 and +0.13[d]	+0.56 and +0.63[d]	-	+0.10 to +0.72[e]

All Zn stable isotope compositions (δ^{66}Zn) are reported relative to JMC-Lyon Zn. [a] non-italicized values represent isotopic differences, whereas italicized values represent the isotope fractionation factor (ε^{66}Zn) for uptake. [b] mean values. [c] mean values for rice grown in anaerobic and aerobic soils, respectively. [d] mean values for wheat grown in soil from two different sites. [e] range of mean values for flag and senescent leaves for wheat. [f] mean values for *Agrostis capillaris* L. grown in soil from two different sites. [g] represents total Zn concentrations in soils. [h] represents total Zn concentration in soil leachates or extracts.

Note A4.1. Depletion of Zn from the hydroponic solutions.

Plants were grown in 3 L hydroponic systems containing 4 plants of the same genotype (see main text for further experimental details). The total Zn mass taken up by one plant from each system was calculated based on the Zn concentrations in each organ and their dry mass. For two of the 19 genotypes (CC 41 and GU 207/H), the total Zn mass was calculated for three plants and an average was taken. Given the good agreement between the total Zn masses for the replicates of CC 41 and GU 207/H, all plants in each system were assumed to take up the same mass of Zn and therefore the total Zn mass of one plant was multiplied by four. This total mass of Zn that was removed from the hydroponic solution was then converted to a percentage of the total Zn mass available in the hydroponic systems (equation A4.1):

$$\text{Hydroponic Zn depletion (\%)} = \left(\frac{\text{Total Zn of 4 plants}}{\text{Total Zn in hydroponic substrate}}\right) \text{x } 100 \quad \text{(Equation A4.1)}$$

The percentages (21±8%, 1SD) were then used to calculate the initial and final Zn isotope compositions of the hydroponic solutions, and ultimately, the Zn isotope fractionation factor ε^{66}Zn during root uptake (see main text for details).

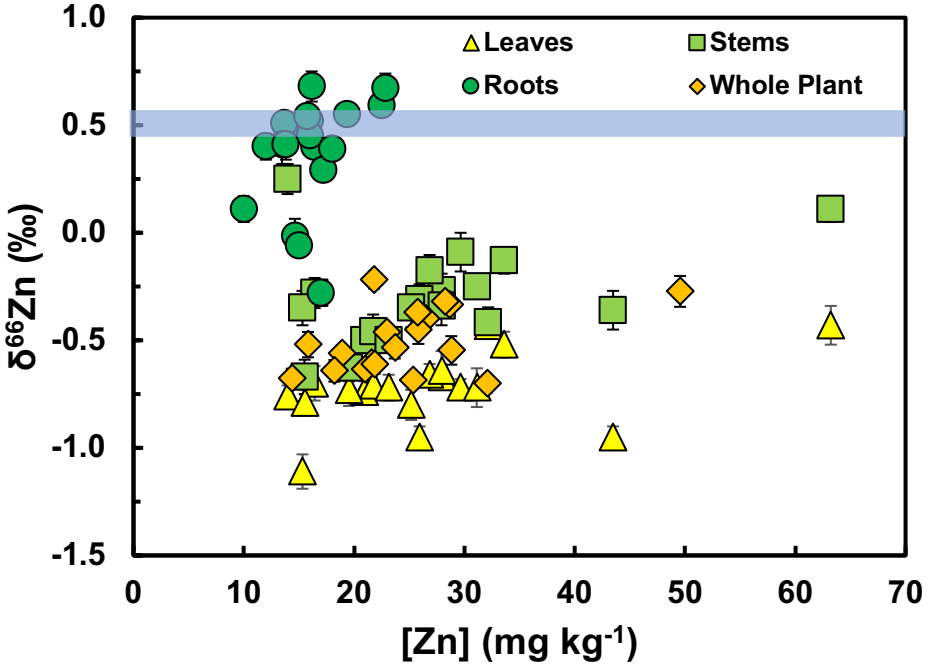


Figure A4.1. Zinc stable isotope compositions ($\delta^{66}Zn$) versus Zn concentrations ([Zn]; mg kg^{-1}) for leaves, stems, roots, and whole plants of the 19 cacao genotypes treated with 20 µmol L^{-1} $CdCl_2$. The error bars denote the 2SD precision determined for multiple analyses of the Zn isotope standard that bracketed the sample runs. The blue line denotes the $\delta^{66}Zn$ value of +0.51±0.06‰ for the $ZnSO_4$ that was added to the hydroponic solutions.

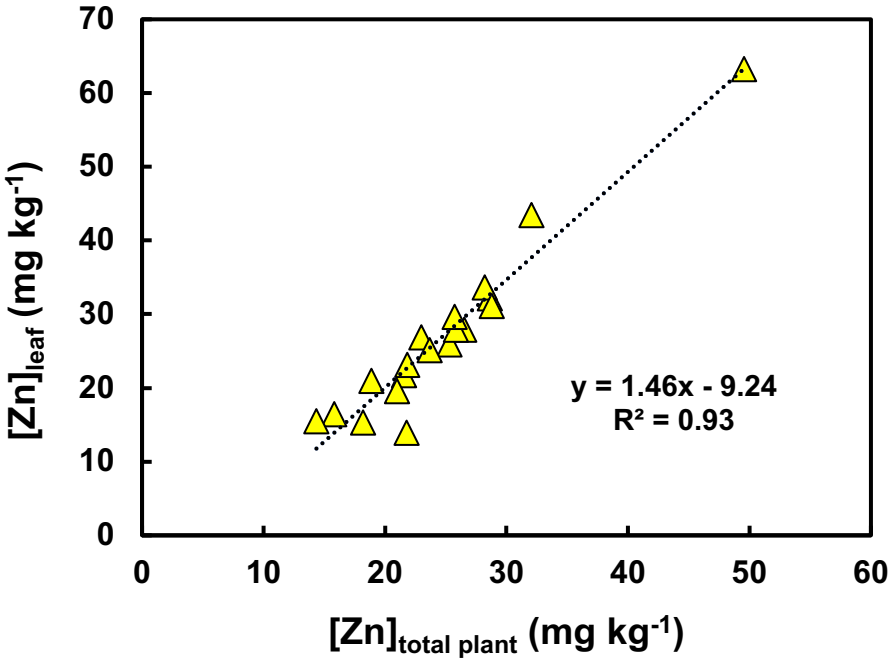


Figure A4.2. Leaf Zn concentrations ([Zn]; mg kg^{-1}) versus total plant Zn concentrations (mg kg^{-1}) for the 19 cacao genotypes.

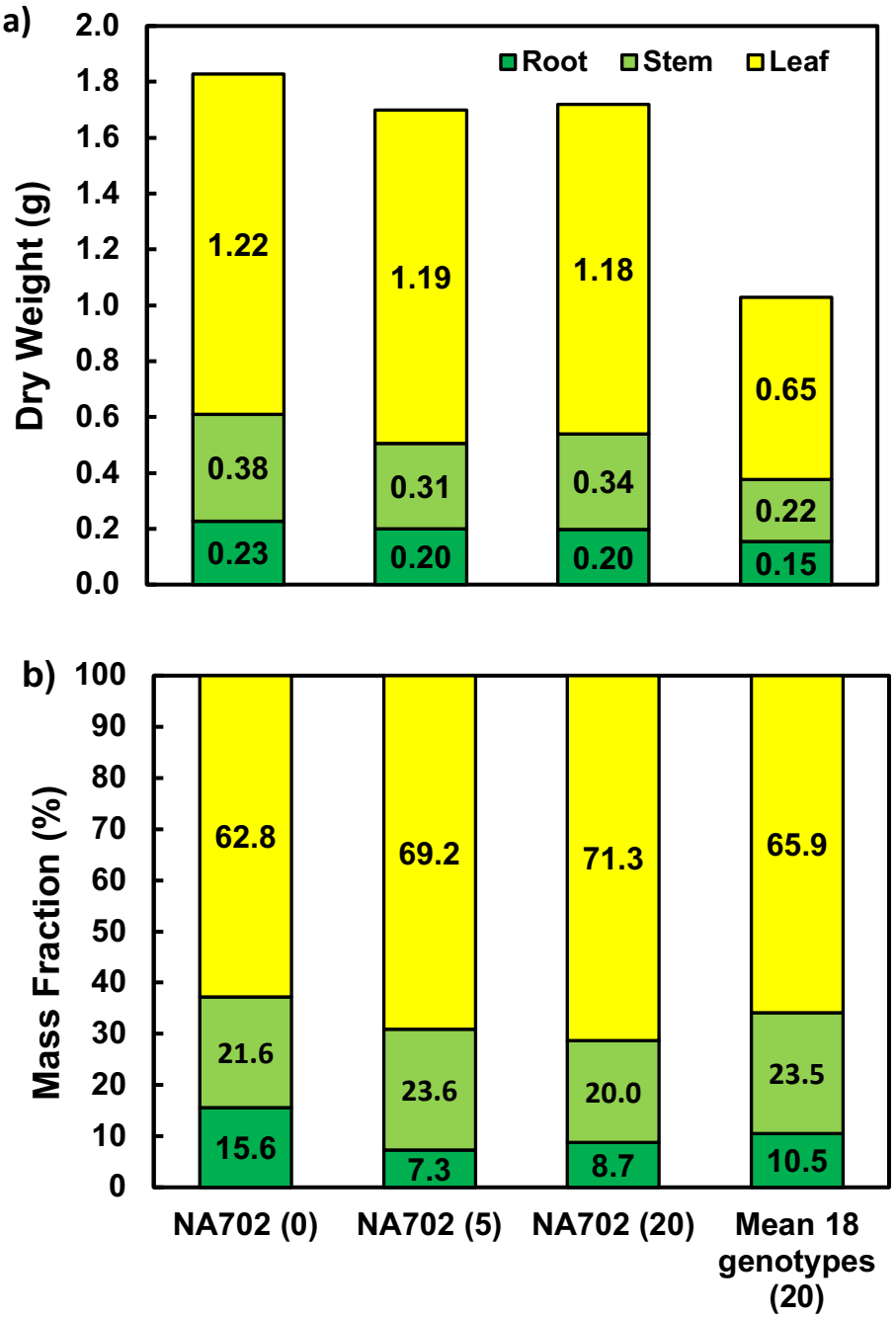


Figure A4.3. (a) Dry weights (g) and (b) mass fraction (%) for organs of NA 702 plants cultured with 0, 5 and 20 µmol L^{-1} $CdCl_2$ and mean results for the other 18 cacao genotypes cultured with 20 µmol L^{-1} $CdCl_2$. The notations (0), (5), (20) represent NA 702 plants treated with 0, 5, and 20 µmol L^{-1} $CdCl_2$, respectively.

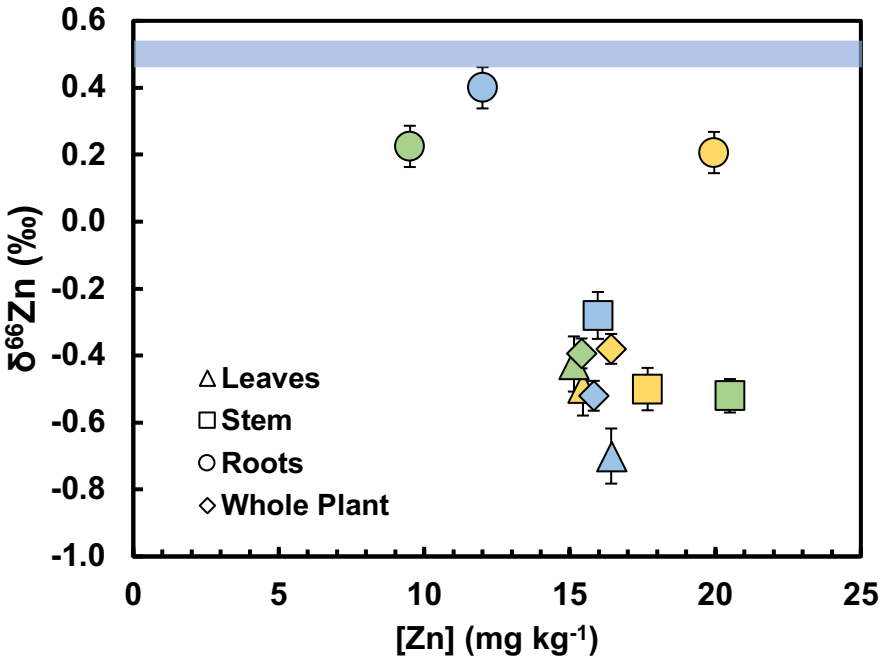


Figure A4.4. Mean Zn stable isotope compositions (δ^{66}Zn) for leaves, stems and roots versus mean Zn concentrations ([Zn]; mg kg^{-1}) of the NA702 seedlings treated with 0 µmol L^{-1} (yellow), 5 µmol L^{-1} (green) and 20 µmol L^{-1} (blue) $CdCl_2$. The error bars denote the 2SD precision determined for multiple analyses of the Zn isotope standard that bracketed the sample runs. The blue line denotes the δ^{66}Zn value of +0.51±0.06‰ for the $ZnSO_4$ that was added to the hydroponic solutions.

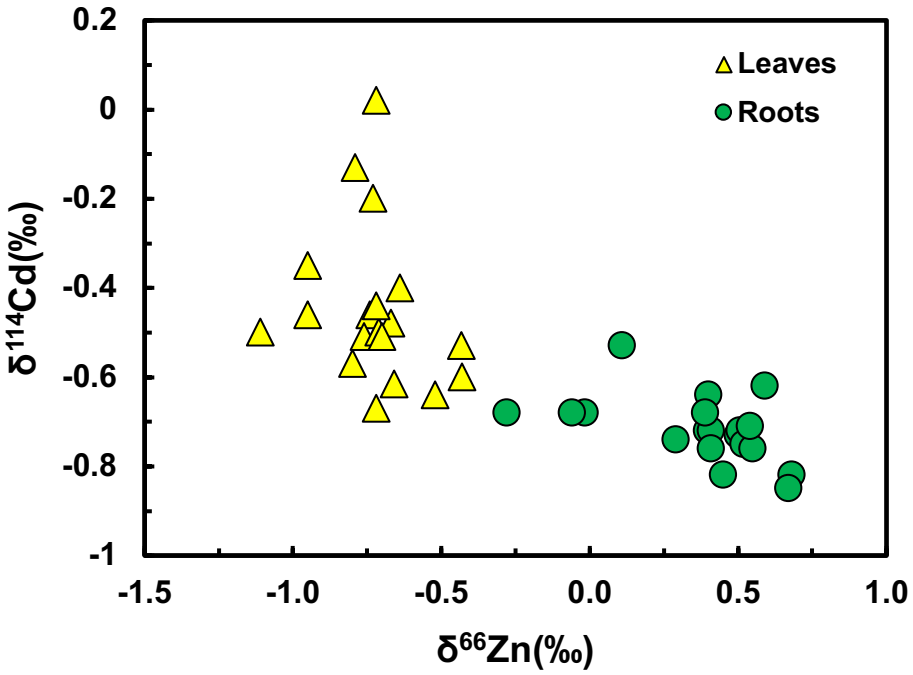


Figure A4.5. Cadmium stable isotope compositions ($\delta^{114}Cd$) versus Zn stable isotope composition ($\delta^{66}Zn$) for roots and leaves of the 19 cacao genotypes treated with 20 µmol L^{-1} $CdCl_2$. The Cd isotope data is from Moore et al. [42].

Appendix II:

Chapter 5

Uptake and translocation of essential and non-essential elements in cacao (*Theobroma cacao* L.): An Ecuador field study



Figure A5.1. Sampling locations situated near the three Ecuadorian villages of Mompiche, Esmeraldas, Atacames, Esmeraldas, and Puerto Inca, Guayas [77].

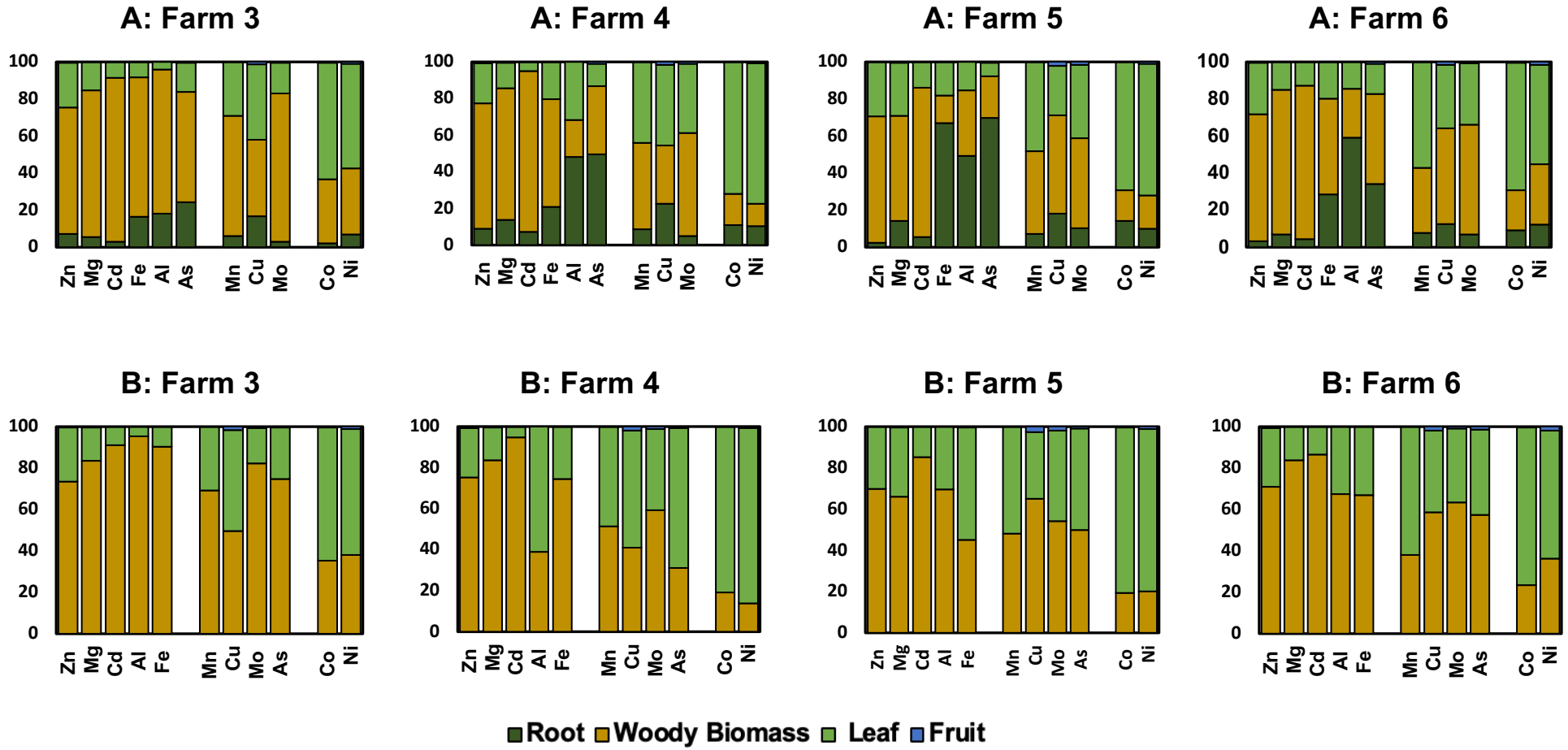


Figure A5.2. Median elemental (mass) distributions (%) determined for (a) total trees with root, woody biomass, leaf and fruit reservoirs and (b) aboveground tree parts with woody biomass, leaf and fruit reservoirs. The data are for six trees from Farms 3 to 6. For Farms 3 and 6 results are averages from data for two trees each; $n = 1$ for the other Farms.

Note A5.1. Sample digestion protocol for cacao, spinach leaf (NIST SRM 1570a) and baking chocolate (NIST SRM 2384) samples.

Seventy samples were digested in 100 mL PFA vessels with 7 mL 15.4 mol L^{-1} HNO_3 and 3 mL of 30–32% Optima™ grade H_2O_2 using a Milestone Ethos EZ microwave system at MAGIC laboratories, Imperial College London. Fifty-two samples were digested in either 7 or 15 mL PFA vessels in 4 mL 15.8 mol L^{-1} HNO_3 using a Milestone ultraWAVE microwave system at the LMF, King's College London. For each set of sample digestions, a procedural blank was prepared. For samples digested using a Milestone Ethos EZ microwave system, the digestion protocol consisted of heating at 90°C for 15 mins and then at 180°C for 30 mins. For samples digested using a Milestone ultraWAVE microwave system at the LMF, the digestion protocol consisted of heating at 220°C for 10 mins. After microwave digestion, the samples were transferred to acid-cleaned 15 mL Savillex Teflon vials and dried on a hotplate. Subsequently, all cacao samples had 700 µL 15.4 mol L^{-1} HNO_3, 300 µL of H_2O_2 and between 20 to 50 µL of 28 mol L^{-1} HF added to them and the digestion continued at 120°C on a hotplate for approximately 48 hours, to ensure all residual organic materials and silica were completely mineralised.

Note A5.2. Sample preparation and extraction protocol for soil leachate samples.

For this study, the soil-to-reagent ratios used for Mehlich-3, AA, EDTA-AA were 1:10, 1:5, and 1:10, respectively. Between 0.25 g and 1 g of soil samples were added to individual centrifuge tubes containing one of the 3 reagents, with each centrifuge tube holding either 10 mL of Mehlich-3 (0.2 mol L^{-1} acetic acid + 0.25 mol L^{-1} ammonium nitrate + 0.015 mol L^{-1} ammonium fluoride + 0.013 mol L^{-1} HNO_3 + 0.001 mol L^{-1} EDTA), 1 mol L^{-1} EDTA-AA, or 5 mL of 1 mol L^{-1} AA, respectively. The centrifuge tubes containing Mehlich-3, EDTA-AA, and AA were then agitated for 5 mins, 120 mins, and 75 mins, respectively. After agitation, the soil leachate samples were centrifuged for 5 mins at 3500 rpm to separate the supernatant from the soil. The supernatant was then extracted into PTFE vials, and subsequently dried on a hotplate at 120°C until all the reagents had evaporated.

Note A5.3. Sample digestion protocol for bulk soil and San Joachim Soil (NIST SRM 2709a) samples.

A quantity of 0.1 g of each soil sample and of San Joachim Soil (NIST SRM 2709a) were added to a Savillex Teflon vial containing 2 mL of 35% H_2O_2 and left for approximately 2 hrs at room temperature to mineralise any residual organic matter. The soil samples were then submerged in a reverse aqua regia solution (composed of 3 mL of 6 mol L^{-1} HCl and 9 mL of 15 mol L^{-1} HNO_3) for 12 hrs at room temperature. The samples were then heated sequentially at four different temperatures on a hotplate: at 60°C for 24 hrs, at 90°C for 12 hrs, at 110°C for 24 hrs and finally at 140°C for 12 hrs. Samples were then evaporated and dried on a hotplate at 80°C and taken up by 0.5 ml of 15 mol L^{-1} HNO_3. The Savillex Teflon vials containing the soil samples were then placed in an ultrasound bath for 30 mins and were then placed on a hotplate at 110°C for 12 to 24 hrs.

Table A5.1. Location of the farms as well as the number, genotype and age of each of the cacao trees grown on the farms.

Ecuador Location	Farm #	Tree #	Genotype	Age (years)
Mompiche, Esmeraldas	1	1	Nacional	50
		2		6
		3		
	2	1	CCN-51	4
Atacames, Esmeraldas	3	1	Nacional	20
		2		
		3		
Puerto Inca, Guayas	4	1	Nacional	50
		2		
		3		
	5	1	CCN51	14
		2		
		3		
	6	1	CCN51	18
		2		
		3	Nacional	24
		4		

Table A5.2. Limits of detection (LOD) and quantification (LOQ) for cacao samples, and certified and measured element concentrations (mean ± SD; μg g^{-1}) for reference materials analysed by ICP-Q-MS together with cacao samples at the LMF.

	Cacao samples (μg g^{-1})[a]		SRM 1570a (Spinach Leaf) (μg g^{-1})		SRM 2384 (Baking Chocolate) (μg g^{-1})		CRM-TMDW-500 (Trace Metal Drinking Water) (μg g^{-1})	
Element	**LOD**	**LOQ**	**Certificate Value**	**Measured (*n* =3)**	**Certificate Value**	**Measured (*n* = 2)**	**Certificate Value**	**Measured (*n* = 8)**
Al	0.0002	0.0008	310 ± 15	304.2 ± 3.2	-	-	0.12	0.11 ± 0.006
As	0.0005	0.0018	0.068±0.012	0.076±0.003	-	-	0.08	0.08 ± 0.002
Co	0.0028	0.0094	0.39 ± 0.03	0.31± 0.01	-	-	0.025	0.022 ± 0.001
Cu	0.0005	0.0018	12.2 ± 0.86	9.3 ± 0.24	23.9 ± 1.0	21.6± 0.4	0.02	0.02 ± 0.002
Fe	0.0028	0.0094	-	-	132 ± 11.0	144 ± 6.2	0.10	0.09 ± 0.003
Mg	0.0002	0.0006	-	-	2610 ± 120	2933±22.7	9.00	9.46 ± 2.61
Mn	0.0005	0.0018	76.0 ± 1.2	67.0 ± 1.7	20.8 ± 1.3	19.6 ± 0.7	0.04	0.04 ± 0.007
Mo	0.0028	0.0094	-	-	-	-	0.10	0.11 ± 0.022
Ni	0.0005	0.0018	2.1 ± 0.06	1.6 ± 0.04	-	-	0.06	0.05 ± 0.003
Zn	0.0028	0.0094	82.3 ± 3.9	71.7 ± 3.9	37.6 ± 1.9	42.9 ± 1.4	0.07	0.08 ± 0.001

[a] represents the LOD and LOQ determined from a total of 5 procedural blanks. *n* represents the number of samples. SD denotes the standard deviation.

Table A5.3. Certified and measured Cd concentrations (mean ± SD; μg g^{-1}) for reference materials analysed alongside cacao plant organ samples at MAGIC Laboratories by MC-ICP-MS using the isotope dilution method.

	BCR 679 (White Cabbage) (μg g^{-1})		SRM1570a (Spinach Leaf) (μg g^{-1})		SRM2384 (Baking Chocolate) (μg g^{-1})	
Element	**Certificate Value**	**Measured (*n*=2)**	**Certificate Value**	**Measured (*n*=3)**	**Certificate Value**	**Measured (*n*=4)**
Cd	1.66 ±0.07	1.70 ±0.01	2.88 ±0.06	2.83 ± 0.11	0.073 ± 0.008	0.072 ± 0.002

SD denotes the standard deviation.

Table A5.4. Limits of detection (LOD) and quantification (LOQ) for bulk soils, and certified and measured element concentrations (mean ± SD; μg g^{-1}) for a reference material analysed primarily by ICP-Q-MS at GET laboratories, except for Cd concentrations, which were analysed at the MAGIC Laboratories by MC-ICP-MS using the isotope dilution method.

	Bulk Soil Samples (μg g^{-1})		**NIST SRM 2709a (μg g^{-1})**	
Element	**LOD**	**LOQ**	**Certificate Value**	**Measured (*n* = 2)**
As	0.001	0.002	10.5 ± 0.3	10.5 ± 0.4
Cd*	-	-	0.37 ± 0.002	0.35 ± 0.002
Cu	0.001	0.003	33.9 ± 0.3	31.9 ± 0.5
Fe	0.067	0.219	33600 ± 700	33300 ± 320
Mn	0.002	0.005	529 ± 18	515 ± 5
Mg	0.065	0.206	14600 ± 200	11861 ±196

*Cadmium was determined using the isotope-dilution method. SD denotes the standard deviation.

Table A5.5. Limits of detection (LOD) and quantification (LOQ) for soil leachates, and certified and measured element concentrations (mean ± SD; μg g^{-1}) for a reference material analysed by ICP-Q-MS at the LMF alongside soil leachate samples.

Element	Soil Leachate Samples (μg g^{-1})		CRM-TMDW-500 (Trace Metal Drinking Water) (μg g^{-1})	
	LOD	LOQ	Certificate Value	Measured (*n* = 15)
Cd	0.00002	0.0001	0.01	0.0096 ± 0.0005
Cu	0.0014	0.0048	0.02	0.018 ± 0.003
Mn	0.0003	0.0009	0.04	0.042 ± 0.001
Zn	0.0001	0.0002	0.07	0.071 ± 0.002

SD denotes the standard deviation.

Table A5.6. Element concentrations (μg g^{-1}) determined for analytical replicates of cacao plant organs from Farms 3, 4 and 6.

Farm #	Tree #	Replicate #	Cacao organ	Al μg g^{-1}	As μg g^{-1}	Cd* μg g^{-1}	Co μg g^{-1}	Cu μg g^{-1}	Fe μg g^{-1}	Mg μg g^{-1}	Mn μg g^{-1}	Mo μg g^{-1}	Ni μg g^{-1}	Zn μg g^{-1}
3	1	1	Mature leaves	19	0.04	1.8	6.3	9.8	45	5143	622	1.7	14	87
		2	Mature leaves	13	0.03	2.5	6.9	8.4	39	4859	689	1.7	14	89
			Mean	16	0.03	2.1	6.6	9.1	42	5001	656	1.7	14	88
			SD	3.1	0.003	0.4	0.3	0.7	2.9	142	34	0.04	0.2	1.2
			CV (%)	19	8.2	17	4.1	7.8	6.7	2.8	5.1	2.1	1.1	1.3
3	1	1	Leaf Litter	6805	0.3	2.1	11	10	3114	4619	676	0.4	15	89
		2	Leaf Litter	7782	0.3	2.1	11	10	3166	4776	649	0.5	14	81
			Mean	7294	0.3	2.1	11	10	3140	4697	662	0.5	14	85
			SD	488	0.02	0.02	0.4	0.04	26	78	14	0.08	0.4	4
			CV (%)	6.7	5.3	0.9	3.4	0.4	0.83	1.7	2.0	17	2.9	4.6
4	1	1	Leaf Litter	840	0.2	4.3	3.1	6.1	332	8656	164	0.4	4.2	71
		2	Leaf Litter	581	0.2	4.3	3.2	5.8	377	5486	192	0.2	4.2	65
			Mean	712	0.2	4.3	3.2	6	355	7071	178	0.3	4.2	68
			SD	130	0.01	0.02	0.04	0.2	22	1585	14	0.1	0.01	3.4
			CV (%)	18	2.8	0.5	1.2	2.5	6.3	22	7.7	31	0.3	4.9
6	1	1	Leaf Litter	3370	0.9	3.2	2.8	5.4	1966	2906	194	0.07	2.7	52
		2	Leaf Litter	2988	0.7	3.4	2.4	4.8	1643	2951	219	0.2	2.5	48
			Mean	3179	0.8	3.3	2.6	5.1	1805	2928	206	0.2	2.6	50
			SD	191	0.08	0.1	0.2	0.3	162	23	13	0.08	0.09	1.8
			CV (%)	6	11	3.5	6.8	6.2	9	0.8	6.1	55	3.5	3.7
3	3	1	Pod husk (ripe)	2.4	0.02	0.9	0.6	10	11	2354	26	1.1	4.9	44
		2	Pod husk (ripe)	1.8	0.02	-	0.6	10	10	2245	25	0.3	4.5	41
			Mean	2.1	0.02	0.9	0.6	10	11	2299	25	0.7	4.7	43
			SD	0.4	0.0003	0	0.02	0.2	0.3	77	0.5	0.5	0.3	2.1
			CV (%)	20	1.5	0	3.2	2.1	2.6	3.4	2.1	76	5.8	4.9
6	1	1	Pod husk (ripe)	8.3	0.09	1	0.1	4.6	16	2635	10	2.3	1.5	48
		2	Pod husk (ripe)	8.9	0.09	1	0.09	4.6	16	2563	10	1.8	1.6	47
			Mean	8.6	0.09	1	0.09	4.6	16	2599	10	2	1.6	48
			SD	0.3	0.00004	0.02	0.001	0.02	0.04	36	0.1	0.2	0.01	0.7
			CV (%)	3.3	0.05	2	1.1	0.4	0.3	1.4	0.7	12	0.9	1.5

*Cadmium was determined using the isotope-dilution method. SD denotes the standard deviation. CV denotes coefficient of variation.

(Table continued on following page)

Table A5.6 (Continued). Element concentrations (μg g^{-1}) determined for analytical replicates of cacao plant organs from Farms 3, 4 and 6.

Farm #	Tree #	Replicate #	Cacao organ	Al μg g^{-1}	As μg g^{-1}	Cd* μg g^{-1}	Co μg g^{-1}	Cu μg g^{-1}	Fe μg g^{-1}	Mg μg g^{-1}	Mn μg g^{-1}	Mo μg g^{-1}	Ni μg g^{-1}	Zn μg g^{-1}
3	1	1	Mucilage (ripe)	4.0	0.07	0.5	1	16	38	2105	16	3.3	8.6	39
		2	Mucilage (ripe)	5.1	0.03	-	0.7	10	22	1333	11	0.2	4.4	22
			Mean	4.6	0.05	0.5	0.9	13	30	1719	14	1.8	6.5	30
			SD	0.6	0.02	0.0	0.2	2.7	8.3	386	2.6	1.6	2.1	8.5
			CV (%)	12	35	0.0	21	21	27	23	19	89	32	28
1	3	1	Mucilage (ripe)	3.1	0.02	0.6	0.1	2.5	7.9	342	1.3	0.1	2.3	7.8
		2	Mucilage (ripe)	1.7	0.02	-	0.1	2.2	7.0	285	1.1	0.09	2.0	6.6
			Mean	2.4	0.02	0.6	0.1	2.4	7.5	314	1.2	0.1	2.2	7.2
			SD	0.7	0.0004	0.0	0.001	0.1	0.4	28	0.08	0.01	0.1	0.6
			CV (%)	29	1.7	0.0	0.6	5.9	5.7	9.0	6.6	14	6.6	8.3
3	2	1	Mucilage (unripe)	10	0.08	0.7	0.7	4.9	21	920	6.8	0.5	14	27
		2	Mucilage (unripe)	11	0.09	-	0.7	5.1	22	968	7.1	0.6	15	29
			Mean	11	0.09	0.7	0.7	5.0	22	944	6.9	0.5	15	28
			SD	0.5	0.004	0.0	0.02	0.1	0.5	24	0.2	0.05	0.4	0.8
			CV (%)	4.8	4.9	0.0	2.3	2.1	2.1	2.5	2.6	10	2.5	2.8
3	1	1	Bean (unripe)	0.6	0.01	0.8	1.4	40	28	4608	60	0.3	11	49
		2	Bean (unripe)	1.0	0.004	0.9	1.3	37	27	4411	57	0.4	9.8	46
			Mean	0.8	0.005	0.9	1.3	38	28	4510	58	0.3	10	47
			SD	0.2	0.0004	0.06	0.06	1.5	0.8	99	1.5	0.03	0.5	1.7
			CV (%)	29	8.3	6.9	4.5	4.0	2.9	2.2	2.5	11	4.8	3.5
3	1	1	Root	817	0.2	1.4	1.7	8.9	555	4671	334	0.08	3.1	36
		2	Root	1046	0.2	1.0	0.7	7.7	573	4103	159	0.8	2.2	21
			Mean	931	0.2	1.2	1.2	8.3	564	4387	246	0.4	2.7	29
			SD	115	0.002	0.2	0.5	0.6	9.0	284	87	0.4	0.5	7.5
			CV (%)	12	1.3	15	41	7.3	1.6	6.5	36	81	17	26

*Cadmium was determined using the isotope-dilution method. SD denotes the standard deviation. CV denotes coefficient of variation.

Table A5.7. Element concentrations (μg g^{-1}) determined for analytical replicates of bulk soil (0-20cm) samples from the six farms.

Farm #	Tree #	Replicate #	As μg g^{-1}	Cu μg g^{-1}	Fe μg g^{-1}	Mg μg g^{-1}	Mn μg g^{-1}
1	1	1	4.2	52.3	38030	8720	428
		2	4.3	52.4	38566	9137	449
		Mean	4.3	52.4	38298	8929	438
		SD	0.03	0.1	268	208	11
		CV (%)	0.8	0.2	0.7	2.3	2.4
1	3	1	4.0	48.3	36705	8382	375
		2	4.1	50.9	35131	7863	373
		Mean	4.0	49.6	35918	8123	374
		SD	0.1	1.3	787	259	1.4
		CV (%)	1.8	2.5	2.2	3.2	0.4
2	1	1	4.8	50.2	36767	6898	1630
		2	4.7	48.3	36567	6919	1362
		Mean	4.8	49.2	36667	6908	1496
		SD	0.1	0.9	100	10	134
		CV (%)	1.8	1.9	0.3	0.2	9.0
3	1	1	1.4	50.3	36148	10729	855
		2	1.6	55.9	39340	11249	1005
		Mean	1.5	53.1	37744	10989	930
		SD	0.8	2.8	1596	260	75
		CV (%)	7.2	5.2	4.2	2.4	8.1
3	2	1	3.1	63.6	42707	12243	580
		2	3.4	65.4	44361	13100	650
		Mean	3.3	64.5	43534	12671	615
		SD	0.2	0.9	827	428	35
		CV (%)	4.8	1.4	1.9	3.4	5.7
4	1	1	24.2	71.0	49168	11735	771
		2	25.4	73.0	51172	12089	831
		Mean	24.8	72.0	50170	11912	801
		SD	0.6	1.0	1002	177	30
		CV (%)	2.5	1.4	2.0	1.5	3.7
5	1	1	21.2	68.5	48447	12087	953
		2	21.6	69.4	48228	11990	1006
		Mean	21.4	69.0	48337	12039	980
		SD	0.2	0.4	110	49	26
		CV (%)	1.1	0.6	0.2	0.4	2.7
6	1	1	13.2	39.2	31304	7131	649
		2	12.9	39.1	31240	7105	653
		Mean	13.1	39.1	31272	7118	651
		SD	0.13	0.04	32	13	2.0
		CV (%)	1.0	0.1	0.1	0.2	0.3

SD denotes the standard deviation. CV represents the coefficient of variation.

Table A5.8. Element concentrations (μg g^{-1}) determined for analytical replicates of soil leachates extracted using Mehlich-3, EDTA-AA and AA.

Soil Leachate				Mehlich-3	EDTA-AA	AA
Element #	**Farm #**	**Tree #**	**Replicate #**			
Cd (μg g^{-1})	4	1	1	0.07	0.08	0.05
			2	0.06	0.07	0.04
			3	0.06	0.08	0.04
			Mean	0.06	0.08	0.04
			SD	0.004	0.002	0.001
			CV (%)	6.8	2.7	1.4
Cu (μg g^{-1})	4	1	1	4.5	7.7	0.2
			2	3.8	7.5	0.2
			3	3.9	7.6	0.2
			Mean	4.1	7.6	0.2
			SD	0.3	0.07	0.01
			CV (%)	7.3	0.9	3.0
Mn (μg g^{-1})	4	1	1	16	23	7.3
			2	14	17	6.5
			3	14	18	6.5
			Mean	15	19	6.8
			SD	0.8	2.6	0.4
			CV (%)	5.4	13	5.6
Zn (μg g^{-1})	4	1	1	1.9	3.1	0.4
			2	1.5	1.9	0.4
			3	1.4	2.0	0.4
			Mean	1.6	2.3	0.4
			SD	0.2	0.5	0.01
			CV (%)	13	23	2.9

SD denotes the standard deviation. CV represents the coefficient of variation.

Table A5.9. Median, min and max element concentrations (μg g^{-1}) in the cacao plant organs from the six farms.

Cacao organs	*n*		Al μg g^{-1}	As μg g^{-1}	Cd μg g^{-1}	Co μg g^{-1}	Cu μg g^{-1}	Fe μg g^{-1}	Mg μg g^{-1}	Mn μg g^{-1}	Mo μg g^{-1}	Ni μg g^{-1}	Zn μg g^{-1}
Bean (unripe)	6	Median	0.64	0.01	2	0.8	35	33	5473	34	0.3	13	62
		Min/Max	0.10/5.1	0.005/0.02	0.8/4	0.5/1	18/41	23/63	3240/7575	18/58	0.1/0.5	7.0/26	36/87
Bean (ripe)[a]	16	Median	0.60	0.02	2	0.5	24	24	3941	16	0.4	5.6	61
		Min/Max	0.022/2.5	0.002/0.1	0.9/3	0.1/2	16/56	17/54	2620/8656	11/58	0.02/1	2.5/17	33/122
Pod husk (unripe)	2	Median	18	0.02	0.8	1	10	18	3404	79	2	4.0	36
		Min/Max	15/22	0.02/0.02	0.8/0.9	1/1	8.7/12	16/20	2941/3867	52/107	0.8/2	3.7/4.2	35/38
Pod husk (ripe)	11	Median	6.4	0.04	1	0.2	6.2	11	2843	19	2	1.0	43
		Min/Max	1.0/30	0.02/0.1	0.9/2	0.04/2	3.0/10	7.4/27	1209/5011	5.9/88	0.2/7	0.3/11	24/70
Mucilage (unripe)	3	Median	11	0.04	0.7	0.9	6.0	22	1174	7.4	0.5	7.1	28
		Min/Max	11/17	0.02/0.1	0.7/0.9	0.7/1	5.0/16	19/26	944/2409	6.9/59	0.4/0.5	5.8/15	25/55
Mucilage (ripe)	15	Median	4.8	0.1	1	0.2	6.7	31	1537	5.0	0.6	2.1	20
		Min/Max	0.9/51	0.01/0.3	0.5/2	0.03/0.9	2.3/15	3.8/41	314/2014	1.2/17	0.1/2	0.60/12	7.2/38
Young Leaves	8	Median	27	0.05	2	0.8	15	46	3473	36	0.9	7.8	60
		Min/Max	6.4/87	0.02/0.2	0.8/5	0.2/2	9.3/26	27 /63	2206/3686	17/84	0.1/2	1.6/12	42/75
Mature Leaves	17	Median	63	0.09	3	2	5.7	69	4656	113	0.9	4.5	80
		Min/Max	12/186	0.01/0.2	1/7	1/7	1.8/9.3	15/151	1685/7410	60/656	0.3/2	1.8/30	31/155
Leaf Litter	10	Median	5384	0.3	4	4	6.1	2719	4248	203	0.5	10	71
		Min/Max	711/11135	0.1/2	2/10	1/18	3.8/12	355/7280	2777/8528	177/662	0.2/2	2.6/27	24/233
Branch[b]	2	Median	197	0.06	3	0.4	11	144	3606	65	1	9.0	48
		Min/Max	165/230	0.05/0.06	3/3	0.3/0.5	7.7/15	132/154	2835/4378	51/78	1/1	8.3/9.8	48/48
Bark	7	Median	87	0.03	7	0.2	2.9	74	7814	29	0.9	0.8	57
		Min/Max	29/365	0.03/0.07	4/11	0.1/1	2.0/4.3	21/185	3668/9611	21/312	0.4/2	0.2/2.2	38/120
Root	6	Median	816	0.2	2	0.3	8.1	416	5145	25	0.5	1.5	30
		Min/Max	127/2351	0.02/0.6	0.6/5	0.1/1	1.2/17	21/630	1250/6377	21/246	0.1/0.7	0.9/2.7	2.9/51
Total Plant	6	Median	164	0.06	5.3	0.5	4.4	121	5412	44	0.7	1.5	59
		Min/Max	95/376	0.03/0.09	2.7/8.9	0.4/1.6	3.2/9.0	81/192	4341/7141	30/317	0.5/1.2	0.8/6.3	37/118

n represents number of samples. [a] $n = 16$ for all elements except Al ($n = 10$). [b] $n = 2$ for all elements except Cd ($n = 3$).

Table A5.10. Element concentrations (in μg g^{-1}) in the organs of the cacao trees.

Region		Mompiche, Esmeraldas				Atacames, Esmeraldas			Puerto Inca, Guayas											
Farm #		Farm 1			Farm 2	Farm 3			Farm 4			Farm 5			Farm 6					
Genotype		Nacional			CCN51	Nacional			Nacional			CCN51			CCN51		Nacional			
Tree #		Tree 1	Tree 2	Tree 3	Tree 1	Tree 1	Tree 2	Tree 3	Tree 1	Tree 2	Tree 3	Tree 1	Tree 2	Tree 3	Tree 1	Tree 2	Tree 3	Tree 4		
Element	**Plant Organ**																		**Mean**	**SD**
Al (μg g-1)	Bean (unripe)	5.1		0.1	3.2	0.8	0.1	0.5											1.6	1.9
	Bean (ripe)	0.2		1.4			2.5	0.1			0.02		2.2	2.3	0.7	0.5		0.2	1.0	0.9
	Pod husk (unripe)					15.1		21.6											18.4	3.3
	Pod husk (ripe)					13.0	7.4	2.1	1.0	1.0	4.3	2.4	6.4	15.5	8.6		30.0		8.3	8.2
	Mucilage (unripe)					10.8	10.9	17.3											13.0	3.0
	Mucilage (ripe)			2.4	11.2	5.1	2.4	18.1	4.8	51.2	2.9	1.7	4.5	4.0	0.9	17.1	7.4	7.3	9.4	12.3
	Young leaves	28.5		26.1	6.4	14.5	63.2	87.1								32.3		18.3	34.5	25.4
	Mature leaves	36.1	16.0	51.5	16.5	16.1	18.7	12.0	136.0	50.8	100.5	114.9	134.3	164.6	63.4	139.6	185.5	133.2	81.7	57.8
	Leaf litter	1113 5.0		9873.0	1542.0	7293.5	1686.9	5553.5	710.6			6646.6			3179.0		5214.6		5283.5	3369.8
	Branch						164.9	229.6											197.3	32.4
	Bark					364.9	52.7	157.9	28.7			86.7			176.9		50.8		131.2	108.6
	Root					931.2		127.1	444.4			789.3			2351.2		843.3		914.4	698.3
As (μg g-1)	Bean (unripe)	0.010		0.020	0.010	0.005	0.020	0.005											0.012	0.006
	Bean (ripe)	0.010		0.020	0.010	0.010	0.020	0.003	0.020	0.002	0.018	0.030	0.070	0.030	0.110	0.100	0.060	0.140	0.041	0.041
	Pod husk (unripe)					0.022		0.016											0.019	0.003
	Pod husk (ripe)					0.025	0.100	0.019	0.040	0.040	0.050	0.040	0.035	0.050	0.100		0.100		0.054	0.029
	Mucilage (unripe)					0.020	0.100	0.039											0.053	0.034
	Mucilage (ripe)			0.020	0.013	0.020	0.090	0.044	0.200	0.100	0.100	0.110	0.130	0.150	0.253	0.200	0.200	0.200	0.122	0.075
	Young leaves	0.020		0.015	0.100	0.040	0.060	0.020								0.130		0.210	0.074	0.064
	Mature leaves	0.040	0.036	0.060	0.010	0.034	0.060	0.045	0.200	0.110	0.120	0.090	0.090	0.120	0.100	0.120	0.130	0.140	0.089	0.047
	Leaf litter	0.300		0.400	0.100	0.300	0.170	0.210	0.200			1.530			0.800		1.210		0.522	0.467
	Branch						0.060	0.050											0.055	0.005
	Bark					0.030	0.040	0.030	0.030			0.030			0.070		0.040		0.039	0.014
	Root					0.200		0.020	0.260			0.610			0.049		0.540		0.280	0.225

SD denotes the standard deviation.

(Table continued on following page)

Table A5.10 (Continued). Element concentrations (in μg g^{-1}) in the organs of the cacao trees.

Region		Mompiche, Esmeraldas				Atacames, Esmeraldas			Puerto Inca, Guayas											
Farm #		Farm 1			Farm 2	Farm 3			Farm 4			Farm 5			Farm 6					
Genotype		Nacional			CCN51	Nacional			Nacional			CCN51			CCN51		Nacional			
Tree #		Tree 1	Tree 2	Tree 3	Tree 1	Tree 1	Tree 2	Tree 3	Tree 1	Tree 2	Tree 3	Tree 1	Tree 2	Tree 3	Tree 1	Tree 2	Tree 3	Tree 4		
Element	**Plant Organ**																		**Mean**	**SD**
Cd (μg g-1)	Bean (unripe)	3.6		3.3	2.0	0.8	1.4	0.9											2.0	1.1
	Bean (ripe)	2.8		2.8	2.0	1.0	1.2	0.9	1.5	1.0	0.9	2.4	2.0	1.7	2.7	1.9	1.6	3.4	1.8	0.8
	Pod husk (unripe)					0.8		0.9											0.8	0.1
	Pod husk (ripe)					0.9	1.2	0.9	1.7	1.5	1.4	1.4	2.3	1.8	1.0		1.8		1.5	0.4
	Mucilage (unripe)					0.9	0.7	0.7											0.8	0.1
	Mucilage (ripe)			0.6	0.7	0.5	1.2	1.0	1.1	1.6	0.5	1.5	0.8	1.5	1.2	0.7	1.3	1.5	1.1	0.4
	Young leaves	2.3		4.6	2.3	1.2	1.9	0.8								2.6		2.2	2.2	1.1
	Mature leaves	5.2	7.2	7.4	2.0	2.1	1.9	1.2	1.2	3.1	2.6	5.5	4.4	5.0	3.4	3.0	2.7	5.1	3.7	1.9
	Leaf litter	5.1		4.8	6.3	2.1	3.5	1.8	4.4			9.9			3.3		2.9		4.4	2.3
	Branch					3.4	2.6	3.1											3.0	0.3
	Bark					7.2	6.4	4.0	7.3			10.7			6.6		6.5		7.0	1.8
	Root					1.3		0.6	4.0			4.7			1.4		3.0		2.5	1.5
Co (μg g-1)	Bean (unripe)	0.5		0.7	1.4	1.3	0.8	0.7											0.9	0.3
	Bean (ripe)	0.3		0.7	1.2	1.8	0.5	0.3	0.2	0.5	0.1	0.3	0.4	0.4	0.6	0.9	0.5	1.1	0.6	0.4
	Pod husk (unripe)					1.1		1.2											1.2	0.0
	Pod husk (ripe)					1.7	0.3	0.6	0.1	0.6	0.04	0.1	0.2	0.2	0.1		0.2		0.4	0.5
	Mucilage (unripe)					1.1	0.7	0.9											0.9	0.2
	Mucilage (ripe)			0.1	0.5	0.9	0.4	0.5	0.1	0.5	0.03	0.1	0.1	0.2	0.2	0.1	0.2	0.2	0.3	0.2
	Young leaves	0.2		0.8	0.8	1.4	0.8	1.5								0.5		0.4	0.8	0.4
	Mature leaves	2.2	2.1	2.5	1.0	6.6	4.2	3.2	1.8	1.9	1.3	1.1	1.5	1.4	1.7	2.0	1.3	1.4	2.2	1.3
	Leaf litter	1.3		3.7	6.3	10.9	6.4	18.1	3.2			2.1			2.6		2.4		5.7	4.9
	Branch						0.3	0.5											0.4	0.1
	Bark					1.0	0.4	0.2	0.1			0.1			0.2		0.1		0.3	0.3
	Root					1.2		0.1	0.3			0.3			0.1		0.6		0.4	0.4

SD denotes the standard deviation.

(Table continued on following page)

Table A5.10 (Continued). Element concentrations (in μg g^{-1}) in the organs of the cacao trees.

Region		Mompiche, Esmeraldas				Atacames, Esmeraldas			Puerto Inca, Guayas											
Farm #		Farm 1			Farm 2	Farm 3			Farm 4			Farm 5			Farm 6					
Genotype		Nacional			CCN51	Nacional			Nacional			CCN51			CCN51		Nacional			
Tree #		Tree 1	Tree 2	Tree 3	Tree 1	Tree 1	Tree 2	Tree 3	Tree 1	Tree 2	Tree 3	Tree 1	Tree 2	Tree 3	Tree 1	Tree 2	Tree 3	Tree 4		
Element	**Plant Organ**																		**Mean**	**SD**
Cu (μg g^{-1})	Bean (unripe)	31.8		39.9	40.5	38.4	18.4	20.3											31.6	9.1
	Bean (ripe)	23.7		41.0	38.9	28.1	23.3	20.8	21.2	23.9	15.9	24.8	34.8	18.6	17.4	26.7	18.3	55.7	27.1	10.3
	Pod husk (unripe)					11.6		8.7											10.2	1.5
	Pod husk (ripe)					8.4	6.9	10.2	6.2	7.0	4.7	9.1	5.4	5.6	4.6		3.0		6.5	2.0
	Mucilage (unripe)					16.0	5.0	6.0											9.0	5.0
	Mucilage (ripe)			2.3	5.4	13.0	7.2	14.5	5.7	10.2	5.1	12.2	5.6	13.0	5.2	3.8	8.1	6.7	7.9	3.7
	Young leaves	12.2		14.4	15.4	14.0	19.1	26.0								9.3		15.3	15.7	4.7
	Mature leaves	9.3	4.8	7.5	1.8	9.1	8.4	7.7	8.4	8.3	5.3	5.4	5.0	6.3	5.0	4.2	5.5	5.7	6.3	2.0
	Leaf litter	3.8		5.9	6.2	10.0	11.7	8.1	6.0			10.0			5.1		5.5		7.2	2.4
	Branch						14.9	7.7											11.3	3.6
	Bark					4.3	3.6	2.5	2.0			3.6			2.9		2.3		3.0	0.8
	Root					8.3		17.4	9.2			7.9			1.2		7.4		8.6	4.7
Fe (μg g^{-1})	Bean (unripe)	56.7		62.5	38.2	27.5	24.6	22.6											38.7	15.7
	Bean (ripe)	23.7		50.6	42.2	27.5	23.9	19.9	24.4	16.7	19.8	21.1	36.0	20.9	22.6	53.7	26.3	49.9	30.0	12.0
	Pod husk (unripe)					15.3		19.6											17.5	2.1
	Pod husk (ripe)					13.0	24.8	10.5	10.3	7.4	10.8	10.9	7.8	11.0	15.6		27.4		13.6	6.3
	Mucilage (unripe)					18.5	21.6	25.9											22.0	3.0
	Mucilage (ripe)			3.8	11.0	30.1	22.9	41.0	35.2	25.3	30.8	36.4	34.2	41.0	30.4	35.4	33.4	21.3	28.8	10.1
	Young leaves	29.8		42.3	27.3	45.1	62.6	62.3								50.0		46.0	45.7	12.2
	Mature leaves	42.1	28.4	63.4	15.1	41.7	38.0	23.1	120.8	52.2	78.7	76.6	91.3	128.7	69.3	133.7	150.7	112.3	74.5	41.0
	Leaf litter	7280.1		3215.7	742.8	3139.8	890.9	2728.6	354.6			3025.6			1805.1		2710.2		2589.3	1866.2
	Branch						154.1	132.8											143.5	10.7
	Bark					185.1	58.7	74.4	116.6			21.0			129.6		47.5		90.4	52.2
	Root					563.4		21.0	268.6			608.8			77.1		630.3		361.5	251.5

SD denotes the standard deviation.

(Table continued on following page)

Table A5.10 (Continued). Element concentrations (in μg g^{-1}) in the organs of the cacao trees.

Region		Mompiche, Esmeraldas				Atacames, Esmeraldas			Puerto Inca, Guayas											
Farm #		Farm 1			Farm 2	Farm 3			Farm 4			Farm 5			Farm 6					
Genotype		Nacional			CCN51	Nacional			Nacional			CCN51			CCN51		Nacional			
Tree #		Tree 1	Tree 2	Tree 3	Tree 1	Tree 1	Tree 2	Tree 3	Tree 1	Tree 2	Tree 3	Tree 1	Tree 2	Tree 3	Tree 1	Tree 2	Tree 3	Tree 4		
Element	Plant Organ																		Mean	SD
Ni (μg g^{-1})	Bean (unripe)	25.6		16.4	16.4	10.3	10.5	7.0											14.4	6.1
	Bean (ripe)	15.5		17.0	16.9	11.8	13.3	9.6	3.9	3.0	2.5	4.5	5.9	3.8	4.6	6.2	4.3	5.3	8.0	5.0
	Pod husk (unripe)					3.7		4.2											4.0	0.3
	Pod husk (ripe)					3.9	11.1	4.7	0.6	1.4	0.3	1.0	0.8	0.7	1.5		0.6		2.4	3.1
	Mucilage (unripe)					7.1	14.5	5.8											9.1	3.8
	Mucilage (ripe)			2.2	6.6	6.5	12.3	6.4	1.3	2.3	0.6	1.7	1.1	1.7	2.3	1.1	2.1	1.1	3.3	3.1
	Young leaves	7.0		8.5	8.7	5.2	12.4	10.7								1.6		2.2	7.0	3.6
	Mature leaves	23.1	23.0	29.5	6.8	13.6	23.4	14.9	5.6	3.5	1.8	4.5	4.5	3.0	2.2	2.0	2.3	2.1	9.7	9.2
	Leaf litter	5.7		15.0	26.5	14.4	25.6	25.0	4.2			4.8			2.6		3.2		12.7	9.4
	Branch						9.8	8.3											9.0	0.8
	Bark					1.0	2.2	1.2	0.3			0.4			0.8		0.2		0.9	0.6
	Root					2.7		2.7	1.6			1.4			0.9		1.3		1.7	0.7
Mg (μg g^{-1})	Bean (unripe)	7575.0		6436.6	6525.1	4509.5	3239.6	3260.5											5257.7	1682.6
	Bean (ripe)	4279.4		6980.7	6183.2	3864.3	3979.2	3420.8	3506.6	2620.2	3475.7	3817.1	5539.7	3855.5	3902.0	6491.0	4353.9	8655.9	4682.8	1571.0
	Pod husk (unripe)					3866.6		2940.8											3403.7	462.9
	Pod husk (ripe)					3269.7	1209.2	2299.1	2678.6	2714.6	5010.9	3752.3	3261.4	3284.0	2598.8		2843.1		2992.9	899.5
	Mucilage (unripe)					2409.0	944.3	1174.0											1509.1	643.2
	Mucilage (ripe)			313.5	976.5	1718.7	1235.7	1655.7	1793.5	1698.0	2013.6	1387.3	1826.6	1613.4	1163.3	1478.7	1305.0	1537.2	1447.8	404.8
	Young leaves	2632.2		2206.3	3479.8	2647.3	3485.3	3685.5								3516.3		3466.1	3139.9	518.7
	Mature leaves	6930.2	4567.6	4530.6	1684.6	5001.0	3674.8	3450.6	3049.2	4655.2	7409.7	5645.9	6262.7	6370.1	3835.2	4656.2	5512.5	4844.8	4828.3	1417.6
	Leaf litter	3593.5		2776.6	4530.3	4697.3	5603.7	3965.6	7071.0			8528.1			2928.2		3931.5		4762.6	1740.0
	Branch						2834.6	4377.5											3606.1	771.4
	Bark					5775.4	8468.5	9611.0	5196.1			3668.1			8335.4		7814.1		6981.2	1973.9
	Root					4387.0		1250.3	6376.6			5903.4			3046.4		6363.8		4554.6	1898.8

SD denotes the standard deviation.

(Table continued on following page)

Table A5.10 (Continued). Element concentrations (in μg g^{-1}) in the organs of the cacao trees.

Region		Mompiche, Esmeraldas				Atacames, Esmeraldas			Puerto Inca, Guayas											
Farm #		Farm 1			Farm 2	Farm 3			Farm 4			Farm 5			Farm 6					
Genotype		Nacional			CCN51	Nacional			Nacional			CCN51			CCN51		Nacional			
Tree #		Tree 1	Tree 2	Tree 3	Tree 1	Tree 1	Tree 2	Tree 3	Tree 1	Tree 2	Tree 3	Tree 1	Tree 2	Tree 3	Tree 1	Tree 2	Tree 3	Tree 4		
Element	**Plant Organ**																		**Mean**	**SD**
Mn (μg g^{-1})	Bean (unripe)	27.9		40.3	49.8	58.3	24.4	18.2											36.5	14.3
	Bean (ripe)	14.3		33.3	43.6	58.0	32.4	14.7	14.3	17.7	14.1	11.2	17.4	11.1	12.1	26.0	14.5	32.0	22.9	13.1
	Pod husk (unripe)					106.6		52.0											79.3	27.3
	Pod husk (ripe)					87.8	10.2	25.1	19.2	57.4	19.8	9.2	10.9	5.9	10.1		23.3		25.4	24.0
	Mucilage (unripe)					58.5	6.9	7.4											24.3	24.2
	Mucilage (ripe)			1.2	5.1	13.5	10.4	9.8	5.2	16.9	4.9	2.8	5.0	3.5	3.0	3.4	6.8	3.6	6.3	4.3
	Young leaves	17.3		43.8	49.7	83.7	78.6	25.0								29.0		21.7	43.6	24.0
	Mature leaves	92.2	129.7	146.5	174.9	655.5	251.1	95.5	60.1	88.6	62.3	78.9	96.7	112.8	173.6	159.2	112.9	104.7	152.7	134.1
	Leaf litter	197.9		176.9	661.8	662.4	538.5	493.6	178.0			199.5			206.2		181.5		349.6	201.3
	Branch						77.8	51.2											64.5	13.3
	Bark					311.9	121.6	28.6	21.1			24.1			33.7		23.9		80.7	100.0
	Root					246.3		15.5	25.5			24.7			19.5		55.0		64.4	82.3
Mo (μg g^{-1})	Bean (unripe)	0.17		0.34	0.49	0.30	0.37	0.10											0.3	0.1
	Bean (ripe)	0.26		0.35	0.61	1.04	0.88	0.10	0.45	0.02	0.10	0.37	0.63	0.81	0.42	0.82	0.26	0.40	0.5	0.3
	Pod husk (unripe)					0.80		2.10											1.5	0.7
	Pod husk (ripe)					0.70	0.20	0.70	4.58	2.34	0.34	3.14	2.00	6.85	2.00		0.80		2.2	2.0
	Mucilage (unripe)					0.50	0.50	0.40											0.5	0.05
	Mucilage (ripe)			0.10	0.10	1.80	0.36	0.70	1.60	0.79	0.30	0.56	1.10	0.10	0.62	0.30	0.88	0.50	0.7	0.5
	Young leaves	1.52		1.04	0.50	0.11	0.83	0.50								1.43		1.11	0.9	0.5
	Mature leaves	0.73	0.30	1.20	0.32	1.70	1.05	0.30	2.10	1.79	1.64	0.89	0.70	0.94	0.76	0.87	1.07	0.72	1.0	0.5
	Leaf litter	1.83		0.50	0.60	0.50	0.57	0.44	0.30			0.50			0.20		0.15		0.6	0.4
	Branch						1.41	1.17											1.3	0.1
	Bark					0.88	1.79	1.44	1.03			0.36			0.67		0.43		0.9	0.5
	Root					0.40		0.10	0.59			0.50			0.10		0.69		0.4	0.2

SD denotes the standard deviation.

(Table continued on following page)

Table A5.10 (Continued). Element concentrations (in μg g^{-1}) in the organs of the cacao trees.

Region		Mompiche, Esmeraldas				Atacames, Esmeraldas			Puerto Inca, Guayas											
Farm #		Farm 1			Farm 2	Farm 3			Farm 4			Farm 5			Farm 6					
Genotype		Nacional			CCN51	Nacional			Nacional			CCN51			CCN51		Nacional			
Tree #		Tree 1	Tree 2	Tree 3	Tree 1	Tree 1	Tree 2	Tree 3	Tree 1	Tree 2	Tree 3	Tree 1	Tree 2	Tree 3	Tree 1	Tree 2	Tree 3	Tree 4		
Element	**Plant Organ**																		**Mean**	**SD**
Zn (μg g^{-1})	Bean (unripe)	87.3		77.1	85.3	47.1	43.5	35.5											62.6	21.1
	Bean (ripe)	58.8		78.1	89.0	53.1	42.9	36.1	60.9	42.9	33.0	60.3	107.5	56.0	80.3	121.7	60.7	113.5	68.4	26.6
	Pod husk (unripe)					35.0		37.8											36.4	1.4
	Pod husk (ripe)					46.2	24.0	42.9	36.8	38.5	23.5	69.7	58.5	56.9	47.4		38.6		43.9	13.4
	Mucilage (unripe)					54.7	28.2	24.9											35.9	13.3
	Mucilage (ripe)			7.2	27.6	30.4	22.9	36.5	16.6	37.7	12.9	19.5	13.9	28.4	18.5	17.6	27.5	17.8	22.3	8.5
	Young leaves	51.9		51.3	41.5	56.5	74.7	69.9								63.4		74.3	60.4	11.3
	Mature leaves	99.8	52.5	90.6	49.5	87.6	53.2	42.8	36.7	80.0	75.7	155.3	133.1	128.0	46.1	30.9	90.6	87.9	78.8	34.9
	Leaf litter	24.4		39.2	233.0	85.2	103.6	60.1	68.0			142.7			49.9		73.4		88.0	57.9
	Branch						47.7	47.5											47.6	0.1
	Bark					68.9	56.9	55.5	37.8			119.8			40.5		69.5		64.1	25.4
	Root					28.5		51.4	31.6			28.6			2.9		38.0		30.2	14.5

SD denotes the standard deviation.

Table A5.11. Mean and median elemental (mass) distributions (%) for the cacao tree reservoirs: roots, woody biomass, leaves and fruit.

Region		Atacames, Esmeraldas		Puerto Inca, Guayas							
Farm #		Farm 3		Farm 4	Farm 5	Farm 6					
Genotype		Nacional		Nacional	CCN51	CCN51	Nacional				
Tree #		Tree 1	Tree 3	Tree 1	Tree 1	Tree 1	Tree 3				
Element	**Plant Organ**							**Mean**	**Median[a]**	**SD**	**CV**
Al	Fruit	0.02	0.04	0.02	0.01	0.01	0.07	0.03	0.02	0.02	89
	Leaf	1.0	7.1	31.6	15.4	3.7	25.3	14.0	12.0	11.3	80
	Woody biomass	71.1	84.3	20.2	35.2	31.6	21.0	43.9	35.7	24.8	57
	Root	28.0	8.5	48.2	49.4	64.7	53.7	42.1	52.2	18.5	44
As	Fruit	0.2	0.4	1.0	0.4	1.4	0.8	0.7	0.6	0.4	57
	Leaf	16.7	16.0	12.3	7.4	22.6	9.6	14.1	14.2	5	36
	Woody biomass	41.0	77.7	37.1	22.3	68.6	29.1	46.0	39.2	20	44
	Root	42.1	5.8	49.6	69.9	7.5	60.5	39.2	46.0	25	63
Cd	Fruit	0.1	0.2	0.2	0.1	0.2	0.2	0.2	0.2	0.03	21
	Leaf	9.0	8.1	4.7	13.8	14.2	11.2	10.2	10.1	3.3	33
	Woody biomass	87.5	89.3	87.8	80.6	82.9	82.8	85.2	85.3	3.2	4
	Root	3.4	2.3	7.3	5.4	2.7	5.8	4.5	4.4	1.8	41
Co	Fruit	0.6	0.4	0.1	0.3	0.4	0.4	0.4	0.4	0.1	39
	Leaf	55.9	69.8	71.9	69.0	71.6	66.2	67.4	70.7	5.5	8
	Woody biomass	40.9	28.4	17.0	16.5	26.1	17.0	24.3	21.9	8.8	36
	Root	2.6	1.4	11.0	14.2	2.0	16.4	7.9	6.9	6.1	78
Cu	Fruit	1.6	1.0	1.6	2.1	1.7	1.7	1.6	1.6	0.3	19
	Leaf	39.9	41.2	44.0	26.6	34.2	33.9	36.7	36.4	5.8	16
	Woody biomass	45.1	37.8	31.8	53.2	60.2	43.0	45.2	43.3	9.4	21
	Root	13.4	19.9	22.6	18.2	3.8	21.3	16.6	18.7	6.4	39

SD denotes the standard deviation and CV represents the coefficient of variation. [a]All median mass distribution values were adjusted (normalised) to ensure the sum was 100%.

(Table continued on following page)

Table A5.11 (Continued). Mean and median elemental (mass) distributions (%) for the cacao tree reservoirs: roots, woody biomass, leaves and fruit.

Region		Atacames, Esmeraldas		Puerto Inca, Guayas							
Farm #		Farm 3		Farm 4	Farm 5	Farm 6					
Genotype		Nacional		Nacional	CCN51	CCN51	Nacional				
Tree #		Tree 1	Tree 3	Tree 1	Tree 1	Tree 1	Tree 3				
Element	**Plant Organ**							**Mean**	**Median[a]**	**SD**	**CV**
Fe	Fruit	0.1	0.2	0.1	0.1	0.1	0.1	0.1	0.1	0.03	25
	Leaf	5.0	11.6	20.1	18.0	13.9	25.5	15.7	15.4	7	42
	Woody biomass	64.6	85.5	58.9	15.0	78.8	24.4	54.5	59.7	26	48
	Root	30.3	2.7	20.9	66.9	7.2	49.9	29.7	24.8	23	77
Mg	Fruit	0.3	0.3	0.3	0.4	0.2	0.2	0.3	0.3	0.1	22
	Leaf	16.3	14.0	13.9	28.8	12.5	17.1	17.1	15.4	5.4	32
	Woody biomass	74.6	83.4	72.1	56.7	82.6	73.4	73.8	75.2	8.8	12
	Root	8.7	2.3	13.6	14.1	4.7	9.2	8.8	9.1	4.3	49
Mn	Fruit	0.1	0.2	0.3	0.1	0.1	0.2	0.2	0.2	0.1	41
	Leaf	25.8	31.9	44.1	48.2	60.9	53.4	44.0	46.3	12.0	27
	Woody biomass	66.0	64.0	46.9	44.6	35.8	34.3	48.6	46.0	12.4	26
	Root	8.0	3.8	8.8	7.1	3.2	12.2	7.2	7.6	3.0	42
Mo	Fruit	0.9	0.3	1.1	1.7	1.0	0.7	0.9	0.9	0.4	45
	Leaf	23.9	9.1	37.8	39.5	26.5	39.4	29.4	31.7	11.0	38
	Woody biomass	70.4	89.6	56.2	48.5	70.9	48.0	63.9	62.5	14.7	23
	Root	4.9	1.1	5.0	10.4	1.6	11.9	5.8	4.9	4.1	70
Ni	Fruit	1.5	0.7	0.7	1.0	1.5	1.8	1.2	1.3	0.4	35
	Leaf	68.0	44.8	76.6	71.0	42.5	64.6	61.2	68.5	13.0	21
	Woody biomass	21.3	50.1	12.4	18.0	48.1	17.1	27.9	20.3	15.3	55
	Root	9.2	4.4	10.2	10.0	7.9	16.5	9.7	9.9	3.6	37
Zn	Fruit	0.4	0.4	0.6	0.3	0.8	0.4	0.5	0.4	0.2	36
	Leaf	24.4	23.7	22.0	29.1	26.9	28.3	25.7	25.8	2.6	10
	Woody biomass	70.7	65.7	68.6	68.1	71.6	65.8	68.4	68.7	2.2	3
	Root	4.5	10.1	8.8	2.5	0.8	5.5	5.4	5.1	3.3	61

SD denotes the standard deviation and CV represents the coefficient of variation. [a] All median mass distribution values were adjusted (normalised) to ensure the sum was 100%.

Table A5.12. Physico-chemical properties and element concentrations of bulk soils (0-20cm) from the six farms (n = 16).

Farm #	Tree #	pH	CEC cmol+ kg^{-1}	OM %	TOC %	C %	N %	C/N	S %	P %	As µg g^{-1}	Cd µg g^{-1}	Cu µg g^{-1}	Fe µg g^{-1}	Mg µg g^{-1}	Mn µg g^{-1}
1	1	6.1	32	2.8	1.4	1.7	0.2	10	0.02	0.1	3.7	0.8	45	33039	7703	378
1	2	5.9	21	1.4	0.7	0.8	0.1	10	0.00	0.06	3.5	0.3	45	30916	6651	359
1	3	5.7	30	4.3	2.3	2.5	0.2	10	0.04	0.08	3.5	0.5	43	30986	7007	323
2	1	5.4	12	4.3	2.4	2.5	0.3	9	0.11	0.05	4.4	0.5	45	33783	6365	1378
3	1	6.3	32	1.2	0.9	0.7	0.1	8	0.02	0.05	1.4	0.4	49	35043	10217	861
3	2	7.5	36	5.4	2.8	3.2	0.3	10	0.01	0.1	2.8	0.8	56	37556	10931	530
3	3	6.5	27	4.2	2.5	2.4	0.3	10	0.01	0.06	1.8	0.5	55	36202	9748	677
4	1	5.8	16	1.8	0.8	1.0	0.1	11	0.03	0.1	23	0.4	66	46225	10975	738
4	2	5.9	21	2.6	1.5	1.5	0.1	11	0.02	0.2	17	0.5	63	42431	11261	643
4	3	6.3	20	2.1	1.2	1.2	0.1	11	0.02	0.1	22	0.7	70	46375	12089	822
5	1	5.5	21	2.1	1.1	1.2	0.1	10	0.02	0.1	20	0.4	64	44536	11092	903
5	3	6.4	27	3.6	1.8	2.1	0.2	11	0.04	0.1	21	1.1	58	42249	9597	908
6	1	6.2	15	2.8	1.3	1.6	0.1	12	0.03	0.07	12	0.9	36	28459	6477	592
6	2	6.1	22	2.4	1.5	1.4	0.1	10	0.04	0.09	13	1.3	39	33278	7404	724
6	3	5.8	5	1.3	0.8	0.8	0.1	11	0.03	0.08	17	0.5	43	37887	8077	727
6	4	6.4	17	2.0	1.1	1.2	0.1	10	0.03	0.1	19	1.8	50	37880	8220	804
	Mean	6.1	22	2.8	1.5	1.6	0.2	10	0.03	0.1	12	0.7	52	37303	8988	710
	SD	0.5	7.9	1.2	0.6	0.7	0.1	1	0.02	0.03	7.9	0.4	10	5464	1896	250
	CV (%)	36	44	11	46	43	44	9	35	21	19	55	12	69	35	15
	Median	6.1	21	2.5	1.3	1.5	0.1	10	0.03	0.1	12	0.5	50	36879	8909	726
	Min	5.4	5	1.2	0.7	0.7	0.1	8	0.0	0.05	1.4	0.3	36	28459	6365	323
	Max	7.5	36	5.4	2.8	3.2	0.3	12	0.1	0.2	23	1.8	70	46375	12089	1378

SD denotes the standard deviation and CV represents the coefficient of variation.

Table A5.13. Element concentrations (μg g^{-1}) of leachates extracted from the bulk soil (0-20cm) samples of the six farms (n = 14) using Mehlich-3, EDTA-AA and AA.

	Farm #	Tree #	Cd μg g^{-1}	Cu μg g^{-1}	Mn μg g^{-1}	Zn μg g^{-1}
Mehlich-3	1	1	0.5	5.5	43	2.9
	1	2	0.08	3.2	21	0.9
	2	1	0.3	4.9	179	5.2
	3	1	0.1	2.6	149	0.7
	3	2	0.4	4.8	144	7.8
	3	3	0.3	4.7	113	3.2
	4	1	0.07	4.5	16	1.9
	4	2	0.2	5.0	24	2.5
	4	3	0.3	5.2	24	3.3
	5	1	0.1	4.6	39	2.2
	5	3	0.4	7.1	64	2.9
	6	1	0.4	4.2	52	5.5
	6	2	0.6	3.9	75	4.8
	6	3	0.2	3.3	42	2.3
		Mean	0.3	4.5	70	3.3
		SD	0.2	1.1	52	1.9
		CV (%)	61	24	74	57
		Median	0.3	4.7	48	2.9
		Min	0.1	2.6	15	0.7
		Max	0.6	7.1	179	7.8
EDTA-AA	1	1	0.4	5.8	30	2.0
	1	2	0.08	3.9	10	0.8
	2	1	0.3	5.6	191	3.8
	3	1	0.1	2.7	60	0.09
	3	2	0.4	3.9	49	4.8
	3	3	0.3	4.7	64	1.9
	4	1	0.08	7.7	23	3.1
	4	2	0.3	8.7	32	3.4
	4	3	0.1	5.9	26	3.9
	5	1	0.1	8.8	59	2.6
	5	3	0.4	10	55	2.6
	6	1	0.4	5.4	47	5.1
	6	2	0.7	6.6	55	4.9
	6	3	0.2	5.3	46	2.8
		Mean	0.3	6.0	53	3.0
		SD	0.2	2.0	41	1.4
		CV (%)	62	33	77	48
		Median	0.3	5.7	48	2.9
		Min	0.08	2.7	10	0.09
		Max	0.7	10	191	5.1

SD denotes the standard deviation and CV represents the coefficient of variation.

Table A5.13 (Continued). Element concentrations (μg g^{-1}) of leachates extracted from the bulk soil (0-20cm) samples of the six farms using Mehlich-3, EDTA-AA and AA.

	Farm #	Tree #	Cd μg g^{-1}	Cu μg g^{-1}	Mn μg g^{-1}	Zn μg g^{-1}
AA	1	1	0.2	0.07	14	0.2
	1	2	0.1	0.07	1.5	0.1
	2	1	0.1	0.07	139	0.7
	3	1	0.04	0.04	1.9	0.05
	3	2	0.06	0.04	4.8	0.1
	3	3	0.07	0.05	7.8	0.1
	4	1	0.05	0.2	7.3	0.4
	4	2	0.1	0.1	22	0.5
	4	3	0.1	0.1	14	0.4
	5	1	0.08	0.2	51	0.6
	5	3	0.1	0.1	16	0.3
	6	1	0.07	0.03	0.05	0.3
	6	2	0.2	0.07	8.6	0.5
	6	3	0.08	0.08	3.9	0.5
		Mean	0.1	0.09	21	0.4
		SD	0.05	0.06	35	0.2
		CV (%)	51	62	168	54
		Median	0.08	0.07	8.1	0.4
		Min	0.04	0.03	0.05	0.05
		Max	0.2	0.2	139	0.7

SD denotes the standard deviation and CV represents the coefficient of variation.

Table A5.14. Fractions of elements extracted (%) from bulk soil (0-20 cm) of the six farms (n = 14) using Mehlich-3, EDTA-AA, and AA.

		Cd (%)	Cu (%)	Mn (%)
Mehlich-3	**Median**	39	8.2	7.9
	Min	19	5.4	2.1
	Max	60	12	27
EDTA-AA	**Median**	41	12	6.8
	Min	21	5.5	2.8
	Max	59	17	14
AA	**Median**	15	0.2	1.2
	Min	7.3	0.1	0.01
	Max	31	0.3	10

Table A5.15. Bioaccumulation factors (BF) determined for elements between the cacao trees (n = 6) of Farms 3 to 6 and bulk soils as well as the Mehlich-3, EDTA-AA, and AA soil leachates.

BF	*n*		As	Cd	Cu	Fe	Mg	Mn	Zn
$BF_{total\ plant\text{-}bulk\ soil}$	6	Median	0.006	11	0.09	0.003	0.5	0.06	-
		Min/Max	0.002/0.04	5.1/21	0.06/0.2	0.002/0.005	0.4/1.1	0.04/0.4	-
$BF_{total\ plant\text{-}\ Mehlich\text{-}3}$	6	Median	-	36	1	-	-	1	27
		Min/Max	-	9.2/93	0.8/2.4	-	-	0.4/2	7/96
$BF_{total\ plant\text{-}EDTA\text{-}AA}$	6	Median	-	34	1.8	-	-	1	27
		Min/Max	-	10/72	0.6/74	-	-	0.6 / 5	8/755
$BF_{total\ plant\ -AA}$	6	Median	-	87	10	-	-	9	172
		Min/Max	-	37/140	7.4 / 119	-	-	0.7/1167	93/1218

n represents number of samples.

Table A5.16. Mean and median elemental (mass) distributions (%) for the cacao tree reservoirs: woody biomass, leaves and fruit.

Region		**Atacames, Esmeraldas**			**Puerto Inca, Guayas**						
Farm #		**Farm 3**		**Farm 4**	**Farm 5**	**Farm 6**					
Genotype		**Nacional**		**Nacional**	**CCN51**	**CCN51**	**Nacional**				
Tree #		**Tree 1**	**Tree 3**	**Tree 1**	**Tree 1**	**Tree 1**	**Tree 3**				
Element	**Plant Organ**							**Mean**	**Median[a]**	**SD**	**CV**
Al	Fruit	0.02	0.04	0.03	0.01	0.02	0.15	0.05	0.03	0.05	104
	Leaf	1.4	7.8	61.0	30.4	10.6	54.6	27.6	20.5	23.2	84
	Woody biomass	98.6	92.2	39.0	69.6	89.4	45.3	72.3	79.5	23.2	32
As	Fruit	0.4	0.4	0.8	0.9	1.3	1.3	0.9	0.9	0.4	44
	Leaf	28.9	21.0	68.2	49.3	31.6	51.1	41.7	40.5	16	38
	Woody biomass	70.7	78.6	31.0	49.8	67.1	47.6	57.5	58.6	16	28
Cd	Fruit	0.1	0.2	0.2	0.1	0.2	0.2	0.2	0.2	0.03	20
	Leaf	9.3	8.3	5.1	14.6	14.5	11.9	10.6	10.6	3.4	32
	Woody biomass	90.6	91.4	94.8	85.3	85.3	87.9	89.2	89.2	3.4	4
Co	Fruit	0.6	0.4	0.1	0.3	0.4	0.5	0.4	0.4	0.1	37
	Leaf	57.4	70.8	80.8	80.4	73.0	79.2	73.6	76.1	8.2	11
	Woody biomass	42.0	28.8	19.1	19.3	26.6	20.3	26.0	23.5	8.1	31
Cu	Fruit	1.8	1.3	2.1	2.5	1.8	2.1	1.9	1.9	0.4	20
	Leaf	46.1	51.5	56.9	32.5	35.6	43.2	44.3	44.7	8.5	19
	Woody biomass	52.1	47.2	41.1	65.0	62.6	54.7	53.8	53.4	8.3	15
Fe	Fruit	0.1	0.2	0.1	0.4	0.1	0.3	0.2	0.2	0.1	55
	Leaf	7.2	11.9	25.4	54.4	15.0	51.0	27.5	20.2	19	68
	Woody biomass	92.7	87.9	74.4	45.2	84.9	48.7	72.3	79.6	19	26

SD denotes the standard deviation and CV represents the coefficient of variation. [a]All median mass distribution values were adjusted (normalised) to ensure the sum was 100%.

(Table continued on following page)

Table A5.16 (Continued). Mean and median elemental (mass) distributions (%) for the cacao tree reservoirs: woody biomass, leaves and fruit.

Region		Atacames, Esmeraldas			Puerto Inca, Guayas						
Farm #		Farm 3		Farm 4	Farm 5	Farm 6					
Genotype		Nacional		Nacional	CCN51	CCN51	Nacional				
Tree #		Tree 1	Tree 3	Tree 1	Tree 1	Tree 1	Tree 3				
Element	**Plant Organ**							**Mean**	**Median[a]**	**SD**	**CV**
Mg	Fruit	0.4	0.3	0.4	0.5	0.2	0.3	0.3	0.3	0.1	26
	Leaf	17.9	14.4	16.2	33.5	13.1	18.8	19.0	17.0	6.8	36
	Woody biomass	81.8	85.4	83.5	66.0	86.6	80.9	80.7	82.7	6.8	8.5
Mn	Fruit	0.1	0.3	0.3	0.1	0.1	0.2	0.2	0.2	0.1	41
	Leaf	28.1	33.2	48.3	51.8	62.9	60.8	47.5	50.1	13.0	27
	Woody biomass	71.8	66.6	51.4	48.0	37.0	39.0	52.3	49.7	13.0	25
Mo	Fruit	0.9	0.3	1.2	1.9	1.0	0.7	1.0	0.9	0.5	47
	Leaf	25.1	9.2	39.7	44.1	27.0	44.7	31.6	33.4	12.7	40
	Woody biomass	74.0	90.5	59.1	54.1	72.1	54.5	67.4	65.7	13.0	19
Ni	Fruit	1.6	0.7	0.8	1.1	1.6	2.2	1.3	1.4	0.5	38
	Leaf	74.9	46.9	85.3	78.8	46.1	77.3	68.2	76.5	15.7	23
	Woody biomass	23.5	52.4	13.9	20.0	52.3	20.5	30.4	22.1	15.8	52
Zn	Fruit	0.4	0.5	0.7	0.3	0.8	0.4	0.5	0.5	0.2	35
	Leaf	25.5	26.4	24.1	29.9	27.1	29.9	27.2	26.8	2.2	8
	Woody biomass	74.0	73.1	75.2	69.9	72.1	69.7	72.3	72.8	2.0	3

SD denotes the standard deviation and CV represents the coefficient of variation. [a] All median mass distribution values were adjusted (normalised) to ensure the sum was 100%.

Table A5.17. Translocation factors (TF) determined for elements between the roots and different aboveground organs of cacao tree from the six farms.

TF	*n*		Al	As	Cd	Co	Cu	Fe	Mg	Mn	Mo	Ni	Zn
			µg g^{-1}	µg g^{-1}	µg g^{-1}	µg g^{-1}	µg g^{-1}	µg g^{-1}	µg g^{-1}	µg g^{-1}	µg g^{-1}	µg g^{-1}	µg g^{-1}
$TF_{bean(unripe)\ -root}$	2	Median	0.002	0.1	1.1	4.1	2.9	0.6	1.8	0.7	0.9	3.2	1.2
		Min/Max	0.001/0.004	0.02/0.2	0.6/1.6	1.1/7.2	1.2/4.6	0.05/1.1	1.0/2.6	0.2/1.2	0.8/1.0	2.6/3.8	0.7/1.7
$TF_{bean(ripe)\ -root*}$	6	Median	0.001	0.1	0.6	1.2	2.8	0.1	0.8	0.5	0.9	3.5	1.9
		Min/Max	-	0.05/2.2	0.4/1.9	0.6/6.4	1.2/14.5	0.03/0.9	0.5/2.7	0.2/0.9	0.4/4.2	2.4/5.2	0.7/27.7
$TF_{pod(unripe)\ -root}$	2	Median	0.1	0.5	1.0	6.6	0.9	0.5	1.6	1.9	11.5	1.5	1.0
		Min/Max	0.02/0.2	0.1/0.8	0.6/1.5	0.9/12.3	0.5/1.4	0.03/0.9	0.9/2.4	0.4 / 3.4	2.0/21.0	1.4/1.6	0.7/1.2
$TF_{pod(ripe)\ -root}$	6	Median	0.7	0.2	0.6	0.7	0.8	0.04	0.7	0.5	6.6	1.1	1.4
		Min/Max	0.002/0.04	0.1/2.0	0.3/1.6	0.3/6.1	0.4 / 3.8	0.02/0.5	0.4/1.8	0.4/1.6	1.2/20.0	0.4/1.7	0.8/16.3
$TF_{mucilage\ (unripe)\ -root}$	2	Median	0.1	1.0	1.0	5.1	1.1	0.6	0.7	0.4	2.6	2.4	1.2
		Min/Max	0.01/0.1	0.1/2.0	0.7/1.2	0.9/9.2	0.3/1.9	0.03/1.2	0.5/0.9	0.2/0.5	1.3/4.0	2.1/2.6	0.5/1.9
$TF_{mucilage\ (ripe)\ -root}$	6	Median	0.01	0.6	0.4	0.6	1.3	0.1	0.3	0.1	3.6	2.0	0.7
		Min/Max	0.0004/0.1	0.1/5.1	0.3/1.7	0.3/5.1	0.6/4.3	0.1/2.0	0.2/1.3	0.1 / 0.6	1.1/7.0	0.8/2.5	0.5/6.4
$TF_{young\ leaves-root}$	2	Median	0.4	0.6	1.1	8.2	1.6	1.5	1.8	1.0	2.6	2.9	1.7
		Min/Max	0.02/0.7	0.2/1.0	0.9/1.3	1.1/15.3	1.5/1.7	0.1/3.0	0.6/2.9	0.3 / 1.6	0.3/5.0	1.9/4.0	1.4/2.0
$TF_{mature\ leaves-root}$	6	Median	0.1	0.5	1.4	6.1	0.8	0.3	1.0	2.9	3.3	3.4	2.7
		Min/Max	0.02/0.3	0.1/2.3	0.3/2.4	2.1/32.7	0.4/4.2	0.1/1.1	0.5/2.8	2.1 / 8.9	1.6/7.6	1.8/5.5	0.8/15.9
$TF_{leaf\ litter\ -root}$	6	Median	7.0	2.4	1.9	10.5	1.0	5.3	1.1	7.5	1.1	3.2	2.6
		Min/Max	1.4/43.7	0.8/16.2	1.0/3.0	3.9/184.6	0.5/4.3	1.3/129.3	0.6/3.2	2.7 / 31.8	0.2/4.4	2.5/9.2	1.2/17.2
$TF_{branch-root**}$	1	Median	1.8	2.6	3.9	4.8	0.4	6.3	1.8	3.3	11.7	3.1	0.9
		Min/Max	-	-	2.5/5.2	-	-	-	-	-	-	-	-
$TF_{bark\ -root}$	6	Median	0.1	0.1	3.5	0.7	0.4	0.4	1.3	1.1	2.0	0.3	2.1
		Min/Max	0.06/1.2	0.05/1.5	1.8/6.7	0.2/2.0	0.1/2.4	0.03/3.5	0.6/7.7	0.4/1.8	0.6/14.4	0.2/0.9	1.1/14.0

n represents the sample size. * *n*=6 for all elements, except for Al with *n*=1. ** *n* = 1 for all elements, except Cd with *n* = 3.

Appendix III:

Chapter 6

A critical review of zinc and cadmium stable isotope fractionation in vascular plant systems

Table A6.1. Summary of measured Zn concentration ± SD (mg kg^{-1}) and $\delta^{66}Zn$ (‰) values of certified reference materials used in published studies.

Type	Material	*n*	Measured [Zn] ± SD (mg kg^{-1})	Measured $\delta^{66}Zn$ ± 2SD (‰)	Reference
Tomato leaves	NIST 1573a	4	-	+0.79 ± 0.09	Araújo et al. [93]
		4	34 ± 2	-	Smolders et al. [63]
		-	-	+0.74 ± 0.06	van der Ent et al. [78]
Rye grass	BCR-281	3	-	+0.40 ± 0.09	Arnold et al. [28]
		9	-	+0.38 ± 0.04	Couder et al. [27]
		6	-	+0.42 ± 0.06	Caldelas et al. [92]
		5	-	+0.50 ± 0.1	Caldelas et al. [61]
		5	31.2 ±6.1	+0.53 ± 0.04	Imseng et al. [67]
		3	35.2 ±6.1	+0.55 ± 0.02	Liu et al. [54]
		12	-	+0.34 ± 0.15	Weiss et al. [50]
		5	29.6±0.1	+0.42 ± 0.04	Wiggenhauser et al. [68]
		9	-	+0.49 ± 0.04	Houben et al. [66]
Olive leaves	BCR-62	-	13±3	-	Caldelas et al. [61]
		9	17.3 ± 0.8	+0.44 ± 0.02	Tang et al. [29]
		4	16.8 ± 0.6	+0.45 ± 0.05	Tang et al. [24]
Spinach Leaf	NIST 1570a	19	79 ± 6	+0.41 ±0.06	Barati et al. [34]
Peach leaves	NIST 1547	16	17.2 ± 0.8	−0.337 ± 0.144	Rodushkin et al. [95]*
Oak leaves	V464	4	26.27 ± 2.28	−0.42 ± 0.02	Tang et al. [29]
Wheat flour	NIST1567b	-	-	+1.27 ± 0.04	van der Ent et al. [78]
		6	11.2±1.2	+1.25 ± 0.05	Wiggenhauser et al. [68]
Pine needles	NIST 1575a	7	37 ± 1	-	Dinis et al. [41]
Black spruce trunk wood	AGBS (in-house sample)	27	9.10 ± 0.20	-	Dinis et al. [41]
Zea mays L.	V463	-	-	-	Jouvin et al. [60]
Wood fuel	NJV 94-5	10	37.7±1.9	+0.075 ± 0.101	Rodushkin et al. [95]*
Celery	GBW10048	-	-	-	Zhou et al. [25]**

All stable isotope compositions are reported relative to standard JMC-Lyon Zn. SD is the standard deviation. *The sample size *n* was 8 for concentrations and 17 for stable isotope compositions. **Concentration and stable isotope values are not declared in the publication or in the corresponding supplementary document, but reference materials are said to be analysed. *** The instrumental reproducibility based on repetitive $\delta^{66}Zn$ measurements of the standard over six months was 0.06‰ (2SD), the $\delta^{66}Zn$ values were not stated.

(Table continues on the next page)

Table A6.1 (Continued). Summary of measured Zn concentration ± SD (mg kg^{-1}) and $\delta^{66}Zn$ (‰) values of certified reference materials used in published studies.

Type	Material	*n*	Measured [Zn] ± SD (mg kg^{-1})	Measured $\delta^{66}Zn$ ± 2SD (‰)	Reference
Lichen	BCR-482	6	-	+0.11 ± 0.05	Aucour et al. [39]
		6	-	+0.11 ± 0.05	Aucour et al. [40]
		-	91±9	-	Caldelas et al. [61]
		3	-	+0.03 ± 0.07	Couder et al. [27]
		8/17***	98.10 ± 2.70	+0.07 ± 0.11	Dinis et al. [41]
		8	-	+0.14 ± 0.03	Viers et al. [42]
		-	-	+0.10 ± 0.08	Viers et al. [43]
		3	-	+0.03 ± 0.07	Deng et al. [37]
Moss	BCR-60	-	309±13	-	Caldelas et al. [61]
Soil	NIST 2709a	-	-	+0.27 ± 0.06	van der Ent et al. [78]
		2	106±1.6	+0.17 ± 0.02	Wiggenhauser et al. [68]
	BCR-142R	-	91±14	-	Caldelas et al. [61]
	GBW07405	-	-	-	Zhou et al.[25]**
	SCL-7003	3	74.2 ±5.1	+0.16 ± 0.09	Imseng et al. [67]
		3	73.1 ±5.1	+0.15 ±0.07	Liu et al. [54]
Basalt	BHVO-2	5	-	+0.25 ± 0.10	Araújo et al. [93]
	BCR-1	-	-	+0.20 ± 0.07	Viers et al. [43]
		8	-	+0.26 ± 0.05	Viers et al. [42]
	BCR-2	1	-	+0.25 ± 0.08	Araújo et al. [93]
		3	132.2 ±5.1	+0.33 ± 0.06	Imseng et al. [67]
		5	132.1 ±5.7	+0.33 ±0.05	Liu et al. [54]
	GBW07105	-	-	-	Li et al. [44]***
Blend ore	BCR-027	4	-	+0.25 ± 0.06	Arnold et al. [28]
		9	-	+0.34 ± 0.08	Caldelas et al. [61]
Andesite	AGV-2	2	-	+0.29 ± 0.07	Araújo et al. [93]
Zn solution	IRMM-3702	30		+0.27 ± 0.06	Araújo et al. [93]
		12	-	+0.27 ± 0.05	Dinis et al. [41]
		11	-	+0.30± 0.07	Imseng et al. [67]
		22	-	+0.30 ±0.07	Liu et al. [54]
		6	-	+0.25 ± 0.07	Markovic et al. [51]

All stable isotope compositions are reported relative to standard JMC-Lyon Zn. SD is the standard deviation. *The sample size *n* was 8 for concentrations and 17 for stable isotope compositions. **Concentration and stable isotope values are not declared in the publication or in the corresponding supplementary document, but reference materials are said to be analysed. *** The instrumental reproducibility based on repetitive $\delta^{66}Zn$ measurements of the standard over six months was 0.06‰ (2SD), the $\delta^{66}Zn$ values were not stated.

(Table continues on the next page)

Table A6.1 (Continued). Summary of measured Zn concentration ± SD (mg kg^{-1}) and $\delta^{66}Zn$ (‰) values of certified reference materials used in published studies.

Type	Material	*n*	Measured [Zn] ± SD (mg kg^{-1})	Measured $\delta^{66}Zn$ ± 2SD (‰)	Reference
Zn solution	JMC 30749 Lyon	-	-	-	Aucour et al. [36]***
		27	-	+0.01 ± 0.05	Deng et al. [37]
		22	-	+0.02 ± 0.08	Tang et al. [29]
		27	-	+0.01 ± 0.05	Tang et al. [24]
	London Zn	30	-	+0.10 ±0.06	Barati et al. [34]
		9	-	+0.10 ± 0.06	Caldelas et al. [61]
	Romil	6	-	−9.00 ± 0.06	Markovic et al. [51]
		12	-	–9.1 ± 0.1	Caldelas et al. [61]
	AA-ETH	150	-	+0.27 ± 0.04	Caldelas et al. [92]
	NIST 683	19	-	+0.12 ± 0.04	Dinis et al. [41]
	In-house Zn standard	24	-	+0.01 ± 0.03	Houben et al. [66]

All stable isotope compositions are reported relative to standard JMC-Lyon Zn. SD is the standard deviation. *The sample size *n* was 8 for concentrations and 17 for stable isotope compositions. **Concentration and stable isotope values are not declared in the publication or in the corresponding supplementary document, but reference materials are said to be analysed. *** The instrumental reproducibility based on repetitive $\delta^{66}Zn$ measurements of the standard over six months was 0.06‰ (2SD), the $\delta^{66}Zn$ values were not stated.

Table A6.2. Summary of measured Cd concentration ± SD (mg kg^{-1}) and $\delta^{114}Cd$ (‰) values of certified reference materials used in published studies.

Type	Material	n	Measured [Cd] ± SD (mg kg^{-1})	Measured $\delta^{114}Cd$ ± 2SD (‰)	Reference
White cabbage	BCR-679	6	1.70 ± 0.06	+0.18 ± 0.03	Blommaert et al. [71]
		2	1.77± 0.05	+0.22 ± 0.02	Wiggenhauser et al. [33]
		2	1.77± 0.05	+0.22 ± 0.02	Wiggenhauser et al. [55]
Cacao leaf	MAGIC NA 702	1	102	–0.50 ± 0.06	Barraza et al. [80]
		10	107±18	–0.55 ±0.13	Moore et al. [35]
Spinach Leaf	NIST 1570a	4	2.709±0.01	+0.44 ± 0.06	Moore et al. [35]
Cabbage leaf	IAEA-359	1	0.123	-	Moore et al. [35]
Wheat flour	NIST 1567b	2	0.0223 ±0.0016	+0.89 ± 0.00	Imseng et al. [70]
		2	0.0223 ±0.0016	+0.89 ± 0.00	Imseng et al. [32]
		6	0.0216 ± 0.0019	+0.93 ± 0.08	Wiggenhauser et al. [30]
Rice flour	GBW10045	-	-	-	Zhang et al. [31]*
Peach leaves	NIST 1547	16	0.0254 ± 0.0011	+0.068 ± 0.148	Rodushkin et al. [95]*
Wood fuel	NJV 94-5	10	0.269 ± 0.013	−0.052 ± 0.084	Rodushkin et al. [95]*
Bush branches and leaves	GBW07603	3	0.37	-	Wei et al. [18]
Celery	GBW10048	-	-	-	Zhou et al. [26]*
Baking Chocolate	NIST 2384	2	0.0645 ± 0.0011	−0.26 ± 0.10	Barraza et al. [80]
		4	0.35 ± 0.07	−0.22 ± 0.04	Blommaert et al. [71]
Soil	NIST 2711	3	-	+0.65 ± 0.01	Zhong et al. [72]
		8	42.5 ± 1.9	+0.80 ± 0.071	Pallavicini et al. [79]**
		2	38.2 ± 0.32	+0.65 ± 0.02	Wiggenhauser et al. [33]
		2	38.2 ± 0.32	+0.65 ± 0.02	Wiggenhauser et al. [55]
		3	-	+0.63 ± 0.07	Yan et al. [64]
		3	-	+0.65 ± 0.01	Zhong et al. [53]
		-	-	-	Zhang et al. [31]*
		3	12.3–54.1	+0.65 ± 0.01	Zhong et al. [56]

All stable isotope compositions are reported relative to standard NIST SRM 3108. SD is the standard deviation. *Concentration and stable isotope values not declared in the publication or in the corresponding supplementary document, but the reference materials are said to be analysed. **See publication for full list of over 20 control and reference materials. ***See publication for full list of over 8 reference materials analysed using dry ashing and high-pressure bomb for sample preparation.

(Table continues on the next page)

Table A6.2 (continued). Summary of measured Cd concentration ± SD (mg kg^{-1}) and $\delta^{114}Cd$ (‰) values of certified reference materials used in published studies.

Type	Material	n	Measured [Cd] ± SD (mg kg^{-1})	Measured $\delta^{114}Cd$ ± 2SD (‰)	Reference
Soil	NIST 2709a	2	0.353 ± 0.036	−0.17 ± 0.05	Barraza et al. [80]
		3	0.3434 ± 0.004	−0.17 ± 0.04	Imseng et al. [70]
		3	0.3434 ± 0.004	−0.17 ± 0.04	Imseng et al. [32]
	NIST 2709	4	0.37 ± 0.02	+0.007 ± 0.089	Pallavicini et al. [79]**
	NIST 2710	2	21.8	−0.17 ± 0.06	Lv et al. [94]***
		3	12.3–54.1	−0.18 ± 0.00	Zhong et al. [56]
		3	-	−0.18± 0.00	Zhong et al. [53]
		3	-	− 0.18 ± 0.00	Zhong et al. [72]
	NIST 2710a	3	-	−0.13 ± 0.05	Zhong et al. [72]
		3	12.3–54.1	−0.13 ± 0.05	Zhong et al. [56]
		3	-	−0.13 ± 0.05	Zhong et al. [53]
	NIST 2711a	3	-	+0.54 ± 0.07	Zhong et al. [53]
		-	-	+0.52 ± 0.03	Gao et al. [73]
		3	12.3–54.1	+0.54 ± 0.07	Zhong et al. [56]
		3	-	+0.54 ± 0.07	Zhong et al. [72]
		2	-	+0.52 ± 0.03	Yan et al. [64]
	GBW07405	-	-	-	Zhou et al. [26]*
Rock	USGS AGV-2	2	0.0666 ± 0.0003	+0.11 ± 0.11	Wiggenhauser et al. [30]
	GSD-12	-	-	− 0.11 ± 0.03	Gao et al. [73]
Cd Solution	Münster Cd	5	-	+4.43 ± 0.06	Blommaert et al. [71]
		-	-	+4.53 ± 0.08	Wei et al. [57]
		12	-	+4.45 ± 0.08	Wei et al. [38]
		12	-	+4.45 ± 0.08	Wei et al. [58]
		12	-	+4.45 ± 0.08	Wei et al. [89]
		5	-	+4.46 ±0.02	Wiggenhauser et al. [33]
		5	-	+4.46 ±0.02	Wiggenhauser et al. [55]
		113	-	+4.5 ± 0.05	Zhong et al. [53]
		113	-	+4.5 ± 0.05	Zhong et al. [56]
	NIST 3108	11	-	+0.04 ± 0.09	Imseng et al. [70]
		11	-	+0.04 ± 0.09	Imseng et al. [32]

All stable isotope compositions are reported relative to standard NIST SRM 3108. SD is the standard deviation. *Concentration and stable isotope values not declared in the publication or in the corresponding supplementary document, but the reference materials are said to be analysed. **See publication for full list of over 20 control and reference materials. ***See publication for full list of over 8 reference materials analysed using dry ashing and high-pressure bomb for sample preparation.

(Table continues on the next page)

Table A6.2 (Continued). Summary of measured Cd concentration ± SD (mg kg^{-1}) and $\delta^{114}Cd$ (‰) values of certified reference materials used in published studies.

Type	Material	n	Measured [Cd] ± SD (mg kg^{-1})	Measured $\delta^{114}Cd$ ± 2SD (‰)	Reference
Cd Solution	Spex-1 Cd	3	-	−1.25 ± 0.06	Wei et al. [38]
		3	-	−1.25 ± 0.06	Wei et al. [58]
		3	-	−1.25 ± 0.06	Wei et al. [89]
	Nancy-Spex Cd	2	-	−0.09 ± 0.01	Wei et al. [38]
		2	-	−0.09 ± 0.01	Wei et al. [58]
		2	-	−0.09 ± 0.01	Wei et al. [89]
	BAM-I012	4	-	−1.33 ± 0.07	Barraza et al. [80]
		36	-	−1.31 ± 0.10	Imseng et al. [70]
		36	-	−1.31 ± 0.10	Imseng et al. [32]
		16	-	–1.32 ± 0.06	Moore et al. [35]
		12	-	–1.30 ± 0.09	Wiggenhauser et al. [30]
		154	-	−1.33 ± 0.05	Zhong et al. [53]
		154	-	−1.33 ± 0.05	Zhong et al. [56]
		77	-	−1.33 ± 0.05	Zhong et al. [72]
	AAS Cd	170	-	−0.69 ± 0.06	Zhong et al. [53]
		170	-	−0.69 ± 0.06	Zhong et al. [56]
		91	-	− 0.69 ± 0.05	Zhong et al. [72]

All stable isotope compositions are reported relative to standard NIST SRM 3108. SD is the standard deviation. *Concentration and stable isotope values not declared in the publication or in the corresponding supplementary document, but the reference materials are said to be analysed. **See publication for full list of over 20 control and reference materials. ***See publication for full list of over 8 reference materials analysed using dry ashing and high-pressure bomb for sample preparation.

Table A6.3. Summary of $\Delta^{66}Zn$ (‰) values associated with uptake and translocation and $\delta^{66}Zn$ (‰) values for roots, shoots and leaves for different vascular plant species.

Plant type	Plant Species	Zn concentrations in medium (mg kg^{-1})	$\Delta^{66}Zn_{x\text{-medium}}$ represents	$\Delta^{66}Zn_{x\text{-medium}}$ (‰)	$\Delta^{66}Zn$ represents	$\Delta^{66}Zn$ (‰)	Root $\delta^{66}Zn$ (‰)	Shoot $\delta^{66}Zn$ (‰)	Leaf $\delta^{66}Zn$ (‰)	Reference
Cereals	*Oryza sativa* L. (rice)	60[+]	Shoot-soil	−0.22 to +0.05[a]	-	-	-	-	-	Arnold et al. [49]
		26[‖]	Total plant (aboveground)–soil extract	−0.27 to −0.08[b]	Grain-shoot	−0.79 to −0.67[b]	-	+0.61 to +0.73[b]	-	Arnold et al. [28]
		29.6 to 243.3[‖]	-	-	-	-	-	+0.01 to +0.58[c]	-	Weiss et al. [50]
		6.5×10^{-3} and 1.3×10^{-2}	Shoot-hydroponic solution	−0.21 to −0.12[d,e]	Shoot-root	−0.30 to −0.25[d,e]	−0.03 to +0.18[d,f]	−0.25 to −0.06[d,f]	-	Weiss et al. [59]
	Triticum aestivum L. (wheat)	0.40 and 10.9[‖]	Total plant–soil extract	−0.33 to +0.13[g]	Straw-root	−0.14 to +0.10[g]	+0.56 to +0.63[g]	-	+0.10 to +0.72[g]	Wiggenhauser et al. [68]
		3.9×10^{-3} and 1×10^{-2}	Shoot-hydroponic solution	−0.36 to −0.28[h]	Shoot-root	−0.51 to −0.25[h,i]	-	-	-	Jouvin et al. [60]
	Zea mays (maize)	0.043 to 0.21	Total plant – soil porewater	−0.20 to −0.02[j]	Shoot-root	−0.39 to −0.37[j]	+0.86 to +0.93[j]	+0.49 to +0.54[j]	+0.50 to +0.57[j]	Liu et al. [54]
Vegetable	*Lactuca sativa* (lettuce)	6.5×10^{-3} and 1.3×10^{-2}	Shoot-hydroponic solution	−0.32 to −0.21[d,e]	Shoot-root	−0.49 to −0.35[d,e]	+0.12 to +0.20[d,f]	−0.39 to −0.22[d,f]	-	Weiss et al. [59]
Fruit	*Lycopersicon esculentum* (tomato)	3.9×10^{-3} and 1×10^{-2}	Shoot-hydroponic solution	−0.43 to −0.33[h]	Shoot-root	−0.51 to −0.30[h,i]	-	-	-	Jouvin et al. [60]
		6.5×10^{-3} and 1.3×10^{-2}	Shoot-hydroponic solution	−0.44 to −0.22[d,e]	Shoot-root	−0.51 to −0.35[d,e]	−0.04 to +0.16[d,f]	−0.54 to −0.14[d,f]	-	Weiss et al. [59]
		<2.0 x10^{-4}, 5.9 x10^{-3} and 6.5 x10^{-3}; 0 and 50[+]	Total plant–hydroponic solution; Shoot-soil	−0.33 to −0.06[k]; −1.09 to −0.57[l]	-	-	+0.16 to +0.33[k]	−0.36 to +0.24[k]; −0.25 to +0.66[l]	-	Smolders et al. [63]
	Theobroma cacao L. (cacao)	2.5 x10^{-3}	Total plant–hydroponic solution	−1.21 to −0.73[m]	Leaf-total plant	−0.54 to −0.09[m]	−0.28 to +0.68[m]	-	−1.11 to −0.43[m]	Barati et al. [34]
Legumes	*Lens culinaris* (lentil)	-	-	-	Leaves-seeds	−0.34 to −0.21[n]	-	-	+0.85 to +1.18[§]	Moynier et al. [62]

(Table continues on the next page)

Table A6.3 (Continued). Summary of $\Delta^{66}Zn$ (‰) values associated with uptake and translocation and $\delta^{66}Zn$ (‰) values for roots, shoots and leaves for different vascular plant species.

	Plant Species	Zn concentrations in medium (mg kg^{-1})	$\Delta^{66}Zn_{x\text{-medium}}$ represents	$\Delta^{66}Zn_{x\text{-medium}}$ (‰)	$\Delta^{66}Zn$ represents	$\Delta^{66}Zn$ (‰)	Root $\delta^{66}Zn$ (‰)	Shoot $\delta^{66}Zn$ (‰)	Leaf $\delta^{66}Zn$ (‰)	Reference
Hyperaccumulator and metal-tolerant plants (including grasses, trees, flowering and marginal aquatic plants)	*Phragmites australis* (common reed)	2.1×10^{-2} and 13.1	Total plant-hydroponic solution	+0.30 to +0.60[o]	Shoot-root	–1.0 to +0.02[p,o]	+0.17 to +0.43[o]	−0.55 to +0.26[o]	−0.54 to +0.03[o]	Caldelas et al. [61]
		0 to 1000	-	-	Shoot-root	−0.71 to −0.52[q]	+0.02 to +0.38[q]	−0.61 to −0.32[q]	-	Caldelas et al. [92]
	Phalaris arundinacea (reed canary grass)	2129[+]	Total plant–soil	−0.60[r]	-	-	+0.24[r]	-	−0.19[r]	Aucour et al. [39]
	Brassica napus L. (rape)	7400 to 74800[+]	Root-soil; Root-soil extract	+0.00 to +0.08; +0.13 to +0.20[s]	Shoot-root	−0.39 to −0.23[s]	+0.05 to +0.31[s]	−0.34 to +0.06[s]	-	Couder et al. [27]
	Lolium multiflorum L. (ryegrass)		Root-soil; Root-soil extract	−0.07 to +0.06; +0.05 to +0.18[s]	Shoot-root	−0.20 to −0.04[s]	−0.10 to +0.32[r]	−0.25 to +0.17[s]	-	
	Agrostis capillaris L. (common bent)	9470 and 56600[+]	Total plant–soil extract	−0.04 to +0.02[t]	Shoot-root	–0.40 to –0.24[t]	+0.17 to +0.36[t]	−0.10 to −0.05[t]	-	Houben et al. [66]
	Alyssum murale (yellowtuft)	1.3×10^{-2} and 3.3×10^{-1}	Total plant–hydroponic solution	−0.17 to −0.04[u]	Shoot-root	−0.76 to −0.37[u]	+0.17 to +0.32[u]	−0.59 to +0.14[u]	−0.74 to −0.12[u]	Deng et al. [37]
	Arabidopsis halleri (thale cress)	6.5×10^{-2} and 1.6	Total plant–hydroponic solution	−0.13 to +0.02[v]	Shoot-total plant	−0.22 to −0.03[v]	+0.60 to +0.96[v]	−0.01 to +0.16[v]	-	Aucour et al. [36]
	Silene vulgaris (bladder campion)	107, 115, 2220 and 2396[+]	Total plant–soil	−0.05[w]	Shoot-total plant	–0.01[w]	+0.58 to +0.76[w]	-	+0.76 to +0.77[w]	Tang et al. [29]
	Typha latifolia (broadleaf cattail)	2089[+]	Total plant–soil	−0.50[r]	Shoot-root	−0.40[r]	+0.03[r]	-	−0.32[r]	Aucour et al. [40]
	Noccaea caerulescens (alpine Pennycress)	107, 115, 2220 and 2396[+]	Total plant–soil	−0.01 to +0.63[w]	Shoot-total plant	−0.05 to +0.00[w]	+0.72 to +0.99	-	+0.19 to +0.88	Tang et al. [29]
		1.3×10^{-2} and 3.3×10^{-1}	Total plant–hydroponic solution	−0.20 to +0.24[u]	Shoot-root	−0.94 to −0.64[u]	+0.54 to +1.12[u]	−0.12 to +0.23[u]	-	Deng et al. [37]
		1.3×10^{-4}, 6.5×10^{-3}, 3.3×10^{-2} and 3.3×10^{-1}	Total plant–hydroponic solution	−0.12 to −0.06[x]	Shoot-total plant	−0.29 to −0.09[x]	+0.55 to +0.82[§]	−0.16 to +0.13[§]	-	Tang et al. [24]

(Table continues on the next page)

Table A6.3 (Continued). Summary of $\Delta^{66}Zn$ (‰) values associated with uptake and translocation and $\delta^{66}Zn$ (‰) values for roots, shoots and leaves for different vascular plant species.

	Plant Species	Zn concentrations in medium (mg kg^{-1})	$\Delta^{66}Zn_{x\text{-medium}}$ represents	$\Delta^{66}Zn_{x\text{-medium}}$ (‰)	$\Delta^{66}Zn$ represents	$\Delta^{66}Zn$ (‰)	Root $\delta^{66}Zn$ (‰)	Shoot $\delta^{66}Zn$ (‰)	Leaf $\delta^{66}Zn$ (‰)	Reference
Hyperaccumulator and metal-tolerant plants (including grasses, trees flowering and marginal aquatic plants)	*Sedum plumbizincicola* (stonecrop)	1006 to 2022[+]; 15.3 to 133[‖]	Shoot-soil; Shoot-soil extract	−0.14 to +0.05; −0.46 to −0.16[y]	-	-	-	+0.08 to +0.24[y]	-	Zhou et al. [25]
	Elsholtzia splendens N. (Shiny Elsholtzia)	1170[+]	Total plant-soil; Total plant-soil solution	+0.41[z]; +0.43	Above-ground tissues- root	+0.47[z]	−0.74[z]	-	−0.55 to −0.42[§§]	Li et al. [44]
	Dichapetalum gelonioides (gelonium poison-leaf)	10 to 65[+]	-	-	-	-	+0.90 to +0.95[ab]	-	+0.45 to +0.70[ab]	van der Ent et al. [78]
	Laguncularia racemosa (white mangrove)	151 to 23,700[+]	-	-	-	-	-	-	+0.08 to +0.23[abc]	Araújo et al. [93]
Non-hyperaccumulator plants (flowering plant)	*Arabidopsis petraea* (northern rock-cress)	6.5×10^{-2} and 1.6	Total plant–hydroponic solution	−0.36 to −0.09[v]	Shoot-total plant	−0.59 to −0.21[v]	+0.19 to +0.31[v]	−0.54 to −0.19[v]	-	Aucour et al. [36]
	Thlaspi arvense (field pennycress)	1.3×10^{-2} and 3.3×10^{-1}	Total plant–hydroponic solution	−0.26 to +0.21[u]	Shoot-root	−0.70 to −0.61[u]	+0.28 to +0.34[u]	−0.35 to −0.31[u]	−0.42 to −0.40[u]	Deng et al. [37]
		1.3×10^{-4}, 6.5×10^{-3}, 3.3×10^{-2} and 3.3×10^{-1}	Total plant–hydroponic solution	−0.26 to +0.16[x]	Shoot-total plant	−0.29 to −0.21[x]	+0.14 to +0.58[§]	−0.26 to −0.10[§]	-	Tang et al. [24]
Trees and shrubs (with non-edible fruits)	Tree (unspecified species)	64 to 122[+]	Total plant-soil	−0.10 to +0.05[abcd]	-	-	-	-	-	Imseng et al. [67]
	Phyllostachys aurea (bamboo)	-	-		Leaves-rhizome/stem	−1.07 to −0.71[n]	+0.48 to +0.62[abcde]	-	−0.55 to −0.19[§]	Moynier et al. [62]
	Picea glauca (white spruce)	1.2 to 15.3[+]	-	-	-	-	-	-	-	Dinis et al. [41]
	Betula pubescens (birch)	-	-	-	-	-	-	-	−0.15 to +0.20*	Rodushkin et al. [95]

(Table continues on the next page)

Table A6.3 (Continued). Summary of Δ^{66}Zn (‰) values associated with uptake and translocation and δ^{66}Zn (‰) values for roots, shoots and leaves for different vascular plant species.

	Plant Species	Zn concentrations in medium (mg kg^{-1})	$\Delta^{66}Zn_{x\text{-medium}}$ represents	$\Delta^{66}Zn_{x\text{-medium}}$ (‰)	Δ^{66} Zn represents	Δ^{66} Zn (‰)	Root δ^{66}Zn (‰)	Shoot δ^{66}Zn (‰)	Leaf δ^{66}Zn (‰)	Reference
Trees and shrubs (with non-edible fruits)	*Megaphrynium macrostachyum* (Yoruba soft cane)	14 to 59[+]	-	-	-	-	+0.75**	+0.42**	+0.52**	Viers et al. [42]
	Milicia excelsa (African teak)		-	-	-	-	-	-	−0.03**	
	Musanga cecropioides (umbrella tree)		-	-	-	-	-	+0.09**	−0.27**	
	Lasimorpha senegalensis		-	-	-	-	+0.57**	+0.69**	+0.63**	
	Raphia vinifera (wine raffia palm)		-	-	-	-	+0.51**	+0.76**	−0.91**	
	Renealmia cincinnata		-	-	-	-	+0.57**	+0.61**	+0.26**	
	Larix gmelinii (larch)	108 to 121[+]	-	-	-	-	+0.48***	-	-	Viers et al. [43]

All Zn stable isotope compositions are reported relative to standard JMC-lyon. The x in x-medium represents either total plant, shoot or root, and the medium represent bulk soil, soil extract, solution (i.e. porewater, seepage water) or hydroponic solution. [+]represents total Zn concentration in soils. [‖] represents total Zn concentration in soil leachates and extracts. [§]represents range of individual values. [§§]represents range of mean values. [a]represents range of mean values for *Oryza sativa* L. (rice) grown in soil sites in Philippines under both Zn deficient and Zn sufficient conditions (this excludes summarized data findings from Weiss et al. [59] discussed in the study for comparison purposes). [b]represents range of mean values for *Oryza sativa* L. (rice) grown in anaerobic and aerobic soils in pots inside greenhouses (Britain). [c]represents the range of individual values for two different genotypes of *Oryza sativa* (rice) grown in soil under both Zn deficient and Zn sufficient conditions and under different planting densities in the Philippines (excludes data from Weiss et al. [59] and Arnold et al. [28,49] used for comparison in this study). [d]represents range of values for *Oryza sativa* (rice), *Lactuca sativa* (lettuce) *and Lycopersicon esculentum* (tomato) grown in either HEDTA+NTA or EDTA in hydroponics-plant systems. [e]represents an approximation for range of mean values taken from both table and graphical figures and these values were taken from Jouvin et al. [60] that declares the apparent fractionation values from Weiss et al. [59]. [f]represents an approximation for individual values taken from a graphical figure and values were converted and reported relative to JMC lyon Zn, from an internal standard used in the laboratory for this study that is 0.04 ± 0.04‰ heavier than JMC lyon Zn. [g]represents range of mean values for wheat grown in two different soil sites in Switzerland. [h]represents range of mean values *Lycopersicon esculentum* (tomato) *and Triticum aestivum* L. (wheat) grown under low Iron (2 μmol L^{-1}) or high Iron (100 μmol L^{-1}) conditions (part of the summarized data from this study for *Oryza sativa* (rice) and *Lactuca sativa* (lettuce) is derived from Weiss et al. [59] and excluded to avoid repetition). [i]represents an approximation for range of mean values taken from a graphical figure. [j]represents the range of mean values for maize grown in three different treatments of native, disturbed, and reconditioned soils from Switzerland. [k]represents range of mean values for *Lycopersicon esculentum* L. (tomato) grown under low and high supply in hydroponics-plant systems. [l]represents range of mean values for *Lycopersicon esculentum* L. (tomato) grown in pots containing soil from Spain either fertilized with Zn (as $ZnSO_4$) or not fertilized (control). [m]represents the range values for 19 cacao genotypes undergoing high Cd treatment (20 μmol L^{-1}) in a hydroponics-plant system. [n]represents range of mean values for apparent fractionation between leaves and rhizome/stem for *Phyllostachys aurea* (bamboo) and between leaves and seeds for *Lens culinaris* (lentil) grown in hydroponics-plant systems. [o]represents range of mean values for *Phragmites australis* grown in two different Zn treatments: control and high Zn treatment. [p]represents apparent fractionation between high shoot and living root for *Phragmites australis.* [q]represents range of mean values for *Phragmites australis* grown in four different hydroponic solutions: non-nano ZnO (bulk), spherical particle nanopowder <100 nm in diameter, <50 nm nanopowder particles of various shapes, and nanowires 50 nm in diameter × 300 nm long. [r]represents mean values of *Typha latifolia* and *Phalaris arundinacea* grown in soil sites situated in France. [s]represents range of mean values for *Brassica napus* L. (rape) and *Lolium multiflorum* L. (ryegrass) grown in soil from three different soil sites in Belgium. [t]represents range of mean values for *Agrostis capillaris* L. grown in soil from two different soil sites in Belgium. [u]represents range of individual values for *Thlaspi arvense*, *Alyssum murale and Noccaea caerulescens* undergoing low and high Zn treatment in hydroponics-plants system. [v]represents range of individual values for *Arabidopsis halleri* and *Arabidopsis petraea* undergoing low and high Zn treatment in hydroponics-plant systems. [w]represents the range of mean values for *Noccaea caerulescens and Silene vulgaris* grown in three soil sites in France. [x]represents range of mean values for *Noccaea caerulescens* and *Thlaspi arvense* under low and high Zn treatment in hydroponics-plant systems. [y]represents range of

mean values for *Sedum plumbizincicola* grown in four different soils from soil sites in China. [z]represents mean values of *Elsholtzia splendens* Nakai grown in soil sites in China. [ab]represents range of mean values for *Dichapetalum gelonioides* at different sites in Malaysian Borneo. [abc]represents range of mean values for *Laguncularia racemosa* from three soil sites in Brazil. [abcd]represents range of mean values for trees grown in soil from three different soil sites in Switzerland. [abcde]represents range values for rhizome. *represents the range of mean values for leaf samples from birch leaves from three different countries (Sweden, Britain and Iceland). **represents range of individual values for six different plant species in different soil sites in Cameroon. *** represents mean value for *Larix gmelinii* (larch) in Russia.

Table A6.4. Summary of Δ^{114}Cd (‰) values associated with uptake and translocation and δ^{114}Cd (‰) values for roots, shoots and leaves for different vascular plant species.

	Plant Species	Cd concentrations in medium (mg kg^{-1})	$\Delta^{114}Cd_{x\text{-medium}}$ represents	$\Delta^{114}Cd_{x\text{-medium}}$ (‰)	Δ^{114}Cd represents	Δ^{114}Cd (‰)	Root δ^{114}Cd (‰)	Shoot δ^{114}Cd (‰)	Leaf δ^{114}Cd (‰)	Reference
Fruit	*Theobroma cacao* L. (cacao)	0.28; 0.08	Total plant-soil; Total plant-soil extract	−0.05; −0.20[a]	Shoot-root	+0.27[a]	−0.58[a]	-	−0.44 to −0.15[a]	Blommaert et al. [71]
		0.17 to 0.52	Leaf-soil	+0.22 to +0.41[b]	Beans–leaves	−0.40 to −0.08[b]	-	-	+0.28 to +0.42[b]	Barraza et al. [80]
		0.13	Total plant-hydroponic solution	−0.34 to +0.01[c]	Leaf-total plant	−0.04 to +0.46[c]	−0.85 to −0.53[c]	-	−0.67 to +0.02[c]	Moore et al. [35]
Cereals	*Triticum aestivum* L. (wheat)	0.19 to 0.51; 2.75×10^{-3} to 3.96×10^{-2}	Total plant-soil; Total plant-soil extract	+0.13 to +0.39; −0.21 to +0.03[d]	Straw-root	+0.21 to +0.41[d]	−0.12 to +0.13[d]	+0.20 to +0.57[d]	-	Wiggenhauser et al. [30]
		2.8×10^{-3} to 4.0×10^{-2}	Total plant-soil extract	−0.28 to −0.04[e]	Shoot-root	+0.35 to +0.45[e]	-	+0.38 to +0.56[e]	-	Wiggenhauser et al. [69]
		0.15 to 1.66	Total plant-soil	−0.56 to −0.34[f]	-	-	-	-	-	Imseng et al. [70]
		0.15 to 1.66	Total plant-soil; Total plant-soil solution	+0.31 to +0.46; −0.36 to −0.20[g]	Shoot-total plant	−0.26[h]	−0.05 to +0.20[g]	-	-	Imseng et al. [32]
	Hordeum vulgare (barley)	0.15 to 1.66	Total plant-soil	−0.83 to −0.71[f]	-	-	-	-	-	Imseng et al. [70]
		0.15 to 1.66	Total plant-soil; Total plant-soil solution	+0.51 to +0.55; −0.18 to −0.06[g]	-	-	+0.05 to +0.20[g]	-	-	Imseng et al. [32]
	Oryza sativa L. (rice)	15	Total plant-soil solution	−0.43 to −0.24[i]	Shoot-root	−0.02 to +0.19[i]	−0.55 to −0.41[i]	−0.57 to −0.22[i]	-	Wiggenhauser et al. [33]
		15	-	-	Grain-root	+0.93[j]	−0.47 to +0.03[k]	−0.31 to +0.14[k]	-	Wiggenhauser et al. [55]

(Table continues on the next page)

Table A6.4. (Continued) Summary of $\Delta^{114}Cd$ (‰) values associated with uptake and translocation and $\delta^{114}Cd$ (‰) values for roots, shoots and leaves for different vascular plant species.

	Plant Species	Cd concentrations in medium (mg kg^{-1})	$\Delta^{114}Cd_{x\text{-medium}}$ represents	$\Delta^{114}Cd_{x\text{-medium}}$ (‰)	$\Delta^{114}Cd$ represents	$\Delta^{114}Cd$ (‰)	Root $\delta^{114}Cd$ (‰)	Shoot $\delta^{114}Cd$ (‰)	Leaf $\delta^{114}Cd$ (‰)	Reference
Cereals	*Oryza sativa* L (rice)	5.87 to 9.73	Leaf- soil	−0.05[l]	Leaf-root	+0.17[l]	−0.31[l]	-	−0.14[l]	Yan et al. [64]
		0.04 to 8.29; 0.95	Grain-soil; Grain-soil solution	+0.58 to +0.22; −0.20 to +0.16[m]	-	-	−0.50 to −0.39[n]	-	−0.98 to −0.31[n]	Zhang et al. [31]
		1.04; 0.40 and 0.81	Total plant-soil; Total plant- soil solution	+0.25 to +0.26; −0.47 to −0.41[o]	Shoot-root	+0.05 to +0.03[p]	+0.27 to +0.29[q]	+0.32[q]	+0.07 to 1.28[q]	Zhong et al. [53]
		0.40 and 0.81	Total plant – soil porewater	−0.39 to −0.15[r]	Shoot-root	−0.67 to +0.19[r]	+0.31 to +0.48[r]	−0.19 to +0.50[r]	+0.14 to +2.10[r]	Zhong et al. [56]
		0.51 to 1.65; 5.35 to 16.71[s]	Total plant-soil solution; Total plant-iron plaque	−0.63 to −0.36; +0.13 to +0.24[t]	Shoot-root	+0.29 to +0.33[t]	−0.13 to −0.04[t]	+0.18 to +0.29[t]	−0.27 to +0.18[t]	Zhong et al. [72]
		0.46 to 0.70	Total plant-soil extract	−0.41 to −0.02[u]	Shoot-root	−0.02 to +0.33[u]	−0.41 to −0.22 [u]	−0.24 to −0.02[u]	−0.31 to −0.14[u]	Gao et al. [73]
		1.53; 0.20 to 0.60	Grain-soil; Root-soil extract	+0.84 to +0.99; −0.002 to +0.22[v]	Shoot-root	+0.037 to +0.056[v]	−0.51 to +0.08[v]	−0.012 to +0.14[v]	-	Wang et al. [45]
Hyperaccumulator and metal tolerant plants (flowering plants)	*Ricinus communis* (castor oil)	2 and 5	-	-	-	-	−0.08[w]	-	−0.12[w]	Wei et al. [18]
		2 and 5	Total plant-hydroponic solution	−0.46 to −0.27[x]	Shoot-total plant	−0.08 to +0.11[x]	−0.22 to −0.01[x]	−0.40 to −0.08[x]	-	Wei et al. [57]
		0.5 and 5	Total plant-hydroponic solution	−0.64 to −0.29[x]	Shoot-total plant	+0.15 to +0.22[x]	−0.65 to −0.29[x]	-	−0.70 to −0.10[x]	Wei et al. [38]
		0.5 and 5	-	-	-	-	−0.49 to −0.26[x]	-	−0.49 to −0.06[x]	Wei et al. [58]
		0.1, 2, and 5	-	-	-	-	−0.36 to −0.23[y]	-	−0.82 to +0.03[y]	Wei et al. [89]

(Table continues on the next page)

Table A6.4. (Continued). Summary of $\Delta^{114}Cd$ (‰) values associated with uptake and translocation and $\delta^{114}Cd$ (‰) values for roots, shoots and leaves for different vascular plant species.

	Plant Species	Cd concentrations in medium (mg kg^{-1})	$\Delta^{114}Cd_{x\text{-medium}}$ represents	$\Delta^{114}Cd_{x\text{-medium}}$ (‰)	$\Delta^{114}Cd$ represents	$\Delta^{114}Cd$ (‰)	Root $\delta^{114}Cd$ (‰)	Shoot $\delta^{114}Cd$ (‰)	Leaf $\delta^{114}Cd$ (‰)	Reference
Hyperaccumulator and metal tolerant plants (flowering plants)	*Solanum nigrum* (black nightshade)	2 and 5	-	-	-	-	−0.37[w]	-	−0.34[w]	Wei et al. [18]
		2 and 5	Total plant-hydroponic solution	−0.48 to −0.41[x]	Shoot-total plant	+0.03 to +0.11[x]	−0.26 to −0.25[x]	−0.14 to −0.09[x]	-	Wei et al. [57]
		0.5 and 5	Total plant-hydroponic solution	−0.84 to −0.31[x]	Shoot-total plant	+0.13 to +0.16[x]	−0.90 to −0.31[x]	-	−0.70 to −0.10[x]	Wei et al. [38]
		0.5 and 5	-	-	-	-	−0.87 to +0.04[x]	-	−0.62 to −0.04[x]	Wei et al. [58]
	Cyperus alternifolius (umbrella Sedge)	2 and 5	-	-	-	-	−0.37[w]	-	-	Wei et al. [18]
	Pteris vittate (Chinese Brake Fern)	2 and 5	-	-	-	-	−0.34[w]	-	-	Wei et al. [18]
	Sedum (stonecrops)	-	-	-	-	-	-	−0.04 to +0.24[ab]	-	Lv et al. [94]
	Sedum plumbizincicola (stonecrops)	20.8 to 29.9	Shoot-soil	+0.02 to +0.14[abc]	-	-	-	−0.15 to +0.04[abc]	-	Zhou et al. [26]
Tree and shrub (with non-edible fruit)	*Betula pubescenes* (Birch)	-	-	-	-	-	-	-	+0.3 to +1.3[abc]	Pallavicini et al. [79]
	Betula pubescens (birch)		-	-	-	-	-	-	+0.40 to +0.51[abcd]	Rodushkin et al. [95]
	Trees (unspecified species)	0.15 to 1.66	Total plant-soil	+0.25[f]	-	-	-	-	-	Imseng et al. [70]

All values are reported relative to standard NIST SRM 3108. The x in x-medium represents either total plant, shoot or root, and the medium represent soil, soil extract, soil solution (e.g., porewater) or hydroponic solution. [a]represents mean values for *Theobroma cacao* L. from Trinidad. [b]represents range of values for *Theobroma cacao* L. from three different soil sites in Ecuador. [c]represents the range of values for 19 cacao genotypes undergoing high Cd treatment in hydroponics-plant systems. [d]represents range of mean values for *Triticum aestivum* L. (wheat) grown in soil from three different soil sites in Switzerland. [e]represents range of mean values for *Triticum aestivum* L. (wheat) grown in soils without (control) and with phosphorus fertilizers (part of the data is an approximation from graphical figures). [f]represents range of values for trees (unspecified species), *Triticum aestivum* L. (wheat) and *Hordeum vulgare* (barley) from three different soil sites in Switzerland. [g]represents range of values for *Triticum aestivum* L. (wheat) and *Hordeum vulgare* (barley) from three different soil sites in Switzerland. [h]represents isotope fractionation (ε) for *Triticum aestivum* L. (wheat) (field samples) grown in soil from three different soil sites. [i]represents range of mean values for flooded and non-flooded rice (including with or without functional membrane transporter *OsHMA3*). [j]represents mean value for rice during flowering and maturity. [k]represents range of mean values for rice during flowering, maturity and grain-filling. [l]represents mean value of rice grown across different soil sites in China. [m]represents range of mean values for rice (with or without functional *OsHMA3*) grown under field conditions in China. [n]represents

range of mean values for wild type and genetically modified (with and without functional *OsNramp5* and *OsHMA3*) rice grown in hydroponics-plant systems. [o]represent range of values for rice in drained and flooded conditions. [p]represents range of mean values for rice in drained and flooded conditions. [q]represents range of mean values for rice for drained and flooded conditions. [r]represents range of mean values for rice rice grown under flooded and non-flooded conditions. [s]represents range of mean values for soil solution and Fe plaque concentrations from soils from China that were drained and not drained. [t]represents range of mean values for rice grown in soils from China during flowering and grain-filling and under drained and not flooded soil conditions. [u]represents range of mean values for rice grown under flooded (during tillering and panicle initiation stages) and drained soils (during maturity stage) from China. [v]represents range of individual values for rice grown in China under different soil redox conditions. [w]represents the range of mean values of *Ricinus communis, Solanum nigrum, Cyperus and alternifolius Pteris vittata* grown in hydroponic solutions with low and high Cd treatment. [x]represents range of mean values (an approximation for part of the values was made using graphical figures) for *Ricinus communis and Solanum nigrum* undergoing low and high Cd treatment. [y]represents range of individual values for *Ricinus communis* undergoing low and high Cd treatments. [z]represents range of mean values for sedum shoot undergoing dry ashing and high-pressure bomb digestion methods. [ab]represents range of mean values for *Sedum plumbizincicola* grown in four different soils. [abc]represents range of individual values for birch leaves across multiple sites across Sweden. [abcd]represents the range of mean values for birch leaf samples from three different countries (Sweden, Britain, and Iceland).